Table 1. Bioassay conditions measured by flow cytometry.

Endpoint	Fluorescent Dye	Cytometer Emission Filter
Viability	Propidium iodide (PI)	ECD, 610 nm
Esterase activity	Fluorescein diacetate (FDA)	FITC, 525 nm
Membrane potential	3,3′-dihexyloxacarbocyanine iodide ($DIOC_6$)	FITC, 525 nm

The used fluorescent dyes and measured parameters are shown in Table 1. The features of using this set of biomarkers for determining the aquatic toxicity of particulate matter on marine organisms were described in our previous works (Pikula et al., 2019; Pikula et al., 2020b).

The morphological changes in the cells were monitored by the Axio Observer A1 optical microscope (Carl Zeiss, Germany).

3 RESULTS AND DISCUSSION

The particle size distribution of coal used in the study was represented by a fine fraction, most susceptible to dusting under the influence of external factors. Altogether, 300 thousand particles from the coal sample were examined by micro-Raman spectroscopy and 1 million particles by flow cytometry. Particles, in general, have oval elongated and broken shapes. The diameter of majority of particles ranges from 150 nm to 10 μm. As shown in Figure 1a, b, the predominant amount of coal particles is in the diameter range of about 300 nm. In the micrometer range, the predominant diameter is 1–2 μm (Figure 1a, c).

It should be noted that the analyzed coal samples taken from the coal seam are represented by a finer size fraction than coal, which was transported, stored, and then sampled directly at the territory of the coal terminal (Kirichenko et al., 2019).

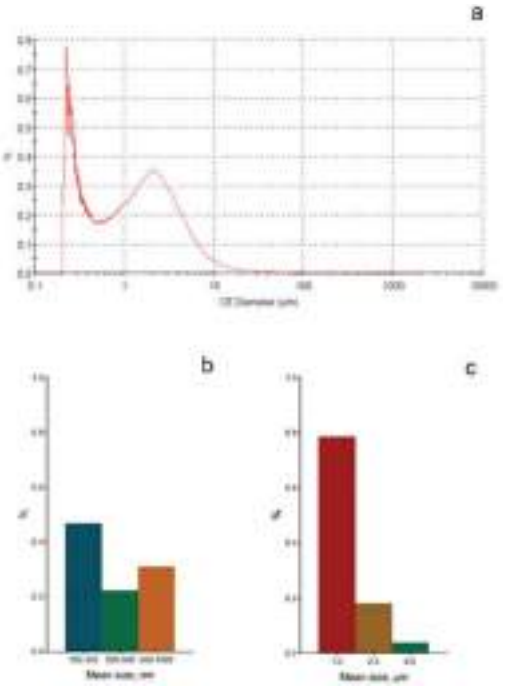

Figure 1. Particle size composition of the coal sample. a) micro-Raman spectroscopy data; b) and c) flow cytometry data.

The results of the exposure of the mollusk *M. modiolus* hemocytes to the coal suspension are presented in Figure 2.

The viability was assessed by the absence of DNA cells staining with PI dye (Ostrander, 2005) registered by the absence of changes in the level of cell fluorescence in the ECD emission channel (Table 1). Dead cells were excluded from the count. According to the results of the tests, we can conclude that the investigated coal sample did not have a significant effect on the viability of the mollusk *M. modiolus* hemocytes. The proportion of alive cells in each measurement series after 2, 4, and 6 hours of exposure to the highest concentration of coal suspension (1000 mg/L) was almost at the same level as the proportion of alive cells in the control group for each series (Figure 1a). The greatest fluctuation and spread of values in different series of measurements was observed for the concentration of coal suspension of 100 mg/L.

The change in the hemocyte esterase activity level after exposure to coal suspension was recorded as the fluorescence intensity of fluorescein formed due to the cleavage of FDA dye with cell esterases (Figure 2b). This index makes it possible to assess the enzyme activity and, therefore, the level of cell metabolism (Fontvieille et al., 1992). We can note that the cell metabolism activity increased slightly when exposed to coal suspension at concentrations of 1 and 10 mg/L, while concentrations of 100 and 1000 mg/L caused the inhibition of cell metabolism. The increase in the time of exposure to coal suspension from 2 to 6 hours did not cause any further decrease in the cell metabolism level, since each series of measurements (2, 4, and 6 hours) had a similar exposure level.

Maintaining the polarization level of cell membranes is an important indicator characterizing the ability of cells to perform barrier and metabolic functions that ensure cell activity.

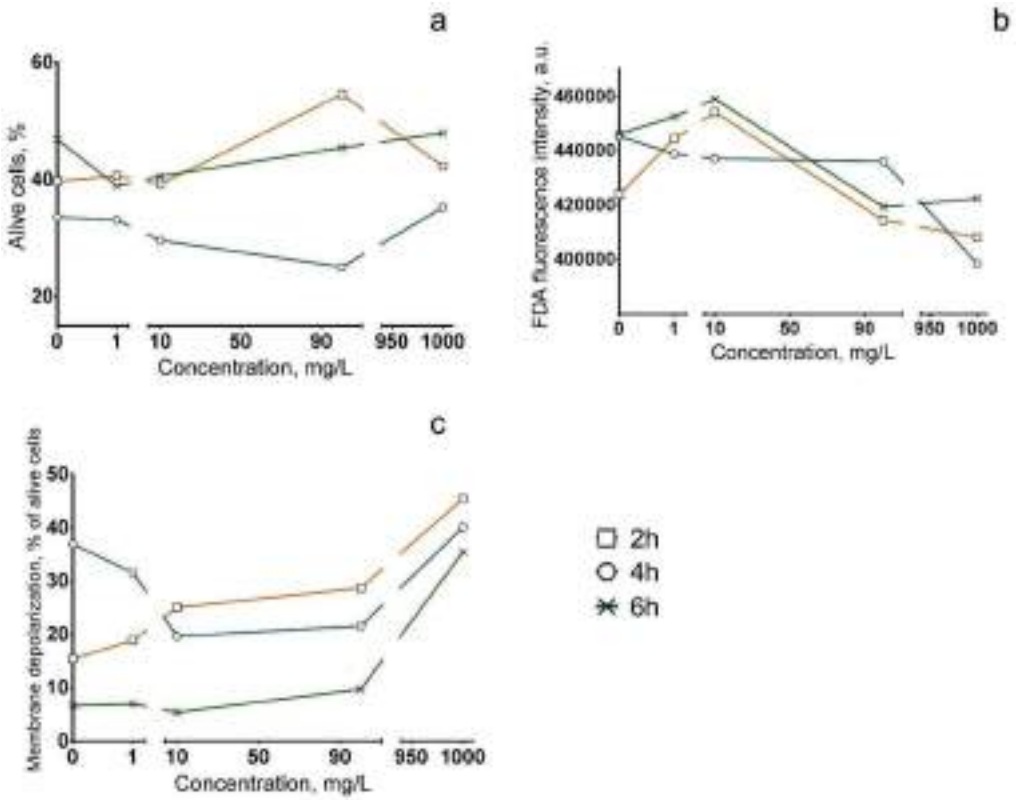

Figure 2. The change in the state of hemocytes of mollusk *M. modiolus* after 2, 4, and 6 hours of exposure to coal suspension at concentrations of 1, 10, 100, and 1000 mg/L. a) percentage of alive cells, b) change in esterase activity of cells, c) change in polarization of cell membranes; a.u. – arbitrary units.

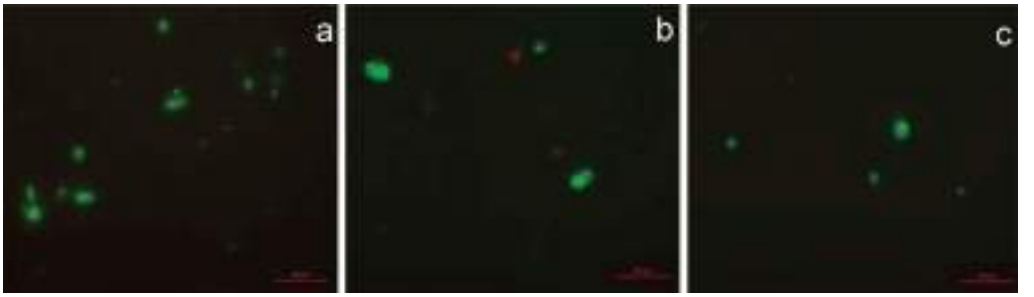

Figure 3. The hemocytes of mollusk *M. modiolus* after 6 hours of exposure. a) control group, b) 100 mg/L, c) 1000 mg/L.

Negatively charged cell membranes bind to the positively charged $DiOC_6$ dye (Sabnis et al., 1997). When cell membrane functions are impaired, their charge decreases and, accordingly, the bound $DiOC_6$ dye is released into the medium (Grégori et al., 2003). As a result of the mollusk *M. modiolus* exposure to the coal suspension, no significant effects were observed at coal suspension concentrations up to 100 mg/L. (Figure 2c). At the coal suspension concentration of 1000 mg/L, membrane depolarization of about 20% of alive cells of hemocytes was observed. A change in the fluorescence level of cell membranes is shown in Figure 3.

It should be noted that the change in polarization of cell membranes during the exposure for 2, 4, and 6 hours has a common trend, which indicates the absence of an increase in the negative effect over time in the measurement range.

4 CONCLUSIONS

We did not detect acute toxicological hazard of coal dust particles to the representatives of marine biota even at extremely high concentrations. There is a decrease in the enzyme activity and partial depolarization of membranes (an average of 20%) exposed to coal particles. The observed changes in the state of hemocytes of mollusk *M. modiolus* suggest that there is a chronic exposure. Further long-term toxicological studies are needed to identify the effects of coal dust on marine aquatic organisms.

This study will be continued using the environmental monitoring system which is planned to be set up at various locations in Nakhodka city.

ACKNOWLEDGEMENTS

The study was funded by RFBR, project number 19-05-50010, and by the grant from the President of the Russian Federation for young candidates of sciences (PhD) MK-2461.2019.5.

REFERENCES

Berry, K., Hoogenboom, M., Flores, F., Negri, A.P. 2016. Simulated coal spill causes mortality and growth inhibition in tropical marine organisms. *Scientific Reports* 6: 25894. doi:10.1038/srep25894.

Berry, K. L., Hoogenboom, M. O., Brinkman, D. L., Burns, K. A., Negri, A. P. 2017. Effects of coal contamination on early life history processes of a reef-building coral, Acropora tenuis. *Marine pollution bulletin* 114(1): 505–514. doi:10.1016/j.marpolbul.2016.10.011.

Christian, P., Von der Kammer, F., Baalousha, M., Hofmann, Th. 2008. Nanoparticles: structure, properties, preparation and behaviour in environmental media. *Ecotoxicology* 17: 326–343. https://doi.org/10.1007/s10646-008-0213-1.

Fontvieille, D.A., Outaguerouine, A., Thevenot, D.R., 1992. Fluorescein diacetate hydrolysis as a measure of microbial activity in aquatic systems- Application to activated sludges. *Environmental Technoogy* 13(6): 531–540. doi: 10.1080/09593339209385181.

Gibson, R., Atkinson, R., Gordon, J. (ed.). 2005. Oceanography and Marine Biology. Boca Raton: CRC Press. doi:10.1201/9781420037449.

Golokhvast, K.S., Kupriyanov, A.N., Manakov, Yu.A., Agoshkov, A.I., 2017. Environmental characteristic of air suspensions at coal production objects: From extraction to combustion. *Gornyi Zhurnal* 4: 87–90. doi:10.17580/gzh.2017.04.18 (In Russian).

Grégori, G., Denis, M., Lefèvre, D., Beker, B., 2003. A flow cytometric approach to assess phytoplankton respiration. *Advanced Flow Cytometry: Applications in Biological Research*. Springer Netherlands, Dordrecht: 99–106. doi:10.1007/978-94-017-0623-0_15

Honarvar, A.R., Sami, A. 2019. Towards sustainable smart city by particulate matter prediction using urban big data, excluding expensive air pollution infrastructures. *Big data research* 17: 56–65. doi:10.1016/j.bdr.2018.05.006.

Johnson, R., Bustin, R.M. 2006. Coal dust dispersal around a marine coal terminal (1977–1999), British Columbia: The fate of coal dust in the marine environment. *International Journal of Coal Geology* 68 (1-2): 57–69. doi:10.1016/j.coal.2005.10.003.

Kholodov, A.S., Golokhvast, K.S. 2016. Complex research of the particles which cause air pollution by laser granulometry, Raman-spectrometry and IR-spectrometry. *Proc. SPIE* 10176: 101760N-1-101760N-6, doi:10.1117/12.2268229.

Kirichenko, K.Yu., Kholodov, A.S., Vakhniuk, I.A., Gusev, D.S., Kiryanov, A.V., Drozd, V.A., Golokhvast, K.S., 2019. Research of air pollution with fine coal dust (Nakhodka, Primorsky krai). *Bulletin of Kamchatka State Technical University* 50: 6–13. doi:10.17217/2079-0333-2019-50-6-13 (In Rusian).

Kumar, P., Fennell, P., Robins, A. 2010. Comparison of the behaviour of manufactured and other airborne nanoparticles and the consequences for prioritising research and regulation activities. *Journal of Nanoparticle Research* 12: 1523–1530. doi:10.1007/s11051-010-9893-6.

Kurilenko, V.V. 2019. Fundamentals of environmental geochemistry. V.V. Kurilenko (ed.), *Ecological Problems Geology: Proceedings of XIX International Youth Scientific Conference-school*; *Saint-Petersburg*, *2-7 June 2019*. Saint-Petersburg: Saint-Petersburg State University (In Russian).

Lebedev, A.A., Tikhonova, O.A., Blinovskaya, Ya.Yu., Chaika, V.V., Kirianov, A.V., Khristophorova, N.K., Pikula, K.S., Shevchenko, V.P., Golokhvast, K.S. 2017. Coal terminal impact on marine suspention composition: Nakhodka Gulf (Japan Sea). *Proceedings of the Russian State Hydrometeorological University* 48: 195–201 (In Russian).

Lelieveld, J., Evans, J. S., Fnais, M., Giannadaki, D., Pozzer, A. 2015. The contribution of outdoor air pollution sources to premature mortality on a global scale. *Nature* 525: 367–371. doi:10.1038/nature15371.

Naumov, Yu.A., Naidenko, T.Kh. 1997. The ecological state of Nakhodka Bay. *Izvestiâ Tihookeanskogo naučno-issledovatel'skogo rybohozâjstvennogo centra* 122: 524–537 (In Russian).

Naumov, Yu.A. 2016. Sea ports and their water areas state of the environment (through the example of Nakhodka Bay port complex on the Sea of Japan). *International journal of applied and fundamental research* 10(4): 623–626. (In Russian).

Ostrander, G.K. (ed.) 2005. Techniques in aquatic toxicology. Boca Raton: CRC Press.

Pikula, K.S., Chernyshev, V.V., Zakharenko, A.M., Chaika, V.V., Waissi, G., Hai, L.H., Hien, T.T., Tsatsakis, A.M., Golokhvast, K.S. 2019. Toxicity assessment of particulate matter emitted from different types of vehicles on marine microalgae. *Environmental research* 179: 108785. doi:10.1016/j.envres.2019.108785.

Pikula, K.S., Zakharenko, A.M., Chaika, V.V., Kirichenko, K.Y., Tsatsakis, A.M., Golokhvast, K.S. 2020a. Risk assessment in nanotoxicology: Bioinformatics and computational approaches. *Current Opinion in Toxicology* 19: 1–6. doi:10.1016/j.cotox.2019.08.006.

Pikula, K., Chaika, V., Zakharenko, A., Markina, Z., Vedyagin, A., Kuznetsov, V., Gusev, A, Park, S, Golokhvast, K. 2020b. Comparison of the level and mechanisms of toxicity of carbon nanotubes, carbon nanofibers, and silicon nanotubes in bioassay with four marine microalgae. *Nanomaterials* 10 (3): 485. doi:10.3390/nano10030485.

Sabnis, R.W., Deligeorgiev, T.G., Jachak, M.N., Dalvi, T.S., 1997. DiOC(6)(3): a useful dye for staining the endoplasmic reticulum. Biotech. Histochem. 72(5),253–258. doi:10.3109/10520299709082249.

Tang, Z., Chai, M., Cheng, J., Jin, J., Yang, Y., Nie, Z., Huang, Q., Li, Y. 2017. Contamination and health risks of heavy metals in street dust from a coal-mining city in eastern China. *Ecotoxicology and Environmental Safety* 138: 83–91. doi:10.1016/j.ecoenv.2016.11.003.

Zhang, Q., Jiang, X., Tong, D.,Davis, S.J., Zhao, H., Geng, G., Feng, T., Zheng, B., Lu, Z., Streets, D. J., Ni, R., Brauer, M., Donkelaar, A., Martin, R.V., Huo, H., Liu, Z., Pan, D., Kan, H., Yan, Y., Lin, J., He, K., Guan, D. 2017. Transboundary health impacts of transported global air pollution and international trade. *Nature* 543: 705–709. doi:10.1038/nature21712.

Advances in Raw Material Industries for Sustainable Development Goals – Litvinenko (Ed)

Air sample system optimization for the raw materials industry objects monitoring

M.V. Volkodaeva
Professor, Saint-Petersburg Mining University, Saint-Petersburg, Russia

Ya.A. Volodina
Postgraduate student, Saint-Petersburg Mining University, Saint-Petersburg, Russia

V.A. Kuznetsov
Postgraduate student, Saint-Petersburg Mining University, Saint-Petersburg, Russia

ABSTRACT: The raw material industry has a negative impact on the environment. In particular, it is an air pollution source. In order to improve the air sampling procedure, it is suggested to use lavsan sample bags. A distinctive feature of these devices is the ease of their use, regeneration and transportation, the possibility of their multiple application and averaging air samples for any period of time. Due to structural features and technical characteristics of bags, the procedure of their delivery to laboratories from remote observing sites is simplified, as well as air samples analysis. To establish the feasibility of using proposed sample bags and to assess the impact of the phosphorite mining enterprise the research was conducted, results of which allow us to conclude that it is advisable to use these devices for sample collection and transportation.

1 INTRODUCTION

Mineral resources are a complex of raw material stocks in the bowels that can ensure the stable development of the country's economy for a significant future (Boyko et al. 2019, Kozlov et al. 2018). Exploitation of natural resources by a mineral resource sector is associated with the extraction, removal of overburden, ore, coal, oil, gas, groundwater, etc. from geosystems. Attendant problems of the use of natural resources are man-made impacts on environmental compartments that cause their changes (Mammadov et al. 2019, Nevskaya et al. 2019). In this regard, the mineral resource complex has a negative impact on the environment (Krutskikh 2019, Pashkevich et al. 2019), in particular, as a source of emission of a wide range of pollutants into the atmospheric air. The main pollutants in the air basin are particulate pollutants, sulfur dioxide, carbon monoxide, nitrogen oxides and volatile organic compounds (State report 2018).

In the total volume of pollutant emissions into the atmosphere from stationary sources, which amounted to 17,476.2 thousand tons in 2017, the largest contribution was made by sources (by type of economic activity): "Manufacturing" - 5 802.2 thousand tons, or 33.2% of all emissions from stationary sources; "Mining" - 4,918.9 thousand tons, or 28.1%; "Provision of electric energy, gas and steam; air conditioning"- 3,542.6 thousand tons, or 20.3% (State report 2018).

Therefore, in order to carry out effective environmental protection activities, it is necessary to be provided with sufficient information about the state of the environment, take into account spatial and temporal factors, the degree of anthropogenic impact, anticipate the possible consequences of human intervention in the course of natural processes. The tool for obtaining such information is environmental monitoring (State report 2018).

2 ENVIRONMENTAL MONITORING SAMPLING

Monitoring conducted by enterprises to assess the impact of their activities on the natural environment (and, first of all, on the most sensitive component of ecosystems - atmospheric air) can be both instrumental and calculated. Calculated monitoring allows you to determine the level of pollution based on the data on emissions of pollutants. Thanks to this approach, it is possible to estimate the level of pollution not only at its source, but also at any distance from the industrial facility. Instrumental monitoring involves sampling on the ground (usually in the area of greatest pollution) and subsequent laboratory analysis, allowing you to obtain data on the level of air pollution in the zone of a particular enterprise influence. However, it should be noted that the largest measurement errors occur at the stage of sampling of atmospheric air (Watson et al. 2011). Also carrying out full-fledged instrumental monitoring is associated with a number of difficulties, for example, the inability to quickly obtain data from remote areas, the operation of obsolete equipment, as well as sampling methods and devices (Yakunina & Popov 2009).

Basically, sampling methods are divided into 2 groups: aspiration (air suction through absorption solutions, filters, sorption tubes or grain sorbents placed in the absorber) and sampling in vessels (bottles, gas pipettes and other containers) that are delivered for the further analysis to the laboratory (Woolfenden 2010).

Air sampling is most often carried out by the aspiration method in order to determine the concentration of chemical compounds. The method is based on aspiration of a known volume of air through an absorption material capable of retaining substances to be determined. This method is used when it is necessary to concentrate the microimpurities in the absorber and to increase the sensitivity of the analysis method.

As an absorption solution, distilled water or special liquids that dissolve toxic substances or interact with them are used. Absorbers with solid sorbents are also used: silica gel, activated carbon, and others. They have a different design: in them, solid sorbents can be stationary or set in motion by an air current, forming a "fluidized bed", which contributes to a greater contact of the sorbents with air and improves the absorption of the substance of interest. Sorption tubes are also used to take and analyze air samples. They are filled with glass powder, impregnated with special solutions for trapping toxic substances. This type of sampling suction systems is most common for environmental monitoring tasks.

For quick sampling with the availability of sensitive research methods, sampling into various vessels and containers is used. The type of gas sampling vessel is determined by the nature of the gas being analyzed and the volume of the sample. It is noteworthy that the volume of the gas sample should be sufficient for analysis by the selected method and for repeated determinations.

Sample storage conditions are an important factor in the analysis of environmental component. For example, air samples taken on active solid sorbents can be stored for a limited time, in some cases cooling is necessary. Air samples taken in vessels are not recommended to be stored for a long time, since reactions with oxygen, water vapor, adsorption of the vessel walls and so on are possible. One of the main problems in determining the concentrations of volatile substances is associated with this.

Typically, gas samples are taken into the device in which the analysis is performed. If the analysis cannot be performed at the sampling site, air samples are delivered to the laboratory. Gas diffusion through some connecting tubes may cause a change in the composition of the gas sample. The composition of the average sample may vary in the sampling device itself. Another important factor is the temperature - a significant temperature difference at the time of selection and during storage can significantly affect the final result of the analysis. Therefore, when optimizing sampling methods, various aspects should be considered that affect the concentration of pollutants in the sample.

Currently, various devices are used in the Russian Federation for air sampling: direct sorption and indicator tubes, various types of absorption vessels (for example, Zaitsev, Richter vessels with a porous plate), cooled traps, syringes, gas pipettes and others. Most of these devices have several disadvantages. For example, when using sorption tubes, the concentration of substances in the sample decreases as a result of adsorption by the tube material, and during subsequent analysis of the sample, false peaks may appear on the gas chromatogram (as a result of desorption of

previously adsorbed substances). The use of syringes and gas pipettes does not comply with the regulatory and technical documentation for sampling (due to the time of sampling), as well as these devices do not allow storing air samples. Moreover, many sampling devices require considerable time for their regeneration, as well as the preliminary preparation of special sorbents and absorption solutions. These shortcomings indicate the need for modernization of the monitoring network, in particular, the introduction of new methods and devices for air sampling for the subsequent determination of the pollutant content in the air.

It should be noted that in recent years, sample bags have increasingly been used for sampling around the world (Watson et al. 2011). They are devices for sampling air, which are used both for basic gases and for specific substances. These bags can be made of various materials (teflon, lavsan, fluoroplastic, polyvinylidene fluoride, fluoroethylene propylene, aluminum film, etc.). The leaders in the production of sampling bags are considered to be Restek (USA), SKC (USA), Cole-Parmer (USA), Merck (Germany), GL Sciences (The Netherlands).

In support of the feasibility and advisability of using these sampling devices, many studies have been carried out around the world. For instance, some scientists consider the problem of storage stability (Akdeniz et al. 2011, Laor et al. 2010); in other works the question regarding the sample loss is raised (Sironi et al. 2014, Kim & Kim 2012); there are also some works on the different types of bags (Kim et al. 2012, Laor et al. 2010) and materials (Salo & Makinen 2019) comparison. Of particular interest is the study of comparing commercial and homemade bags (Parker et al. 2010, Abruzzi et al. 2019). All in all, the results allowed concluding that air sample bags can be an alternative to the widely used sampling devices and are suitable for many areas, including industrial hygiene, landfill (biogas), ambient air, indoor air and stationary source testing. The disadvantage of these devices is their high cost, often the inability to reuse, as well as the inability to store some volatile organic compounds.

For the needs of industrial environmental control and atmospheric air monitoring in the Russian Federation, which includes the regular determination of the pollutant concentrations over immense territories and in remote areas, as well as for studying the content of specific compounds in samples, there is no universal sampling device. This is due to the need to fulfill a number of conditions: ease of sampling, ease of the device regeneration, a low background level of substances in the device, economic affordability, the possibility of long-term storage of samples and comparisons with established environmental standards.

In order to improve the atmospheric air sampling procedure, the authors propose the use of lavsan sample bags, which allow subsequent determining of the concentrations of pollutants that are characteristic of mineral resource complex enterprises. Due to the design features and technical characteristics of the bags, the procedure of their delivery to laboratories from remote observation points and analysis of air samples is simplified, and the cost of devices is reduced.

To establish the feasibility and advisability of using the proposed sample bags with the participation of the authors numerous studies were carried out: the concentrations of pollutants at control points without sampling were determined and also in laboratory conditions with preliminary sampling of atmospheric air into the lavsan bags (Volkodaeva & Volodina 2017); the optimal methods for the sample bags regeneration were identified (Volkodaeva et al. 2019b); the possibility of using these devices at the border of the sanitary protection zone was demonstrated (Volkodaeva et al. 2019a).

3 SAMPLE BAGS APPLICATION

Sample bags made of polymer films are intended to be used for the collection and storage of gaseous samples for subsequent analysis on laboratory equipment (chromatographs, stationary gas analyzers, etc.). The bags can be used to control the pollution of the atmosphere, air of the working area, industrial emissions, as well as to control production processes in the chemical, petrochemical, pharmaceutical, food industries, medicine, agriculture, etc.

Sampling in bags is carried out by means of portable sampling pumps or vacuum samplers. The capacity of the packages can vary from 0.5 to 100 liters. The bags are equipped with

various fittings: stainless steel, polypropylene, teflon, designed both for sampling from the bag with a syringe, and using an external pump. The number of fittings may also vary.

Compared to other sampling devices (gas pipettes, gas syringes, etc.), bags of polymer films have several advantages:

- flexibility: a variety of organic and inorganic compounds can be sampled and stored in bags;
- high stability of sample storage;
- the ability to automatically average samples over a 20-minute (or other) time interval;
- the ability to automatically adapt the sample to the conditions of analysis (temperature and pressure);
- the variety of fitting types and their quantity;
- lightness, strength and durability.

A study of a great variety of sample bags produced by world leaders, as well as Russian manufacturers, showed that there is no appropriate device for the collection, storage and transportation of samples of volatile organic compounds (control of such compounds is mandatory in large cities and near enterprises-sources of these substances) for the purpose of environmental monitoring of atmospheric air. Some samples are disposable and cannot be regenerated, others are not able to hold the specific contaminants necessary for determination, and others are equipped with fittings that are inconvenient to use. Thus, the absence of a suitable sampling device leads to the search for technical solutions to optimize the procedure of sample collection, storage, transportation, as well as the procedure of bags regeneration.

Currently, the monitoring of the content of volatile organic compounds in the air is carried out over vast territories. It implies sampling on site and delivering air samples to specialized laboratories. Due to the remoteness of some observation points, as well as the load of analytical equipment in laboratories, the solution is to increase the storage time of samples in bags.

The authors propose to make some changes to the design of the sample bag, namely, to improve the seams and fittings of the device. The use of reinforced double seams has a positive effect on the duration of storage of samples and less diffusion of pollutants through the seams of the bag - the most fragile part of the sampling device. There is also a need for better cleaning of devices, which can be achieved by identifying the optimal regeneration method, as well as placing an additional fitting on the opposite side of the bag.

4 SAMPLE BAG DESIGN OPTIMIZATION

The authors propose to make changes to the design of the sample bags, as well as to use the identified effective ways of regenerating these devices.

The manufacture of sample bags from an ultra-pure lavsan film with a thickness of 50 μm can be considered the optimal solution, because with the small weight of the bag the barrier functions necessary for storing the samples are performed. The material prevents the diffusion of gases through the walls of the bag, which is similar to preserving the air sample inside the device. The usage of double seams increases the storage time of volatile organic compounds in atmospheric air samples. Seams are made by the agency of a welding machine.

Moreover, it is also possible to place a fluoroplastic tube with a diameter of 1-2 mm in the space between two seams (Figure 1). This tube, located around the entire perimeter of the bag, will make it possible to make a kind of frame and at the same time reduce the likelihood of deformation of the device and, as a result, loss of atmospheric air sample.

The use of two polypropylene fittings increases the "flexibility" of the sampling. In other words, it allows taking samples in different conditions, varying the way the bag is attached to the sample feeder and the sampling speed, and also improves the quality of the bag regeneration by the through-bag purging.

Another feature of lavsan sample bags is the possibility of their multiple use. For the purpose of this, devices should be regenerated properly. The authors propose the use of ozone and nitrogen as gases for cleaning bags. The choice of a regeneration method is based on the physicochemical characteristics of substances acting as purifiers (Volkodaeva et al. 2019b).

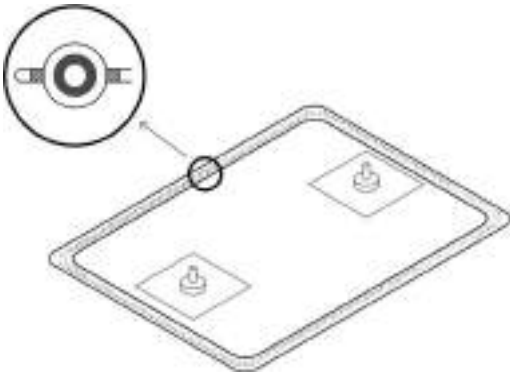

Figure 1. Sample bag with a fluoroplastic tube.

From an environmental point of view, lavsan material can be recycled and disposed of. There are two main ways of processing polyethylene terephthalate: mechanical and physico-chemical; biological methods are actively developing (Yoshida et al. 2016). Moreover, polypropylene processing is practiced. It includes the stages of sorting, crushing and temperature exposure, granulation.

Thus, the proposed characteristics of the sample bags make it possible to obtain reliable data from remote areas (relevant for objects of the mineral resource complex), as well as to conduct numerous sampling while monitoring air quality at the border of the sanitary protection zone. It should be noted that there are various ways to recycle and dispose of the material from which the bags are made.

5 FIELD STUDY

To assess the impact of the phosphorite mining enterprise, measurements were made on site and 20-minute air samples with an hourly interval during the active phase of the production process were taken. As a part of the study, the concentrations of the following pollutants were determined: benzene, toluene, ethylbenzene, isomers of xylene, styrene, acetone.

In order to obtain more complete and representative environmental information about the state of the air basin, as well as to conduct a comparative experiment, the authors decided to use several different devices for sampling (in addition to direct measurements on site). Such devices were sorption tubes (filled with Carbopack™ B), Tedlar® sample bags (manufactured by SKC) and homemade lavsan sample bags. The measurements on site were carried out by the agency of portable gas chromatograph FGH (manufactured by Research and Production Company Ekan).

Samples were taken in an open field, without obstacles to capture pollutants from the leeward side of the source of pollution at the border of the sanitary protection zone.

After sampling, all samples were delivered to the laboratory within three hours for further analysis (by means of a gas chromatograph FGH).

The averaged results of determining the pollutant concentrations in different ways are presented in Table 1 and Figure 2.

The results of direct measurements made on site should be considered as reference, since such measurements do not have factors affecting the sample such as its storage and transportation. Moreover, background concentrations of sampling devices can also distort the final result.

According to the research, all the devices used provide fairly good stability of the samples during their transportation and preservation of volatile organic compounds. However, there is a decrease in the concentration of pollutants in the samples due to

Table 1. Averaged results of determining the pollutant concentrations in samples of atmospheric air.

Pollutant	Direct measurements (on site)	Preliminary sampling in sorption tubes	Preliminary sampling in Tedlar® bags	Preliminary sampling in lavsan bags
benzene (mg/m3)	0.023	0.011	0.015	0.018
toluene (mg/m3)	0.091	0.124	0.065	0.071
ethylbenzene (mg/m3)	0.018	0.009	0.012	0.015
m-xylene (mg/m3)	0.184	0.104	0.122	0.151
p-xylene (mg/m3)	0.159	0.113	0.135	0.142
o-xylene (mg/m3)	0.078	0.043	0.061	0.068
styrene (mg/m3)	0.002	<0.001	0.001	0.002
acetone (mg/m3)	0.016	0.007	0.004	0.011

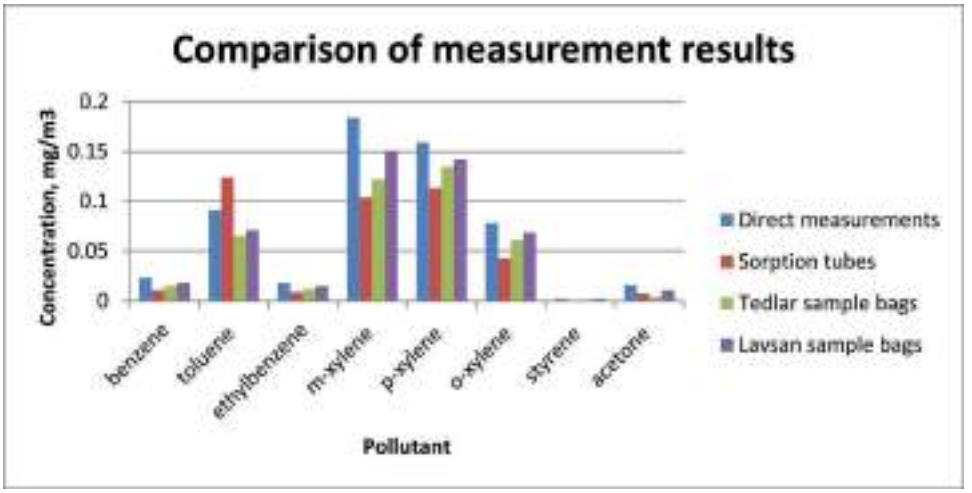

Figure 2. Comparison of results of a quantitative measurement of pollutants.

volatilization, adsorption (in the case of tubes) or deposition (on the inner walls of the bags). An exception is the result of the determination of toluene, collected using sorption tubes, which may be caused by the desorption of previously adsorbed substances. The correlation coefficient between the results of direct measurements and measurements using sorption tubes amounted to 0.86, Tedlar® bags - 0.98, lavsan bags - 0.99. The discrepancies between the values obtained during measurements on site and during the analysis of samples taken in bags under laboratory conditions vary within a few tens of percent, which is acceptable when conducting such studies.

All in all, the results obtained during the research allow us to conclude that it is possible and advisable to use devices for sampling and transportation of samples, in particular, lavsan sample bags, in order to control the quality of atmospheric air. Despite a slight decrease in pollutant concentrations in lavsan bags, the use of these devices for the purposes of environmental monitoring is a good alternative to outdated methods.

It should also be noted that the results of this study, similar to the results reflected in the Abruzzi's research (Abruzzi et al. 2019), show that homemade containers are a good alternative to commercial ones for storing air samples and further analysis by chromatographic method. The Abruzzi's work also says about the possibility of stable storage of samples in homemade borosilicate glass containers for up to 96 hours, while in our lavsan bags the time of stable storage is about 72 hours. However, lavsan bags are also suitable for volatile organic compounds sampling and it is easier to transport and store them due to their light weight and shape.

Moreover, Kim's research (Kim et al. 2012) on the storage of volatile organic compounds in polyester aluminum (PEA) and polyvinyl fluoride (PVF) sample bags showed more stable storage of substances in PEA containers than in PVF ones. Homemade lavsan sample bags showed similar results in our research.

6 CONCLUSION

The raw material industry has a significant negative impact on the environment and atmospheric air, in particular. In this regard, it is mandatory to conduct continuous air quality monitoring both at the facilities themselves and at the border of the sanitary protection zone, which implies sampling. Since widely used methods and devices have certain drawbacks, the authors propose the use of lavsan sample bags. When using these bags, it becomes possible to average the air samples over different time intervals, to deliver the samples from distant observation points to the laboratory for subsequent analysis. Bags can be used multiply, which is also a cost-effective solution for monitoring systems of different levels. In support of the feasibility and advisability of using these sampling devices, many studies have been carried out around the world.

In a similar vein authors conducted an experiment in order to compare different sampling devices – sorption tubes, manufactured and homemade sample bags. According to the research, all the devices used provide fairly good stability of the samples during their transportation and volatile organic compounds preservation. The discrepancies between the values obtained during measurements on site and during the analysis of samples taken in bags vary within a few tens of percent, which is acceptable when conducting such studies. Homemade lavsan sample bags also showed good results and, consequently, could be used for environmental monitoring purposes despite a slight decrease in pollutant concentrations in them.

Thus, the optimization of the sampling system through the introduction of specialized bags will improve the quality and speed of obtaining reliable information necessary for decision-making on environmental protection, as well as assessing effectiveness of nature protection measures.

REFERENCES

Abruzzi, R.C., Bonetti, B., Marçal, J.R.P., Berenice, A.D. & Bitencourt, A.K. 2019. Artifacts in the analysis and assessment of low-cost containers for sampling and storing greenhouse gases. *Quimica Nova* 42(1): 84–94.

Akdeniz, N., Janni, K.A., Jacobson, L.D. & Hetchler, B.P. 2011. Comparison of gas sampling bags to temporarily store hydrogen sulfide, ammonia, and greenhouse gases. *Transactions of the ASABE* 54: 653–661.

Boyko, N.A., Chvileva, T.A. & Romasheva, N.V. 2019. The impact of coal companies on the socio-economic development of coal mining regions and its assessment. *Ugol* 11(1124): 48–53.

Kim, Y.-H. & Kim, K.-H. 2012. Experimental approach to assess sorptive loss properties of volatile organic compounds in the sampling bag system. *Journal of Separation Science* 35(21): 2914–2921.

Kim, Y.-H., Kim, K.-H., Jo, S.-H., Jeon, E.-C., Sohn, J. R. & Parker, D. B. 2012. Comparison of storage stability of odorous VOCs in polyester aluminum and polyvinyl fluoride Tedlar® bags. *Analytica Chimica Acta* 712: 162–167.

Kozlov, A.V., Teslya, A.B. & Chernogorsky, S.A. 2018. Game Theory Model of State Investment into Territories of Advanced Development in the Regions of Mineral Resources Specialization. *Journal of Mining Institute* 234: 673–682.

Krutskikh, N.V. 2019. Assessment of nature transformation in the mining influence zone by earth remote sensing data. *Gornyi Zhurnal* 3: 88–93.

Laor, Y., Ozer, Y., Ravid, U., Hanan, A. & Orenstein, P. 2010. Methodological aspects of sample collection for dynamic olfactometry. *Chemical Engineering Transactions* 23: 55–60.

Mammadov, V.A., Salamov, A.M. & Khalilova, H.Kh. 2019. Study of the anthropogenic impact on the change of geoecological conditions of the Khojahasan lake, Azerbaijan. *Journal of Mining Institute* 239: 603–610.

Nevskaya, M.A., Seleznev, S.G., Masloboev, V.A., Klyuchnikova, E.M. & Makarov, D.V. 2019. Environmental and business challenges presented by mining processing waste in the Russian Federation. *Minerals* 9(7): 445.

Parker, D.B., Perschbacher-Buser, Z.L., Cole, N.A. & Koziel, J.A. 2010. Recovery of agricultural odors and odorous compounds from polyvinyl fluoride film bags. *Sensors* 10(9): 8536–8552.

Pashkevich, M.A., Matveeva, V.A. & Danilov, A.S. 2019. Migration of pollutants from the mining waste disposal territories on the Kola Peninsula. *Gornyi Zhurnal* 1: 17–21.

Salo, H. & Makinen, J. 2019. Comparison of traditional moss bags and synthetic fabric bags in magnetic monitoring of urban air pollution. *Ecological indicators* 104: 559–566.

Sironi, S., Eusebio, L., Capelli, L., Boiardi, E., Del Rosso, R. & Guillot, J.M. 2014. Ammonia diffusion phenomena through Nalophan bags used for olfactometric analyses. *Journal of Environmental Protection* 5: 949–961.

State report. 2018. *On the State and Environmental Protection of the Russian Federation in 2017*. Moscow: Ministry of Natural Resources and Environment of the Russian Federation, Research and Production Enterprise Kadastr.

Volkodaeva, M.V. & Volodina, Y.A. 2017. Comparing the results of measurements of concentrations of volatile organic compounds using different sampling methods. *Ecological systems and devices* 7: 3–6.

Volkodaeva, M.V., Volodina, Y.A. & Kuznetsov, V.A. 2019a. Development of industrial environmental control methods. *IOP Conf. Series: Earth and Environmental Science* 378(2019) 012108.

Volkodaeva, M.V., Volodina, Y.A. & Kuznetsov, V.A. 2019b. On the selection of the lavsan sample bags regeneration for their repeated use. *Danish Scientific Journal* 21(1): 65–68.

Watson, N., Davies, S., Wevill, D. 2011. Air Monitoring: New Advances in Sampling and Detection. *Scientific World Journal* 11: 2582–2598.

Woolfenden, E. 2010. Sorbent-based sampling methods for volatile and semi-volatile organic compounds in air - part 1: sorbent-based air monitoring options. *Journal of Chromatography A*. 1217(16): 2674–2684.

Yakunina, I.V. & Popov, N.S. 2009. *Methods and instruments for environmental control. Environmental Monitoring: A Training Manual*. Tambov: Publishing house of Tambov State technical university.

Yoshida, S., Higara, K., Takehana, T., Taniguchi, I., Yamaji, H., Maeda, Y., Toyohara, K., Miyamoto, K., Kimura, Y. & Oda, K. 2016. A bacterium that degrades and assimilates poly(ethylene terephthalate). *Science* 351: 1196–1199.

Advances in Raw Material Industries for Sustainable Development Goals – Litvinenko (Ed)

Method of MSW landfill reclamation using waste conversion products

N.O. Milyutina
Postgraduate student, Saint Petersburg State University, Saint Petersburg, Russia

N.A. Averianova
PhD, Chief process engineer, JSC Avtopark №1 «Spectrans», Saint Petersburg, Russia

E.S. Velikoselsksya
Ecologist, LLC Novyj Svet.EKO, Saint Petersburg, Russia

D.M. Malyuhin
Deputy general Director, LLC Novyj Svet-EKO, Saint Petersburg, Russia

N.A. Politaeva
DSc, Professor, Peter the Great Saint Petersburg Polytechnic University, Saint Petersburg, Russia

ABSTRACT: Mostly, municipal solid waste in Russia is disposed of in landfills. It is known that the main problems in landfill reclamation are the leachate purification and the application of a fertile layer. The most commonly used technology of leachate purification nowadays is reverse osmosis, but the result of this method are two substances: clean water and new waste – concentrate. The creation of a fertile layer is related to the destruction of natural land. A new method of leachate utilization without the generation of new waste is presented in this paper. Also, it is proposed to use the biological potential of the organic waste fraction to create a fertile layer. As a result, a resource-saving scheme for landfill reclamation using waste potential has been developed.

1 INTRODUCTION

About 35 to 40 million tons of municipal solid waste (MSW) are annually generated in Russia. Only 4-5% of them are sent for recycling while the remaining waste is disposed of in landfills and dumps. However, this type of waste management is the least preferred according to the hierarchy of accepted methods (Wilson, 1999, Umanets, 2014, Yousefloo, 2020).

Under the influence of biological, physical and chemical factors, the processes of substance transformation occur in the body of MSW landfill. The formed leachate and biogas determine the polluting effect of MSW landfills on the environment (Gourc, 2010, Popovych, 2020, Wilson, 1999). MSW landfills remain sources of pollutants despite the observance of protective measures on the spot. Problems associated with the emission of MSW transformation products remain even after the closure of landfills. Therefore, it is necessary to conduct landfill reclamation.

Reclamation is a combination of engineering, technical and sanitary-hygienic measures that allow to restore the ecological balance of the environment near landfills. Reclamation is divided into technical and biological stages. The technical stage includes the selection of technologies for collecting, purifying and utilizing biogas and leachate as well as slopes formation and application of recultivation layers, the final of which is a fertile soil layer. The biological stage is a set of agrotechnical and phytomeliorative measures to restore the territory of closed

landfills. The main economic and environmental problems in landfill reclamation are related to purification and disposal of the leachate, as well as the creation of a fertile layer (Lassini, 1999, Weng, 2015).

2 LITERATURE REVIEW

Most of the MSW landfills currently operating in Russia are not equipped with a local leachate treatment station. The most common way to reduce leachate during landfill operation is its recirculation. However, this does not solve the problem completely and becomes impossible to use after landfill reclamation (He, 2005). Therefore, an important issue in the technical stage of reclamation is the selection and installation of a treatment plant.

The main methods for purifying the leachate can be divided into biological (aerobic and anaerobic), mechanical (sedimentation, filtration, separation) and physicochemical (coagulation, flocculation, flotation, ion exchange, sorption, micro and ultrafiltration, reverse osmosis, ozonation, electrolysis, ultraviolet radiation) (Henze, 1995, Renou, 2008, Salem, 2008, Silva, 2004, Trebouet, 2001). To achieve a high degree of purification, a combination of these methods is necessary. The most commonly used technology nowadays is reverse osmosis with preliminary mechanical and/or physicochemical treatment of the leachate. The permeate (purified water) obtained as a result of such a purification scheme corresponds to the quality required for its discharge to surface water (Renou, 2008). On the other hand, the use of reverse osmosis leads to the formation of a concentrate representing 25-50% of the raw leachate, which is itself a new form of waste that must be disposed of.

The second problem of the technical stage of reclamation is applying the fertile layer which is necessary for the realization of the biological stage. The creation of this reclamation layer is an environmental and economic problem due to the shortage of soil. It is estimated that up to 10 000 m^3 of fertile soil is required for the reclamation of 1 hectare of landfill, which corresponds to the destruction of 5 hectares of natural land. It should be kept in mind that when using mineral loam soils as a recultivation layer, the processes of humus formation occur very slowly. In fact, in 15 years, only 1.5-2 cm of a continuous humus horizon is formed. In order to save natural resources and accelerate biological processes during reclamation work, the soil can be replaced with organogenic substrates from MSW (Ilinykh, 2015, Awasthi, 2020). The high biological potential of these substrates that are due to their rich plant nutrients and humified organic matter content is universally recognized (Bolan, 2013, Gauhey, 1953).

Waste composting can be carried out in biodrums or in storage pits by the field method. Before composting, it is necessary to sort waste. The activation of biological processes based on the microflora contained in the compostable mass is ensured by aeration using a compost turner (Werf, 2000). The rotating shaft of the turner mixes the mass of the storage pits in such a way that it keeps its trapezoidal shape.

The processes that occur during composting of waste can be divided into 3 phases. The first is characterized by the rapid reproduction of mesophilic microorganisms at an optimal temperature of 20-35 ℃. Easily biodegradable organic compounds, mainly found in food waste (carbohydrates, organic acids, proteins), serve as an energy source for bacteria. As a result of their vital activity, thermal energy is released, which contributes to the heating of the composted material to a temperature of 50 ℃. In the second phase, this increase in temperature creates favorable conditions for the development of thermophilic microorganisms, which, as a result of their vital activity, increases even more the heat generation and accelerate the decomposition of organic substances. The temperature of the composted material rises to 55-60 ℃. The third phase is a slow drop in temperature, indicating the exhaustion of easily decomposable organic compounds. At this stage, a part of the thermophilic microflora dies and the other part goes into a state of spore formation. The mesophilic microflora begins to multiply again due to its more diverse and powerful enzymatic system, with the help of which more stable organic compounds (fiber, lignin) are decomposed. Antibiotic substances with bactericidal properties produced by the biothermal process inhibit the development or cause the death of pathogenic microflora (zhu, 2019, Jain, 2020, Ilinykh, 2015, Liwarska-Bizukoje, 2001).

3 METHODS AND MATERIALS OF INVESTIGATION

The objects of this study consisted of the leachate from one of the MSW landfills of the Leningrad Region, the stabilized leachate and the technogenic soil. The leachate stabilized by solidification was obtained at different periods of time (six samples). The technogenic soil (ten samples) was produced by field composting of sorted municipal solid waste.

In the course of this research, the heavy metals content and agrochemical indicators of the studied objects have been determined. The analysis of the heavy metals content was carried out by Inductively Coupled Plasma Optical Emission Spectroscopy (ICP OES). The toxicity of the stabilized leachate was determined by biotesting. The organic carbon content was determined by the Tyurin method. The active forms of phosphorus were determined by the Denizha colorimetric method after effectuating a Kirsanov extraction. The analysis of the active forms of potassium was carried out using a PAZh-2 flame analyzer from a Kirsanov extract. The active forms of nitrogen were determined by the colorimetric method; nitrate nitrogen with disulfophenolic acid and ammonium with the Nessler reagent.

4 THE RESULTS AND DISCUSSION

4.1 *Leachate utilization*

In the course of this research, a new technology for the leachate utilization based on a change in the aggregation state of a liquid into a solid product has been developed. This new product is obtained by the mechanical mixing of the leachate with special reagents. The process is divided in two main stages: the first stage consists of water coagulation, the result of which is the basis for the activation of the second stage - hardening of the mixture due to the formation of mineral components. Various known compounds widely used for MSW leachate purification (Trebouet, 2001) serve as coagulation activators in the present technology. The selection of a particular coagulant depends on the chemical composition of the raw leachate. The main binder additive is the mineral residue from the burning of oil shale in thermal power plants.

The high porosity of the particles of the binder additive leads to the sorption of neutralization reaction soluble products and other soluble impurities of the leachate. Also, as a consequence of chemical reactions, poorly soluble humates of heavy metals are formed. During the mixing of the components, gases are released and are sent to a gas purification filter based on fibrous composite material. The composition of the resulting gases includes nitrogen dioxide (NO_2), carbon monoxide (CO), hydrogen sulfide (H_2S), nitric oxide (NO) and methane (CH_4). A plastic paste-like mass of material obtained after mixing components is formed, which hardens and gains strength within 21 days.

The chemical composition of the leachate depends on a number of factors. The main ones are the morphological composition of the deposited waste and the landfill stage of life, which corresponds to a certain stage of biochemical and physicochemical transformation of the waste. The leachate is conditionally divided into "young" and "old" according to its chemical composition. The "young" leachate is formed at the first stages of waste decomposition in the acetogenic phase after the 2-7 years of waste storage. The "old" leachate is formed at the methanogenic stages (salem, 2008). Depending on the amount of organic carbon (COD and BOD), basic anions and heavy metals (HM) in the leachate, the ratio of the main components when converting the leachate to a solid product can be varied for obtaining a high-quality product.

The studied leachate was determined as "old" and the appropriate ratio of components and mixing have been selected, after which, a product of solidification was obtained. The content of the active forms of HM in the new product is presented in Table 1.

The total content of HM in this product is presented in Table 2. These concentrations represent the average contents in the six samples.

From the data obtained, it follows that the content of heavy metals in the solid product does not exceed permissible concentrations for settlement soils.

Table 1. Active form of heavy metals content in the solid product.

Heavy metal (active form)	Concentration, mg/kg	LOC*, mg/kg
Ni^{2+}	1.1±	4.0
Co^{2+}	<1.0	5.0
Cu^{2+}	<1.0	3.0
Mn^{2+}	28.0±4,2	80.0
Cr^{3+} and Cr^{6+}	1.7±	6.0
Pb^{2+}	2.7±	6.0
Zn^{2+}	5.3±	23.0

* Level of concern from the Hygienic Standards 2.1.7.2041-06.

Table 2. Total heavy metals content in the solid product.

Heavy metal (total)	Concentration, mg/kg	LOC*, mg/kg
Hg	0.068±0.0078	2.1
As	10.02±0.83	10.0
Ni	3.60±0.32	80.0
Co	1.43±0.14	-
Cu	2.21±0.17	132.0
Mn	72.0±4.3	1500
Cr	6.02±0.54	-
Pb	7.98±0.61	130.0
Zn	16.0±1.1	220.0
Cd	0.162±0.015	2.0

* Level of concern from the Hygienic Standards 2.1.7.2511-09.

The toxicological studies carried out on white rats and guinea pigs as well as the bioassays realized on *Daphnia magna Straus* and *Chlorella vulgaris* did not show any toxic effects of the product (Table 3, 4).

The resulting solid product is proposed to be used during reclamation as a leveling layer (when grinded to a fraction of 1-5 mm diameter), and also as a drainage layer under a fertile soil (when crushed to a fraction of 20-40 mm diameter). Moreover, this product can be used as an inert material when refilling waste during the operation of the MSW landfills and for building roads to the facility. Thus, the leachate is converted into a solid product without receiving new waste and can be implemented directly at its production site.

4.2 *Creation of the fertile layer*

In the course of this work, it was confirmed that 180 days are needed for obtaining the product of waste field composting in Saint-Petersburg climate. However, the use of additional biological additives can reduce the ripening time of the product, i.e. the technogenic soil, to 90 days. Currently, due to the relevance of using the potential of MSW landfills, various modifications of biological additives with antimicrobial effects have been designed to accelerate the decomposition of organic substances. Tests on the influence of several Russian brands of biological additives on the raw mass of sorted waste have revealed a more rapid humus formation and, consequently, a faster ripening of technogenic soil.

The chemical composition of the technogenic soil obtained after field composting of sorted waste is presented in Table 5.

According to the obtained data, the technogenic soil is a very agrochemically favorable substrate for plant growth and significantly exceeds the sod-podzolic soil in terms of nutrient content. The total content of heavy metals does not exceed the normative indicators for composts

Table 3. Toxicological studies of the new solid product on laboratory animals.

Indicator	Units	Research results	Russian normative document on the research method
Acute toxicity by intragastric gavage DL_{50} (white rats)	mg/kg	DL_{50}>5000	Instruction 1.1.11-12-35-2004 "Experimental research requirements for primary toxicological evaluation and hygienic regulation of substances"
Inhalation hazard by static inhalation inoculation, (n.c.), exposure for 2 hours, (white rats)	-	The volatile components did not cause irritation of the mucous membranes of the eyes and upper respiratory tract. The death of animals was not recorded.	"Recommendations for preliminary assessment of chemical substance toxicity by accelerated method"
Skin-irritant effect (white rats) -singly -repeatedly	points points	0 0	Methodical guidelines №2102-79 "Assessment of the impact of harmful chemical compounds on the skin and the justification of extremely acceptable levels of skin contamination"
Irritation of the mucous membranes of the eyes (guinea pigs)	points	0	Methodical guidelines № 2196-80 "Setting up studies of irritating properties and justification of maximum permissible concentrations of selectively acting irritating substances in the air of the working area"

Table 4. Toxicological studies of the new solid product by bioassays.

Indicator	Units	Research results				Permissible level	Russian normative document on the research method
Dilution of the extract tested on the hydrobionts:	%	24 h	48 h	72 h	96 h	A ≤ 10	FR 1.39.2007.03222 "Methods for determining water toxicity and water extracts from soil, sewage sludge, waste on mortality and fertility changes of Daphnia"
-without dilution		0	0	0	0		
-control		0	0	0	0		
Sensitivity of Chlorella at multiple rates of dilution: -without dilution -control	%	+9,6 0				-30<I<+20	FR 1.39.2015.20001 "Method of the measurement of the optical density of cultures of Chlorella algae for the determination of drinking, fresh, natural and waste water, water extracts from soil, sewage sludge, and waste toxicity"

from MSW. It should be noted that the bioavailable forms of HM are even less (Kabata-Pendias, 2001). Despite that it is not planned to use the plants that naturally sprouted on the technogenic soil for feed, results have shown that these plants were within the standards of fodder crops of farm animals.

Table 5. Chemical composition of the technogenic soil.

Elements	Concentration	Measurement units
C total	11.3±0.8	%
N total	0.54±0.07	%
C:N	20.9	unit fraction
N-NH_4 (active form)	22.4±1.3	mg/kg
N-NO_3 (active form)	31.2±2.5	mg/kg
P (active form)	343±31	mg/kg
K (active form)	339±20	mg/kg
Cu (total)	103±7	mg/kg
Zn (total)	208±9	mg/kg
Pb (total)	134±8	mg/kg
Cd (total)	3.32±0.28	mg/kg
Ni (total)	31.4±2.3	mg/kg
Mn (total)	4.50±0.39	mg/kg
Hg (total)	4.21±0.33	mg/kg
As (total)	2.13±0.17	mg/kg

Thus, the technogenic soil obtained from the organic part of MSW is a rational and affordable method for replacing the fertile layer during reclamation.

4.3 *Use of the MSW potential in landfill reclamation*

During landfill reclamation, the following layers are used: a drainage layer to collect biogas, a waterproof layer to isolate the landfill body, a drainage layer to drain surface water and a fertile soil layer (Figure 1).

According to the obtained data, a method for landfill reclamation using the potential of waste coming to landfill is proposed. The product of the leachate solidification can serve as a drainage layer and technogenic soil as a fertile soil. The scheme of using waste transformation products during reclamation is presented in Figure 2.

Today, many landfills of the Russian Federation created at the end of the last century need to be reclaimed, and therefore the development of a landfill reclamation scheme using the potential of waste is relevant and opportune.

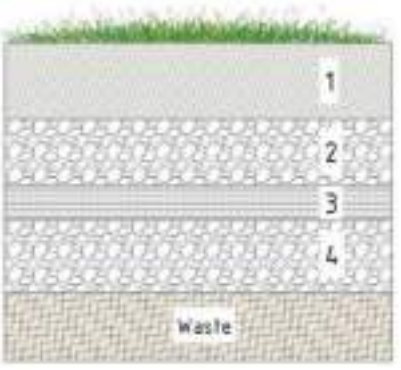

Figure 1. Reclamation layers of landfill: 1 – fertile layer, 2 – drainage layer for water, 3 – waterproof layer (clay), 4 – drainage layer for biogas.

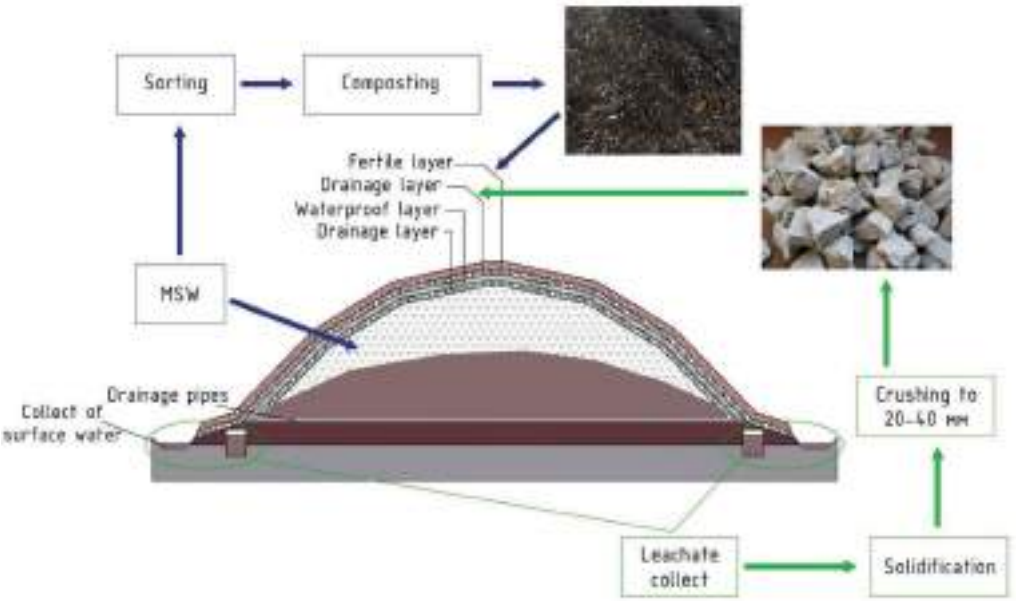

Figure 2. Scheme of using waste transformation products during reclamation.

5 CONCLUSIONS

1. A new method for the utilization of leachate has been developed, which allows the leachate to be converted into a solid product without generating new waste;
2. The content of heavy metals in the solid product did not exceed permissible concentrations for settlement soils and thus, does not represent a secondary source of pollution. Moreover, the toxicological studies confirmed the safety of this product;
3. It was confirmed that the technogenic soil obtained from the organic fraction of MSW has the necessary agrochemical parameters for its use as a fertile layer;
4. A resource-saving scheme for landfill reclamation using waste transformation products as reclamation layers was presented, which is economically and environmentally friendly.

REFERENCES

Awasthi, S.K., Sarsaiya, S., Awasthi, M.K. et al. 2020. Changes in global trends in food waste composting: Research challenges and opportunities. *Bioresource Technology* 299: 122555.

Bolan, N.S., Thangarajan, R., Seshadri, B. et al. 2013. Landfills as a biorefinery to produce biomass and capture biogas. *Bioresource Technology* 135: 578–587.

Gauhey, P., Golueke, C. 1953. *Reclamation of Municipal Refuse by Composting*. Berkeley: Univ. of Calif.

Gourc, J. P., Staub, M. J., Conte, M. 2010. Decoupling MSW settlement into mechanical and biochemical processes – Modelling and validation on large-scale setups. *Waste Management* 30: 1556–1568.

He, R., Shen, D., Wang, J., He, Y., Zhu, Y. 2005. Biological degradation of MSW in a methanogenic reactor using treated leachate recirculation. *Process Biochemistry* 40: 3660–3666.

Henze, M. 1995. *Wastewater treatment. Biological and chemical processes*. Berlin: Springier.

Ilinykh, G.V., Visman, YA.I., Slyusar, N.N., Korotaev, V.N. 2015. Municipal solid waste composition of the city of Perm, Russia: main changes over time. *Intern. multidisciplinary scientific geoconference surveying geology and mining ecology management*. Albena: SGEM.

Jain, M.S., Paul, S., Kalamdhad. A.S. 2020. Kinetics and physics during composting of various organic wastes: Statistical approach to interpret compost application feasibility. *Journal of Cleaner Production* 255: 120324.

Kabata-Pendias, A., Pendias, H. 2001. *Trace elements in soils and plants*. Boca Raton: CRC Press.

Lassini, P., Sala, G., Sartori, F. 1999. Reclamation of old and new landfills and their integration with the invironment. *Environmental impact, aftercare and remediation of landfills; 7th intern. waste management and landfill symp*. Sardinia: SIWMLS.

Liwarska-Bizukoje, E., Ledakowicz, S. 2001. *Elemental balance for the biodegradation process of the organic fraction of municipal solid waste*. Lodz: Technical university of Lodz.

Popovych, V., Telak, J., Telak, O. et al. 2020. Migration of hazardous components of municipal landfill leachates into the environment. *Journal of Ecological Engineering* 21: 52–62.

Renou, S., Givaudan, J.G., Poulain, S. et al. 2008. Landfill leachate treatment: review and opportunity. *Journal of Hazardous Materials* 150: 468–493.

Salem, Z., Hamouri, K., Djemaa, R., Allia, K. 2008. Evalution of landfill leachate pollution and treatment. *Desalination* 220: 108–114.

Silva, A. C., Dezotti, M., Sant'Anna, G. L. 2004. Treatment and detoxitation of a sanitary landfill leachate. *Chemosphere* 55: 207–214.

Trebouet, D., Schlumpf, J. P., Jaouen, P., Quermeneur, F. 2001. Stabilized landfill leachate treatment by combined physicochemicalnanofiltration process. *Water Research* 35: 2935–2945.

Umanets, V.N., Chusov, A.N., Umanets, E.V. 2014. Solution approach to historical pollution and accumulated production wastes. *Ecology & environmental protection*: 607–614.

Weng, Y., Fujiwara, T., Houng, H.J. et al. 2015. Management of landfill reclamation with regard to biodiversity preservation, global warming mitigation and landfill mining: experiences from the Asia–Pacific region. *Journal of Cleaner Production* 1041: 364–373.

Werf, P. 2000. *Assessment and evaluation of outlets of compost produced from municipal waste*. Wexford: Environmental Protection Agency.

Wilson, I.M., Garlick, C. 1999. Management and statistical analysis of landfill monitoring data. *Environmental impact, aftercare and remediation of landfills; 7th intern. waste management and landfill symp*. Sardinia: SIWMLS.

Yousefloo, A., Babazadeh, R. 2020. Designing an integrated municipal solid waste management network: A case study. *Journal of Cleaner Production* 244: 118824.

Zhu, L., Zhao, Y., Zhang, W. et al. 2019. Roles of bacterial community in the transformation of organic nitrogen toward enhanced bioavailability during composting with different wastes. *Bioresource Technology* 285: 121326.

Advances in Raw Material Industries for Sustainable Development Goals – Litvinenko (Ed)
© 2021 Taylor & Francis Group, London, ISBN 978-0-367-75881-3

Microalgae biotechnology multiple use of *Chlorella sorokiniana*

N.A. Politaeva, Y.A. Smyatskaya & I.V. Dolbnya
Peter the Great St. Petersburg Polytechnic University, St. Petersburg, Russia

D.S. Sobgaida
Saratov State Medical University named after V.I. Razumovsky, Saratov, Russia

ABSTRACT: This study is dedicated to realization closed biotechnology using *Chlorella sorokiniana* microalgae. It is a new source of valuable components for various kinds of industry and for obtaining energy such as biofuel and biogas. This technology includes several main stages: microalgae cultivation; extraction of lipids, pigments, pectic substances and carotenoids from the biomass; creation sorption materials based on residual biomass of microalgae for water treatment; using residual biomass and saturated sorbents as a fuel, as a co-substrate for organic waste fermentation and as fertilizers. It is shown that the realization of presented biotechnology allows to use each product on every step of the technology.

1 INTRODUCTION

Nowadays, biomass of different microalga species is used widely in various industries such as: the ecological industry, in water purification, biotechnology, pharmacy, in the food industry and for biofuel production. Green microalgae grow fast. They do not require large soil territories like in the case of conventional food crops and they can be cultivated in closed or open cultivation systems (cultivators and photobioreactors) (Azad, 2019). And they need provision of light, nutrients and aeration. Microalgae is a source of many valuable components such as: lipids, proteins, pigments, carotenoids, pectic substances. These components are extracted from the biomass and can be used in different fields of production.

One of the main ecological problems is water pollution by organic and inorganic substances. Fresh water is widely used in different fields of industry, for agricultural and domestic needs; after technological processes wastewater is formed. They contain various kinds of pollutants including suspended particles and dissolved ones. Often, they are toxic, for example heavy metal ions (Afroze, 2018). Microalgae are good sorption materials for water purification (Abdel-Raouf, 2012). It is possible to grow them with the use of wastewater as a nutrient medium or to use their residual biomass which is formed after extraction valuable components.

Sorption is the one of the effective methods for water treatment. It is a process of concentration pollutants on the surface or the porous area of the material (sorbent). If it occurs on the surface of solid material, the adsorption arises. If liquid or gas phase is used as a sorbent, and in this case, contaminants are concentrated in the volume of the phase, the absorption occurs (Gregg, 1982; Dąbrowski, 2001). At the same time, sorption is a complicated method. Therefore, it is important to develop research in this field, accumulate new knowledge, find new materials which can be used as sorbents, establish modern modification methods for sorption materials creation. Herewith, technologies which are invented for a solution of some problems have not to be the reason of other difficulties, it is important to apply them in a complex way.

Thus, innovative biotechnology multiple use of *Chlorella sorokiniana* microalgae was developed. It includes stages from biomass cultivation, extraction of pigments, lipids and pectic substances, creation sorption materials based on residual biomass for water treatment, and

end up with biogas production by organic waste fermentation with residual biomass and saturated sorbents as co-substrate. The realization of this biotechnology allows to use of each component on every step and totally avoid waste accumulation, because all materials are considered as the resources.

2 LITERATURE REVIEW

2.1 *Microalgae biomass and its cultivation*

Microalgae are cultivated in cultivators and photobioreactors with different constructions; they can be closed or open, Figure 1.

All cultivation technics are divided into two categories: the first one is laboratory conditions and a controlled environment, Figure 2; the second one is outdoor conditions which allow to produce large amount of biomass (Vonshak, 1985; Brennan, 2010). Each type of this technic has advantages and disadvantages. The closed system prevents contamination by other microalgae species and some pollutants, but the open pond should be controlled to avoid such problems. Some construction of the cultivator has a special electro and mechanical providing which allows to move panels with cultivators in the direction of sunlight, Figure 1b.

Microalgae are living microorganisms, for their growth they need in nutrients medium supply. The nutrients medium should consist of following elements: carbon, hydrogen, oxygen, calcium, potassium, magnesium, nitrogen, iron, phosphorus, sulfur, and copper, manganese, zinc or selenium as trace elements. But three elements such as carbon, nitrogen and

Figure 1. Types of cultivation systems (outdoor conditions): a – open raceway pond; b – closed photobioreactor.

Figure 2. Microalgae cultivation in laboratory conditions (closed photobioreactors).

phosphorus are the most important for growth (Geada, 2017; Richmond, 2013). The use of additional external physical actions (e.g. laser radiation, magnetic field) allows to maximize biomass growth in the shortest time (Politaeva, 2018; Smyatskaya, 2019).

Microalgae represent green carbon as an alternative to fossil carbon (fuels); these microorganisms capable to produce biomass enriched with valuable components using sun energy. As all green plants they absorb CO_2 and convert it into O_2. Thus, they provide decrease of CO_2 concentration in the air and take part in minimization of global warming. So, the use of microalgae as a new source of energy has a lot of advantages and perspectives (Geada, 2017).

Chlorella sorokiniana is widely used to obtain the biomass containing lipids and proteins. It is a singlecelled green microalga characterized by its small size (2–10 μm in diameter) and high division rate (1division every 17 to 24 hours). It is non-flagellated and has thick cell wall. These microalgae contain high amounts of valuable compounds: 40 % protein, 30-38 % carbohydrate, 18-22 % lipid, pigments (lutein), etc. (Niccolai, 2019; De Andrade, 2017).

2.2 *Wastewater treatment*

Water contamination is the main ecological problem in the world. Industry and agriculture use a large amount of fresh water for production needs. And after technological processes wastewater are formed, which include in their composition various kinds of substances specific for certain activity. In the most cases these substances are hazardous even in small concentrations and have the ability to accumulate in body tissues of living organisms and then can reach the human body by movement along the food chain. It is extremely important to apply special technological methods and equipment to get purified water. Even for now the planet has such territories with lack of fresh water and for some people it is very hard to have it in a sufficient amount.

Water treatment technology consists from following methods: physical, chemical, physicochemical, biological. The choice of one method or another or their group depends on initial water contamination and purposes of its further usage. Wastewater containing suspended substances go through a stage of pretreatment; during this process large particles such as wood, rags, fecal material and others are removed. Then sewage flow in sedimentation tanks, where sedimentation of settleable solids occurs by gravity. Water prepared in this way is directed on a stage of more deep sorption purification where dissolved impurities are removed. At the end of the process purified water flows on biological treatment, then its disinfection is curried out and after this water can be used again.

Microalgae widely used in the process of water purification. As they capable to actively accumulate biomass by transformation of sun energy it is possible to use of wastewater as nutrient medium for their growth (De la Noüe, 1988; Abdel-Raouf, 2012).

Algae have a good accumulation ability in relation to different heavy metal ions: Cu^{2+}, Pb^{2+}, Cr^{3+}, Ni^{2+}, Cd^{2+}, Co^{2+}, Fe^{2+}, Mn^{2+}, Zn^{2+}. And these elements are included in the biological process of microalgae growth, at the same time metal detoxication occurs. Different mechanisms lead to reducing heavy metals concentration by microalgae. It depends on the algae species, the type of metal ion and its valency, the condition of aqueous solution and the state of algae cells, which can be living or nonliving (Abdel-Raouf, 2012). And it is possible to use a residual biomass of microalgae which is formed after extraction of valuable components for water treatment as sorption materials.

2.3 *Sorption process and sorption materials*

Sorption is surface phenomenon when accumulation of substances near an interface takes place. This process may be defined as partitioning of chemical species between bulk phase and interface. It can be a contact of such systems as solid-liquid, liquid-liquid, liquid-gas and solid-gas. The possibility of change in concentration of a given substance at the interface in comparison with bulk phase underlies many directions of technology including purification nature environments such as water, gas, soil (Dąbrowski, 2001; Bajpai, 1999).

Sorption is the general determination of the process, but when this phenomenon caries out on a surface or porous space of solid phase, adsorption occurs. But in the case of concentration of the substances in the volume of liquid or gas phase, absorption arises. It is important to distinguish these specific terms. Also, sorption has different types; when physical interactions caused by Van der Waals forces take place, the process is called physical sorption; when interactions between two phases are caused by chemical mechanisms with formation of new substances, in this case sorption has the chemical type.

Now, a lot of different materials are used as sorbents for water treatment. The most famous is activated carbon. This material is widely used as adsorbent for the removal of different kinds of contaminants, which have organic and inorganic origin. Activated carbon has good sorption properties, high values of adsorption capacity and surface area (Rodriguez-Reinoso, 2016). But it also has some disadvantages in application as difficulties with regeneration after sorption and this is expansive material. Because of it, there are many research dedicated to development of new materials with the same properties like activated carbon has; and now in the most cases researches pay attention on the use of waste to create sorption materials based on them. It can be agricultural waste such as wheat and millet husk, sunflower husk, nuts shells, rice straw; also, it can be chitosan, zeolites, waste of food production and other kinds of industry (Crini, 2018; Jagruti, 2015; Khalil, 2018; Politaeva, 2019a). Due to the use of waste for these purposes another one urgent ecological problem related to this can be solved. As it was previously mentioned the biomass of microalgae is the good sorbent for many substances in aqueous solutions; and it is possible to use residual biomass for water purification, because of the composition of this natural material consisting of cellulose, hemicellulose, lignin, etc. On practice in the most cases row materials have such sorption characteristics which are not so good enough. Therefore, various kinds of modification are applied to improve sorption properties (thermal and chemical modification). In order to increase the sorption capacity composite sorption materials can be created with different composition. As a binder substance chitosan can be used in obtaining of granulated sorbents. It is a biopolymer and it has good sorption properties in relation to contaminants in water solutions. And in water treatment technology it is also used as a sorbent, but because of its high cost, chitosan doesn't find a wide application. But residual microalgae biomass included in the composition with chitosan increases sorption characteristics of a new created granulated sorbent and leads to improvement of chitosan resistance to dissolution in acid environment.

2.4 *Biogas production with the use of microalgae*

Another advantage to develop the biotechnology of microalgae treatment is biogas production. Nowadays it is third generation biofuel. Microalgae produce an oil that can be refined into biodiesel. It is a renewable one and it includes methane, carbon dioxide and biohydrogen. The grow rate of microalgae is very high; large land territories for biomass production is not needed. Because of it, microalgae as a source of energy is more profitable in comparison with materials used as a basis for first and second generation fuels. In general, the process of biogas production from microalgae biomass is commercially viable, when firstly all by-products are extracted from the initial biomass. And after that for the purposes of biogas production the residual biomass is applied (Alam, 2015; Brennan, 2010; Azad, 2019; Tang, 2016). Converting the biomass into biogas components (methane, hydrogen and CO_2) carries out at anaerobically digested conditions (Chusov, 2019). Thus, the complex use of microalgae potential through all stages of the biotechnology allows to get a lot of useful by-products, new materials and energy.

During implementation of international project entitled «Development and implementation of innovative biotechnologies for treatment of microalgae *Chlorella sorokiniana* and the duckweed *Lemna minor*» a closed loop biotechnology using *Chlorella sorokiniana* microalgae biomass has been developed. It includes following stages: cultivation microalgae in bioreactors; harvesting; extraction lipids and fatty acids, and pigments; obtaining sorption materials based on residual biomass for water treatment; producing biogas by fermentation of used sorbents and other waste which are formed.

3 MATERIALS AND METHODS

3.1 *Cultivation of Chlorella sorokiniana microalgae in laboratory conditions and its harvest*

Chlorella sorokiniana microalgae were cultivated in closed photobioreactors which are presented in Figure 2. For its growth nutrition medium was prepared based on modified Hoagland solution including composition of macro- and micronutrients, which are important for microalgae cell formation (Richmond, 2004). Specific growth conditions were provided such as illumination of photobioreactors using fluoriscence lamps with duration 18 hours per day in the regime of day/night with constant aeration by air. This aeration was conducted by bubbling Xilong AP-003 device (5 W, 2Kh2, 5 l/mines). The optical density of the biomass from the beginning of the cultivation was measured by spectrophotometer Shimadzu UV-1280 at λ = 750 nm. It allows to control cells culture accumulation. And after 10 days the biomass growth reaches maximum amounts at the stationary phase of the growth (Politaeva, 2018b).

The next step after cultivation is harvest. Biomass concentration was carried out by microfiltration through membrane filters or by centrifugation. After this step, the biomass was dried by freeze-drying.

3.2 *Extraction of valuable components*

Chlorella sorokiniana biomass is the source of many valuable components such as: lipids including fatty acids which can be used for Omega - 3 and biofuel production; carotenoids which are widely used in pharmaceutic industry; green pigments which can be used in the fields of cosmetology and in the food industry as dietary pigments; pectic substances which are useful ingredients in the food production. The extraction of lipids and this process are described in following scientific article (Politaeva, 2019b).

3.3 *Sorption material for water treatment based on residual biomass and chitosan*

After the extraction of valuable components, a residual biomass is formed. It is a kind of waste, but at the same time it is a material with useful properties. Therefore, it can be used for obtaining sorption material for water treatment from heavy metal ions. It is known that these substances are toxic and are often contained in wastewater, so it is relevant to look for new methods to remove these heavy metal ions and get purified water. So, the technology of obtaining sorption material based on carbonized residual biomass and chitosan as a binder substance consists of following steps. First, the residual biomass is carbonized at high temperatures in order to be activated. The second step is the dissolution of chitosan in a 3 % solution of acetic acid. Then all components are mixed and the next, the granulation step is carried out by the addition of the mixture drop by drop to a 5 % solution of sodium hydroxide. The granules are then left to soak in this solution for 24 hours. Then the granules are washed using distilled water until reaching neutral pH values. After this, the material is by ambient air drying.

The determination of the sorption properties of the obtained sorbent was conducted. Sorption isotherms were experimentally obtained. The initial and equilibrium concentrations of heavy metal ions in the modal water solution have been measured with the use of TA-Lab device (Russia, LLC Research production enterprise Tom'analit) which work based on inversion voltammetric method of analysis, using standard Russian method Environmental Protection Regulation 14.1:2:4.222-06. The inaccuracy of measuring technique is 25 %. Experimental conditions of purification model water solutions consisted of Zn^{2+}, Cd^{2+} and Cu^{2+} ions: $m_{sorbent}/V_{solution}$ = 2 g/l; $t_{sorption}$ = 24 hours; T = 20 ± 2 °C; pH = 4.0 ± 0.2. The experiment accuracy is within the limits of 5-10 %. The sorption capacity was calculated using Equation 1:

$$q = \frac{(C_i - C_e) \cdot V}{m} \quad (1)$$

where C_i and C_e – initial and equilibrium concentrations of heavy metal ions (mmol/l); V – solution volume (l); and m – mass of the sorbent (g).

To describe sorption process two sorption models were applied: Lengmuir (Equation 2) and Freundlich (Equation 3) isotherm models. Equation 2 is a linearized form of Lengmuir sorption model (Ayawei, 2017).

$$\frac{1}{q} = \frac{1}{q_{max}} + \frac{1}{Kq_{max}C_e} \tag{2}$$

where q – sorption capacity (mmol/g); q_{max} – maximum sorption capacity of the sorbent (mmol/g); C_e – equilibrium heavy metal ions concentration in the solution (mmol/l); K – Langmuir constant which notices on sorption rate and it is also a coefficient or constant of sorption equilibrium (l/mmol).

Equation 3 is a logarithmic form of Freundlich sorption model (Ayawei, 2017).

$$log\ q = log\ K + 1/n\ log\ C_e \tag{3}$$

where q – sorption capacity (mmol/g); K and n – constants of Freundlich sorption model; C_e – equilibrium heavy metal ions concentration (mmol/l).

In order to establish sorption character (physical or chemical mechanism) Gibbs free energy has been calculated by Equation 4 (Gautam, 2016):

$$\Delta G = -R \cdot T \cdot ln\ K \tag{4}$$

where R – universal gas constant which equal to 8,314 (J/mol·K); T – absolute temperature (K); K – coefficient or constant of sorption equilibrium (l/mmol).

If $\Delta G < 0$, there is an absence of energy consumption during sorption process, therefore the physical mechanism of interaction between sorbate and sorbent is observed. In that case if $\Delta G > 0$, chemisorption caries out, some amounts of energy are expended on interactions between dissolved substance with sorbent with formation of tough chemical bond or new compound. If $\Delta G = 0$, a system is in equilibrium. The results are presented in Table 3.

Microstructure of obtained sorption material was identified by scanning electron microscopy with the use of JSM 7001F (JEOL, Japan) equipment. The graphs of the sorption isotherms and all data of the experiment were statistically calculated with the help of Microsoft Office Excel 2019 software (Politaeva, 2019b).

The process of biogas production using *Chlorella sorokiniana* microalgae residual biomass is presented and described in detail in following article (Chusov, 2019).

4 RESULTS AND DISCUSSION

Obtained sorption material (carbonized residual biomass + chitosan (CRB+Chitosan)) has a shape of granules and it is presented in Figure 3a. The sorbent microstructure (1000) is shown on Figure 3b.

The structure of the material has roughness, porous and cracks which determine the sorption of contaminants from aqueous solution. Studying the surface of the sorbent it is possible to presume the physical adsorption. To establish the sorption mechanism more accurately sorption isotherms have been obtained by conducting of the bunch of the experiments with certain conditions, Figure 4. They have the shape of Langmuir type of isotherm or the first type of isotherm of BET classification (Abebe, 2018). It is the first sign of sorption conducted by physical mechanisms. After mathematical conversion the isotherms were linearized. The constants of Langmuir and Freundlich sorption models have been graphically determined. A suitability of the isotherms in relation to studied sorption models was established by values of correlation coefficient (r) and approximation coefficient (R^2), Table 1 and Table 2. If they

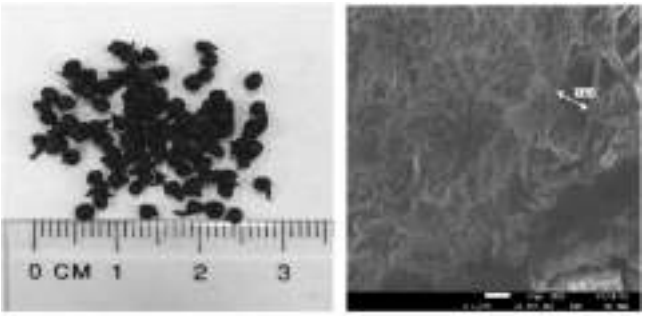

Figure 3. Sorption material CRB+Chitosan.

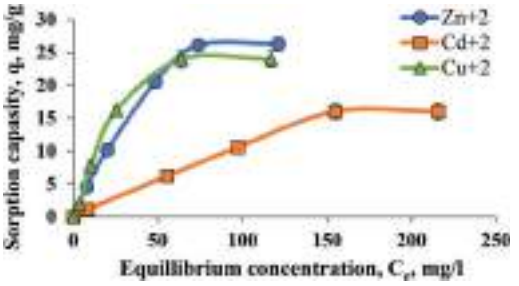

Figure 4. Sorption isotherms.

Table 1. Application of Langmuir sorption model.

Sorbent	Heavy metal ions	q_{max}, mmol/g	$tg\alpha = 1/q_{max}$	K, l/mmol	r	R^2
CRP+Chitosan	Zn^{+2}	0.78	1.28	0.8	0.999	0.998
	Cd^{+2}	0.12	8.67	1.4	0.995	0.871
	Cu^{+2}	7.23	0.14	0.1	0.991	0.981

Table 2. Application of Freundlich sorption model.

Sorbent	Heavy metal ions	K	1/n	n	r	R^2
CRP+Chitosan	Zn^{+2}	0.33	0.682	1.5	0.978	0.956
	Cd^{+2}	0.10	0.860	1.2	0.994	0.989
	Cu^{+2}	0.35	0.712	1.4	0.949	0.900

Table 3. Gibbs free energy and type of sorption.

Sorbent	Heavy metal ions	ΔG, kJ/mol	Type of sorption
CRP+Chitosan	Zn^{+2}	0.5	Chemisorption
	Cd^{+2}	-0.8	Physical sorption
	Cu^{+2}	5.6	Chemisorption

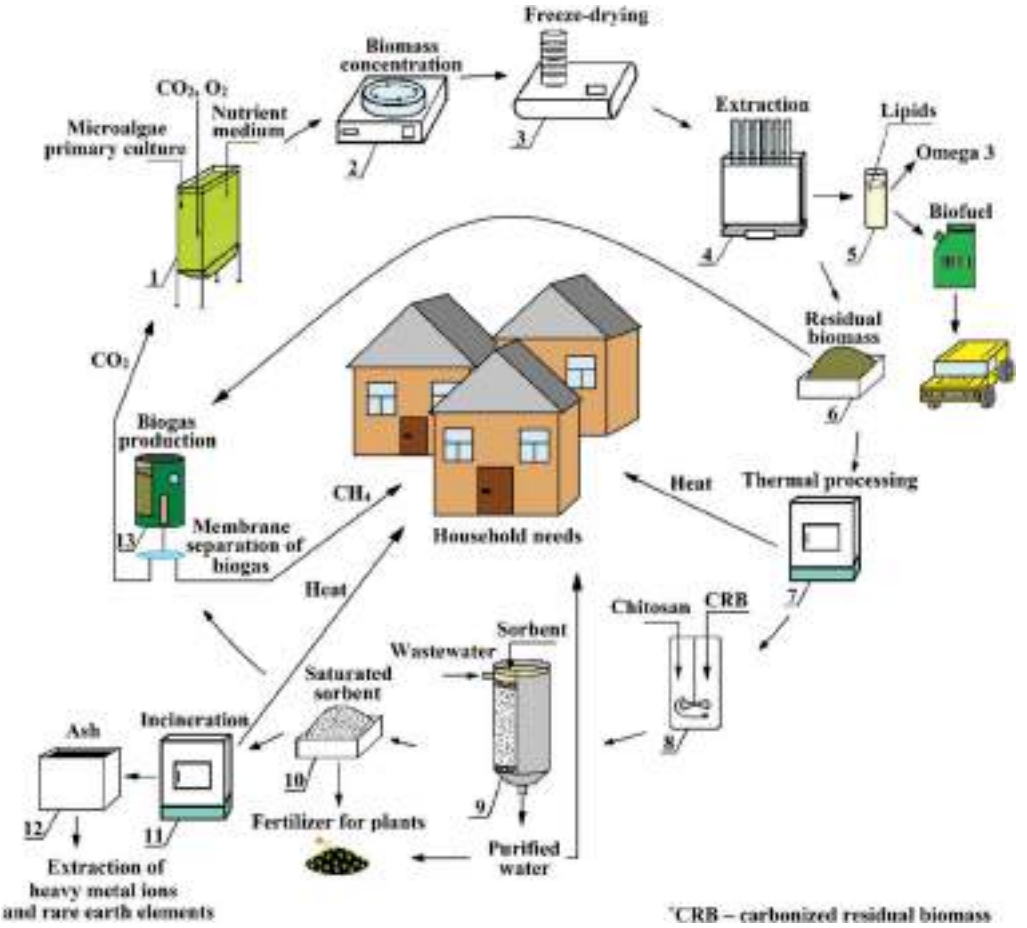

Figure 5. Microalgae biotechnology multiple use of *Chlorella sorokiniana* (general scheme).
1 – photobioreactor; 2 – centrifuge; 3 – freeze-dryer; 4 – Soxhlet extractor; 5 – lipids extracted from mi-croalgae; 6 – storage tank for residual biomass; 7, 11 – muffle furnace; 8 – mixing apparatus; 9 – appa-ratus for water treatment (adsorber); 10 – storage tank for saturated sorbent; 12 – storage tank for ash; 13 – bioreactor.

are close to 1.0, experimental results are described in an appropriate way, and this or that isotherm refers to one of two studied models or even both of them.

Thus, the results indicate the possibility to use obtained sorption material in the fields of industry where wastewater are formed containing heavy metal ions including the mining industry.

After a sorption process saturated sorbents can be utilized by three ways such as: use it as a fuel, as a co-substrate for organic waste fermentation and as fertilizers.

The general scheme of cyclic ecotechnology is presented on Figure 5. It includes all steps which have been reviewed previously. The main idea is the complex use of each component on every step of the technology.

5 CONCLUSIONS

To conclude, *Chlorella sorokiniana* biomass presents several promising applications. It is the source of valuable components which can be used in different fields of industry. Sorption material based on residual biomass and chitosan have been proved effective for water

purification from heavy metal ions. The realization of this closed loop biotechnology using microalgae biomass allows to get new resources, products, materials, energy, that can be used in a complex way.

ACKNOWLEDGEMENTS

The research was performed within the implementation of Federal Target Program for Research and Development in Priority Areas of the Russian Scientific and Technological Complex for 2014 - 2020, the project «Development and implementation of innovative biotechnologies for treatment of microalgae *Chlorella sorokiniana* and the duckweed *Lemna minor*» (Agreement № 14.587.21.0038 of 17.07.2017), the unique project identifier is RFMEFI58717X0038.

REFERENCES

Abdel-Raouf, N., Al-Homaidan, A.A. & Ibraheem, I.B.M. 2012. Microalgae and wastewater treatment. *Saudi Journal of Biological Sciences* 19(3): 257–275.

Abebe, B., Ananda Murthy, H.C. & Amare, E. 2018. Summary on Adsorption and Photocatalysis for Pollutant Remediation: Mini Review. *Journal of Encapsulation and Adsorption Sciences* 8: 225–255.

Alam, F., Mobin, S. & Chowdhury, H. 2015. Third generation biofuel from Algae. *6th BSME International Conference on Thermal Engineering (ICTE 2014); Procedia Engineering* 105: 763–768.

Afroze, S. & Kanti Sen, T. 2018. A Review on Heavy Metal Ions and Dye Adsorption from Water by Agricultural Solid Waste Adsorbents. *Water, Air & Soil Pollution* 229:225.

Ayawei, N., Ebelegi, A.N. & Wankasi, D. 2017. Modelling and Interpretation of Adsorption Isotherms: Review Article. *Hindawi Journal of Chemistry* vol. 2017: 11 pages.

Azad, K. 2019. *Advances in eco-fuels for a sustainable environment. Woodhead publishing series in energy*. Elsivier.

Bajpai, A.K. & Rajpoot, M. 1999. Adsorption Techniques – A Review. *Journal of Scientific & Industrial Research* 58: 844–860.

Brennan, L. & Owende, P. 2010. Biofuels from microalgae – A review of technologies for production, processing, and extractions of biofuels and co-products. *Renewable and Sustainable Energy Reviews* 14: 557–577.

Chusov, A. et al. 2019. Determination of biogas potential of residual biomass of microalgae *Chlorella sorokiniana. IOP Conf. Series: Earth and Environmental Science* 403 012225.

Crini, G. & Litchfouse, E. 2018. *Green adsorbents for pollutant removal: Fundamentals and Design. Environmental chemistry for a sustainable world*. Springer.

Dąbrowski, A. 2001. Adsorption from theory to practice. *Advances in Colloid and Interface Science* 93: 135–224.

De Andrade, C.J. & De Andrade, L.M. 2017. An overview on the application of genus Chlorella in biotechnological processes. *Journal of Advanced Research in Biotechnology* 2(1): 1–9.

De la Noüe, J. & De Pauw, N. 1988. The potential of microalgal biotechnology. A review of production and uses of microalgae. *Biotechnol. Adv*. 6: 725–770.

Gautam, R.K. & Chattopadhyaya, M.C. 2016. Kinetics and Equilibrium Isotherm Modeling: Graphene-Based Nanomaterials for the Removal of Heavy Metals From Water: Chapter 5. *Nanomaterials for Wastewater Remediation*: 79-109.

Geada, P. et al. 2017. Microalgal Biomass Cultivation: Chapter 13. *Algal Green Chemistry*: 257-284.

Gregg, S.J. & Sing, S.W. 1982. *Adsorption, Surface Area and Porosity*. London: Academic Press.

Jadava, J.N., Maindb, S.D. & Bhaleraoa, S.A. 2015. Competitive biosorption of lead (II) ions from aqueous solutions onto *Terminalia Catappa l.* leaves as a cost effective biosorbent. *Octa Journal of Environmental Research* 3(1): 067–079.

Khalil, A., Sergeevich N. & Borisova, V. 2018. Removal of ammonium from fish farms by biochar obtained from rice straw: Isotherm and kinetic studies for ammonium adsorption. *Adsorption Science and Technology* 36(5-6): 1294–1309.

Niccolai, A. et al. 2019. Microalgae of interest as food source: Biochemical composition and digestibility. *Algal Research* 42 101617.

Politaeva, N. et al. 2018a. Effect of laser radiation on the cultivation rate of the microalga *Chlorella sorokiniana* as a source of biofuel. *IOP Conf. Series: Earth and Environmental Science* 115 012001.

Politaeva, N. et al. 2018b. Chlorella Microalga Biomass Cultivation for Obtaining Energy in Climatic Conditions of St. Petersburg. V. Murgul and Z. Popovic (eds.), *International Scientific Conference Energy Management of Municipal Transportation Facilities and Transport EMMFT 2017, Advances in Intelligent Systems and Computing* 692: 555–562.

Politaeva, N. et al. 2019a. Research of pH influence on sorption properties of sorbents on a basis of residual biomass of microalgae Chlorella sorokiniana and duckweed Lemna minor. *E3S Web of Conferences* 124 01050.

Politaeva, N., Smyatskaya, Yu. & Toumi, A. 2019b. Influence of SHF Treatment on Lipid Output from Microalga *Chlorella sorokiniana. IOP Conference Series: Earth and Environmental Science* 272 032056.

Richmond, A. 2013. Biological principles of mass cultivation of photoautotrophic microalgae: Chapter 11. A. Richmond, Q. Hu (eds.), *Handbook of Microalgal Culture*. Oxford: John Wiley & Sons.

Richmond, A. 2004. *Handbook of Microalgal Culture: Biotechnology and Applied Phycology*. Hoboken: Blackwell Science.

Rodriguez-Reinoso, F. & Silvestre-Albero, J. 2016. Activated Carbon and Adsorption. *Reference Module in Materials Science and Materials Engineering*. Elsivier.

Smyatskaya, Y.A. et al. 2019. Study of chemical composition and properties of biomass of *Chlorella sorokiniana* under influence of different physical factors. *Izvestiya Vysshikh Uchebnykh Zavedenii, Seria Khimia i Khimicheskaya Tekhnologiya* 62(2): 72–78.

Tang, Y. et al. 2016. Microalgae as a feedstock for biofuel precursors and value-added products: green fuels and golden opportunities. *BioResources* 11(1): 2850–2885.

Vonshak, A. 1985. Micro-algae: laboratory growth techniques and outdoor biomass production: Chapter 15. *Techniques in bioproductivity and photosynthesis*: 188-200.

Advances in Raw Material Industries for Sustainable Development Goals – Litvinenko (Ed)

Geochemical traits of urban landscapes

V.A. Alekseenko
Doctor of geological and mineralogical Sciences, Institute for Water and Environmental Problems of Siberian Branch of the Russian Academy of Sciences, Barnaul, Russia;
Southern Federal University, Rostov-on-Don, Russia;
Admiral Ushakov Maritime State University, Novorossiysk, Russia

N.V. Shvydkaya
Kuban State Agrarian University, Krasnodar, Russia

A.V. Puzanov
Institute for Water and Environmental Problems of Siberian Branch of the Russian Academy of Sciences, Barnaul, Russia

A.V. Nastavkin
Southern Federal University, Rostov-on-Don, Russia

ABSTRACT: The study examines environmental quality in residential landscapes. From the point of view of the migration of elements, urban landscapes are almost identical to industrial ones located beyond the city's borders. The greater impact on all residents – not only on the employees of an enterprise – is the key environmental difference that should be emphasized. In addition, pollutants, especially aerosols, are dispersed less effectively in cities than outside them. Considering these landscapes, it should be borne in mind that very peculiar pollution types like electromagnetic, thermal, sound (noise), and radioactive can occur in the course of life activities within a city. These pollution types cause certain environmental changes as well. For large-scale studies conducted in megacities, as well as for ecological and geochemical certification, a more detailed classification of landscapes is required. Patterns of technogenic migration and concentration of chemical elements are still the basis of division in these cases.

1 INTRODUCTION

Classification of urban geochemical landscapes is carried out taking into account the characteristics of the leading type of migration of chemical elements, i.e. the technogenic patterns. On this basis, first of all, landscapes of industrial, residential, and recreational areas, streets, military zones, wastelands, and cemeteries are distinguished. Industrial landscapes include territories located within localities and occupied by various production enterprises (factories and their separate workshops, transport parks, power plants, etc.), and in certain cases quarries and underground mines (Ajmone-Marsan & Biasioli 2010; Bech et al. 2015; Ermolin et al. 2017; Gallagher et al. 2008; Ngun et al. 2018; Tepanosyan et al. 2019). The same landscapes include territories occupied by buildings necessary for the operation of the named enterprises.

First of all, it is advisable to separate out the landscapes of quarries and underground mines, dumps of mine workings, various factories, power plants, garages, tram and trolleybus parks, gas stations, waste processing facilities, bazaars, as well as the landscapes of automobile and railway stations, airports, and river and seaports. All of them differ from each other in the composition, occurrence form and amount of pollutants, both distributed within their limits, and in neighboring landscapes of a locality.

Landscapes of residential areas normally take a major part of settlements (Grebenshchikova et al. 2017; Naylo et al. 2019; Seleznev et al. 2019; Timofeev et al. 2019). In addition, a significant share of residents spends most of their lives there. Therefore, the assessment of the ecological and geochemical situation of such zones and its improvement are among the most important environmental issues.

Quite often, biological cycles of elements play a significant role in the evolution of landscapes in residential areas. This is especially true for small settlements with one-story houses and homesteads. However, the biological cycles in residential areas of cities differ significantly from those in neighboring industrial, recreational and other urban landscapes (Kabata-Pendias & Pendias 2001).

The building height in residential areas, directly and indirectly, affects the pathways of numerous chemical elements and compounds that end up being accumulated or removed from the urban environment. Wind direction and speed, as well as the ratio of turbulent and laminar air flows, are also often dependent on the number of stories. All other things being equal, these indicators become decisive for the content of many substances, including toxic ones, in the air, and consequently for the ingress from it into soils, plant and animal organisms (including humans).

The number of floors alters the density of the population in a residential area; the volume of municipal waste and ways of disposal are associated with it too. Stories largely determine water supply and heating, which, in turn, control the input and removal of not only elements in the form of solutions and gas mixtures, but also elements in other forms. Species diversity and the number of domestic animals also largely depend on this indicator, and consequently, the features of migration, and often the forms of chemical elements in the landscapes of residential areas. The number of floors in residential areas also affects the level of comfort of residents living in them, as well as the speed and level of spread of various infections and even specific diseases (often mental disorders). These features largely determine the ecological status of many areas.

2 MATERIALS AND METHODS

Field studies in urban areas were carried out during the summer seasons with sampling the upper (0-5 cm) horizon of soils and technogenic superficial formations, which is the most indicative part of the soil cover from the point of view of pollution – the depositing geochemical environment. The work was carried out following a regular grid with a step of 1 km, which is the most representative in the field research conditions, covering all the main geochemical landscapes of the research area. Soil sections were studied within the residential urban parts, with a description of the horizons and sampling. The full list of the studied urban areas categorized by population or primary component of the local economy includes cities with the number of citizens equal to over 1 million, half a million, over 100 thousand, and less than 100 thousand, as well as resort towns and villages of agricultural specialization (Alekseenko & Alekseenko 2014).

The combination of buildings of different height in the landscapes of residential zones can be considered as a main ecological and geochemical indicator for them. In accordance with this indicator, the considered landscapes should be divided more detailed for special studies. It should be noted that in recent years, in many cities, development is conducted on the principle of creating neighborhoods with a specific combination and mutual location of buildings of different stories. When detailing these areas, it is advisable to consider them as separate landscapes. Their ecological and geochemical features should be taken into account when developing the research methodology.

The study of surface horizons of soils was carried out according to the method of an averaged sample: the soil was collected at least three times from the laid-down digs with a depth of 0-5 cm on a plot of approximately 10 sq. m, samples were placed in a single package, their total weight was about 3 kg. Mixing and averaging were performed in the laboratory. The analyses of soil and plant samples were carried out in the certified and accredited Central Testing Laboratory at Kavkazgeolsyomka using emission spectral analysis.

3 RESULTS

Streets are the closest in geochemical features to roads that are allocated outside of localities, and also have no natural analogs. These include roadways and sidewalks (often with plantings of various bushes and trees) near residential buildings, industrial enterprises or barriers that fence off homesteads or other landscapes of the locality. Despite the usual plantings along sidewalks, biological cycles are low-developed in the considered landscapes, since all the fall and dry branches of trees and shrubs, as a rule, are taken out of a city or burned, and the ash is most often dispersed, not concentrating in the street landscapes.

As in other landscapes of settlements, a significant part of the elements in the street comes through the atmosphere. At the same time, unlike neighboring landscapes, car exhaust gases play a significant role in the atmospheric air of streets. They are also the most toxic compounds that are constantly present in the atmospheric gases on the streets. Their concentration is related to the traffic intensity. The latter is largely responsible for the dustiness and receipt of specific compounds in the described landscapes due to the wear of tires, engines, tram tracks, etc.

Indirectly, the traffic intensity is related to the type of road surface (paved, unpaved, etc.). Special cases are streets where railway traffic occurs; in such landscapes, the flow of chemical elements is unpredictable, in various forms: although in relatively small quantities due to spilling out of the cars.

There is usually no significant accumulation of substances from neighboring landscapes on the streets. They themselves are a source of numerous compounds that enter the surrounding landscapes through the atmosphere. The height of buildings that limit streets, as well as the plantings and the type of plants that make up them, have a great influence on this movement of elements. A significant share of different substances is removed from the streets by surface and underground water. They can be concentrated on certain geochemical barriers, creating technogenic anomalies (Table 1) that are not associated with any enterprises, which must be taken into account when making special maps for ecological and geochemical studies.

Table 1. Comparison of the average contents of a number of chemical elements in the soils of various groups of settlements.

Categories of urban areas by population or primary component of the local economy	Heightened average contents		Decreased average contents	
	Number of elements	Elements	Number of elements	Elements
Over 1 million population	17	Ag, As, Be, Bi, Cd, Co, Cr, Cu, Ga, Mn, Ni, P, Pb, Sn, Ti, V, and Zn	2	Li and W
Half a million population	4	Ba, La, Li, and W	11	Ag, As, Mo, Nb, P, Sc, Sn, Ti, Tl, V, and Yb
Over 100 thousand population	11	Ag, Bi, Mo, Nb, P, Sn, Sr, W, Y, Yb, and Zr	10	Ba, Cd, Co, Cr, Cu, Ga, Ge, Mn, Ni, and Ti
Less than 100 thousand population	7	Ge, Nb, Se, Tl, Y, Yb, and Zr	10	Be, Bi, Cu, Ga, Li, Mn, Ni, Pb, Sr, and Zn
Resort towns	16	As, Ba, Cd, Co, Cr, Cu, Ge, Li, Mn, Ni, Pb, Sc, Sr, Tl, V, and Zn	6	Mo, P, W, Y, Yb, and Zr
Villages of agricultural specialization	4	Be, Ga, Mo, and Ti	18	Ag, As, Ba, Bi, Cd, Co, Cr, Ge, Nb, Pb, Sc, Sn, Sr, Tl, V, Y, Zn, and Zr

In the case of special and detailed studies, it is advisable to separate street landscapes taking into account the traffic intensity, the prevailing mode of transport, and the characteristics of the road surface.

Landscapes of recreation areas are located both in the center and on the outskirts of settlements. These include parks, stadiums, squares, sports fields, alleys, recreation lines along banks of rivers, reservoirs, seas, etc. Biological properties of some of them (parks, squares, etc.) are close to the forest-engineering landscapes that are allocated outside of settlements. The landscapes under consideration do not receive any specific compounds, except for oxygen and various solid, liquid and gaseous products of life activity of organisms. Most of the substances entering the recreation areas are transported by air from nearby localities (Mazhari et al. 2018). In recent years, pollution of these landscapes by exhaust fumes from cars and motorboats has become widespread.

For urban areas, especially large ones, very important environmental indicators are the percentage of city's territory occupied by recreation areas, and the uniformity of distribution of the latter over the entire area of the city.

The landscapes of zones occupied by military departments are currently among the least studied. The specific environmental pollution caused by them and the need for their ecological and geochemical study has been discussed only recently, in connection with the withdrawal of troops from Eastern Europe.

In addition to the actual environmental and geochemical pollution, they can cause radiation, electromagnetic, noise, heat, and other types of environmental pollution. Therefore, such landscapes should be highlighted even if they are small and impossible to study. Their classification has not been developed yet for large-scale and detailed studies.

4 DISCUSSION

The relationship between the content of most chemical elements in soils – including metals – with the development of living organisms and the concentration of these elements in them is considered in several works (Bourotte et al. 2019; Lenoir et al. 2019; Tepanosyan et al. 2017). We note only that, as when studying other landscapes, the following factors must be taken into account in urban areas at this level:

- redox conditions, oxidizing with free oxygen and reducing with either gley or sulfides;
- alkaline-acid conditions, which are best divided as strongly acidic, acidic, neutral, and highly alkaline;
- a set of typomorphic elements and, as a result, a class of water migration of chemical elements.

Quite often, especially for detailed work, in the conditions of urban landscapes, the considered selection is not enough. In such cases, a set of typomorphic elements in groundwater should be considered at the same level. It is advisable to note the alkaline-acid properties of groundwater and the acid-sulfur regime, since these indicators in the waters and soils of different parts of settlements may differ very significantly and represent significant ecological and geochemical changes.

Urban landscapes are combined taking into account the geomorphological features of a territory. In terms of the land topography, it is convenient to combine eluvial, trans-eluvial, trans-accumulative, and accumulative positions. First of all, they differ from each other in the features of the mechanical migration of elements and their compounds. Moreover, additional maps of the material's surface drift are often required.

Wasteland landscapes have been developed in many localities. Their appearance is usually associated either with the demolition of old buildings, or with the reconstruction of cities, or with uneven development of certain areas, which usually leave empty areas for a short time. In the first case, landscapes (especially in old cities) may have a large geochemical diversity. However, as a rule, the main ecological and geochemical impact on neighboring urban landscapes is not caused by them, but by the construction waste that is brought from them. Quite

often, vacant lots themselves become temporary storage areas for a variety of garbage — from household waste to construction debris. In this case, they should be given great attention, studying them as a kind of social geochemical barriers.

Cemetery landscapes can be divided into old and operating ones. Old cemeteries are usually located next to a city center and are similar to the landscapes of recreation areas in terms of their ecological and geochemical features. When designing new cemeteries, first of all, one should pay attention to the surface and underground water flow from them. It should not take place in the direction of existing or projected urban districts.

Among the urban landscapes of almost all localities, there are various educational institutions, kindergartens, hospitals, and public baths (Bourotte et al. 2019; Famuyiwa et al. 2019). When assessing the overall environmental situation in localities, special attention should be paid to both their number and the uniformity of distribution. On maps of urban geochemical landscapes, all these institutions should be marked with extra-scale signs.

The second taxonomic level is not less important. At this level, despite the practical poor development of biological cycles in localities, it is advisable to combine urban landscapes based on the characteristics of plant communities and their preservation. There are two main reasons for this.

First, plants are very sensitive to changes not only in the complex of ecological and geochemical conditions but also in such important indicators for normal human life as radiation conditions, thermal pollution, etc. Based on the state (or even survival) of certain plant species (Bezel' et al. 2015; Drozdova et al. 2019; Yalaltdinova et al. 2018), it is often possible to pre-judge changes in the urban environment without analyses, which are sometimes rather expensive.

Secondly, in many localities, especially with a small number of residents, a significant part of agricultural products (fruits, vegetables, and various herbs for vegetable seasonings) is supplied from homesteads. In order to avoid poisoning and to obtain environmentally friendly products, areas with certain agricultural crops located within the boundaries of a city should be identified and their geochemical features studied in detail.

Detailed and special ecological and geochemical studies often require a more fractional division of landscapes. In these cases, one can select separate landscapes with certain agricultural crops, both perennial and annual, ornamental plants, or with their various combinations. In addition, for special studies, separate maps of the sanitary state of plantings should usually be drawn up (Famuyiwa et al. 2019; Grebenshchikova et al. 2017; Tume et al. 2018).

5 CONCLUSIONS

Geochemical traits of natural landscapes are constantly affecting the urban environment. The study of landscapes is performed following the developed scheme, depending on the composition of the rocks. However, when compiling ecological and geochemical maps of localities at the considered level, it is necessary to take into account the thickness of loose formations located between bedrock and soil, as well as the position of zones of discontinuous disturbances. These factors can be crucial in the design of residential and industrial buildings, especially in unstable environments.

The certain associations of plants were also affected by the background elements concentrations in soils of several cities. The increased concentrations of elements were more often detected – other things being equal – in the landscapes with mixed decorative fruit and berry plant association (Cu, Pb, Co, Mn, Ti, Sr), less often – with agricultural fruit and berry plant association (Zn, Ag, Sn, Ba, Cr). In parks with just decorative kinds of plants, the increased concentrations of V and Sc were identified. The traffic intensity could also have some influence in this case.

ACKNOWLEDGMENTS

The analyses of soil and plant samples were carried out in the certified and accredited Central Testing Laboratory at Kavkazgeolsyomka using emission spectral analysis.

REFERENCES

Ajmone-Marsan, F. & Biasioli, M. 2010. Trace elements in soils of urban areas. *Water Air and Soil Pollution* 213, 121–143.

Alekseenko, V. & Alekseenko, A. 2014. The abundances of chemical elements in urban soils. *Journal of Geochemical Exploration* 147 (B), 245–249.

Bech, J., Tume, P., Roca, N. & Reverter, F. 2015. Geochemical distribution of potentially harmful elements in periurban soils of a Mediterranean region: Manresa (Catalonia, Spain). *Fresenius Environmental Bulletin* 24(12A), 4379–4389.

Bezel', V.S., Zhuikova, T.V. & Gordeeva, V.A. 2015. Geochemistry of grass biocenoses: Biogenic cycles of chemical elements at contamination of the environment with heavy metals. *Geochemistry International* 53(3), 241–252.

Bourotte, C.L.M., Sugauara, L.E., De Marchi, M.R.R. & Souto-Oliveira C.E. 2019. Trace metals and PAHs in topsoils of the university campus in the megacity of São Paulo, Brazil. *Anais da Academia Brasileira de Ciencias* 91(3), 20180334.

Drozdova, I., Alekseeva-Popova, N., Dorofeyev, V., Bech, J., Belyaeva, A. & Roca, N. 2019. A comparative study of the accumulation of trace elements in Brassicaceae plant species with phytoremediation potential. *Applied Geochemistry* 108, 104377.

Ermolin, M.S., Fedotov, P.S., Ivaneev, A.I., Fedyunina, N.N. & Eskina, V.V. 2017. Isolation and quantitative analysis of road dust nanoparticles. *Journal of Analytical Chemistry* 72(5), 520–532.

Famuyiwa, A.O., Davidson, C.M., Oyeyiola, A.O., Lanre-Iyanda, Y. & Babajide, S.O. 2019. Pollution characteristics and health risk assessment of potentially toxic elements in school playground soils: A case study of Lagos, Nigeria. *Human and Ecological Risk Assessment* 25(7), 1729–1744.

Gallagher F.J. 2008. Soil metal concentrations and vegetative assemblage structure in an urban brownfield. *Environ Pollut* 153, 351–361.

Grebenshchikova, V.I., Efimova, N.V. & Doroshkov, A.A. 2017. Chemical composition of snow and soil in Svirsk city (Irkutsk Region, Pribaikal'e). *Environmental Earth Sciences* 76(20), 712.

Grebenshchikova, V.I., Gritsko, P.P., Kuznetsov, P.V. & Doroshkov, A.A. 2017. Uranium and thorium in soil cover of the Irkutsk-Angarsk industrial zone (Baikal region). *Bulletin of the Tomsk Polytechnic University, Geo Assets Engineering* 328(7), 93–104.

Kabata-Pendias, A. & Pendias, H. 2001. *Trace elements in soils and plants*. CRC Press LLC, Boca Raton.

Lenoir, T., Duc, M., Lassabatere, L. & Bellagh, K. 2019. Identification of the artifact contribution to two urban Technosols by coupling a sorting test, chemical analyses, and a least absolute residual procedure. *Journal of Soils and Sediments* 19(2), 683–701.

Mazhari, S.A., Bajestani, A.R.M., Hatefi, F., Aliabadi, K. & Haghighi, F. 2018. Soil geochemistry as a tool for the origin investigation and environmental evaluation of urban parks in Mashhad city, NE of Iran. *Environmental Earth Sciences* 77(13), 492.

Naylo, A., Almeida Pereira, S.I., Benidire, L., Schwartz, C. & Boularbah, A. 2019. Trace and major element contents, microbial communities, and enzymatic activities of urban soils of Marrakech city along an anthropization gradient. *Journal of Soils and Sediments* 19(5), 2153–2165.

Ngun, C.T., Pleshakova, Y.V. & Reshetnikov, M.V. 2018. Soil diagnosis of an urban settlement with low levels of anthropogenic pollution (Stepnoe, Saratov region). *IOP Conference Series: Earth and Environmental Science* 012067.

Seleznev, A., Yarmoshenko, I., Malinovsky, G., Kiseleva, D. & Gulyaeva, T. 2019. Snow-dirt sludge as an indicator of environmental and sedimentation processes in the urban environment. *Scientific Reports* 9(1), 17241.

Tepanosyan, G., Sahakyan, L., Belyaeva, O., Maghakyan, N. & Saghatelyan, A. 2017. Human health risk assessment and riskiest heavy metal origin identification in urban soils of Yerevan, Armenia. *Chemosphere* 184, 1230–1240.

Tepanosyan, G., Sahakyan, L., Zhang, C. & Saghatelyan A. 2019. The application of Local Moran's I to identify spatial clusters and hot spots of Pb, Mo and Ti in urban soils of Yerevan. *Applied Geochemistry* 104, 116–123.

Timofeev, I., Kosheleva, N. & Kasimov, N. 2019. Health risk assessment based on the contents of potentially toxic elements in urban soils of Darkhan, Mongolia. *Journal of Environmental Management* 242, 279–289.

Tume, P., Roca, N., Rubio, R., King, R. & Bech, J. 2018. An assessment of the potentially hazardous element contamination in urban soils of Arica, Chile. *Journal of Geochemical Exploration* 184, 345–357.

Yalaltdinova, A., Kim, J., Baranovskaya, N. & Rikhvanov L. 2018. *Populus nigra* L. as a bioindicator of atmospheric trace element pollution and potential toxic impacts on human and ecosystem. *Ecological Indicators* 95, 974–983.

Advances in Raw Material Industries for Sustainable Development Goals – Litvinenko (Ed)

Soil evolution and reclamation of technogenic landscapes in Siberia

V.A. Androkhanov
Doctor of Biological Sciences, Acting Director, Institute of Soil Science and Agrochemistry, Novosibirsk, Russian Federation

D.A. Sokolov
Candidate of Biological Sciences, Senior Researcher, Institute of Soil Science and Agrochemistry, Novosibirsk, Russian Federation

ABSTRACT: Specific features of soil evolution were revealed as a result of the long-term studies of soils developing on the coal mining spoils in Siberia. The evolutionary trends and transformation rates of young soils were shown to be determined by the spoil parent rock material, as well as by the environmental and climatic conditions of the area. Biological reclamation carried out taking into account regional soil evolution features provides the possibility a) to use the parent rock lithogenic resources more efficiently and economically, b) to avoid unfavorable combinations of parent rock properties, climate and biota species, used at the biological stage of recultivation, and c) to increase technogenic landscape diversity due to scientifically based alternation of parent rocks in spoil surface layers.

1 INTRODUCTION

Currently the impact of industrial production on natural landscapes of some regions in Russia reached such a level when negative consequences exert significant influence on natural processes and environment. Continuous development of mining industry, wide use of surface mining, as well as other aspects of economy increase the areas used for waste dumping. Reclamation or revegetation due to natural succession (Shrestha, Lal, 2010; 2011; Huot et al., 2015; Ahirwal et al., 2016; Feng et al., 2019) can minimize such negative consequences. Transformation of ecological functions of technogenic landscapes under both approaches result in soil cover evolution alongside with biogeocenoses succession and changes in microclimate and parent rock material. Soil evolution from the initial parent rock towards the state of equilibrium with environmental conditions is usually referred to as ontogenesis. The specificity of soil ontogenesis in technogenic landscapes is manifested by continuous changes taking place over short time spans (Ivanov et al., 2015). Following the ontogenetic one, the post-ontogenetic stage of soil evolution results in meta-stable, i.e. relatively equilibrated, soil state.

Assessing the above-mentioned soil formation features from the practical aspect makes it obvious that soil evolution process in technogenic landscapes should be aimed at spoil rock substrate transformation in such a way as to increase its beneficial soil ecological functions. The combination of such functions in the short term, i.e. at the ontogenetic stage, ensures surface compaction and vegetation cover, whereas in the medium and long term, i.e. at the post ontogenetic stage, promotes sustainability of biotic communities, able to reproduce their main components.

So the aim of the study was to reveal the regularities and specific features of soil evolution in the technogenic landscapes with the view to use the findings for increasing efficiency of reclamation approaches.

2 METHODS

The soils developed on the coal mining spoils of the major coal mining areas in Siberia were used at the objects of the study. We studied the soil cover of the coal mining spoils located in the montane taiga (humid) and forest-steppe (sub-humid) areas of the Kemerovo region, in the steppe (semi-arid) areas of Khakassia and dry steppe (arid and extra continental) areas of the Tyva Republic. Some brown coal and anthracite mining sites in the Krasnoyarsk and Novosibirsk regions, where spoil parent rocks differ in metamorphosis, were also studied. The parent rock material of all spoils was not phytotoxic.

To reveal specifics of soil evolution we examined soil cover by using macromorphometry description, widely used in pedology (Rosanov, 1983). Soil identification was performed using soil classification of technogenic landscapes, a methodology developed by the Institute of Soil Science and Agrochemsitry of the Siberian Branch of the Russian Academy of Sciences (Gadzhiev, Kurachev, 1992) and then further improved by V.M.Kurachev and V.A.Androkhanov (2002). According to this classification, the identification of a corresponding diagnostic horizon allows to discriminate four types of embryozems on the surface of coal mining spoils. The so called initial embryozems do not have any diagnostic horizons that are morphologically well expressed. The OM-accumulating embryozems are distinguished by the presence of horizons where accumulation of non-specific organic matter (represented by plant material) occurs. Soddy and humus-accumulating embryozems are diagnosed by the presence of respective horizons. According to the World Reference Base for Soil Resources (World Reference. . ., 2015), embryozems are classified as Technosols.

The study was carried out on the horizontally leveled sites, differing in age and parent rock material.

3 RESULTS

The results showed that soil cover formation at the ontogenetic stage of soil evolution in different climatic environments and parent rock materials is going at different rates. All four embryozem types, i.e. initial, OM-accumulating, soddy and humus-accumulating (Table 1), were found in the studied areas. Each embryozem type corresponds to a certain stage of soil evolution, identified by the degree of visualization of OM-accumulating, soddy and humus-accumulating processes in an embryozem profile (Sokolov et al., 2015). The rate of transformation from initial into OM-accumulating and further into soddy and humus-accumulating embryozems was found to be determined by parent rock properties and climate of the regions.

Soil cover of technogenic surface layers, consisting of sandstone, is characterized by minimal diversity of soil types as compared with the soil cover developed on other dense

Table 1. Ontogenetic differentiation of soil cover composition at different technogenic substrates as dependent on environmental and climatic conditions.

			Parent rock material		
Climate type	Sandstone	Siltstone	Mudstone	Sand	Loams and clays
Humid	EI, EOA	EI, EOA, ES	EI, EOA, ES, EHA	EOA	EOA, ES, EHA
Sub-humid	EI, EOA, ES	EI, EOA, ES, EHA	EI, EOA, ES, EHA	EOA, ES	EOA, ES, EHA
Semiarid	EI, EOA, ES	EI, EOA, ES, EHA	EI, EOA, ES EHA	EI, EOA	EOA, ES, EHA
Arid	EI	EI, EOA	EI, EOA, ES	EI, EOA	EOA, ES
Arid Extracontinental	EI	EI, EOA	EI, EOA	EI	EI, EOA

EI – initial embryozem; EOA – organic matter accumulating embryozem; ES – soddy embryozem; EHA – humus-accumulating embryozem.

sedimentary rocks. Such situation is due to a) significant resistance of sandstone to hypergenic transformation, and b) low (5–20%) contribution of swelling minerals in rock cement (Ragimzade, 1992); both factors impede the formation of humus-accumulating embryozems on such surfaces and, consequently, sustainable grass communities (Glebova, 2005). As a result, in all climatic regions during 20–25 years of technogenic landscapes' existence initial embryozems comprise substantial fraction of soil cover. Under climatic conditions ranging from humid to semi-arid ones initial embryozems are accompanied by OM-accumulating embryozems, and in sub-humid regions soddy embryozems are also present in the soil cover. Notably, the same sandstone properties that limit multicomponent composition of soil cover, under humid climate promote eluvial processes in embryozems and hence the formation of woody plant communities.

More favorable conditions for soil cover differentiation occur in those technogenic landscapes, where surface layers consist of silt- or mudstone. These materials are more susceptible for hypergenic transformation as compared with sandstone and are often of laminated texture, impeding eluvial processes in embryozems. At the same time relatively high content of expansive minerals in rock cement (15–35% in siltstone and 55–65% in mudstone) together with carbonaceous inclusions promote formation of sustainable grass communities. All these facilitate the formation of OM-accumulating embryozems in the studied regions, with soddy embryozems developing under less arid climatic conditions (Table 1). Humus-accumulating embryozems can also develop on such parent rocks, i.e. on siltstone under sub-humid climate and mudstone under humid and semiarid climate.

Alongside with soils of the later stages of embryozem genesis, initial and OM-accumulating embryozems persist in the surface layers composed of silt- and mudstone. Such soil cover differentiation results from the differential content of stone fractions and differential metamorphosis of parent rock material.

Ontogenetic differentiation of soil cover on sands is similar to the one on sandstone. However, as soil formation on loose parent material is not accompanied by disintegration of fragments, sufficient precipitation results in practically no initial embryozems in soil cover developed over 20-25 yrs.

The best conditions for transformation of sandy substrate by pedogenic and biotic processes occur in regions with humid climate, where from the first years of phytocenoses' development soil environment benefits predominance of woody vegetation and OM-accumulating embryozems in soil cover. Under sub-humid climate due to low intensity of eluvial processes soddy embryozems contribute significantly into the soil cover. In arid regions there is minimal differentiation of soil cover, developed on sand material. This is also facilitated by deflation processes, increasing with the increased climate aridity. Frequent denudation renewal of surface sandy layers also leads to predominance of initial embryozems in the soil cover.

Clay and clay loams are the most common loose sedimentary materials of the coal mining spoils in Siberia. Transformation of such surface spoil layers, similar to the sandy ones, by pedogenic and biogenic processes begins in the substrate, most favorable for soil formation. High content of fine-sized fractions results in formation of soddy and humus accumulating embryozems over 20-25 years of revegetation.

Soil cover differentiation at the post ontogenetic stage of evolution occurs after embryozems reach meta-stable stage of development. At this stage soil transformation occurs mainly as changes in properties of organogenic horizons. The main driver of the process is substitution of the successional stages of phytocenoses with climax communities, adequate for the surrounding natural environment and climatic conditions. In different regions such substitution does not occur in a similar way. Under moderate arid and humid conditions the meta-stable state as a result of soil evolution is reached at the stage of a closed phytocenosis (Glebova, 2005). In arid conditions the meta-stable state is reached when various sagebrush species become predominating over legumes (Titlyanova, Sambuu, 2016). In humid conditions the meta-stable state of soils is reached when tree crowns close and surface illumination regime changes.

The described changes in phytocenoses directly affect the properties of the upper part of soil profile, allowing more detailed diagnostics of surface differentiation according to soil

formation conditions. In embryozems with the same sequence of genetic horizons it becomes possible to diagnose processes in order to ascribe soils to a certain subtype. There was a need to identify soil subtypes on the old (20-25 yrs) coal mining spoils in Siberia. So among initial embryozems, along the usually identified typical subtype, common at the initial stages of parent substrate transformation by pedogenic and biogenic processes, a cryptopedogenic subtype was distinguished. Such initial cryptopedogenic subtypes are formed after initial embryozems reach the meta-stable state, and thus usually develop on substrates with low lithogenic potential for soil formation. Similar to initial ones, the cryptopedogenic embryozems do not visually manifest genetic horizons, the presence of which more often results from the absence of conditions for preservation, rather than formation.

The soil type of OM-accumulating embryozems can be differentiated into three subtypes according to soil forming environment. For example, the soils with their type-identifying horizon represented by herbs and grasses' residues, are referred to as OM-accumulating felt embryozems; in litter and peat subtypes this horizon is represented by tree litter and moss phytomass.

The identification of soddy embryozem subtypes is more complicated. A combination of features is used to discriminate between xerophytic and hygrophytic subtypes, including the character of interaction between the type-diagnostic horizon with the underlying mineral soil, as well as the composition of the horizon above the soddy one, with sedge residues contributing significantly into the litter of the latter one.

Because humus-accumulating embryozems can form in a quite narrow range of climatic and lithogenic conditions, their differentiation into subtypes according to soil formation conditions is rather problematic. Identified earlier as an individual soil type (Gadzhiev, Kurachev, 1992), currently coarse humus-accumulating embryozems are considered to be a subtype of humus-accumulating embryozems. We believe their development results from the transformation of humus-accumulating horizon, developed during the preceding stage of grass vegetation, rather than from specific humus accumulation in technogenic forest ecosystems.

As post ontogenetic stage of soil evolution starts simultaneously with establishment of constant phytocenotic structure, its specific moment of establishment varies due to conditions, determining the syngenetic transformation of substrate by pedogenic and biogenic processes. It was shown to take 25-26 years under the most favourable conditions in Siberia, i.e. on clay loamy spoils in Kansk-Achinsk coal mining region in Central Siberia (Mironycheva-Tokareva, 1998). On substrates formed by dense sedimentary rocks sustainable soil cover can be developed over 50 years or more (Kurachev, Androkhanov, 2002).

Alongside with soil cover features, mentioned above, another characteristic feature of metastable soil cover is not only its temporal stability, but also its constant composition irrespective of heat- and water supply in some years or over a period of several years. This peculiarity results in low soil cover differentiation on territories composed of the same parent rock material. Such stability of soil cover can best be seen in pedogenesis under humid conditions on sandstone material (Table 2). Development and closinging of tree crowns ensures plant litter input practically on entire soil surface. Similar situation can be observed under sub-humid climate with an exception that the sites with herb and grass communities are dominated by the subtype of soddy xerophytic embryozems. Pedogenesis under arid conditions on sandstone results in formation of OM-accumulating felt embryozems. With increasing climate aridity the contribution of this subtype into soil cover becomes less than the one of the initial cryptopedogenic embryozem subtype.

On siltstone surface layers soil cover differentiation at the stage of its stabilization is mostly driven by the same factors as on sandstone spoils. However, due to the production of fine-sized particles from siltstone material via its destruction, the formation of humus-accumulating and soddy xerophytic embryozems becomes possible in sub-humid and semiarid climatic conditions, respectively. In regions with typical arid climate this siltstone characteristic results in the dominance of the OM-accumulating felt embryozems.

In regions where spoil parent rock material is mudstone (Table 2), soil cover in technogenic landscapes is the most differentiated. High variability of mudstone properties resulted in the prevalence of OM-accumulating litter embryozems and coarse humus accumulating

Table 2. Post ontogenetic differentiation of soil cover developed on different substrates in the technogenic landscapes under different climatic conditions.

			Parent rock material		
Climate type	Sandstone	Siltstone	Mudstone	Sand	Loams and clays
Humid	EOAl	EOAl	EOAl, EOAp, EHAch	EOAl	EOAl, ESh, EHAch
Sub-humid	EOAl, ESx	ESx, EHA	ESx, ESh, EHA	ESx	EHA
Semiarid	EOAf	EOAf, ESx	EOAf, ESx, EHA	EOAf, ESx	EHA
Arid	EIC, EOAf	EOAf	EOAf, ESx	EOAf	ESx
Arid extracontinental	EIc	EIc, EOAf	EIc, EOAf	EIc	EOAf

EIc– initial cryptopedogenic embryozem; EOAl – organic matter accumulating litter embryozem; EOAf – organic matter accumulating felt embryozem; EOAp – organic matter accumulating peat embryozem; ESx – soddy xerophytic embryozem; ESh – soddy hygrophytic embryozem; EHA – humus accumulating embryozem; EHAch – coarse humus accumulating embryozem.

embryozems in soil cover of the humid regions. OM-accumulating peat embryozems develop on highly compacted surface layers, composed of highly metamorphosed mudstone. Under sub-humid climate the dominant OM-accumulating embryozems are substituted by humus accumulating and soddy xerophytic and hygrophytic ones. With further increase in aridity the share of the above-mentioned soils in the soil cover decreases, whereas the share of OM-accumulating felt embryozems increases. Under arid extra continental climate the contribution of initial cryptopedogenic embryozems becomes more pronounced.

Soil cover composition on sand rock is similar to the one on sandstone. However, high dispersion, resulting in the relatively high water-holding capacity of sands, shifts pedogenesis towards prevailing formation of soddy xerophytic embryozems in sub-humid and semi-arid regions and towards OM-accumulating felt embryozems in arid regions.

Soil cover differentiation at the post ontogenetic evolution stage is less pronounced in loamy and clay surface layers, as their properties promote quick implementation of specific zonal soil formation. Thus more than 20-years-old areas of coal mining spoils, composed of such parent rock material, display similar soil cover composition in most climatic regions except for the humid ones, where soddy hygrophytic embryozems are widely spread alongside with OM-accumulating litter embryozems, with" residual" coarse humus accumulating embryozems being often identified as well.

4 CONCLUSION

Thus our studies showed different potential of parent rock substrates for pedogenesis and differentiated soil cover formation in technogenic landscapes, as related to embryozem types and subtypes. Taking into account that each soil type and subtype under different climatic conditions develops under certain vegetation formation, one can design adequate approaches for technical and biological reclamation. The latter, based on the revealed features of soil evolution, allows to 1) use lithogenic resources more efficiently and economically; 2) to minimize or avoid those combinations of parent rocks, climatic conditions and plant species, which are unfavourable for pedogenesis; 3) to increase biological diversity of technogenic landscapes by reasonably alternating parent rock materials in surface layers.

Overall it can be concluded that parent rock substrates with higher content of physical clay or that are able to produce it due to weathering, i.e. clays, loams, mudstone, are more beneficial for greenery landscaping. The less metamorphised the parent rocks are, the higher their

capacity to release fine-sized fractions is, and hence better the chances to reach the reclamation goals. Mechanic fixing of a surface, i.e. providing geomorphologic stability for a landscape, requires other parent rock substrates. In such cases dense sedimentary materials, resistant to hypergenic transformation (sandstone, strongly metamorphised siltstone and mudstone) are better. The mentioned features enable development of efficient and economically relevant reclamation actions. Their implementation is possible by employing selective spoil formation by using loose or alternating dense sedimentary parent materials for surface layer construction in technogenic landscapes.

REFERENCES

Ahirwal, J. & Maiti S.K. 2016. Assessment of soil properties of different land uses generated due to surface coal mining activities in tropical Sal (Shorea robusta) forest, India. *Catena* 140: 155–163.

Feng, Y., Wang J., Bai Z. et al. 2019. Effects of surface coal mining and land reclamation on soil properties: A review. *Earth-Science Reviews* 191: 12–25.

Gadzhiev, I.M. & Kurachev V.M. 1992. Genetic and environmental aspects of the study and classification of soils of technogenic landscapes. In V.G. Mordkovich, V.I. Volkovintser & T.P. Slavlina (eds), *Ecology and remediation of technogenic landscapes*: 6–15. Novosibirsk: Science. Sib. Br. [in Russian]

Glebova, O.I. 2005. *Biogeographic diagnosis of Kuzbass embryozems*. Novosibirsk: Institute of Soil Science and Agrochemistry SB RAS. [in Russian]

Huot, H., Morel J.L. & Simonnot, M.-O. 2015. Pedogenetic trends in soils formed in technogenic parent materials. Soil Sciences 180 (4-5): 182–192.

Ivanov, I.V. & Kudeyarov, V.N. 2015. *Evolution of soils and soil cover. Theory, diversity of natural evolution and anthropogenic transformations of soils*. Moscow: GEOS. [in Russian]

Kurachev, V.M. & Androkhanov, V.A. 2002. Classification of soils of technogenic landscapes. *Siberian Journal of Ecology* 9 (3): 255–261. [in Russian]

Mironycheva-Tokareva, N.P. 1998. *Dynamics of vegetation during overgrowing of dumps (on the example of KATEK)*. Novosibirsk: Science. Sib. Br. [in Russian]

Ragim-zade, F.K. 1992. Soil-forming rocks of technogenic landscapes. In V.G. Mordkovich, V. I. Volkovintser & T.P. Slavlina (eds), *Ecology and remediation of technogenic landscapes*: 15–45. Novosibirsk: Science. Sib. Br. [in Russian]

Rozanov, B.G. 1983. *Soil morphology*. Moscow: MSU Pubs. [in Russian]

Shrestha, R.K. & Lal, R. 2010. Carbon and nitrogen pools in reclaimed land under forest and pasture ecosystems in Ohio, USA. *Geoderma* 157 (3): 196–205.

Shrestha, R.K. & Lal, R. 2011. Changes in physical and chemical properties of soil after surface mining and reclamation. *Geoderma* 161 (3-4): 168–176.

Sokolov, D.A., Androkhanov, V. A., Kulizhskii, S. P. et al. 2015. Morphogenetic diagnostics of soil formation on tailing dumps of coal quarries in Siberia. *Eurasian Soil Science* 48 (1): 95–105.

Titlyanova, A.A. & Sambuu, A.D. 2016. *Succession in grasslands*. Novosibirsk: Publishing house of the SB RAS. [in Russian]

World reference base for soil resources 2015. International soil classification system for naming soils and creating legends for soil maps. Update 2015. *World soil resources reports, 106. Food and agricuture organization of the United Nations*. Rome.

Advances in Raw Material Industries for Sustainable Development Goals – Litvinenko (Ed)

Lightning exposure of oil tanks with changing roof position

A.I. Adekitan & M. Rock
Group for Lightning and Overvoltage Protection, Technische Universität Ilmenau, Germany

ABSTRACT: Crude oil and related petroleum products are major fossil fuels for the supply of energy globally. Floating Roof Tanks (FRTs) are used for storing crude oil after production to ensure product stability before product export, but FRTs are susceptible to lightning strikes. Lightning is a major threat to operational safety in crude oil storage terminals, particular in the tropics with a very high number of thunderstorm days per year (Td/yr). Protecting crude oil storage tanks against the high-energy lightning current with a continuing current charge of 200 Coulomb requires the design and implementation of a purpose-specific lightning protection system. An evaluation of the probability of a lightning strike to a FRT using the dynamic electro-geometrical model (DEGM) was performed using numerical techniques. The results for the cases considered show that the total probability of a direct strike to the circular tip of the tank shell at its topmost height varies from about 85% to 99% depending on the dimension of the tank and the position of the floating roof within the tank.

Keywords: Floating roof tank, lightning strike probability, dynamic electro-geometrical model, lightning protection system, lightning current distribution, numerical methods, oil and gas facility, fire, process safety

1 INTRODUCTION

Lightning is a natural phenomenon that is as old as the earth itself. Lightning strikes to structures on earth may be very dangerous to facilities, and equipment depending on the level of risk associated with the structure as a function of the geographic location, nature and dimension of the structure, and adjoining facilities. The geographic location determines the number of lightning flashes that the structure is exposed to annually. Lightning strike can either be direct i.e. when the flash terminates on a structure or indirect, when the flash terminates near the structure and connected services. Out of 102 floating roof tank fires studied in China by Ren et al. (2012), it was discovered that 65% of these were due to direct lightning strikes (Wei et al., 2018). Lightning strike to structures and equipment can result in damage, fire, and even injury to living beings. A lightning flash can either be negative or positive, and fact as shown that about 90% of lightning flashes are of the negative type while positive flashes carry about six times more current than the negative type (Afa, 2012, Akinyemi et al., 2014).

A number of lightning-induced floating roof tank and facility fire incidents, and equipment damage have occurred across the globe resulting in equipment and facility destruction, expensive repair cost, loss of production time, and man-hours expended on incident reviews. An external floating roof tank has a floating roof that moves with the level of the liquid within the tank in order to limit the vapor space above the liquid crude oil. This helps to reduce the evaporation of light oil fractions and petroleum products by 90-98% (Kulikov & Chekardovskiy, 2018). The roofs are made of pontoons which aid the buoyancy of the roof. The gap between the floating roof and the tank shell is covered by rim seals which prevent crude oil from leaking onto the roof. Also, it limits vapor escape from the shell-roof gap. The rim seal region of a floating roof tank is the most likely starting point for a lightning-induced tank fire during a thunderstorm (Chang & Lin, 2006, Adekitan & Rock, 2019a).

Any vapor that escapes from the crude oil during service will bubble to the surface, and escape to the atmosphere through breather valves that are set at atmospheric pressure. High-pressure liquids should not be diverted to a floating roof tank because it can generate sufficient vapor pressure to jam the roof. High crude-oil true vapor pressure (TVP) coupled with inefficient safety barriers from the production end can result in excessive vapor release on the floating roof tank (Adekitan & Rock, 2019b). The accumulation of escaped flammable vapor around the tank, and the rim seal region can be ignited when lightning strikes.

1.1 *Modes of FRT ignition by lightning*

A floating roof tank can be ignited by lightning in three ways, and these are:

a. Roof surface electrostatic charging due to the charge separation occurring in the clouds which creates a pre-strike electromagnetic field that setup transient currents.
b. When lightning strikes, sparks can easily be generated between intended and unintended gaps existing on the floating roof tank. Sparks can either be a thermal spark resulting from the formation of incendiary materials at a spark point, or a voltage spark that results in the electrical breakdown of air-vapor mixture within the gap.
c. Heating due to the flow of heavy lightning current which can cause thin tank materials that are less than 5 mm in thickness to melt.

A floating roof tank is a massive structure with a large diameter and tall height, and a gap at the shell-roof interface where flammable fuel vapor may accumulate, and this makes it difficult to design a simple and effective conventional lightning protection system for a floating roof tank. To ensure continuity for the flow of lightning current from the tank shell to the roof during lightning strike, the shell-roof linkage provided by the roof stairs, the use of bypass conductors, and shunts have all been considered, and each has been found to be defective in one way or the order, as they do not continuously provide the optimal low resistance shell-roof connection that can effectively prevent sparks at the rim seal region of the floating roof tank [7]. For example, bypass conductors create dangling cables on the roof, shunts can be easily coated with crude oil which increases its contact resistance. Also, floating roof tank may lose its perfect roundness over time, or when tank subsidence occurs the shunts become disconnected from the tank shell creating a gap it was installed to prevent.

A device called a retractable grounding array (RGA) was developed in order to address the issues created by the extensive length of bypass cables. RGA is made of retractable weaved cable strands that adjust its length based on the position of the roof. Although the RGA may be better than the bypass cable which conducts the continuing, and the intermediate components of the lightning current by ensuring minimal length at any roof position (Hu & Liu, 2012), but its sufficiency as a replacement for shunts which are meant to conduct the fast (rising) lightning current pulse needs to be determined. Also, due to continuous extension and retraction of the RGA with the changing floating roof position, a number of RGAs tend to snap off from the roof over time, as observed on some tanks. The roof of the floating roof tank constantly changes its vertical position within the tank based on the level of the liquid content, and as such, the portion of the roof exposed to direct lightning strike varies depending on the position of the roof.

Currently, there is no approved air termination design based on conventional lightning protection system for FRT. This is due to the intricacies of how direct and indirect lightning strikes interact with FRT. In this study, the interaction of lightning with FRT is investigated by evaluating the probability of lightning strikes to different points on a FRT using the dynamic electro-geometrical model. Based on the result of the numerical model, an air termination configuration that can adequately intercept and safely dissipate the high energy lightning current while preventing sparking at the shunt-shell interface can now be developed.

2 MATERIALS AND METHODS

The methodology applied in this study has three key aspects. First, a volume from which lightning can strike a FRT is defined as the attractive volume as discussed in section 2.1, while section 2.2 highlights the details of a numerical model termed the dynamic electro-geometrical model (DEGM) for computing the probability of a direct lightning strike to structures within the defined volume. Finally, the DEGM model is applied to various dimensions of a FRT as described in section 2.3.

2.1 *The attractive volume of a FRT*

The risk of a lightning strike to a structure can be evaluated using the concept of the attractive volume. The attractive volume defines a space volume around a structure to be protected within which lightning strikes can hit the object. The object is deemed naturally protected from all lightning downward leaders which do not enter the attractive volume of the protected object. The concept was developed to explain the stochastic nature of the descent of a downward leader, and the orientation point at which the object to be struck by lightning is determined (Horváth, 1991). The distance between the orientation point, and the object to be struck or the ground is known as the striking distance. It is a function of the lightning-induced electrical field strength on the ground, and this also depends on the magnitude of the electric charge in the lightning leader channel.

By applying increasing striking distance, various rolling sphere radii that can touch the FRT and the ground were computed, the centers of such spheres as shown by the curved black line in Figure 1 represent the boundary of the interception volume of the FRT on the "right" side of the structure. The same concept applies on all sides around the structure, and this will generate a volume within which downward leaders can orientate towards the floating roof tank.

2.2 *The dynamic electro-geometrical model (DEGM)*

The peak value of lightning current has been measured and recorded at different regions of the world, and this has been used to develop a distribution function for the striking distance (r) using logarithm normal functions (Horváth, 2006). In terms of the striking distance, the probability density function (PDF) is defined by Equation 1. By applying the median value of lightning current distribution and the standard deviation for positive and negative lightning, the distribution obtained is shown in Figure 2. Also, the effective probability distribution

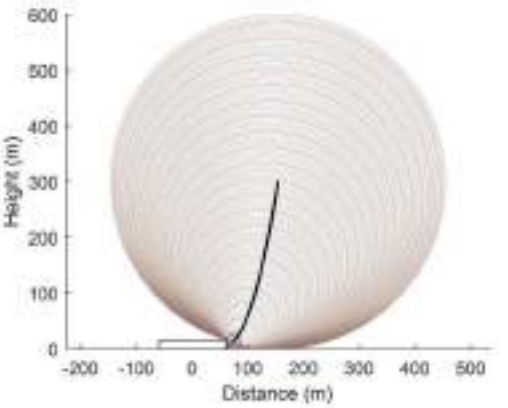

Figure 1. Interception boundary at one side of FRT.

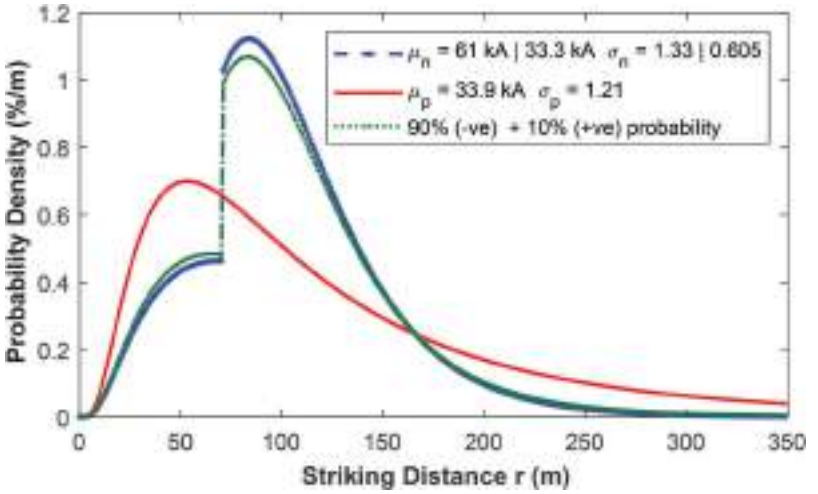

Figure 2. Striking distance probability density (blue, n – negative lightning, red, p – positive lightning).

resulting from the summation of 90% of the PDF for negative lightning and 10% for positive lightning is also plotted in comparison in Figure 2. From lightning observations over time, about 90% of all lightning strikes have negative polarity, and as such, the effective probability distribution will be applied in the numerical computation of the dynamic electro-geometrical model (Hannig et al., 2014).

The DEGM applies the concept of probability weighted collection volume (Horváth, 2006), which modulates collection volume by the probability density function i.e. the striking distance density. To apply the DEGM concept to a floating roof tank (FRT), the surface of the FRT is first discretized into various surface points, and the associated interception volume enclosed by the circle centers as shown in Figure 1 is also discretized into multiple orientation points from which lightning can orientate towards the FRT. For each orientation point in space, the distance to various points on the FRT is computed, and the point(s) on the FRT having distances equal to the lowest geometric distance are determined as the final strike point(s) from that specific orientation point in space above the FRT (Adekitan & Rock, 2020). The associated probability is computed using Equation 1, and the process is repeated for all the orientation points within the interception volume. The probability of a strike to the same point on the FRT from different orientation points is cumulated. Finally, the overall probability for all the points on the FRT is summed, and from this value, the percentage of the probability of a strike for each point on the FRT can be computed. This is a numerical computation which has also been applied by Kern et al. (Kern et al., 2010) for various structures.

$$PDF(r) = \frac{10^{\frac{-1}{0.65}}}{0.65} r^{\frac{0.35}{0.65}} \frac{1}{\sigma\left(\frac{r}{10}\right)^{\frac{1}{0.65}}\sqrt{2\pi}} e^{\frac{-\left\{\ln\frac{\left(\frac{r}{10}\right)^{\frac{1}{0.65}}}{\mu}\right\}^2}{2\sigma^2}} \quad (1)\leftarrow$$

Where r is the striking distance, μ is the median value and σ is the standard deviation (σ) of the lightning current distribution.

2.3 *Numerical simulation of various FRT dimensions and roof positions*

Large floating tanks are more susceptible to lightning induced ignition and fires. This is due to the increased surface area that is exposed to direct lightning strikes, and the consequences

of indirect strikes as charges accumulate on, and around the tank. The position of the floating roof changes within a FRT based on the level of the liquid in the tank. Due to the changing roof position, the exposed area of the roof that can be struck by lightning from above the tank, and within the interception volume of the FRT i.e. cloud-to-ground strikes (Wang et al., 2018), varies with the position of the roof (Adekitan & Rock, 2019b).

In this study, the effect of tank height and the position of the roof within the tank on the probability of lightning strike to different points on a FRT is examined. Three different tank heights were considered; 10 m, 15 m, and 20 m high FRTs with a diameter of 60 m. The roof positions were simulated to determine the effect of changing roof position. The first roof position is at the top, when the roof is most exposed to direct lightning strikes. The middle position, at half the height of the tank was also considered, and the bottom position which for this simulation was set at 0.5 m from the ground. Usually, the roof does not get to 0 m on the ground. At the base of the tank, the roof sits on adjustable legs, that may be as high as 2 m to allow for man-entry for maintenance checks.

3 RESULTS AND DISCUSSION

The results of the numerical analysis for the various roof positions are presented in this section.

In Figure 3, the floating roof of the 30 m radius tank with 20 m in height is at the topmost position, and at this point, the roof has the highest exposure to direct lightning strikes. In Figure 4, the roof is at half the height of the tank and only a small portion of the tank roof

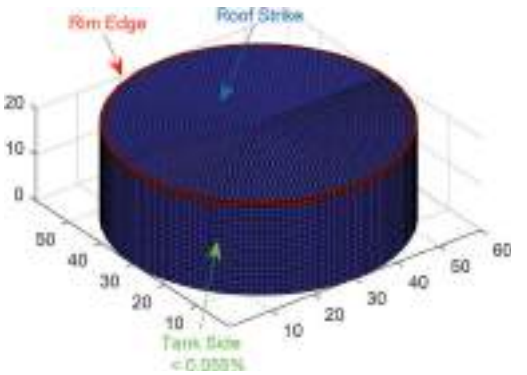

Figure 3. Floating roof at the highest position within the tank.

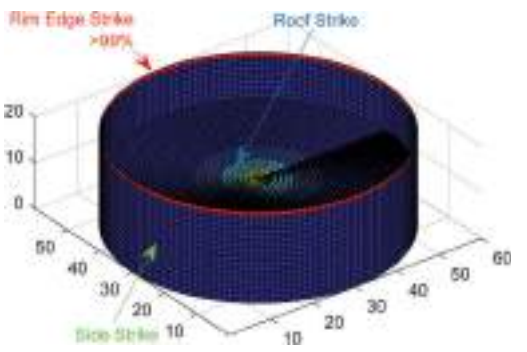

Figure 4. Floating roof at the middle height of the tank.

around the center is exposed to direct cloud-to-ground strikes. In Figure 5, the roof is shown at the base of the tank, and at this position the risk of a direct lightning strike to the roof is extremely small.

The surface of the FRT is categorized into three: the roof, the rim edge which refers to the topmost circular portion of the cylindrical tank shell, and the side of the tank which encompasses the remaining cylindrical wall of the tank below the rim edge. The probability of a strike to each of these three parts is presented for the 10 m, 15 m, and 20 m high FRT in Figure 6, Figure 7, and Figure 8 for the various roof positions (top, middle, and bottom).

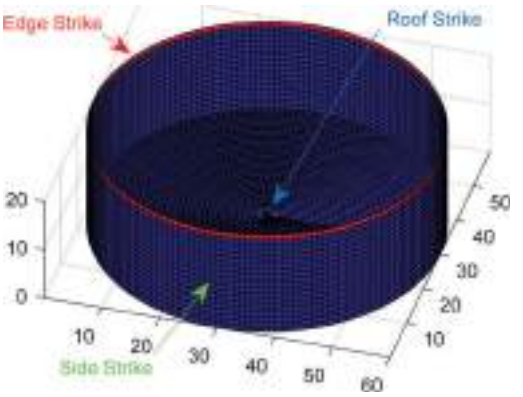

Figure 5. Floating roof at the base of the tank.

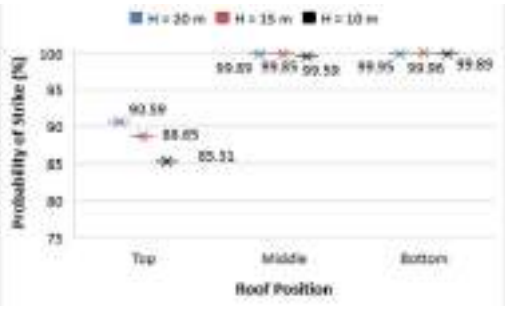

Figure 6. Probability of a lightning strike to the rim edge of the tank cylinder.

Figure 7. Probability of a lightning strike to the side of the tank.

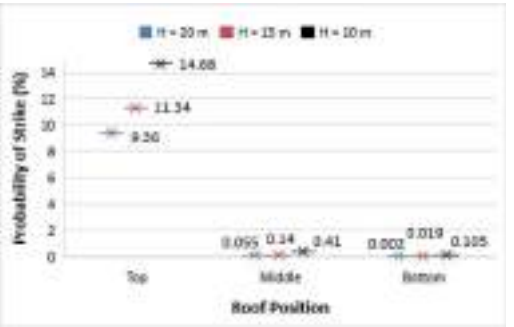

Figure 8. Probability of a lightning strike to the roof of the FRT.

The probability of a lightning strike to the rim edge of the tank cylinder for the three different tank heights considered is shown in Figure 6. It was observed that the probability of a strike to the rim of the cylindrical tank shell increased with tank height at the topmost roof position. At other roof positions i.e. midway, and at the bottom, the probability of a strike to the rim edge is greater than 99%, and this did not change significantly with tank height.

As shown in Figure 7, the probability of a strike to the remaining part of the tank cylindrical shell referred to as tank side increases with tank height (i.e. more exposed tank wall surface area), but the probability of a strike is relatively constant with changing roof position.

For the floating roof as shown in Figure 8, the probability of a direct lightning strike reduces with increasing tank height when the roof is at the topmost height. At the middle position, the probability of a strike to the roof reduces slightly with increasing height, and at the bottom, the probability of a strike is relatively constant irrespective of tank height.

The highest probability of a direct strike occurs when the roof is at the topmost position. The probability of a direct strike to the rim edge, i.e. the rim-seal area of the tank where shunts are positioned, with a high probability of flammable vapor presence is highest as compared with the risk of a strike to the side of the tank or the floating roof. When heavy currents flow through the shunt-shell contact within the rim-seal region, the risk of spark formation is high. Hence, it is necessary to ensure that lightning currents flowing down to the rim edge is minimal. This may be achieved by using interconnected, parallel air termination arrangements, which create multiple flow paths for the lightning current and associated energy. This cannot be achieved by using vertical air termination rods on the FRT shell that will only intercept strikes and conduct the full currents down to a single point on the tank shell.

From the simulated results, the frequency of lightning strike (N_i) can be computed for the rim edge, the roof, and the side of the tank by applying Equation 2.

Frequency of lightning strike (N_i) = ground flash density (N_G) × probability modulated collection volume (CP)

$$N_i = N_G \times CP \tag{2}$$

Where N_G is the ground flash density in flashes/km^2/year, and CP is the computed probability using DEGM for the rim seal, the roof, and the side of the tank. Assuming, the tank is located in the Niger Delta region of Nigeria; the analysis is therefore based on a ground flash density of 16 flashes/km^2/year. The estimated frequency of a lightning strike to the three categorized areas of the FRT is computed for the different tank heights and roof positions. The result is presented in Table 1 for the 10 m high FRT, Table 2 for the 15 m high FRT, and Table 3 for the 20 m high FRT. The variation in the estimated frequency of lightning strikes for the different roof positions is because of the changing total exposed area of the FRT that is susceptible to direct lightning strike as the roof changes position.

Table 1. The frequency of lightning strike per year for the 10 m high FRT.

	Rim Edge	Side Wall	Roof
Top	0.2479	0.000008	0.0427
Middle	0.2929	0.000008	0.0012
Bottom	0.2943	0.000008	0.0003

Table 2. The frequency of lightning strike per year for the 15 m high FRT.

	Rim Edge	Side Wall	Roof
Top	0.3336	0.00006	0.0427
Middle	0.3796	0.00006	0.0005
Bottom	0.3802	0.00006	0.0001

Table 3. The frequency of lightning strike per year for the 20 m high FRT.

	Rim Edge	Side Wall	Roof
Top	0.4129	0.00024	0.0427
Middle	0.4593	0.00024	0.0003
Bottom	0.4596	0.00024	0.0000

4 CONCLUSIONS

The risk of a strike to various points on a floating roof tank (FRT) is dynamic, and it is influenced by the position of the roof within the tank. The dimension of a FRT plays a significant role in the manner of exposure of such tanks to direct lightning strikes. The dynamic electro-geometrical model simulations carried out in this study reveals that the height of a FRT and the position of the floating roof determines the risk of a direct lightning strike to the roof. The numerical simulation shows that when the roof is at the uppermost point, the risk of a strike to the rim edge (around the rim seal region) where flammable vapor concentration is often present, increases with increasing tank height for the same diameter tank. As the roof descends into the tank, the probability of a lightning strike to the rim edge increases with reducing roof height. By the time the roof is at half the height of the tank, the probability of a strike to the rim edge of the tank shell is around 99%.

In line with the realities of the result of this simulation, conventional air terminations positioned on the FRT must be designed, not only to be able to intercept lightning strikes e.g. by using air termination rods, but also, it must be able to divide the lightning current into multiple flow parts in order to reduce the risk of sparking when the current gets to the rim seal region of the tank shell where arcing may occur at the shunt-shell region. This study as revealed the likelihood of lightning strikes to various parts of a FRT with respect to floating roof position. The knowledge provided here, will serve as bases for the design and investigation of various conventional air termination arrangements for reliably protecting a FRT from direct strikes while also preventing arcing at the rim-seal region.

ACKNOWLEDGMENT

This is to appreciate the support of the Nigerian Petroleum Technology Development Fund (PTDF) through the Overseas Scholarship Scheme in partnership with the German Academic Exchange Service (DAAD).

REFERENCES

Adekitan, A. I. & Rock, M. 2019a. Lightning induced fires: A case study of floating roof tanks. XII Russian-German Raw Materials Forum: Youth Day, St Petersburg, Russia. Saint-Petersburg Mining University, 156–157.

Adekitan, A. I. & Rock, M. 2019b. Performance investigation of Lightning Protection Systems for Floating Roof Tanks in Nigeria. 13. VDE Blitzschutztagung, 24. – 25. Oktober 2019 Aschaffenburg. VDE Fachberichte, 71–77.

Adekitan, A. I. & Rock, M. 2020. The impact of space point definition on dynamic electro-geometrical model of lightning strike probability. *Electric Power Systems Research*.

Afa, J. T. 2012. Lightning Activities and Ground Flash Density in Niger Delta Coast. *Journal of Engineering and Applied Sciences*, 7, 339–341.

Akinyemi, M., Boyo, A., Emetere, M., Usikalu, M. & Olawole, O. 2014. Lightning a Fundamental of Atmospheric Electricity. International Conference on Environment Systems Science and Engineering, 47–52.

Chang, J. I. & Lin, C. 2006. A study of storage tank accidents. *Journal of Loss Prevention in the Process Industries*, 19, 51–59.

Hannig, M., Hinrichsen, V., Hannig, R., & Brocke, R. 2014. An analytical consideration on the striking probability and the total amount of strikes to simple structures according to standardized regulations. *32nd International Conference on Lightning Protection (ICLP*). IEEE.

Horváth, T. 1991. Computation of lightning protection. *Cargese Lectures in Physics*.

Horváth, T. 2006. Interception of lightning air termination systems constructed with rolling sphere method. Proc. *28th International Conference on Lightning Protection (ICLP*).

Hu, H. & Liu, Q. 2012. Research on lightning sparks discharge and protection measures of large floating roof tank. *31st International Conference on Lightning Protection (ICLP)*. IEEE, 1–4.

Kern, A., Schelthoff, C. & Mathieu, M. 2010. Probability of lightning strikes to air-terminations of structures using the electro-geometrical model theory and the statistics of lightning current parameters. *30th International Conference on Lightning Protection (ICLP*). IEEE.

Kulikov, A. M. & Chekardovskiy, S. M. 2018. Improving the safety of operation of tanks with a floating roof in the winter period. IOP Conference Series: Materials Science and Engineering, IOP Publishing, 445 012010.

Ren, X., Fu, Z., Yan, N., & Sun, W. 2012. Analysis and experimental investigation of direct lightning protection for floating roof oil tanks. *Electric Power Systems Research*, 94 134–139.

Wang, C., Sun, Z., Jiang, R., Tian, Y. & Qie, X. 2018. Characteristics of downward leaders in a cloud-to-ground lightning strike on a lightning rod. *Atmospheric Research*, 203, 246–253.

Wei, T., Qian, X., & Yuan, M. 2018. Quantitative risk assessment of direct lightning strike on external floating roof tank. *Journal of Loss Prevention in the Process Industries*, 56, 191–203.

Advances in Raw Material Industries for Sustainable Development Goals – Litvinenko (Ed)
© 2021 Taylor & Francis Group, London, ISBN 978-0-367-75881-3

Simulating the formation of wax deposits in wells using electric submersible pumps

A.N. Aleksandrov
Engineer, Saint Petersburg Mining University, Saint Petersburg, Russia

M.A. Kishchenko
Master student, Saint Petersburg Mining University, Saint Petersburg, Russia

Thang Nguyen Van
Postgraduate student, Saint Petersburg Mining University, Saint Petersburg, Russia

ABSTRACT: In this paper, based on the known physicochemical characteristics and the component composition of the reservoir high-wax oil from D_{2ef} formation of the Kirtaelsky field, a phase behavior model of the studied high-wax oil was developed through the Multiflash Wax module, which allows us to determine the conditions for phase transition of paraffinic hydrocarbons in the gas-liquid mixture. It is established that for the given conditions, the closest to the actual value of the depth of organic deposit formation was obtained through the complex mechanistic model of the vertical multiphase flow OLGAS. The nature of the change in WAT along the wellbore was determined. The changes were highly noticeable when creating a depression in the reservoir and increasing the pressure in the electric submersible pumps (ESP) together with the degassing process of well products. A study focused on the influence of operating parameters of a well equipped with an ESP on conditions leading to the wax formation was conducted. Practical recommendations for the conditions under consideration were obtained.

1 INTRODUCTION

A principal challenge in many oil industry production situations is paraffin wax. Up to 75% of the world's oil suffers when wax precipitates out and solidifies in formation pores and fluid flow channels, at the wellbore, on the sidewalls of wells, in the tubing, casings, pump strings, and processing system. Wax deposition is costly and one of the oil industry's most expensive inconveniences, leading to dramatic reductions in production, equipment failures, loss of storage and transport capacity, and loss of efficiency.

Wax is a complicated blend of n-paraffin, i-paraffin and c-paraffin with carbon numbers from 18 to 65 (Lake et al. 2006). Fadairo et al. (2010) and Kasumu et al. (2013) showed that waxes are precipitated as solids with the changing thermodynamic equilibrium when the oil temperature cools down lower than the wax appearance temperature (WAT). In other words, the temperature at which the first organic wax crystalizes in oil as a deposit is referred to as the WAT. Berne-Allen et al. (1938) and Paso et al. (2009) suggested that the WAT is one of the main factors, which needs to be taken into account when developing preventative strategies for handling wax deposition in oil wells.

For a scientifically-based method to the prevention and removal of wax, it is important to take into account the conditions that cause a phase transition of paraffin to a solid-state. This process is influenced concurrently by several factors (Glushchenko et al. 2009, Ibragimov et al. 2010, Rogachev et al. 2006):

- geological, physical and technological conditions of field production;
- physicochemical properties and component composition of reservoir oil;

- changes in thermobaric conditions along the wellbore;
- violation of hydrodynamic equilibrium;
- changes in the structure and flow rate;
- the intensity of oil degassing;
- the amount of solid contained in oil;
- water-cut;
- condition of the internal surface of the equipment (roughness).

The intensity of the wax formation depends on the predominance of one or more factors, which might vary in time and depth, hence, the amount and nature of organic deposits are not constant (Struchkov et al. 2018).

Regarding the analysis of the prevailing situation on the dewaxing of a well of the studied production object, it was found that the measures taken to remove wax deposits, for one reason or another, have low efficiency. Solving the problem of preventing the formation and removing wax deposits will reduce current and capital costs in the exploitation of high-wax oil.

One of the acknowledged methods to reduce the intensity of the formation of organic deposits in the well is to choose the optimal technological regime of its operation. During the production of the high-wax oil well using ESP, the most important operating parameters affecting the conditions for the formation of wax deposits are the changes in the ESP rotation frequency and the number of stages, as well as the buffer pressure.

Despite the fact that wax formation simulation is one of the more challenging questions facing engineers, owing to the extremely complicated and limited data, there are a number of wax simulation programs developed to predict and control wax formation, the amount of precipitated wax, and wax deposition rates.

Detailed design of production systems is required to improve the efficiency of oil production and exploitation. There are a tremendous number of software packages used to predict the crystallization process of high-molecular components of oil such us the PVTsim software package (developed by the Calsep company), the PVTP software package (developed by the Petroleum Experts company), and the OLGA and PIPESIM software packages (developed by the Schlumberger company).

One of the leading software systems in the field of analysis and optimization of oil production systems is the product of the Schlumberger Company - PIPESIM. For the most part, this software package is a wax simulation used for building and calculation of a static model of steady-state multiphase flow moving from the reservoir to the objects of the collection and preparation system. PIPESIM allows for the solution of many complicated problems with the help of numerous modules included in this package (Schlumberger PIPESIM [Electronic resource]).

The novelty of this paper is to provide a detailed study of the effect of parameters of the electric submersible pump on wax formation. In addition, this work also proposes practical recommendation for given conditions, which play a pivotal role in predicting and measuring wax formation.

2 MATERIALS AND METHODS

In this work, we used the results of laboratory studies of the physicochemical properties of the high-wax oil in the Kirtaelskoe field, as well as the results from modeling the movement of the specified high-wax oil along the wellbore of a well using electric submersible pump through the Schlumberger PIPESIM software package.

3 RESULTS AND DISCUSSION

3.1 *Initial data*

The object of the study is a hypothetical well, simulating the conditions of the Timan-Pechora oil and gas province with geometric, geological and physical parameters characterized for the

Table 1. Well parameters.

Parameter	Value
Flow rate of the fluid at standard conditions, m^3/d	85
Productivity Index, $m^3/d*MPa$	15
Gas/oil ratio, m^3/m^3	72
Surface pressure, MPa	1.8
Oil bubble point pressure, MPa	8.8
Well depth, m	3000
Perforation depth, m	2925
Tubing depth, m	2400
Average angle of inclination of the well, °	2
Internal diameter of the production string, m	0.144
Internal diameter of tubing, m	0.062
Temperature of the neutral layer, °C	4
Depth of the neutral layer, m	30

Table 2. Physical and chemical properties of degassed oil from the D_{2ef} pool.

Main properties	Value
Density at 20°C, kg/m^3	802
The pour point, °C	39
WAT, °C	43.5
Hydrocarbon group composition, % by mass:	
Wax content (wt %)	32.3
Asphaltene content (wt %)	0.7
Resin content (wt %)	4.7
Reservoir temperature, °C	62
Reservoir pressure, MPa	29.1

conditions of the developed oil reservoir D_{2ef} (given in Table 1). The temperature for the specified reservoir is 62 °C, and the current reservoir pressure is 19.6 MPa.

The results of laboratory studies of the physical-chemical properties of the wellhead non-water oil sample are shown in Table 2. Degassed oil is extremely light (density 802 kg/m^3). The pour point is 39 °C.

In terms of group analysis, the oil has a high wax content (32.3 % by mass), and is resinous (resin content is 4.7 % and asphaltene content is 0.7 % by mass). Physical and chemical properties of degassed oil from the D_{2ef} pool are given in Table 2.

3.2 *Pump selection*

At the first stage, a method of well productivity evaluation was applied in the form of nodal analysis. It allows us to divide the system "reservoir-well-pump" into components connected by nodal points (Guo et al. 2009), to visually evaluate the influence of various parameters on the formation productivity and the performance of the lift and submersible pump. The behavior of the well is determined by the energy of the reservoir ensuring the flow of fluid to the well and the ability of the fluid to rise to the surface. The intersection point of the inflow curve (indicator curve) and the outflow curve is called the working point of the system. Modeling of fluid flow at the bottom of the well, which determines the flow rate of the reservoir at the depression established on it was carried out by setting the well productivity index, taking into account the Vogel correction. In the developed model, the nodal point is located opposite the perforated interval.

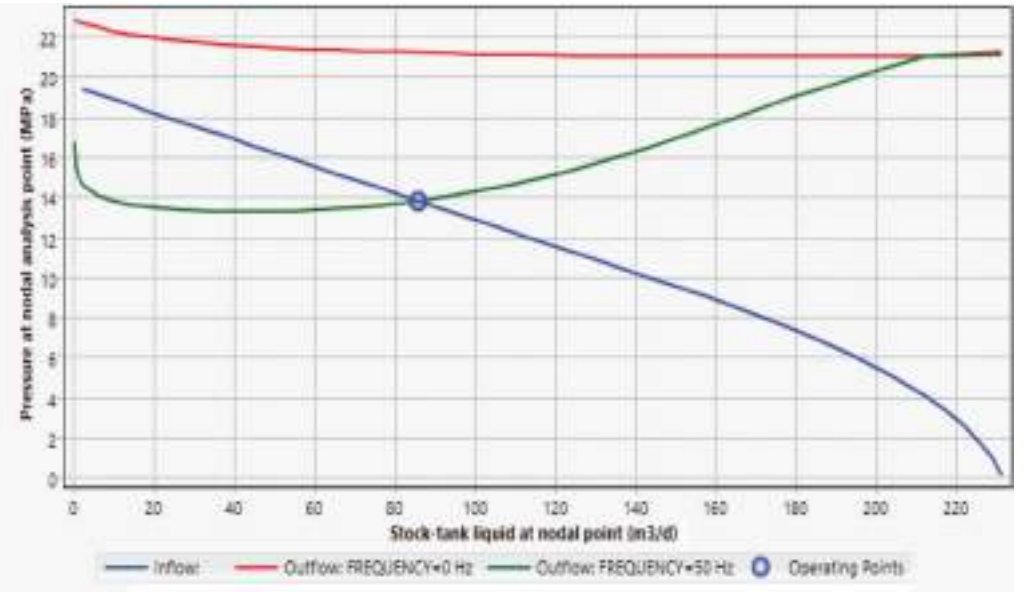

Figure 1. Combined characteristic of the reservoir-well system without a pump and with its use.

During production, the initial reservoir pressure dropped to 19.6 MPa. The use of nodal analysis makes it possible to establish that the energy for lifting the well is not enough to move the fluid from the downhole to the wellhead - well blowout is impossible (red line, Figure 1).

In order to provide the well with sufficient energy to lift fluid to the surface and achieve the planned flow rate (85 m^3/day), an ESP TD600 was chosen. The green line in Figure 1 represents the characteristic of the well with a working pump. The most suitable pump is selected from the vast database with the highest efficiency, which is made for the selected pump model 65 %. When choosing a pump, losses between steps, viscosity correction, and downhole separation effects were taken into account.

3.3 *Phase equilibrium diagram*

With regard to the known physical-chemical characteristics and component composition, a model of high-wax oil was developed, which allows us to determine the conditions for the wax formation in a gas-liquid mixture. The wax formation line shown on the phase diagram corresponds to the temperature of the studied wax appearance temperature – 44 °C. According to the graph, at the temperature of 20 °C, the wax content is 32.3 % by mass. The values of the WAT and wax mass content in the presented model are quite close to the experimentally obtained data at 20 °C and the atmospheric pressure, given in Table 2.

Under normal conditions, different hydrocarbon components contained in the oil form a three-phase system. At reservoir conditions (high temperature and pressure), all the components form one phase which is a liquid mixture. Oil is a multicomponent system, so the phase equilibrium diagram in the "temperature-pressure" coordinates, unlike in individual substances, is not a single curve, but an area limited by condensation line and evaporation line.

The first stage of the simulation is to plot a phase diagram of the hydrocarbon system for the D_{2ef} pool (Figure 2). To the left of the critical point (C) and above the evaporation line (area 1) hydrocarbons are in a liquid state; to the right and below the condensation line (area 2) hydrocarbons are in a gaseous state. Inside the two-phase boundary between the

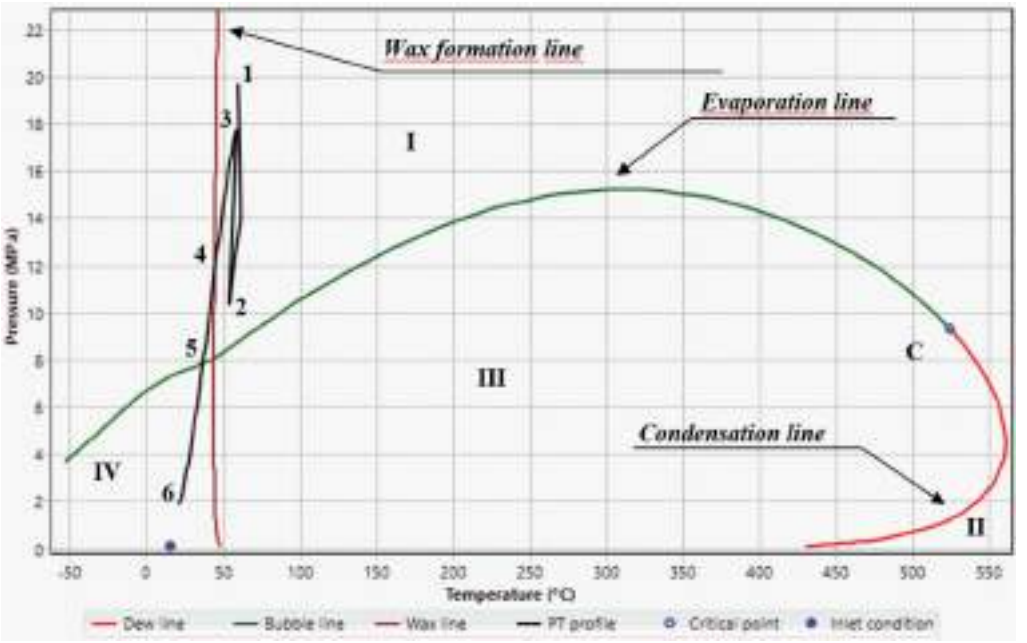

Figure 2. Phase equilibrium diagram for the D_{2ef} pool hydrocarbon system.

evaporation and condensation line (area 3) gas and liquid can coexist. When the temperature drops below the wax formation line, the system turns into a three-phase state (area 4) with an additional solid phase – wax.

Additionally, the phase diagram is a simulated PT (pressure and temperature) - profile during fluid movement from the reservoir to the wellhead. The beginning of the calculation of the model occurs at point 1, which illustrates the reservoir conditions. Points 2 and 3 correspond to the thermobaric conditions at the intake, discharge of the ESP, and illustrate the pressure and temperature rise occurring in the pump. When moving along the tubing string, the flow temperature decreases to the WAT (point 4), which contributes to the beginning of wax formation. Then the pressure decreases to the point of oil saturation with gas (bubble point, point 5), which initiates the loss of light hydrocarbon fractions and contributes to the extensive formation of wax deposits. In the area between points 5 and 6 (wellhead), there is a movement of a 3-phase system (liquid, gas and solid particles).

3.4 *Determination of the depth of wax formation*

Figure 3 shows a comparison of the real (actual) temperature log with temperature distribution profiles along the wellbore, which is calculated by using formulas 1, 2, 3 and through complex mechanical model of the vertical multiphase flow OLGAS. In this model, two types of correlations are observed: the two-phase model considering the gas-liquid flow and the three-phase model additionally counting solid particles.

The complex mechanical flow model OLGAS is applied for all tilt angles, pipe diameters, and fluid properties. In this model, we used independent continuity equations for gas and liquid droplets, which are related to interfacial mass transfer.

The wax appearance temperature curve obtained using the Coutinho model in the Multiflash module was shown in Figure 3, which allows us, when crossing with temperature profiles, to determine the depth of the formation of wax deposits in the well (Table 3).

The model Coutinho is a thermodynamic model based on the concept of predicting the formation of a solid phase. The use of this model in combination with the state equation

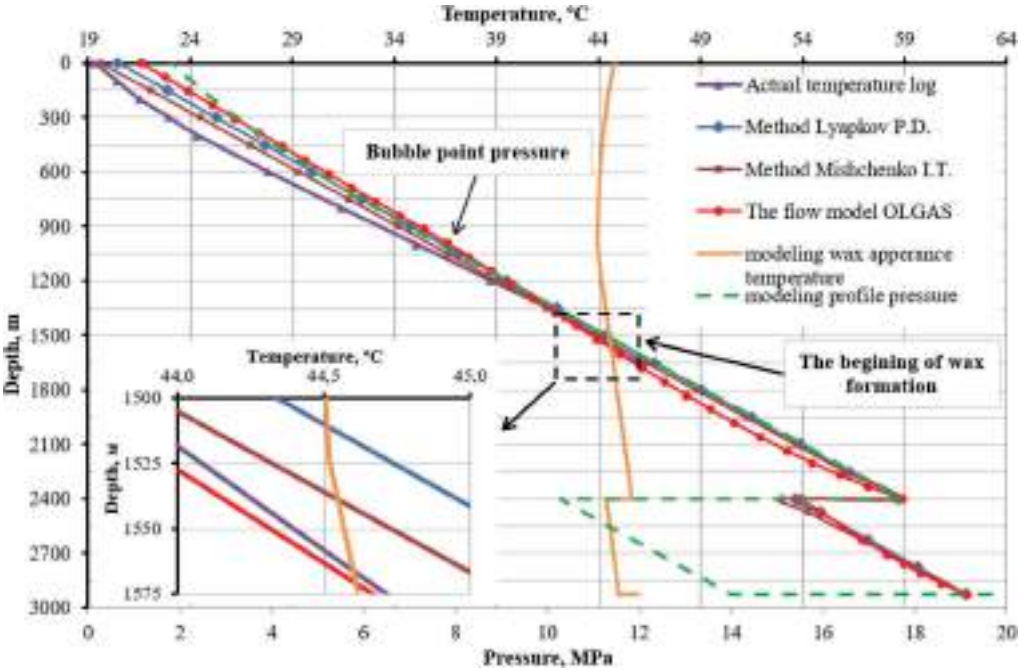

Figure 3. Determination of the depth of the formation of wax deposits.

Table 3. Determination of the depth of wax formation.

Method	WAT, °C	$H_{wax\ formation}$, m
According to Lyapkov P.D.	44,51	1510
According to Mishchenko I.T.	44,55	1540
According to actual temperature log	44,59	1566
According to the flow model OLGAS	44,62	1572

(UNIQUAC model) makes it possible to predict the behavior of oil and its model solutions at low temperatures with high accuracy (Coutinho J. et al. 2001).

Temperature distribution at the wellbore using the method of Lyapkov P.D. (Lyapkov P.D. 1987):

$$T(H) = T_r - (L_c - H) \cdot \frac{0.0034 + 0.79 \cdot \omega \cdot cos\alpha}{10^{\frac{q}{86400 \cdot 20 \cdot d^{2.67}}}}, \quad (1)$$

where T_r is the reservoir temperature, K; L_c is the well depth, m; H is the current depth, which is measured from the wellhead, m; ω is the average geothermal gradient in the well, K/m; α is the angle of deviation of the well from the vertical, degree; q is the flow rate, m^3/s; d is the diameter of the lift, m.

Temperature distribution at the wellbore using the method of Mishchenko I.T. (Mishchenko I.T. 2003):

- For tubing

$$t(h) = t_r\left\{1 - \frac{h}{c}\left[0.544\left(623.7\frac{d_t}{Q_m} + 1\right)\right]\right\}, \quad (2)$$

- For the casing string

$$t(h) = t_r\left\{1 - \frac{h}{c}\left[0.544\left(311.85\frac{d_c}{Q_m} + 1\right)\right]\right\}, \tag{3}$$

where t_r is the reservoir temperature, °C; h is the depth, which is measured from the bottom hole, m; Q_m is the mass flow rate, t/d; d_t is the internal diameter of the tubing, m; d_c is the internal diameter of casing string, m; c is the specific heat of well product, J/kg·°C.

Thus, the comparison of the actual temperature log with the temperature distribution profiles along the wellbore, which was calculated according to the methods of Lyapkov P.D., Mishchenko I.T. and built using the complex mechanical model of the vertical multiphase flow OLGAS, showed that the study has an excellent result. For the given conditions, the greatest convergence with field study results of the temperature distribution along the wellbore and the actual depth of the beginning of the wax formation is given by using the multiphase flow model OLGAS.

3.5 *The nature of the change in the wax appearance temperature*

As previously noted, the WAT is known as the temperature at which wax from the dissolved state transfers to the solid phase (the first wax crystal is deposited in the oil). This parameter is influenced by many factors, which are: physical-chemical properties, component composition of reservoir oil, wax content, degassing intensity, pressure gradient along the wellbore (Kamenshchikov F.A. 2005).

Figure 4 Shows the joint profile of the wax appearance temperature and pressure along the wellbore. It is important to notice that the nature of changes in these parameters corresponds to the phase equilibrium diagram of the hydrocarbon system (Figure 3).

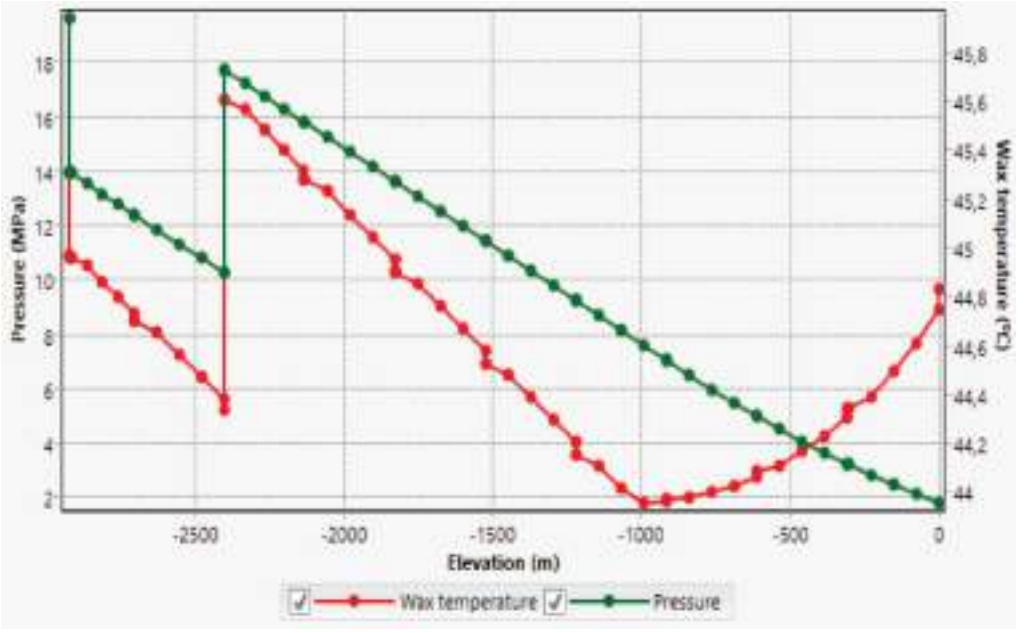

Figure 4. The pressure profile and the wax appearance temperature.

The decrease in the WAT as it moves to the bottom of the well is due to the manifestation of the throttle effect when creating a depression on the reservoir. Moreover, a significant increase in the WAT occurs in the pump, which is caused by a sharp increase in the pressure in the system. In the sections from the perforation interval to the pump intake (2925-2400 m) and from the pump discharge to the "bubble point" (2400-1000 m), there is a linear dependence of the decline in wax appearance temperature with decreasing pressure in the system. Starting from a depth of 1000 meters, an increase in the wax appearance temperature is observed, which is due to the intensive release of light oil fractions and, consequently, a decrease in the solvent capacity of oil relative to (compared to) wax, as well as due to the cooling of the oil flow in the wellbore. It should be noted that the gas globules arising in this process are mass-exchange promoters of the growth of wax crystals (Pashali A.A. et al. 2011 & Tronov V.P. 1970).

3.6 *The effect of the water cut of the test oil on the depth of wax formation*

The study of Glushchenko V.N. (Glushchenko V.N. et al. 2009) presents a thorough analysis of the literature and field material focused on the effect of water-cut on the formation of organic solids. In many works, a decrease in the intensity of the wax formation with an increase in water-cut of wells production was demonstrated. This owes to a decrease in adhesion to the hydrophilic steel surface, a decrease in the rate of cooling due to the greater heat capacity of water compared to oil. In Figure 5, it can be seen that with an increase in water cut, the wellhead temperature increases due to a decrease in the rate of cooling of the flow.

Additionally, in the work (Glushchenko V.N. et al. 2009), a number of researchers were highlighted, whose studies showed the negative effect of water cut. This is explained by the general decrease in the temperature of the watering fields, a significant gas absorption by water with a decrease in the wax solubility in oil, and an increase in the WAT by several degrees.

The simulation results showed that with an increase in the water cut of well production, there is a decrease in the depth of wax formation in the tubing string (Figure 6).

Thus, reducing the interval of wax formation in the well for the given conditions is caused by a decrease in the portion of high-molecular hydrocarbons in the well production during the field development, hydrophilization of the internal surface of the tubing string, as well as a decrease in the rate of flow cooling.

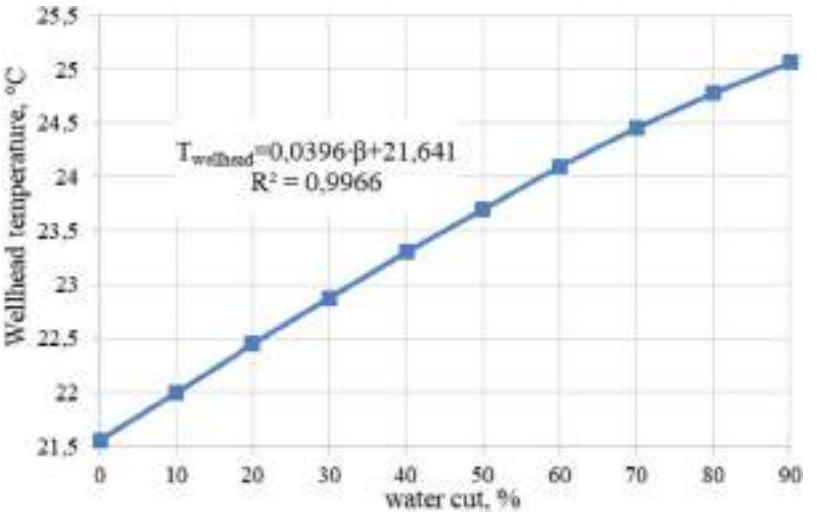

Figure 5. The dependence of wellhead temperature on water cut.

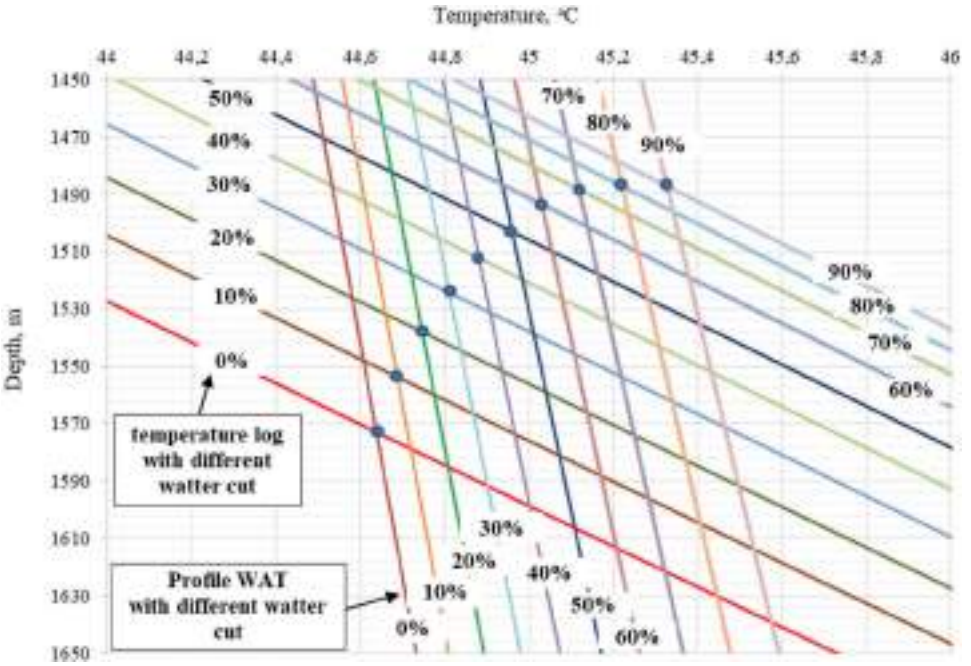

Figure 6. Dependence of the wax formation depth in the well with an increase in water cut.

3.7 *The influence of the buffer pressure on the depth of wax formation*

A considerable amount of field data demonstrates a reverse dependence of the residual gas saturation value of oil to the depth of wax formation in the wellbore (Glushchenko V.N. et al. 2009). For instance, in the Zhanazhol field, an increase in wellhead pressure prevented a sharp degassing, which led to a sharp decrease in the wax formation. Another example is the production of high-wax oil in the Tengutinskaya area in Kazakhstan. At the beginning of field operation with a high gas factor, there were no complications with the formation of wax deposits. During the development of the reservoir, the reservoir, buffer pressures, and the gas factor decrease, which led to intensive waxing of underground and surface equipment.

Hence, one of the effective methods to handle wax formation is to prevent the negative impact of the released gas by using the choke restriction method to increase the buffer pressure (Glushchenko V.N. et al. 2009). The positive effect is to reduce the time finding wells with a simultaneous increase in their flow rates.

The obtained simulation results confirmed that an increase in backpressure at the wellhead leads to a shift in the depth of the start of degassing up along the wellbore (Figure 7). From this point of view, an increase in the buffer pressure at the wellhead can serve as one of the methods for preventing wax formation in the tubing on the condition that the wax formation interval is located above the point of initial degassing.

For the given conditions, when the formation of organic deposits in the wellbore occurs before the start of oil degassing, a negative result is observed, at which point an increase in buffer pressure leads to an increase in the WAT and, therefore, an earlier onset in the formation of organic deposits in the wellbore (Figure 8). Thus, the area of effective application of the choke restriction method as a way to cope with the formation of ARPD has been identified.

In the above example, a sensitivity assessment tool was used for the boundary conditions of the model. It is necessary to consider that when changing one parameter in the model, all the others remain unchanged.

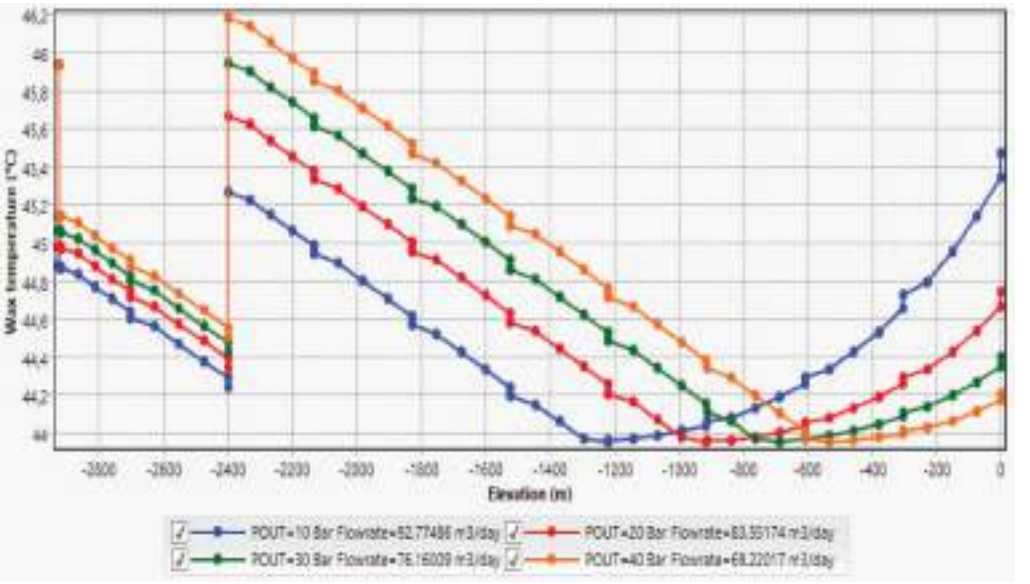

Figure 7. Change in the WAT when creating different buffer pressure.

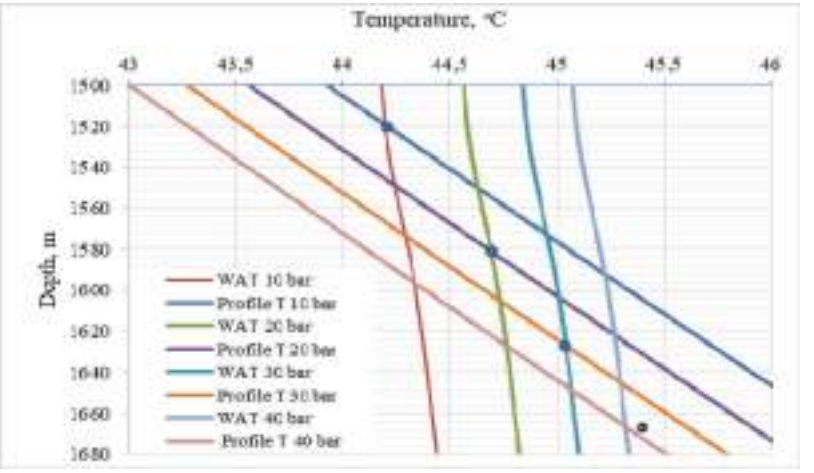

Figure 8. The influence of buffer pressure on the depth of wax formation.

3.8 *The effect of the rotational frequency of the ESP on the depth of wax formation*

One of the most important parameters that affect the intensity of the wax formation of the downhole equipment is the flow rate. Acceleration of the oil flow leads to a decrease in fluctuation of temperature along the wellbore, a change in the structure and dispersion of the gas-liquid flow as well as a decrease in the rate of solid deposits accumulation. In general, a positive effect of the parameter under consideration is perceived when it changes to a certain critical value, corresponding the transition from a laminar to a turbulent flow regime (Glushchenko V.N. et al. 2009, Ibragimov N.G. et al. 2010 & Coutinho J. et al. 2001).

Figure 9 Shows the change in the depth of wax formation in the well depending on the rotation frequency of the ESP. Furthermore, the flow rate can be influenced by change in the

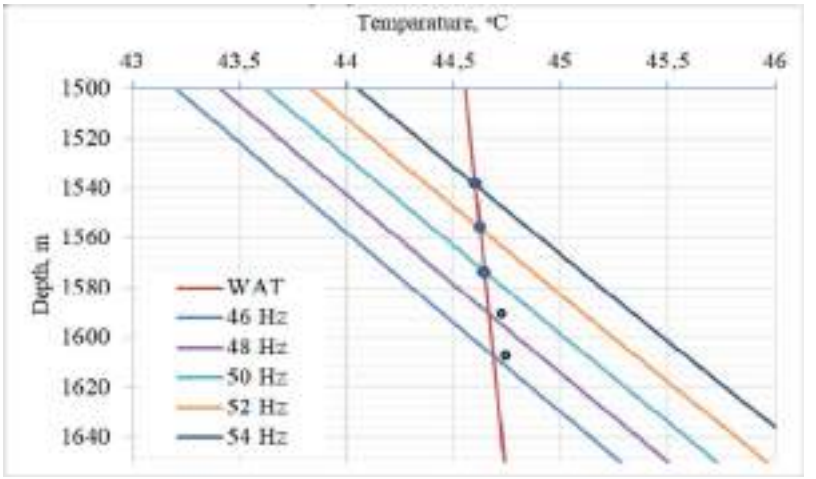

Figure 9. Effect of ESP rotation frequency on the depth of wax formation in the well.

number of stages in the pump and the diameter of the tubing, which also leads to change in the pressure-flow characteristics of the pump.

4 CONCLUSIONS

1. By modeling the movement of high-wax oil in wellbores, we are be able to study the influence of various factors affecting the depth of the formation of organic deposits.
2. High convergence of the actual temperature log with the calculated temperature profiles with regard to the methods of Lyapkov P.D. and Mishchenko I.T. was obtained. This allows us to rely on the accuracy of these methods on the condition that the results of field studies of the temperature distribution in the wellbore are not available. Nevertheless, for the given conditions, the closest to actual value of the depth of organic deposit formation was obtained through the complex mechanistic model of the vertical multiphase flow OLGAS.
3. The nature of the change in WAT along the wellbore was determined. It is important to note that those changes were highly noticeable when creating a depression on the reservoir and increasing the pressure in the ESP. During degassing, the WAT increases due to a decrease in the content of light fractions.
4. Temperature is considered as one of the key factors affecting wax formation in wells. It is recommended to use a nominal size ESP with higher productivity than that, which is required to achieve the planned flow rate, which will provide additional heating to the production of the well.
5. The influence of ESP rotation frequency on the depth of wax formation was established. On top of the increase in frequency, it is possible to influence the growth of the flow rate by reducing the internal diameter of the tubing and adding the number of stages, which also leads to a change in the pressure-flow characteristics of the pump.
6. The dependence of the depth of wax formation along the wellbore on the water content of the high-wax oil was established. The decrease in the interval of wax formation in the well is the result of the reduction in the proportion of high-molecular hydrocarbons in the well production during the development of the field, the hydrophilization of the internal surface of the tubing string, and the decrease in the rate of flow cooling.
7. Identified the area of effective application of the choke restriction method (an increase in buffer pressure) as a way to handle wax formation. A positive effect is observed when the formation of deposits in the well occurs after the start of degassing. Contrarily, a negative

result is observed, when an increase in the buffer pressure leads to an increase in the WAT and consequently, an earlier onset in the formation of organic deposits in the wellbore.

ACKNOWLEDGMENTS

We acknowledge Evgeny A. Kibirev, head of oil production technology, technology and methods of the oil production department (Gazpromneft-NTC LLC, Saint Petersburg, Russian Federation), for his assistance during the experiments. We acknowledge Dr. M.K. Rogachev for his assistance during the experiments. Finally, we would like to thank Saint-Petersburg mining university (Saint-Petersburg, Russian Federation) for providing laboratory equipment, support and samples for this research.

REFERENCES

Bern, P.A., Withers, V.R., & Cairns, R.J. 1980. Wax deposition in crude oil pipelines. In *European offshore technology conference and exhibition*. Society of Petroleum Engineers.

Berne-Allen, Jr.A., & Work, L.T. 1938. Solubility of refined paraffin waxes in petroleum fractions. *Industrial & Engineering Chemistry*, *30*(7): 806–812.

Brown, T.S., Niesen, V.G., and Erickson, D.D., 1993, "Measurement and Prediction of the Kinetics of Paraffin Deposition", *68th Annual Conference of the Society of Petroleum Engineers*, paper no. SPE 26548.

Creek, J.L., Lund, H.J., Brill, J.P., & Volk, M. 1999. Wax deposition in single phase flow. *Fluid Phase Equilibria*, *158*, 801–811.

Fadairo, A.S. A., Ameloko, A., Ako, C.T., & Duyilemi, O. 2010. Modeling of wax deposition during oil production using a two-phase flash calculation. *Petroleum & Coal*, *52*(3): 193–202.

Glushchenko, V.N., Silin, V.N., & Gerin, Yu.G. 2009. Prevention and elimination of asphaltene-resin-paraffin deposits. *Oilfield chemistry*: 480 p.

Guo, B., Song, S., Chacko, J. and Ghalambor, A. "Offshore Pipelines", Elesvier Inc., Oxford, UK, 2005.

Guozhong, Z., & Gang, L. 2010. Study on the wax deposition of waxy crude in pipelines and its application. *Journal of Petroleum Science and Engineering*, *70*(1-2), 1–9.

Huang, Z, Zheng, S., & Fogler, H.S. 2016. Wax Deposition: Experimental Characterizations, Theoretical Modeling, and Field Practices. CRC Press, Boca Raton.

Ibragimov, N.G., Tronov, V.P., & Guskova, I.A. 2010. Theory and practice of methods for controlling organic deposits in the late stages of oil field development. - 240 p.

Jennings, D.W., & Weispfennig, K. 2005. Experimental solubility data of various n-alkane waxes: effects of alkane chain length, alkane odd versus even carbon number structures, and solvent chemistry on solubility. *Fluid phase equilibria*, *227*(1), 27–35.

Jung, S.Y., Lee, D.G., & Lim, J.S. 2014. A simulation study of wax deposition in subsea oil production system. In *The Twenty-fourth International Ocean and Polar Engineering Conference*. International Society of Offshore and Polar Engineers.

Kamenshchikov, F.A. 2005. Thermal dewaxing wells. Izhevsk: 254 p.

Kasumu, A.S., Arumugam, S., & Mehrotra, A. K. 2013. Effect of cooling rate on the wax precipitation temperature of "waxy" mixtures. *Fuel*, 103, 1144–1147.

Kohse, B.F., & Nghiem, L.X. 2006. Asphaltene and waxes. Petroleum. Engineering Handbook. *Society of Petroleum Engineering*, Richardson Texas, USA.

Lake, L.W., Kohse, B.F., Fanchi, J.R., & Nghiem, L.X. 2006. Petroleum Engineering Handbook: Volume I General Engineering. *SPE, Texas, USA*: 397–453.

Leontaritis, K.J., & Geroulis, E. 2011. Wax Deposition Correlation-Application in Multiphase Wax Deposition Models. *In Offshore Technology Conference*. Offshore Technology Conference.

Lyapkov, P.D.1987. Selection of the installation of a submersible centrifugal pump to the well. M.: MING.

Mishchenko, I.T. 2003. Oil Well Production: A Textbook for High Schools. M.: FSUE Publishing House "Oil and Gas" Russian State University of Oil and Gas named after IM Gubkin. – 816 p.

Pan, H., Firoozabadi, A., & Fotland, P. 1997. Pressure and composition effect on wax precipitation: experimental data and model results. *SPE Production & Facilities*, *12*(04), 250–258.

Pashali, A.A., Mikhailov, V.G., & Petrov, P.V. 2011. Investigation of the effect of the concentration of gas bubbles on the value of the coefficient of natural separation//Bulletin of the Ufa State Aviation Technical University, T. 15. - No. 1 (41).

Paso, K., Kallevik, H., & Sjoblom, J. 2009. Measurement of wax appearance temperature using near-infrared (NIR) scattering. *Energy & Fuels*, *23*(10), 4988–4994.
Rogachev M.K., Strizhnev K.V. Fighting complications in oil production. *Nedra*, 2006, 296 p.
Schlumberger PIPESIM [Electronic resource]. – Access mode: http://www.sis.slb.ru/pipesim/(accessed date 04/15/18).
Struchkov, I.A., & Rogachev, M.K. 2018. The challenges of waxy oil production in a Russian oil field and laboratory investigations. *Journal of Petroleum science and Engineering*, 163, 91–99.
Tronov, V.P. 1970. Mechanism of the formation of resin-paraffin deposits and the fight against them// M.: Nedra, T. 192. - p. 5.

Advances in Raw Material Industries for Sustainable Development Goals – Litvinenko (Ed)
© 2021 Taylor & Francis Group, London, ISBN 978-0-367-75881-3

Separation of water-oil emulsions in device with enlarged throughflow capacity

O.S. Dmitrieva
Candidate of Technical Sciences, Associate Professor of the Department of Processes and Devices of Chemical Technology, Kazan National Research Technological University, Kazan, Russia

I.I. Sharipov
Candidate of Technical Sciences, Associate Professor of the Department of Theoretical Foundations of Heat Engineering, Kazan State Power Engineering University, Kazan, Russia

V.E. Zinurov
Master's Student of the Department of Theoretical Foundations of Heat Engineerin, Kazan State Power Engineering University, Kazan, Russia

ABSTRACT: The growth of production capacities of industrial enterprises leads to an increase in emission concentration of pollutants and requires the use of separators. This scientific paper includes the research of separation of emulsions with similar densities. The emulsions with similar properties are separated very slowly, so it is necessary to use special inserts to accelerate the separation process. The authors have chosen inserts with corrugated baffles, located at an angle of 45°, inserts with corrugated baffles, located at an angle of 135°, as well as inserts with cross-corrugated baffles. As a result of experimental research, it was found that with an increase in the emulsion rate inside of apparatus, the separation efficiency decreases, upon the condition that all the studied inserts are installed. When the concentration of hydrocarbons in the original mixture is less than 25%, it is most appropriate to use inserts with corrugated baffles, located at an angle of 45°.

1 INTRODUCTION

In recent years, the separation of oil and water was considered as one of the main problems all around the world due to an increased production of industrial oil-containing wastewaters. Nowadays, the separation of oil and water is still considered as a critical technical problem due to a complex composition and a high content of oily hydrocarbons in wastewaters. The traditional separation methods have low efficiency, high cost, and other types of pollution take place when these methods are implemented (Jiang et al., 2019, Li et al., 2020, Patterson, 1985).

The separators are usually the first stage between the oil source (for ex. oil field well) and oil process pipeline. When being transported inside the pipeline, the crude oil, by-produced water and gas move in a complex multiphase mode, and a finely dispersed emulsion usually creates a number of difficulties. The gas phase can be quite easily separated from the liquid flow; emulsions are usually stable and more difficult to be separated. As a rule, emulsions of "water in oil" type are very common for the oil production (Chen et al., 2009, Harpura et al., 1997, Sadeghi et al., 2013, Wang et al., 2012, Wang et al., 2016). They are mainly formed due to availability of amphiphilic hydrocarbons in the crude oil, such as asphaltenes, resins, and acids. Moreover, some chemical additives or solid particles, used inside of production piping network, contribute to the formation of stable emulsion. The stability of oil emulsified systems is highly dependent on the crude

oil composition. Due to a wide range of compounds in the crude oil, the mathematical modeling of separation processes often gives significant errors, that`s why some problems can be solved only by conducting experimental studies. When producing the crude oil, the emulsions are mostly separated by gravity in vertical or horizontal apparatuses. Since the difference in the density of emulsion components is small, the apparatuses are usually designed with very large dimensions (Berman & Tamir, 2003, Cambiella et al., 2006, Sadeghi et al., 2011, Yang, 2007). Thus, the development, study and application of new apparatuses for the separation of stable emulsions are critical tasks.

In most cases, the choice of a particular type of design is based on a technical and economic analysis and takes into account local conditions, for example, the vertical settling tanks are used at low ground water level. Also, the choice of design is significantly affected by throughput capacity. The vertical, horizontal and radial settling tanks are used at the following throughput capacity of sewage treatment plants: not more than 10000, 15000-20000 and from 20000 m^3/day, respectively. As of today, one of the most promising ways to increase the efficiency of water-oil emulsion separation at the oil fields is to study different methods of improving the settling tanks. One of these methods is to study various inserts, to be installed inside the settling tanks, which have the form of webs, shields and other geometric bodies that increase the rate of water-oil emulsion stratification into components by changing the flow structure when moving along the obstacles. It should be noted that currently the flow rate of water-oil emulsions inside the settling tanks does not exceed a few millimeters per second, since at higher rates, the separation efficiency decreases significantly due to the phase mixing. Increasing the efficiency and separation rate of water-oil emulsions will reduce the costs for obtaining the finished petroleum products. Thus, the research and the use of new devices for the separation of stable emulsions is a relevant task. The purpose of this research paper is to study the increase in efficiency and separation rate of oil-water emulsions inside of continuously operating settling tanks.

2 RESEARCH PROBLEM

The purpose of this paper is to study the extraction of liquid oily hydrocarbon compounds from the emulsion. Two methods are usually used to separate the water-oil emulsions: reagent, using a demulsifies, and reagent-free.

The chemical method includes adding of various chemical reagents into the water to react with it. As a result of chemical reaction, the water is settled out as insoluble residues. This method helps to purify the emulsion by 95%. With a further increase in purification degree due to the use of chemical reagents, the water is contaminated with these chemical reagents. That is disadvantage of this method. The root of reagent-free method is to remove oil and oil products from the water by water settling out with the subsequent collection of oil by special devices: settling tanks, hydrocyclones, oil traps, etc. The main disadvantage of these apparatuses is a low degree of separation of water-oil emulsions (Diederen et al., 1998, Kou et al., 2019, Vanhoutte et al., 2011, Young et al., 1994, Zeng et al., 2016, Zhou et al., 2010,). In some cases, it is advisable to use the membranes for separation of water-oil emulsions (Babiker et al., 2019). However, if oil emulsions contain the components that can form a precipitate on the surfaces, then the membranes are very difficult to be used.

In order to improve the efficiency and to speed up the separation of water-oil emulsions, the authors developed several models of inserts, designed for continuously operating devices (settling tanks, separators), which are to be installed inside of these apparatuses. The research tasks also included the evaluation of possibility of developed inserts by experimental method to increase the efficiency of water-oil emulsion separation, to speed up its stratification, to determine the most effective rate ranges for each insert model, as well as to analyze the process of emulsion separation when it directly contacts with a certain model of insert.

3 RESEARCH METHODS

The experimental apparatus (Figure 1) consisted of separator (Dmitriev et al., 2019) with a cross-section of 60×60 mm with experimental inserts (Figure 2), valves for adjusting the flow rates of light and heavy phases, samplers for determining the concentration of hydrocarbon compounds after separation of emulsion, flowmeters LOUCHEN ZM FS300A G3/4" with an error of ±5% to calculate the rate of separated flows, tanks with a stirrer for remixing the separated emulsion and pump OASIS CRP 15/9 for feeding the emulsion into the separator.

In the course of experimental research, the following parameters were assumed to be constant: ambient temperature t_0 = 20°C; water density ρ_b = 998.2 kg/m^3; coefficient of water dynamic viscosity μ_b = 0.001003 kg/(m·s); density of oily hydrocarbon compounds ρ = 883 kg/m^3; coefficient of dynamic viscosity of hydrocarbon compounds μ_c = 0.0198 kg/(m·s). The concentration of oily hydrocarbons at the inlet of apparatus varied from 15% to 25%.

Various inserts were studied (Figure 2): *a* – insert with corrugated baffles, located at an angle of 45°; *b* – insert with corrugated baffles, located at an angle of 135°; *c* – insert with cross corrugated baffles. The depth of corrugations was equal to 10 mm. Along the entire length of plate, the holes were executed with a diameter of 1 mm and a uniform two-way pace of 3.5 mm. The holes were executed in such a way so that the sharp edges formed around them.

In the course of experimental research, the prepared emulsion was mixed in a tank by means of stirrer and the separated emulsion was fed into the apparatus by means of pump. When the tank was filled, the valves were opened to adjust the required flow rates of emulsion components, which were measured by flowmeters and after that, the emulsion, separated into

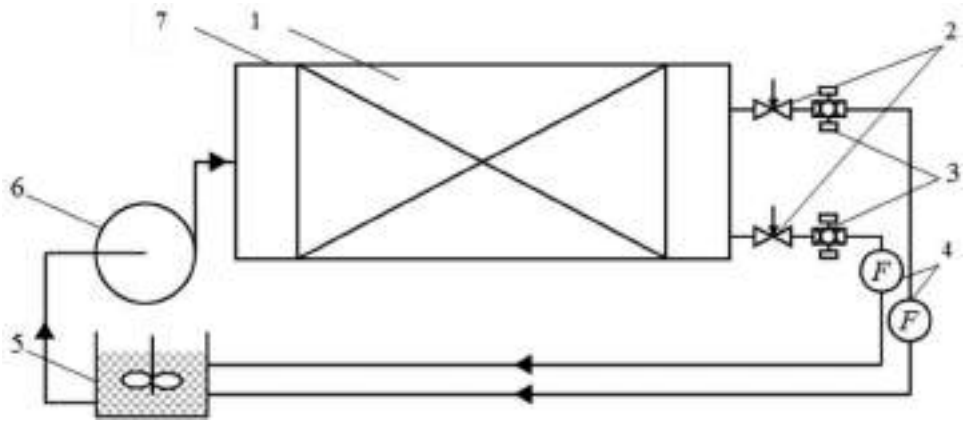

Figure 1. Experimental apparatus: 1 – experimental insert; 2 – control valves; 3 – samplers; 4 – flowmeters LOUCHEN ZM FS300A G3/4; 5 – tank for re-mixing of separated emulsion; 6 – pump OASIS CRP 15/9; 7 – experimental unit.

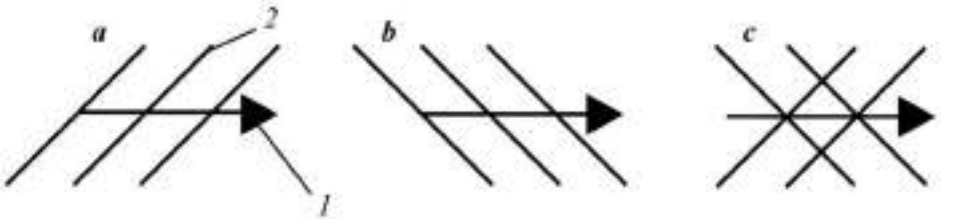

Figure 2. Models of experimental inserts: *a* – insert with corrugated baffles, located at an angle of 45°; *b* – insert with corrugated baffles, located at an angle of 135°; *c* – insert with cross corrugated baffles; *1* – direction of liquid flow movement inside of apparatus; *2* – corrugations.

light and heavy phases, was again fed into the tank. The concentration of hydrocarbon compounds at the outlet of apparatus was determined by the weight method. For this purpose, the sampling was carried out (at least 3 times, every 30 minutes) by samplers, on the scales R-25 with an error of ± 0.05.

4 RESULTS

The results of experimental research are shown graphically in Figures 3-5. With an increase in the emulsion flow rate, entering the experimental apparatus, the efficiency of extracting the liquid oily hydrocarbon compounds from the emulsion decreases. This is due to the fact that an increase in the input rate leads to an increase in the flow turbulence, resulting in a large number of vortex points that prevent the separation of oily hydrocarbon compounds from the emulsion. In order to intensify the processes of extraction of hydrocarbon compounds from the emulsion, it is necessary to use various inserts that are located inside of apparatus, contributing to the stratification of multiphase emulsion, i.e. arrangement of flow structure, contributing to the separation of compounds with different than the water has density.

In the course of research, it was found that the greatest efficiency of separator is achieved when using inserts with corrugated baffles, located at an angle of 45°. Such design increases the efficiency of stratification of oily compounds from the emulsion due to the orientation of corrugated surfaces, which shift the flow direction of lighter oily components against the water i.e. these components move upwards inside of apparatus, thereby intensifying the stratification process.

It should be noted that when the corrugated baffles are located at an angle of 135°, the emulsion separation efficiency is lower than when the baffles are located at an angle of 45°, because the orientation angle of baffles is almost coincident with the emulsion flow direction, that does not allow additionally affect the emulsion separation into different fractions. In the case of cross-corrugated baffles, an unordered emulsion flow is observed, resulting in two simultaneous processes throughout the whole insert, i.e. separation and mixing of mixture that leads to the lower efficiency.

The apparatuses without inserts provide the lowest efficiency of emulsion separation. This is caused by lack of elements inside of apparatus for intensification of separation of oily hydrocarbon compounds from the emulsion. The efficiency of extraction of liquid oily

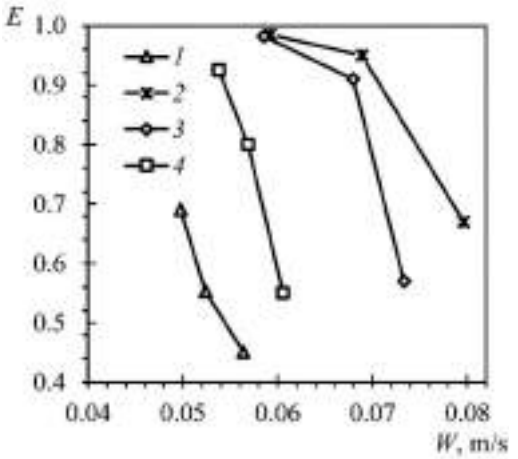

Figure 3. Dependency of liquid oily hydrocarbon compounds extraction efficiency from an emulsion, having 15 % concentration of hydrocarbons in the original mixture, on the input rate with various experimental inserts: *1* – without inserts; *2* – inserts with corrugated baffles, located at an angle of 45°; *3* – inserts with corrugated baffles, located at an angle of 135°; *4* – inserts with cross corrugated baffles.

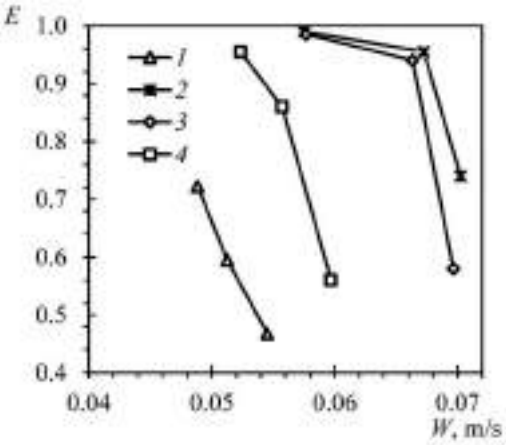

Figure 4. Dependency of liquid oily hydrocarbon compounds extraction efficiency from an emulsion, having 20% concentration of hydrocarbons in the original mixture, on the input rate with various experimental inserts: *1* – without inserts; *2* – inserts with corrugated baffles, located at an angle of 45°; *3* – inserts with corrugated baffles, located at an angle of 135°; *4* – inserts with cross corrugated baffles.

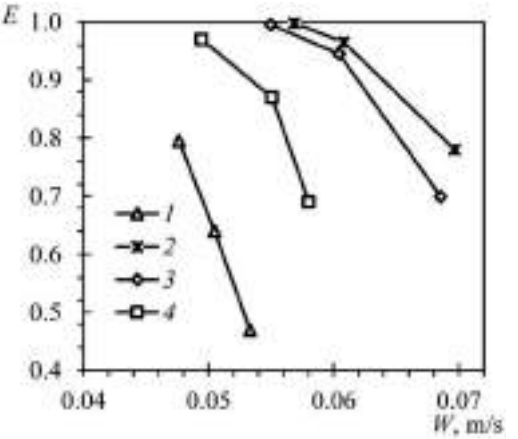

Figure 5. Dependency of liquid oily hydrocarbon compounds extraction efficiency from an emulsion, having 25% concentration of hydrocarbons in the original mixture, on the input rate with various experimental inserts: *1* – without inserts; *2* – inserts with corrugated baffles, located at an angle of 45°; *3* – inserts with corrugated baffles, located at an angle of 135°; *4* – inserts with cross corrugated baffles.

hydrocarbon compounds from the emulsion, with the concentration of them in original mixture of not more than 25%, on average is equal to 89.2, 84.5, 79.8 and 59.8% – when using the inserts with corrugated baffles, located at an angle of 45°, at an angle of 135°, inserts with cross corrugated baffles and without inserts, respectively, at the input rate within the range of 0.047–0.08 m/s.

5 DISCUSSION

When extracting the liquid oily compounds from the emulsion, with 15% concentration of them in the original mixture, the efficiency of apparatus on average was equal to 56.4, 86.8,

82.1 and 75.8% – when using the apparatus without inserts, with inserts with corrugated baffles, located at an angle of 45°, at an angle of 135°, and inserts with cross corrugated baffles, respectively. With an increase in the emulsion flow rate inside of apparatus, the separation efficiency decreased: when using the apparatus without inserts, an increase in the flow rate by 10% resulted in a decrease in efficiency by 52%; when using inserts with corrugated baffles, located at an angle of 45°, an increase in the flow rate by 25% decreased the separation efficiency by 32%; when using inserts with corrugated baffles, located at an angle of 135°, an increase in the flow rate by 20% decreased the separation efficiency by 42%, when using inserts with cross corrugated baffles, an increase in the flow rate by 11% decreased the separation efficiency by 41%. The highest efficiency of emulsion separation was equal to 69.1, 98.5, 98.2 and 92.5% – when using an apparatus without inserts, with inserts with corrugated baffles, located at an angle of 45°, at an angle of 135°, and inserts with cross corrugated baffles, respectively (Figure 3).

When extracting the liquid oily compounds from the emulsion, with 20% concentration of them in the original mixture, the efficiency of apparatus on average was equal to 59.5, 89.5, 83.5 and 79.2% – when using the apparatus without inserts, with inserts with corrugated baffles, located at an angle of 45°, at an angle of 135°, and inserts with cross corrugated baffles, respectively. An increase in the emulsion flow rate inside of apparatus on average by 0.006 m/s resulted in a decrease in the emulsion separation efficiency on average by 33.8%. An increase of liquid oily hydrocarbon compounds concentration in the emulsion from 15 to 20% led to an increase in the separation efficiency on average by 2.7% (Figure 4).

When extracting the liquid oily compounds from the emulsion, with 25% concentration of them in the original mixture, the efficiency of apparatus on average was equal to 63.5, 91.4, 87.9 and 84.3% – when using the apparatus without inserts, with inserts with corrugated baffles, located at an angle of 45°, at an angle of 135°, and inserts with cross corrugated baffles, respectively. An increase in the emulsion flow rate inside of apparatus on average by 0.008 m/s resulted in a decrease in the emulsion separation efficiency on average by 31.8%. The highest efficiency of emulsion separation was equal to 79.5, 99.8, 99.5 and 91.7% – when using the apparatus without inserts, with inserts with corrugated baffles, located at an angle of 45°, at an angle of 135°, and inserts with cross corrugated baffles, respectively. An increase of liquid oily hydrocarbon compounds concentration in the emulsion from 20 to 25% led to an increase in the separation efficiency on average by 4.9% (Figure 5).

6 CONCLUSIONS

The conducted research shows that in order to intensify the processes of extracting the liquid oily compounds from emulsions, various inserts, increasing the efficiency of apparatus at least by 17% in comparison with the apparatus without any inserts, shall be used. In the course of research, it was found that the most effective are the inserts with corrugated baffles, located at an angle of 45°, providing the most qualitative process of emulsions separation as a result of inhibition of liquid oily components by the surfaces of corrugations, moving upwards inside of apparatus due to a lower density than the water has. An obligatory requirement for achieving the highest possible efficiency of emulsion separation is to provide the relatively low flow rates. The highest efficiency of emulsions separation with a concentration of liquid oily hydrocarbon compounds in it within the range of 15-25% was on average equal to 73.1, 98.7, 99.1 and 94.3% – when using an apparatus without inserts, with inserts with corrugated baffles, located at an angle of 45°, at an angle of 135°, and inserts with cross corrugated baffles, respectively at minimum flow rates, which correspond to the following values: for an apparatus without inserts – 0.047 m/s, inserts with corrugated baffles, located at an angle of 45° – 0.057 m/s, inserts with corrugated baffles, located at an angle of 135° – 0.055 m/s, inserts with cross corrugated baffles – 0.049 m/s. The advantages of apparatus are high efficiency of liquid oily hydrocarbon compounds separation from emulsions, design simplicity, minimum capital and operating costs.

ACKNOWLEDGMENTS

The reported study was funded by grant of the President of the Russian Federation, project number MK-616.2020.8.

REFERENCES

Babiker, D.M.D., Zhu, L., Yagoub, H., Xu, X., Zhang, X., Shibraen, M.H.M.A. & Yang, S. 2019. Hydrogen-bonded methylcellulose/poly(acrylic acid) complex membrane for oil-water separation. *Surf. Coat. Technol*. 367: 49–57.

Berman, Y. & Tamir, A. 2003. Kinetics of droplets' sedimentation in a continuous gravity settler. *Chem. Eng. Sci*., 58: 2089–2102.

Cambiella, A., Benito, J.M., Pazos, C. & Coca, J. 2006. Centrifugal separation efficiency in the treatment of waste emulsified oils. *Chem. Eng. Res. Des*. 84: 69–76.

Chen, W., Peng, J., Su, Y., Zheng, L., Wang, L. & Jiang, Z. 2009. Separation of oil/water emulsion using Pluronic F127 modified polyethersulfone ultrafiltration membranes. *Sep. Purif. Technol*. 66(3): 591–597.

Diederen, A.M., Zee, G.van, Veenman, A.W. & Graauw, J.de. 1998. A novel apparatus for countercurrent sorption separation processes using fibrous sorbents. *Chem. Eng. Process.: Process Intensification* 37(3): 217–221.

Dmitriev, A.V., Zinurov, V.E., Vinh, D. & Dmitrieva, O.S. 2019. Removal of moisture from contaminated transformer oil in rectangular separators. *E3S Web Conf*. 110: 01026.

Harpura, I.G., Wayth, N.J., Bailey, A.G., Thew, M.T., Williams T.J. & Urdahl O. 1997. Destabilisation of water-in-oil emulsions under the influence of an A.C. electric field: Experimental assessment of performance. *J. Electrost*. 40-41: 135–140.

Jiang, W., Chen, Y., Chen, M., Liu, X., Liu, Y., Wang, T. & Yang J. 2019. Removal of emulsified oil from polymer-flooding sewage by an integrated apparatus including EC and separation process. *Sep. Purif. Technol*. 211: 259–268.

Kou, J., Chen, Y. & Wu, J. 2019. Numerical study and optimization of liquid-liquid flow in cyclone pipe. *Chem. Eng. Process.: Process Intensification* 107725.

Li, X., Shan, H., Zhang, W. & Li, B. 2020. 3D printed robust superhydrophilic and underwater superoleophobic composite membrane for high efficient oil/water separation. *Sep. Purif. Technol*. 237: 116324.

Patterson, J.W. 1985. *Industrial wastewater treatment technology*. 2nd ed., Butterworths, Stoneham: MA.

Sadeghi, I., Aroujalian, A., Raisi, A., Dabir, B. & Fathizadeh, M. 2013. Surface modification of polyethersulfone ultrafiltration membranes by corona air plasma for separation of oil/water emulsions. *J. Membr. Sci*. 430: 24–36.

Sadeghi, R., Mohebbi, A., Sarrafi, A., Soltani, A., Salmanzadeh, M. & Daneshpojooh, S. 2011. CFD simulation and optimization of the settler of an industrial copper solvent extraction plant: A case study. *Hydrometallurgy* 106: 148–158.

Vanhoutte, D.J.D., Eeltink, S., Kok, W.Th. & Schoenmakers, P.J. 2011. Construction and initial evaluation of an apparatus for spatial comprehensive two-dimensional liquid-phase separations. *Anal. Chim. Acta* 701(1): 92–97.

Wang, S., Qin, W. & Dai, Y. 2012. Separation of oil phase from dilute oil/water emulsion in confined space apparatus. *Chin. J. Chem. Eng*. 20(2): 239–245.

Wang, X., Yu, J., Sun, G. & Ding, B. 2016. Electrospun nanofibrous materials: a versatile medium for effective oil/water separation. *Mater. Today* 19(7): 403–414.

Yang, C.L. 2007. Electrochemical coagulation for oily water demulsification. *Sep. Purif. Technol*. 54: 388–395.

Young, G.A.B, Wakley, W.D., Taggart, D.L., Andrews, S.L. & Worrell J.R. 1994. Oil-water separation using hydrocyclones: An experimental search for optimum dimensions. *J. Pet. Sci. Eng*. 11 (1): 37–50.

Zeng, Q., Wang, Z., Wang, X., Zhao, Y. & Guo, X. 2016. A novel oil-water separator design and its performance prediction. *J. Pet. Sci. Eng*. 145: 83–94.

Zhou, N., Gao, Y, An, W. & Yang, M. 2010. Investigation of velocity field and oil distribution in an oil-water hydrocyclone using a particle dynamics analyzer. *Chem. Eng. J*. 157(1): 73–79.

Advances in Raw Material Industries for Sustainable Development Goals – Litvinenko (Ed)

Increasing the efficiency of pipeline transport of viscous oil based on rheological features

N.A. Zaripova
Postgraduate student, Saint Petersburg Mining University, St. Petersburg, Russia

A.K. Nikolaev
Professor, Saint Petersburg Mining University, St. Petersburg, Russia

Y.G. Matveeva
Engineer, Saint Petersburg Mining University, St. Petersburg, Russia

ABSTRACT: This article discusses existing methods for increasing the efficiency of pipeline transport of viscous oils. In more detail, the authors considered a method for transporting viscous oil using various additives. It is known that the rheological properties of oil are the basic initial data for the selection of a rational method of transportation. In this regard, an analysis of rheological models of viscous fluids is presented. Also, this paper considers the calculation of the effectiveness of the use of additives and their influence on the rheological properties of viscous oil. Taking into account the parameters of the studied pipeline, an anti-turbulent additive was chosen. This additive reduces the coefficient of hydraulic resistance and increases the throughput of the pipeline. The results of experimental studies of the rheological properties of viscous oil are presented. Based on the results of the experiments, the authors obtained the dependence of the shear stress on the shear rate in the temperature range of 10-30 ℃ at different concentrations of the additive used and without it. Taking into account the obtained dependences, conclusions were drawn about the presence of non-Newtonian properties in the investigated oil. In addition, an analysis is made of the change in the rheological model when the concentration of the additive and the temperature of the transportation change. Based on the results of the studies, the authors performed the selection of the optimal pumping regime for the investigated oil.

1 INTRODUCTION

Currently, the issue of increasing the efficiency of pipeline transport of viscous and high-viscosity oils is discussed in the works of many scientists.

The rheological properties of hard-to-recovery oil are the main initial data for the solution of design and operational tasks in field development and further pipeline transport. In this regard, the task of studying the rheological properties of high-viscosity oil is topical.

For the correct choice of technological regimes of various processes of extraction, transportation and processing of oil, it is necessary to know the rheological properties of the oil, as well as oil products and working fluids involved in these processes (Martinez-Palou, 2011).

For the efficient pumping of viscous oil, several basic methods are used (Hart, 2014):

- oil heating;
- using of hydrocarbon diluents;
- hydrotransport;
- construction of loopings and inserts;
- increasing of the number of pumping stations (PS) along the pipeline;
- Increasing of the station capacity;
- Using of additives.

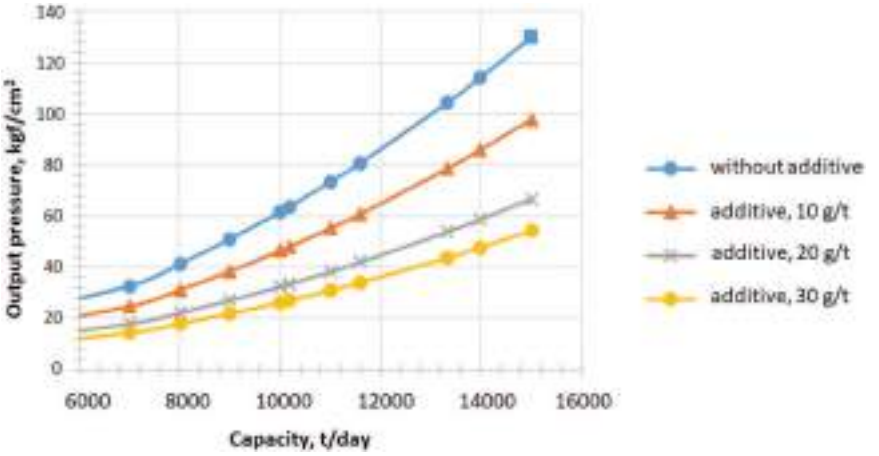

Figure 1. Head capacity curve of the pipeline, transporting oil with the anti-turbulent additive at various concentrations and without it.

The most common method for transporting viscous oil by pipelines is to pump preheated oil. This method consists in preheating oil before the enter to the main oil pipeline. Then oil heating stations are installed on the route at a certain distance, where the oil is heated (Nikolaev. 2016).

Previously, the authors conducted studies on the use of the M-FLOWTREAT grade C anti-turbulent additive in sections of a pressure oil pipeline (Nikolaev et al. 2019).

According to the results of the study, the head-capacity curves of the pipeline pumping oil without additives and with an additive concentration of 10, 20 and 30 g/t were obtained (Figure 1).

In this paper authors provided theoretical and experimental studies of methods for transporting high-viscosity oil. They also got necessary rheological dependencies and calculated effectiveness of using additive.

2 METHODOLOGY

The rheological properties of oil are the main source data for solving design and operational problems in the development of the field and further pipeline transport.

The initial data is a pipeline, the route of which runs under conditions of water-flooded and marshy area and eternal congelation along the territory of the Yamalo-Nenetskiy and Khanty-Mansiisk Autonomous District of the Tyumen Region. In addition to the Arctic climate, the construction area is characterized by unique geological and hydrological conditions. It is not rational to increase throughput only by heating, in order to avoid environmental impact (Nikolaev et al. 2018). In this regard, the authors have suggested the use of additives. An analysis of the using the various additives in domestic and foreign practice was made.

The additives used by the type of commodity form. We can divide additives into two groups: dispersion and gel (Muratova. 2014).

Additives of the first type are a suspension of the polymer in various liquids that do not enter into a chemical reaction with it. Alcohols, glycols and their esters are usually used as such liquids. The content of the active polymer in these additives reaches 25%. Such anti-turbulent additives include Necadd 447, Liquid Power, FLO XL, FLO MXA, M-FLOW-TREAT, Alfacauchuk-S, Koltek PTN 3170, TurbulentMaster 8010.

Gel additives (CDR 102, FLO, Necadd 547, Viol, X-PAND, HIPR) are made in the form of a polymer solution in any hydrocarbon liquid (gasoline, kerosene, etc.). The active polymer in such additives contains about 10%.

The use of gel additives is especially beneficial for pipelines, where the processes of speed of their dissolution are important. These can be short pipelines of offshore fields, loading and shipping terminals.

Recently, work has been underway on the development and implementation of suspension-emulsion additives, designed for use in oil and gas production in field pipelines.

Due to the variety of physicochemical properties of the pumped oil and oil products through pipeline systems, in each case the use of chemical reagents is an individual feature of the pipeline.

Taking into account the parameters of the studied pipeline, an anti-turbulent additive was chosen, which reduces the coefficient of hydraulic resistance and increases the throughput of the pipeline (Avksentiev. 2017, Khudyakova et al. 2018).

The effectiveness (%) of anti-turbulent additive in a stationary mode of operation of the pipeline (Nikolaev et al. 2018):

$$DR = \left[1 - \frac{\Delta P_f}{\Delta P_0} \cdot \left(\frac{Q_0}{Q_f}\right)^{2-m} \cdot \left(\frac{\nu_0}{\nu_f}\right)^{m}\right] \cdot 100\% \quad (1)$$

where f and 0 correspond to the flow of crude oil with and without additives; ΔP = friction pressure loss, kg/cm²; Q = volume flow rate, m³/h; ν = kinematic viscosity with average temperature, m²/c; m = criteria of flow mode. Turbulent in zone hydraulically smooth pipe m = 0,25, zone of mixed friction m = 0,123.

One of the main tasks of rheological research is to determine the correlation between the forces acting on the investigated fluid and the deformations caused by these forces.

Fluids called Newtonian are described by the following equation:

$$\tau = \mu \cdot \dot{\gamma} \quad (2)$$

where τ = the shear stress, Pa; μ = the coefficient of dynamic viscosity, Pa c; $\dot{\gamma}$ = the velocity gradient, c^{-1}.

The hypothesis of linear correlations between shear stresses and the velocity gradient proposed by Newton is not valid for all liquids.

Liquids whose rheological behavior differs from the equation are called non-Newtonian. Non-Newtonian fluids are divided into three groups (Mirzajanzade. 1999, Rogachev. 2000):

1. nonlinearly viscous fluids (shear stress is a nonlinear function of shear rate);
2. liquids with unsteady rheological characteristics (the functional relationship between shear stress and shear rate depends on the time or process history);
3. viscoelastic fluids (exhibit elastic restoration of shape after stress relief).

The studied oil sample can be attributed to nonlinearly viscous liquids.

A general classification of rheological models of nonlinearly viscous fluids proposed by various researchers was given in (Mirzajanzade. 1999.).

3 RESULTS AND DISCUSSION

Experimental studies were carried out at the Center for Engineering Surveys (Mining University), on a Kinexus ultra + rotational rheometer. The principle of operation of the Kinexus ultra + rotational rheometer is to apply an adjustable shear strain to the test sample in order to measure the flow properties.

As a result of experimental studies, the main rheological dependencies were obtained. The obtained dependences show the presence of non-Newtonian properties in oil transported without additives (Figure 2) and in oil samples transported with an additive of 20 g/t (Figure 3) in the temperature range 10-30 ℃.

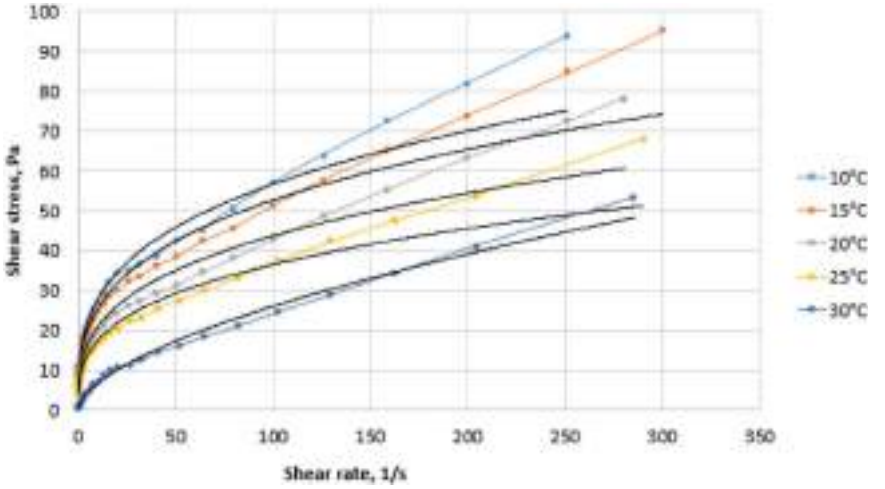

Figure 2. The dependence of shear stress on shear rate without additive.

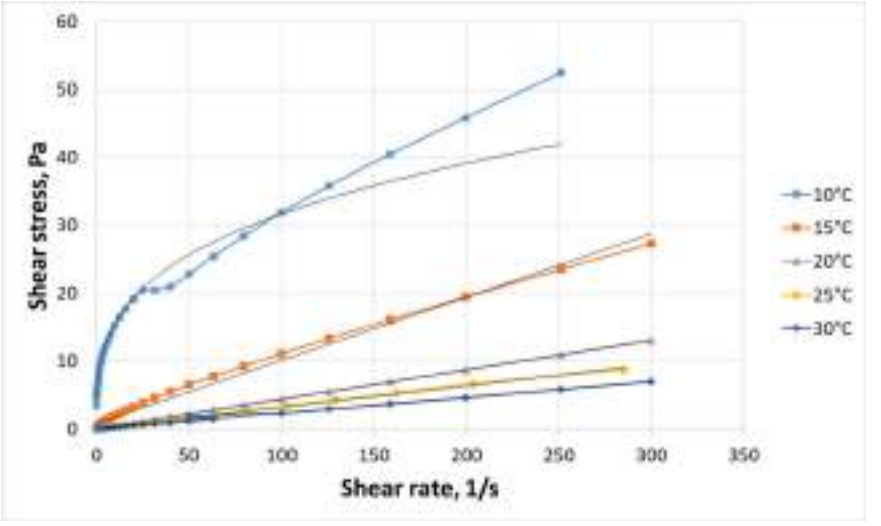

Figure 3. The dependence of shear stress on shear rate with an additive concentration of 20 g/t.

During data processing the authors obtained the following dependences for a sample of oil transported without the use of an anti-turbulent additive:

Sample heating to 10℃:

$$\tau = 13,863\dot{\gamma}^{0,3057} \tag{3}$$

Sample heating to 15℃:

$$\tau = 12,5\dot{\gamma}^{0,3123} \tag{4}$$

Sample heating to 20℃:

$$\tau = 10,197\dot{\gamma}^{0,3161} \tag{5}$$

Sample heating to 25℃:

$$\tau = 8,4988\dot{\gamma}^{0,3168} \tag{6}$$

Sample heating to 30℃:

$$\tau = 1,7589\dot{\gamma}^{0,5857} \tag{7}$$

According to the results of dependences (3-7) and according to the data in Table 1, the oil corresponds to the Ostwald - de Waal model. During the pumping oil without using an additive, the oil sample belongs to nonlinearly viscous liquids and shows the presence of non-Newtonian properties when heated to 30 ℃.

During data processing, authors obtained the following dependences for oil sample transported with an anti-turbulent additive with a concentration of 20 g/t.

Sample heating to 10℃:

$$\tau = 7,7621\dot{\gamma}^{0,3052} \tag{8}$$

Sample heating to 15℃:

$$\tau = 0,0931\dot{\gamma} + 0,8074 \tag{9}$$

Sample heating to 20℃:

$$\tau = 0,0435\dot{\gamma} + 0,0241 \tag{10}$$

Sample heating to 25℃:

$$\tau = 0,0318\dot{\gamma} + 0,0372 \tag{11}$$

Sample heating to 30℃:

$$\tau = 0,0232\dot{\gamma} + 0,0183 \tag{12}$$

According to the obtained dependence 8 and the data of Table 1 the oil corresponds to the Ostwald - de Waal model. According to the obtained dependence of 8, the oil corresponds to the Shvedov-Bingham model. But we can notice that it has a transitional form. According to dependences 9-12, it is clear that when transported with an additive of 20 g/t and when heated to 20 ℃, oil acquires Newtonian properties.

Table 1. The results of calculating the effectiveness of anti-turbulent additive «M-FLOWTREAT» brand C.

Stage	Rate of additive, g/t	Output pressure, kgf/cm²	Inlet pressure, kgf/cm²	Volume flow rate, m³/h	Effectiveness DR, %	Increase in capacity, %
1	-	63.8	2.8	535.00	-	-
2	10	63.7	2.4	610.24	21.59	14.06
3	20	53.9	3.2	700.50	49.86	30.93
4	30	47.7	2.6	734.79	59.08	37.34

4 CONCLUSION

Based on the results obtained during the studying of viscous oil samples at various concentrations of additive from 0 to 20 g/t and heating oil samples from 10℃ to 30℃, the following conclusions and recommendations can be made:

At a certain content and temperature of oil, its properties change slightly. Therefore, increasing the cost of regulation of the temperature and the content of the additive is not rational, because efficiency during pumping does not change significantly.

With an increase in additive concentration and temperature, oil with non-Newtonian properties begins to correspond to the model described by Newton.

The optimal mode for pumping this oil is pumping at 20 ℃ with an additive concentration of 20 g/t. Moreover, increasing in additive concentration will not lead to efficiency improvement.

REFERENCES

Abarasi Hart. 2014. A review of technologies for transporting heavy crude oil and bitumen via pipelines. Journal of Petroleum Exploration and Production Technology – Vol. 4, 327–336.

Avksentiev S.Y., Nikolaev A.K. 2017. Influence of Rheology on Pressure Losses in Hydrotransport System of Polymetallic Ores Tailings. IOP Conference Series: Earth and Environmental Science Volume 87, Issue 5: 6.

Grachev S.I., Korotenko V.A., Kushakova N.P. Study on influence of two-phase filtration transformation on formation of zones of undeveloped oil reserves. Journal of Mining Institute. 2020. Vol.241, p. 68–82. DOI: 10.31897/PMI.2020.1.68

Dolgii I.E. Methods to Enhance Oil Recovery in the Process of Complex Field Development of the Yarega Oil and Titanium Deposit. Journal of Mining Institute. 2018. Vol.231, p.263–267. DOI: 10.25515/PMI.2018.3.263

Khudyakova, I.N. et al. 2018. Raw peat production and processing from flooded fields and approaches to maintain dehydration IOP Conference Series: Earth and Environmental Science.

Martinez-Palou R, Maria de Lourdes M, Beatriz Z-R, Elizabeth M-J, Cesar B-H, Juan de la Cruz C-L, Jorge A. 2011. Transportation of heavy and extra-heavy crude oil by pipeline: a review. J Pet Sci Eng 75:274–282

Mirzajanzade A.H. 1999. Studies on the modeling of complex oil production systems. Nonlinearity, nonequilibrium, heterogeneity. Ufa, Russia.

Muratova V.I. 2014. Assessment of the effect of anti-turbulent additives on the hydraulic efficiency of oil pipelines. Ufa, Russia: 462

Nikolaev A K, Klimko V.I., 2016. Selection of rational heating temperature for pipeline pumping high-viscosity and high pour point crude oil, Journal of Mining Institute, T. 217, 50–54.

Rogachev M.K., Kondrasheva N.K. 2000. Rheology of oil and oil products. Ufa, Russia: 89.

Advances in Raw Material Industries for Sustainable Development Goals – Litvinenko (Ed)

Development of detergent for drilling muds while directional drilling

R.R. Gizatullin
Postgraduate student, Saint-Petersburg Mining University, Saint-Petersburg, Russia

M.E. Budovskaya
Postgraduate student, Saint-Petersburg Mining University, Saint-Petersburg, Russia

M.V. Dvoynikov
Doctor of technical sciences, Saint-Petersburg Mining University, Saint-Petersburg, Russia

ABSTRACT: Research is devoted to the development of formulations detergent for drilling muds in order to reduce the adhesion of clay particles to drill pipes while deepening complex sections of the trajectory of a directional well in the intervals composed of clay rocks. Three types of glycerol-based additive composition with the addition of emulsifiers and water repellents were investigated in various concentrations in the range of 0.5 - 2%. As a result of complex studies which including measurements of the rheological parameters of drilling fluids and bench tests on the model according to the methodology presented in the report, the optimal formulation of detergent was determined. The best results were determined for the additive at a concentration of 1% for all test samples of the presented drilling fluids. The effectiveness of the detergent is estimated in the mass reduction degree of oil seal which formed on the simulator. It amounted to 65-71% in the experiments.

1 INTRODUCTION

The main part of graphic log in Russia (especially Western Siberia) is made up of plastic rocks, in the total mass of which prevail clays. Drilling rocks of this kind with water-basedmuds is often accompanied by various complications, such as bit balling leads, column tacking. Oil seal formation is the process of sticking of soft sticky rocks (usually clays) on the cutting edges of the bit, which leads to their temporary inefficiencies on the elements of the drill string in the places of transition from a large diameter to a smaller one (Guseynova et al. 2016). This process leads to a decrease in the rate of penetration, an increase in the forces of resistance to movement of the tool in the well, the occurrence of talus and rockfall due to the effect of pistoning at lifting the drill string with the oil seal (Nikolaev et al. 2014; Idress et al. 2020). The cause of oil seal formation is insufficient breed inhibition, in particular hydration and drilling of granular highly permeable formations.

Resistance forces to tool movement in wells largely depend on the quality of the drilling fluid and, above all, on the level of its antifriction and adhesive properties (Durkin et al. 2013; Petrov et al. 2015). It should be noted that the worsening of the structure, thixotropic and rheological properties of the drilling mud causes the bit balling. In this case, the bit balling leads to an increase in uncontrolled hydrodynamic pressures in the wellbore and possibility of oil and gas shows and hydraulic fracturing (Morenov et al. 2017; Petrov et al. 2015). In this regard, relevant is the development of formulations detergent and lubricant additives to reduce friction between the borehole walls and the drill string and to reduce bit and elements of the bottom hole assembly balling (BHA) (Alsaba et al. 2017; Nikolaev et al. 2016).

Currently, research is underway in the field of lubricating and anti-oil additives. There are Russian and foreign production. For example, SONBUR manufactured by CJSC "PETROCHEM EXPERIMENTAL PLANT" (Russia), K-LUBE (KEM-TRON INC, USA), TORQ-TRIM II (Halliburton), OPTIBUR ("BURINTEKH", Ltd, Russia). All of these anti-oil additives are successfully used in production, but they all have approximately the same component composition. A distinctive feature of the developed detergent is the replacement of an water base with glycerin (anhydrous), which currently has no analogues in the production of additives for drilling fluids.

Three types of additive compositions (COMPOSITION 1, COMPOSITION 2, COMPOSITION 3), each of which consists of glycerol (glycerol) C3H5(OH)3, monoalkyl ether of polyethylene glycol based on fatty acid with the addition of oxyethylene and monoalkylamine in different volume fraction, were studied in order to solve the task of developing formulations of detergent additives for drilling muds. To determine the effectiveness of the fight against bit balling, these COMPOSITIONS (1-3) in concentrations of 0.5-2.0% were added to the basic drilling muds. Further measurements of rheological parameters and comparison of bench tests on the model were made. It was carried out to find the best additive composition in the muds at which the mass reduction degree of oil seal will be noticed.

2 MATERIALS AND METHODS

Together with the company "Service Center SBM" for the experiment, a technique was developed that simulates the process of the bit balling leads. A laboratory stirrer was used as the basis for an experimental setup in which the standard polished rod with blades for mixing the solution was replaced with an unpolished steel rod of equal diameter (the layout and appearance of the stirrer are shown in Figure 1 a, b).

This was done in order to bring the experimental conditions closer to real ones, since drill pipes and BHA elements have a higher roughness than polished metal parts of laboratory devices (Bulatov 1977; Ganjumyan et al. 2000; Kalinin 2008). The rod is wetted with the solution while it is in it for 5 minutes before the start of the experiment. The rod rotates in a solution with a frequency close to standard conditions of rotation of a drilling tool with rotary drilling - 50 rpm.

Installation elements simulate a well with a diameter D, a drill string with a diameter d_1, a calibrator with a diameter d_2. In this case, these values will accordingly have values D = 40 mm, d_1 = 20 mm, d_2 = 30 mm, taking into account the proportional reduction of the actual dimensions.

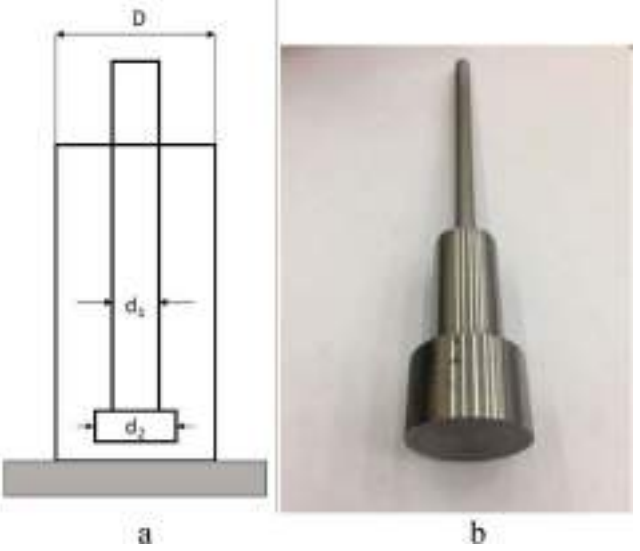

Figure 1. Scheme and type of experimental setup.

The choice of the calibrator as the bottom element of the BHA is due to a small difference in its diameter with the bit and a large role in the danger of the formation of an oil seal in the transition zone from the calibrator in the drill string. The cavernosity coefficient is 1.3 (Idress et al. 2020).

The application of this technique makes it possible to see the process of the bit balling leads during the rotation of a metal rod in the test drilling mud. Researches were carried out using a polymer solution.

3 RESULTS AND DISCUSSION

The grade of clay powder for COMPOSITION 1 was selected after a comparative analysis of the ability of clay powders of various grades to form an oil seal in a polymer solution, as well as taking into account the availability of material (Litvinenko 2007; Chubik 1999; Leusheva et al. 2017). We also recommend the use of dried clay sludge obtained from the interval in which intensive an oil seal is observed.

For example, consider research conducting with COMPOSITION 2. Pour 350 grammes a polymer solution into a 500 ml glass, then use a paddle stirrer with a stirring speed of 100-150 rpm and add the detergent reagent gradually to the solution. Mixing is carried out until the component is completely dissolved. Then 42 grammes of clay powder is gradually dispersed into a glass at a stirring speed of 400-500 rpm. It is necessary to ensure that the minimum amount of clay is dispersed on the mixer blades when dispersing. Dispersion is carried out within 10-12 seconds. Next, pour the suspension into metal cups into which the rods are lowered for subsequent rotation at a speed of 50 rpm. An oil seal is formed within 20 minutes then the rod is washed in distilled water for 20 minutes. Weigh the rods, calculate the average weight of the oil seal in 3 parallel experiments. The effectiveness of the reagent is determined by reducing the weight of the oil seal in comparison with a dummy experiment (without additives).

The optimal formulation of the detergent additive was determined as a result of comprehensive researches which included measurements of the rheological parameters of drilling fluids and bench tests on the model according to the presented methodology. The best results were determined for the additive COMPOSITION 2 with a concentration of 1%.

The graphs (Figures 2-5) show the correlation between two values: the degree of decrease in plastic viscosity and mass reduction degree of oil seal for: gypsum-lime drilling mud, clay drilling mud, biopolymer saline inhibited mud, non-clay mud. Detergent additive COMPOSITION 2 was introduced into all samples at concentrations of 0.5–2%.

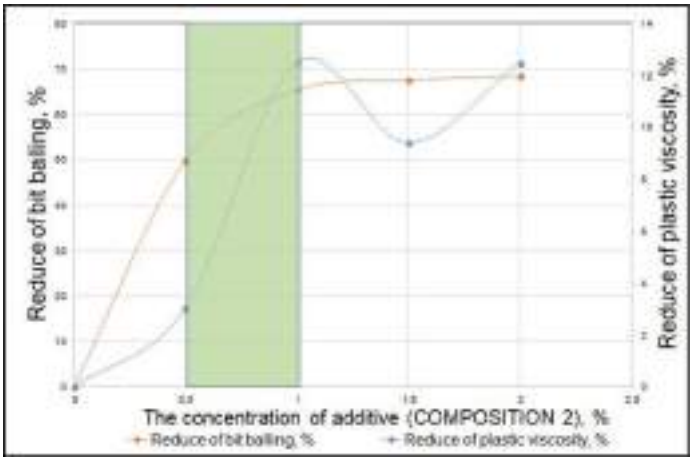

Figure 2. The effect of additives on the reduction the bit balling leads and changes in the viscosity of gypsum-lime mud.

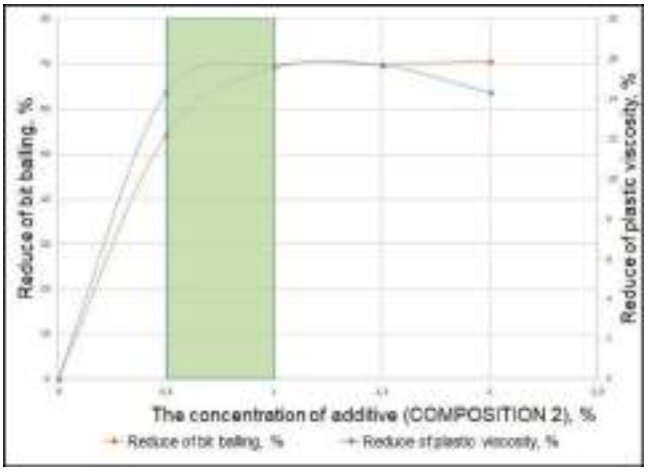

Figure 3. The effect of additives on the reduction the bit balling leads and changes in the viscosity of biopolymer saline inhibited mud.

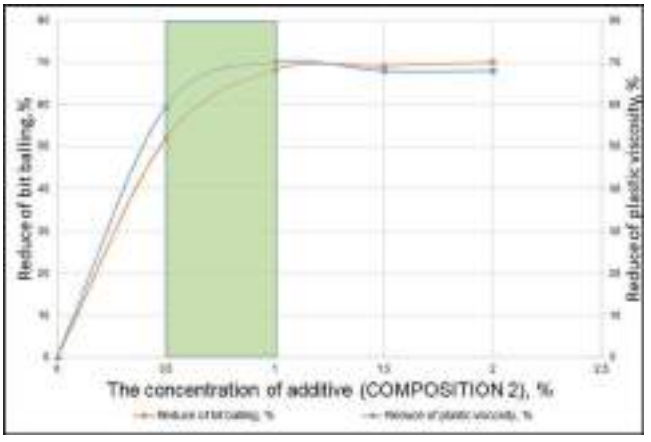

Figure 4. The effect of additives on the reduction the bit balling leads and changes in the viscosity of clay mud.

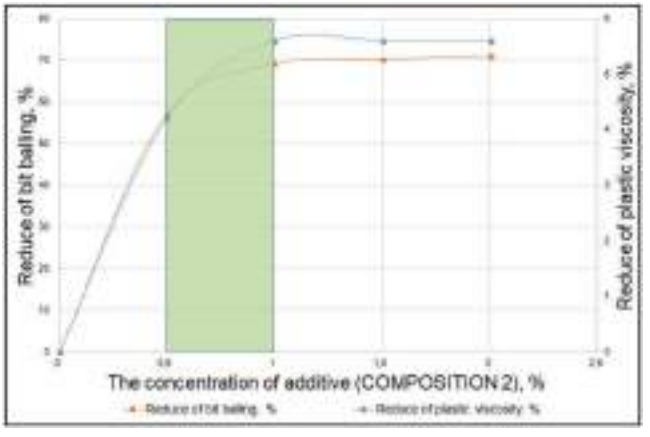

Figure 5. The effect of additives on the reduction the bit balling leads and changes in the viscosity of non-clay mud.

The criterion for the success of detergent additives is the achievement of an effect in which mass reduction degree of oil seal is reduced by more than 50%. An increase in the content of introduced additives of more than 1% does not have a noticeable effect on the elimination of oil seals on BHA elements. The zones of dependence of the change in mass of oil seal with the introduction of additives for each solution are highlighted in green in Figures 2–5. Researches have shown a mass reduction degree of oil seal with the introduction of additives by 67-71% and a decrease in plastic viscosity - up to 15%.

4 CONCLUSION

The use of a new detergent additive leads to a decrease in oil seal formation on the elements (BHA) and bit due to a decrease in the adhesion of clay particles to metal surfaces. This detergent additive improves the rheological properties of the drilling fluid and increases the lubricating properties. A regulation has been developed for regulating the technological properties of the system on the basis of the studies as well as a draft instruction for the use of detergent additives.

REFERENCES

Alsaba, M, Al Dushaishi, MF., Nygaard, R., Nes O-M & Saasen, A. 2017. Updated criterion to select particle size distribution of lost circulation materials for an effective fracture sealing. *Journal of Petroleum Science and Engineering* 149: 641–648.

Bulatov, A.I. 1977. *Grouting materials and well cementing technology*. Moscow: Nedra.

Chubik, P.S. 1999. *Qualimetry of drilling fluids*. Tomsk: NTL.

Durkin, V. V. & Ionov, I. V. 2013. Integrated solution of the problem relating to bit packing prevention during wells' upper intervals drilling. *Journal Construction of oil and gas wells on land and sea*, (4): 13–22. Moscow: Russia.

Ganjumyan, R.A., Kalinin, A.G. & Nikitin, B.A. 2000. *Engineering calculations when drilling deep wells: A reference guide under the general*. Moscow: Nedra.

Guseynova, E. L. & Zernov, M. N. 2016. Application of lubricant and antiadhesive additives to drilling fluids. *Collection of scientific papers of the 43rd International Scientific and Technical Conference of young scientists, post graduate students and students, dedicated to the 60th anniversary of the branch of USTU*: 141–145. Oktyabrsky: Russia.

Idress, M. & Hasan, M.L 2020. Investigation of different environmental-friendly waste materials as lost circulation additive in drilling fluids. *Journal of Petroleum Exploration and Production Technology* 10: 233–242. Bandar Seri Iskandar, Perak Darul Ridzuan: Malaysia.

Kalinin, N.G. 2008. *Drilling oil and gas wells (lecture course): Textbook Russian State Geological Exploration University*. Moscow: TsentrLitNefteGaz.

Litvinenko, V.S. & Kalinin, A.G. 2007. *Basics of drilling oil and gas wells: a Training manual*. Moscow: Higher School.

Leusheva, E. & Morenov, V. 2017. Research of clayless drilling fluid influence on the rocks destruction efficiency. International Journal of Applied Engineering Research, 12(6): 945–949. India.

Morenov, V. & Leusheva, E. 2017. Development of drilling mud solution for drilling in hard rocks. *International Journal of Engineering, Transactions A: Basics*, 30(4): 620–626. Iran.

Nikolaev, N.I. & Leusheva, E.L. 2016. Increasing of hard rocks drilling efficiency. *Neftyanoe Khozyaystvo - Oil Industry*, 3: 68–71. Russia.

Nikolaev, N.I., Liu, T., Wang, Z., Jiang, G., Sun, J., Zheng, M. & Wang, Y. 2014. The experimental study on a new type low temperature water-based composite alcohol drilling fluid. *Procedia Engineering*, *73*: 276–282. Netherlands.

Petrov, N.A., Yangirov, F.N., & Davydova, I.N. 2015. Research of domestic and foreign lubricant additives of drilling fluids. *Network publication "Oil and Gas Business"*, 5: 150–171. Russia.

Advances in Raw Material Industries for Sustainable Development Goals – Litvinenko (Ed)
© 2021 Taylor & Francis Group, London, ISBN 978-0-367-75881-3

Stress-stain state of a vertical steel tank affected by bottom sediments in conditions of extreme temperature differences

R.R. Sultanbekov
Postgraduate student, Saint-Petersburg Mining University, Saint-Petersburg, Russian Federation

R.D. Terekhin
Student, Saint-Petersburg Mining University, Saint-Petersburg, Russian Federation

M.N. Nazarova
PhD, Associate professor, Saint-Petersburg Mining University, Saint-Petersburg, Russian Federation

ABSTRACT: This article describes the analysis of the stress-strain state of the tank taking into account bottom sediments of oil products and the influence of the temperature of the oil product and the environment using the Ansys software package. Effects that oil product has separately and oil product with bottom sediments have on a stress-stain state are compared. Oil products having different temperatures of 20, 30, 40, 50 °C are examined in different series. Calculations at various ambient temperatures (-60, -50, –40 °C; –20 °C; 0 °C; +20 °C; +40 °C) are presented in each series. Different densities of oil product and bottom sediment were considered. Based on the analysis of the stress-strain state using finite element modeling on the example of a vertical steel tank, it was shown that the stresses in the zone of the miter weld, as well as in the places of installation of the receiving-distributing branch pipe and the manhole, are maximum. It is in these zones that the influence of bottom sediment and temperature is significant, since they form local elevated stress zones, which increase significantly when the walls are thinned.

1 INTRODUCTION

The subject of this work is vertical steel tank of the PBC series, and bottom sediments which can appear during normal operation.

Actuality of the work is dictated by absence of scientific research on the theme and by need in increasing reliability, efficiency and safety of oil tank operation.

The study is aimed on testing the following hypothesis: temperature of the bottom sediment affects the stress-stain state of a steel tank; more accurately, the higher change in temperature of a bottom sediment is, the greater stress values are observed in the wall of the tank. This statement is based on the fact that the density of a liquid depends on its temperature. Moreover, temperature stresses appear when the metal wall is heated by bottom heaters of a reservoir. However, it is unclear whether these phenomena can lead to serious consequences, up to reservoir destruction, and is there a significant interplay between temperature changes and the presence of bottom sediments.

The theme of this study is new and is uncovered in previous works. There are a number of studies related to stress-stain study of a steel tank in correlation with cyclic operation loads (Prokopov & Tkachyova., 2015), in correlation with temperature changes (Kuzeev et al., 2013).

The first work considers the same oil tank series as in the current study, but with a different volume, and uses finite element method. Results show influence of loads on the bottom part of the tank and especially its foundation. The second work shows the stress in the zone of

a nozzle using the same finite element method. However, none of these studies consider the affect that bottom sediments can have on a stress-stain state of a tank.

The only work on the theme is made by the authors of this work. Authors have been doing research on the theme for quite a long time, and have articles published (Sultanbekov et al., 2019). In this work temperature changes are greater; moreover, environment temperature is also taken into account. The previous work did not take this aspect into consideration.

In this article authors model the stress-stain state of a vertical steel tank in ANSYS software package, figure out the value of stresses in the wall in different temperatures, make conclusion about connection between stress level and sediment temperature.

2 THEORY AND METHOD

2.1 *Theoretical background*

Tanks for oil and oil product storage are one of the main technological objects of oil depots and trunk oil pipelines (Sherstobitova et al., 2008). The ecology of the area where tank farms and human safety are located depends on their reliability. Ensuring the required level of reliability of the steel vertical cylindrical tank is carried out at the operation stage. In case of tank accidents, oil products pollute adjacent territories and water basins (Bykova et al., 2019). The economic damage from accidents involving leakage of petroleum products includes not only direct losses, but also the costs of environmental measures to restore the environment, as well as the costs of replenishing the stock of petroleum products.

Modern regulatory documents, (GOST R 52910 - 2008) do not establish the maximum service life of tanks. Tank dismantling is done only according to the results of a diagnostic examination - instrumental and calculated (Kuzeev et al., 2013). The tank is a vertical shell with a bottom; however, the presence of geometric features significantly changes the symmetry of the structure, the distribution of stresses and strains in local zones, which is difficult to take into account when performing analytical calculations.

Thanks to the use of software systems for finite element calculations, such as Ansys, it becomes possible to determine the most dangerous zones and predict the stress-stain state (SSS) during operation, taking into account additional factors. One of such is bottom sediment, which is formed during storage and mixing of oil products (Sultanbekov & Nazarova, 2019). Especially active sedimentation is observed when different types of residual oil products are mixed due to their incompatibility (Mitusova et al., 2018). Sedimentation occurs due to imbalance and instability of fuels, when the amount of aromatic hydrocarbons decreases, so the proportion of paraffin and asphaltenes in the mixture increases (Kondrasheva et al., 2019). Cases of "incompatibility" during the mixing of petroleum products are associated with the emergence of strong intermolecular interactions caused by changes in the structural group composition and the mutual ratio of the concentrations of high molecular weight compounds of petroleum products (Karimov & Mastobaev, 2012), which leads to the formation of molecular associates, bulk colloidal particles of various shapes and structures (Kondrasheva et al., 2018). The problem of "incompatibility" of oil products is extremely urgent, since due to the precipitation of sediment on the tanks during operation, the useful volume decreases and the need to clean the tanks arises, and when mixing fuels because of the "incompatibility", the quality of the whole product deteriorates in the first place, the subsequent use of which increases the risk of equipment wear (ISO 8217, 2017).

When there is a big temperature difference, especially in zones of extremely low temperatures, the problem of reservoir operation is quite important (YUhtorov et al., 2018). Such conditions can be found in some northern regions, in the Arctic zone. Tank's wall metal is exposed to greater loads, and this fact should be taken into consideration during tank design to ensure its safe and reliable operation (Bondarev et al., 2017).

2.2 *Method*

To determine the effect of bottom sediment, mainly consisting of asphaltene-tar paraffin deposits, on SSS diagram, we consider vertical steel tank PBC-20000, which stores a mixture of residual fuels of the RMK-700 grade with a density of 958 kg/m3 at 15 °C and has a viscosity of 550 sSt at 50 °C. Liquid surface height is 12 meters, the material of the tank is Steel 3. There is a fixed roof, the weight with the equipment installed on it is 10,000 N. Laboratory tests of viscosity were performed using a Stabinger SVM 3000 laboratory instrument, and Anton Paar DMA 4100 M equipment used to measure density. The results are shown in Table 1.

The reservoir model was created and the tank SSS calculations were performed in the Ansys software package, taking into account the stored residual fuel and total sediments at a temperature of 20 °C (Figure 1).

Table 1. Density of the residual fuel and total sediment depending on the measurement temperature.

Temperature, °C	Total sediment, kg/m3	Residual fuels RMK-700, kg/m3
15	1090.0	958.0
20	1087.2	954.8
25	1084.4	951.6
30	1081.5	948.4
35	1078.7	945.1
40	1075.9	941.9
45	1073.0	938.7
50	1070.2	935.4
55	1067.4	932.2
60	1064.5	928.9
65	1061.6	925.7
70	1058.8	922.4

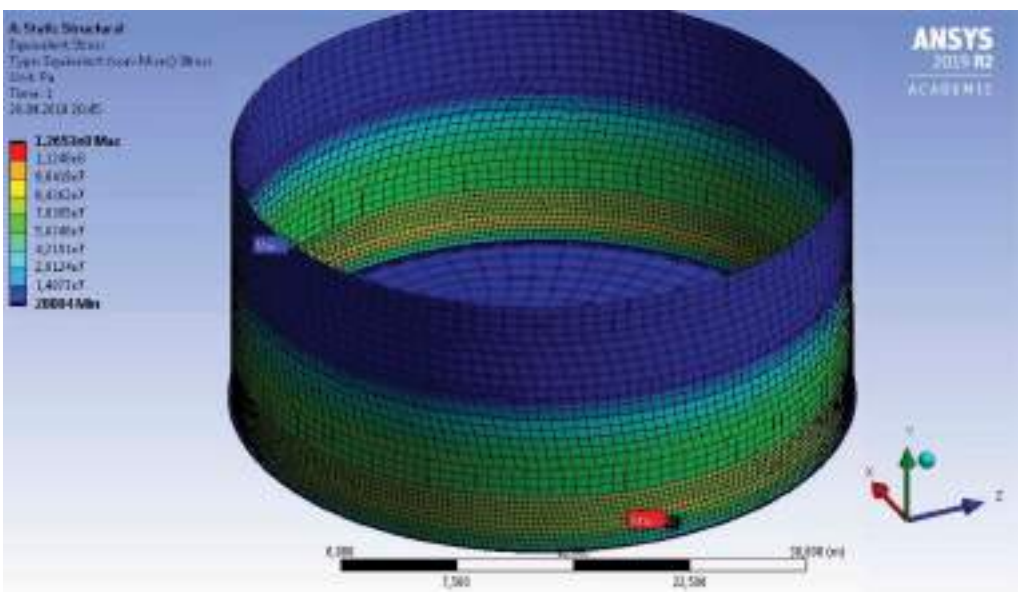

Figure 1. SSS of a reservoir without bottom sediment, 20 °C.

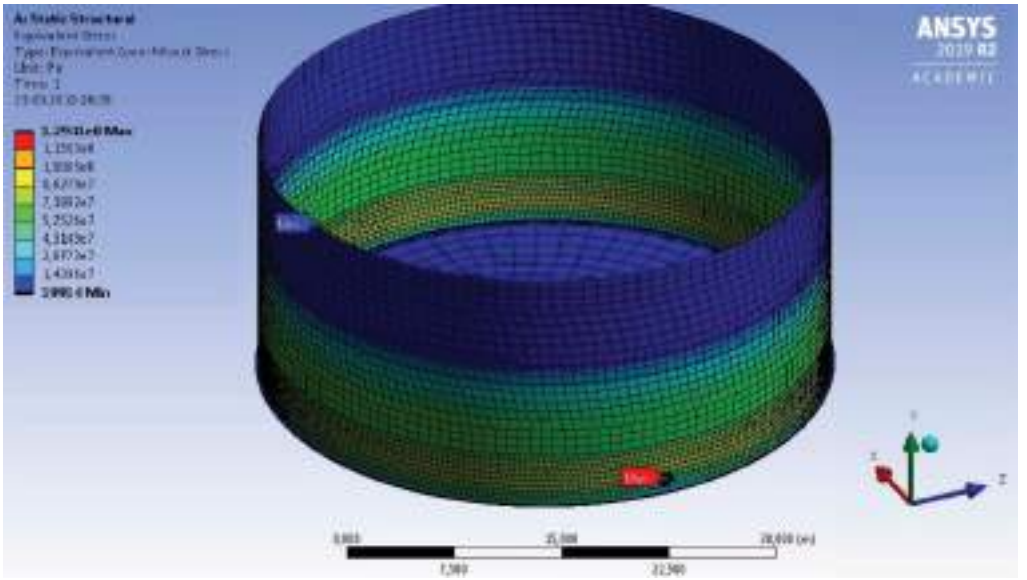

Figure 2. SSS of a reservoir, 1,3 meter of bottom sediment, 20 °C.

In the absence of sediments, the maximum stresses of 126 MPa are observed in the zone of the masonry weld, as well as in the places of installation of the dispensing nozzle and manhole.

Another calculation is made with bottom sediment with a height of 1.3 meters. The density of sediments is 1090 kg/m^3 at 15 °C. (Figure 2).

Attention should be paid to an increase in the maximum stresses created by the liquid column. Unaccounted stress in the metal can lead to negative consequences, especially under bad circumstances. Especially when you consider that the tank is loaded cyclically, and metal failure may occur earlier than anticipated. Especially when you consider that the tank is loaded cyclically, and metal failure may occur earlier than anticipated.

The ambient temperature changes, so does the magnitude of the stresses in the tank wall. This is due to the thermal expansion of the metal. Bottom sediments also affect the stress experienced on the tank wall. So, with a large temperature difference, the maximum stress in the metal can exceed the yield strength, which leads to the destruction of the tank.

Several series are to be calculated. Let the fluid in the tank be heated, its density and temperature are constant during one series. Totally there are four series for each temperature of the stored product – 20, 30, 40, 50 °C. Calculations for different ambient temperatures (-60, -40, -20, 0, 20, 40 °C) are made in one series.

2.3 *Product's temperature is 50 °C.*

Results are shown on Figure 3. Calculation is present for six different ambient temperatures and the same product temperature, which is constant and is 50 °C.

As expected, maximum stress values are obtained with greater temperature difference, and are located in the zones of nozzle and manhole. As the temperature gets higher, stress is lowered at first and gets bigger then, but its distribution is almost the same. Points of max and min values in these cases differ because of low mesh resolution due to free license limitations. Results of calculations are in the Table 2.

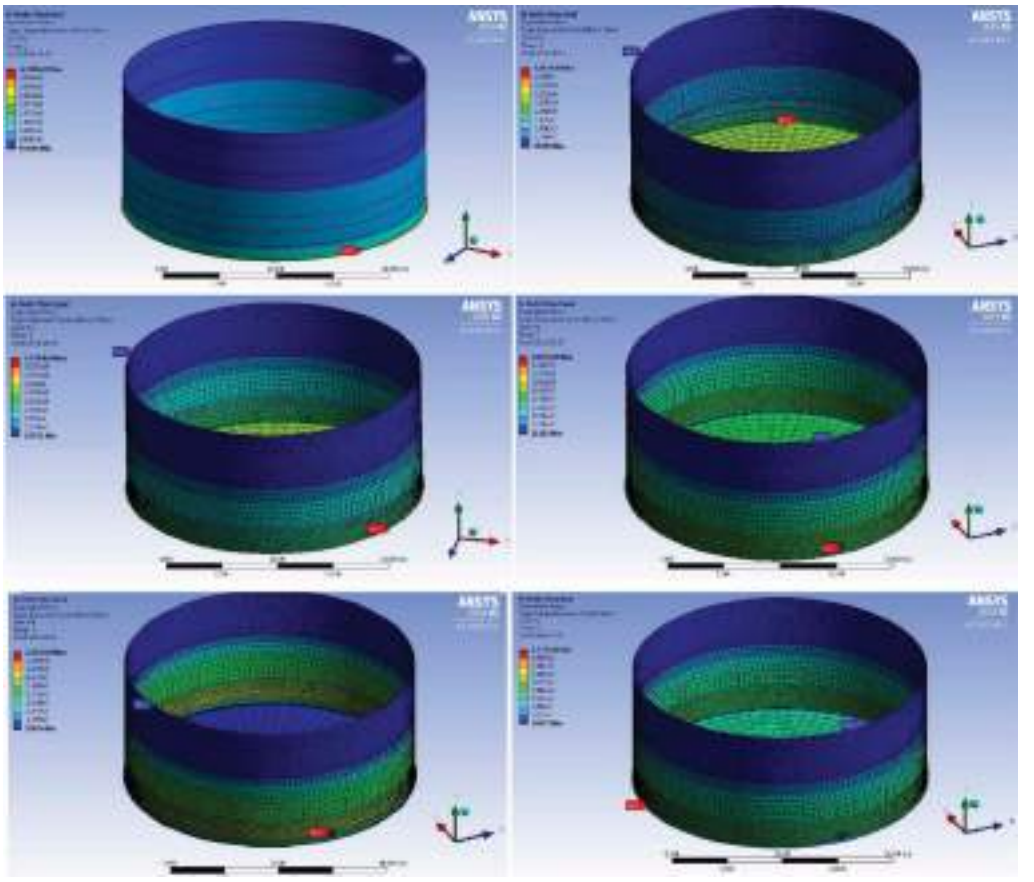

Figure 3. SSS of a reservoir, 1.3 meter of bottom sediment, different ambient temperatures, product at 50 °C.

Table 2. Stress depending on the temperature, product at 50 °C.

Ambient temperature, °C	Maximum stress in a wall, Mpa
-60	444
-40	336
-20	227
0	159
20	129
40	177

2.4 *Series representing product at 40 °C*

As well as in the previous set of calculations, product temperature is constant while ambient temperature is changing. SSS remains almost the same while values change dramatically (Figure 4).

Slight increase in stress due to increased densities of product and sediment is worth mentioning.

Results are shown in the Table 3. Some values representing stress in nozzle or man-hole (the bigger one) are shown separately. Theoretically such different values are caused

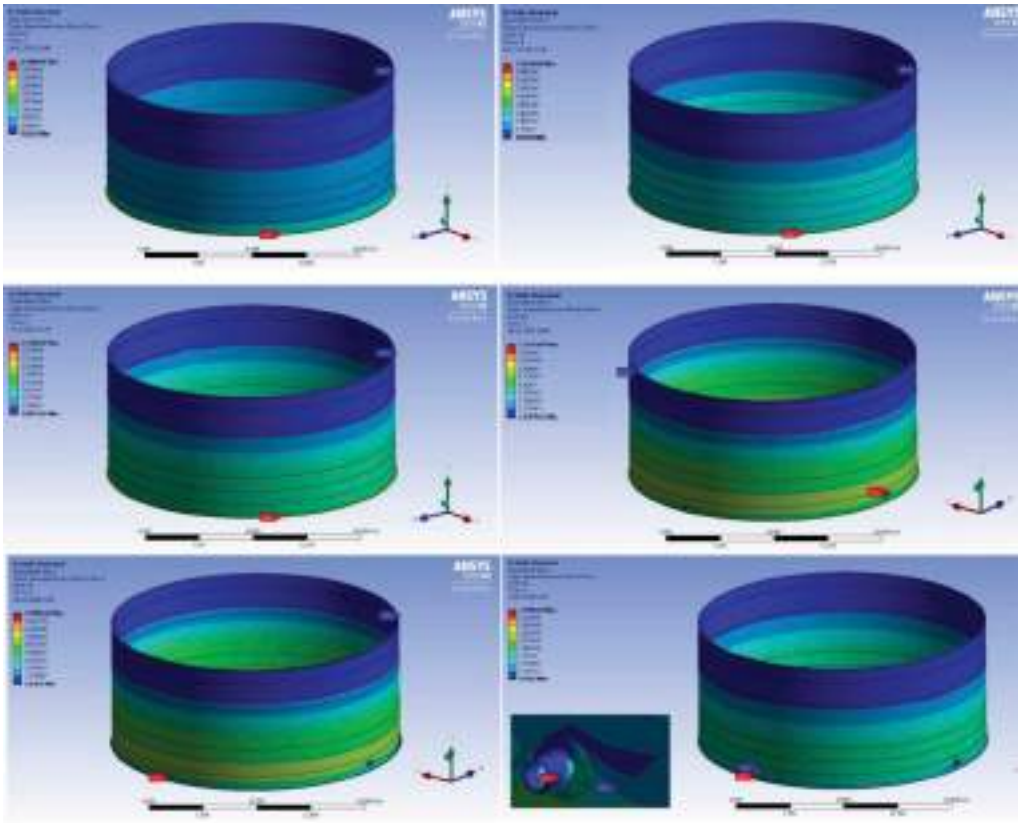

Figure 4. SSS of a reservoir, 1.3 meter of bottom sediment, different ambient temperatures, product at 40 °C.

Table 3. Stress depending on the temperature, product at 40 °C.

Ambient temperature, °C	Maximum stress in a wall, MPa	Maximum stress in nozzle or manhole, MPa (if differ from the other parts)
-60	445	
-40	336	
-20	228	
0	105	157
20	124	159
40	133	239

by low-resolution mesh rather than actual load on the part. It can be understood while closely examining the results: only one mesh node has such great values.

2.5 *Series representing product at 30 °C*

The same as above. Calculation results are shown on Table 4.

Stress measured in manhole and nozzle zones doesn't necessarily represent actual stresses in a real reservoir. Calculation results are shown in Table 4.

Table 4. Stress depending on the temperature, product at 30 °C.

Ambient temperature, °C	Maximum stress in a wall, MPa	Maximum stress in nozzle or manhole, MPa (if differ from the other parts)
-60	446	
-40	337	
-20	229	
0	106	158
20	125	160
40	133	240

Table 5. Stress depending on the temperature, product at 20 °C.

Ambient temperature, °C	Maximum stress in a wall, MPa	Maximum stress in nozzle or manhole, MPa (if differ from the other parts)
-60	447	
-40	337	
-20	229	
0	107	159
20	126	162
40	135	242

2.6 *Series at 20 °C*

In previous cases the product was heated. Now let's consider the situation without heating. Product density reaches its maximum, so the highest values of stress are expected.

As expected, stresses are mostly to the thermal expansion of wall metal. The most dangerous points are again the nozzle and the manhole. Stress values change while the distribution remains the same. Results are shown in Table 5.

3 CONCLUSIONS

As a result of the analysis of the stress-strain state of the tank, taking into account the operational loads of the reservoir models, it was established that the stress in the casing increases during the operation of the reservoir.

Analysis of SSS using finite element methods showed that with active sedimentation and an increase in the temperature of the stored product, an increase and redistribution of stresses occurs in the lower zone. Also, calculations of the influence of ambient temperature and bottom sediment on SSS showed the highest stresses in the lower zone at the most negative values, namely -60 C. As a result, stress concentration zones arise that are located directly in the zone of the weld seam and in the places of installation of the receiving-distributing branch pipe and manhole, which are not taken into account when calculating by standard methods.

REFERENCES

Bondarev E., Rozhin I., and Argunova K. 2017 Features of mathematical modeling of natural gas production and transportation systems in the Arctic zone of Russia. Journal of Mining Institute, 228 (6), 705. DOI: http://dx.doi.org/10.25515/pmi.2017.6.605.

Bykova M.V., Pashkevich M.A., Matveeva V.A., Sverchkov I.P. 2019. Assessment and abatement of the soil oil-contamination level in industrial areas. In: Litvinenko V. (ed.), Topical Issues of Rational Use

of Natural Resources – Proceedings of the International Forum-Contest of Young Researchers, pp. 347–359.
GOST R 52910–2008. Rezervuary vertikal'nye cilindricheskie stal'nye dlja nefti i nefteproduktov. Obshhie tehnicheskie uslovija. M.: Standartinform. 56 c. [in Russian].
ISO 8217 Fuel Standar. – 2017. - URLhttps://https://www.wfscorp.com/sites/default/files/ISO-8217-2017-Tables-1-and-2-1-1.pdf (date of the application10.01.2019).
Karimov R M, Mastobaev B N. 2012. Vliyanie soderzhaniya parafinov, smol i asfal'tenov na tovarnye kachestva neftej//Bashkirskij himicheskij zhurnal.-Tom 19.
Kondrasheva N. K., Eremeeva A. M., & Nelkenbaum K. S. 2018. Development of domestic technologies of produsing high quality clean diesel fuel. Izvestiya vysshikh uchebnykh zavedenii Khimiya Khimicheskaya Tekhnologiya, 61(9-10), 76–82. https://doi.org/10.6060/ivkkt.20186109-10.5651.
Kondrasheva N. K., Eremeeva A. M., Nelkenbaum K. S., Baulin O. A. & Dubovikov O. A. 2019. Development of environmentally friendly diesel fuel, Petroleum Science and Technology, 37:12, 1478–1484, DOI: 10.1080/10916466.2019.1594285.
Kondrasheva N K, Rudko V A, Kondrashev D O, Konoplin R R, Smyshlyaeva K I, and Shakleina V S. 2018. Functional influence of depressor and depressor-dispersant additives on marine fuels and their distillates components. Petroleum Science and Technology 36 (24), 2099–2105. DOI: 10.1080/10916466.2018.1533858.
Kondrasheva N K, Rudko V A, Kondrashev D O, Shakleina V S, Smyshlyaeva K I, Konoplin R R, Shaidulina A A, Ivkin A S, Derkunskii I O, Dubovikov O A. 2019. Application of a Ternary Phase Diagram to Describe the Stability of Residual Marine Fuel /// Energy & Fuels. Vol. 33, № 5. P. 4671–4675.
Kuzeev I.R., Tlyasheva R.R. and others. 2013. Technique of definition the stress-strain state of the steel cylindrical tank. FSBEI HPE "Ufa state petroleum technological university", Ufa, Russian Federation. – №4 – pp. 339–347. http://ogbus.ru/article/view/metodika-opredeleniya-napryazhenno-deformirovannogo-sostoyaniya-stalnogo-cilindricheskogo-rezervuara.
Mitusova T N, Kondrasheva N K, Lobashova M M, Ershov M A, and Rudko V A. 2017. Influence of dispersing additives and blend composition on stability of marine high-viscosity fuels. Journal of Mining Institute 228, 722–725. DOI: 10.25515/PMI.2017.6.722.
Mitusova T N, Kondrasheva N K, Lobashova M M, Ershov M A, and Rudko V A and Titarenko M A. 2018. Determination and Improvement of Stability of High-Viscosity Marine Fuels. Chemistry and Technology of Fuels and Oils 53 (6), 842–845. DOI: 10.1007/s10553-018-0870-.
Prokopov A.Y., Tkachyova K.E. 2015. A study of stress-strain state of foundation of vertical vessel subject to dynamic operating loads. Inzhenerniy vestnik Duna, №3. https://ivdon.ru/ru/magazine/archive/n3y2015/3200 [in Russian].
Sherstobitova R T, et al. 2008. Povyshenie bezopasnosti RVS, dlitel'no jekspluatiruemyh v uslovijah nizkih temperature, Ufa: UGNTU, 131 c. [in Russian].
Sultanbekov R. R., Nazarova M. N. 2019. Determination of compatibility of petroleum products when mixed in tanks. EAGE., Tyumen, DOI: 10.3997/2214-4609.201900614. Available at: http://earthdoc.eage.org/publication/publicationdetails/?publication=96369 (Accessed 30 March 2019).
Sultanbekov R.R., Terekhin R.D., Nazarova M.N. 2019. Effect of temperature fields and bottom sediments of oil products on the stress-strain state of the design of a vertical steel tank. Journal of Physics Conference Series, 1431:012055, DOI: 10.1088/1742-6596/1431/1/012055.
YUhtorov V. N., Korol'chenko I. A., Ulanin S E., Sokolov D. N. 2018. Obosnovanie sposoba prognozirovaniya sohranyaemosti kachestva nefteproduktov pri dlitel'nom hranenii (Substantiation of method for forecasting of preserved quality of oil products during long storage).//Mir nefteproduktov. Vestnik neftyanyh kompanij. - №3. - S. 20–27 [in Russian].

Advances in Raw Material Industries for Sustainable Development Goals – Litvinenko (Ed)
© 2021 Taylor & Francis Group, London, ISBN 978-0-367-75881-3

Modification of sodium lignosulfonate with reagent obtaining for drilling fluids

R.A. Fedina
Applicant of the Department of Physical and Organic Chemistry, Federal State Budgetary Educational Institution of Higher Education Ufa State Petroleum Technological University, Ufa, Russia

A.D. Badikova
Doctor of Engineering Sciences, Professor, Head of the Department of Physical and Organic Chemistry, Federal State Budgetary Educational Institution of Higher Education Ufa State Petroleum Technological University, Ufa, Russia

I.N. Kulyashova
Candidate of Engineering Sciences, Head of laboratory of the Department of Physical and Organic Chemistry, Federal State Budgetary Educational Institution of Higher Education Ufa State Petroleum Technological University, Ufa, Russia

D.A. Dubovtsev
Master's Degree Student of the Department of Oil and Gas Technology, Federal State Budgetary Educational Institution of Higher Education Ufa State Petroleum Technological University, Ufa, Russia

M.A. Tsadkin
Doctor of Engineering Sciences, Professor of the Department of High-molecular Compounds and General Chemical Technology, Federal State Budgetary Educational Institution of Higher Education Bashkir State University, Ufa, Russia

ABSTRACT: Analysis of lignosulfonate drilling reagents showed that the reagents based on modified lignosulfonates, that is ferrochrome lignosulfonates (FCLS) are part of most drilling fluids. However, the content of toxic chromium (2.0-3.5% wt), high bottomhole temperatures (150-190°C), as well as a decrease in the volume and quality of sulfite lignosulfonate, which is the main source of raw materials, limits the possibility to use them. To obtain an effective drilling reagent capable of regulating the properties of the drilling fluid, the basic method for modifying the neutral sulfite lignosulfonate to produce drilling reagents with high qualitative characteristics has been improved - the liquefaction index is up to 60%, the filtration index is 6.0-6.5 cm^3/30 min, the nominal viscosity is 24 s, and to increase the stability and resistance of the washing (drilling) liquid to temperature aggression, additional modifiers containing phosphonic compounds are introduced.

Keywords: sodium lignosulfonate, neutral sulfite liquor, modification, phosphonic compounds, drilling reagent, infrared spectroscopy (IR spectroscopy), X-ray fluorescence (XRF)

1 INTRODUCTION

In drilling, a group of reagents based on lignosulfonates is widely used, i.e. oxidized and chromium-substituted lignosulfonate (oxyl), ferrochrome lignosulfonate (FCLS), spent sulfite-alcohol liquor (SSAL), sulfite yeast mash (SYM), condensed spent sulfite-alcohol liquor

(CSSAL), etc. The main disadvantage of these reagents is the weak effect under conditions of high bottomhole temperatures.

Acrylic polymers, in particular, gipan, metas, K-4, M-14, Lacris-20, and others, are very resistant to heat. However, their use is not always effective because of their instability to polyvalent metal salts, for example, to the effect of calcium ions; the high cost of imported macromolecular substances and the scarcity of domestic ones (the needs for polymer reagents are satisfied only by 40-50%) (Komkova, 2011).

Tretyak A.Ya. proposed a drilling fluid containing 0.5-2.0% carboxymethyl cellulose, dextrin crumb, which is a mixture of hydrocarbons formed during the hydrolysis of potato and maize starch 0.5-3.0% and water (Pat. RF 2038362, 1995). Dextrin crumb is a colmatation filler, and the rest of the solution is very sensitive to polysalt mineralization, so the use of this solution is limited, it can be used only in fresh systems.

The same author proposed the composition of the solution containing 0.5-3.0% dextrin groats, 0.5-2.0% CMC, 0.1% sodium hydroxide and water (Bulatov et al., 1999). The presence of caustic soda creates an increased pH value of the medium (up to 14), which limits their use under conditions of using aluminum pipes and adversely affects the stability of the borehole walls (Kulyashova, 2016).

An analysis of the papers of domestic and foreign researchers showed that the most optimal stabilizing reagents for mineralization conditions and high temperatures may be linear polymeric substances containing non-ionic functional groups that provide optimal adsorption on the solid phase (Komkova, 2011).

A method of obtaining a reagent for processing drilling fluids (Levik, 1982) is known, including the oxidation of spent sulfite-alcohol liquor with alkali metal dichromates, followed by condensation, where the oxidation and condensation being carried out for 1-2 hours at 20-30ºC at pH 6.0-6.5 of the initial raw mixture in the presence of fatty acids of vegetable oils. The disadvantage is that due to high pH and reaction medium dilution, a low degree polycondensation reagent is formed and as a sequence of this, with lower stabilization efficiency and reduced filtration of drilling fluids. In addition, the reagent is used in overdosages.

A method of obtaining a reagent is also known (Pat. RF 2152419, 2000), which is constant in composition and qualitative characteristics, with high performance properties, obtained by polycondensation of lignosulfonates with formaldehyde and a co-condensing agent in an aqueous medium with an acid catalyst when heated, followed by neutralization of the reaction mass with alkali metal hydroxides, characterized in that polycondensation is carried out stepwise: initially, lignosulfonates interact with formaldehyde, then into the reaction mass a co-condensing reagent is introduced and additional polycondensation is carried out, and the neutralized reaction mass is dried. The disadvantage of this production method is that it is proposed to use highly toxic phenol, phenolsulfonic acid, etc., as a co-condensing reagent, which increases the environmental risks when using this drilling reagent.

In the structure of lignosulfonates, there are active centers capable of entering into the polycondensation reaction (of the phenolaldehyde type) with the enlargement of the starting substances (Bulatov et al., 1999). This leads to an increase in the antifiltration and thermostabilizing properties of condensed lignosulfonates as reagents for drilling fluids. Condensed lignosulfonates are obtained, for example, by their interaction with formaldehyde in an aqueous medium when heated with an acid catalyst (Badikova, 2014). The disadvantage is condensed lignosulfonates (CSSAL) are ineffective in the presence of sodium chloride and at high temperatures (Pat. RF 2098447, 1997).

Lignosulfonate macromolecules are disordered, branched helices with varying degrees of compaction. Low molecular fractions can be of a linear structure. Polydispersity, the presence of ionogenic groups, and a high degree of molecular dissociation indicate that strongly associated highly hydrophilic polyions should prevail in the solution. The structure of lignosulfonates in the shape of polyaromatic chains with functional groups included in them, determines their diphilic nature, surface activity, and high adsorption activity (Badikova et al., 2014).

The qualitative and quantitative composition of lignosulfonates obtained during the wood delignification process depends on the main chemical processes timing during various cooking

methods, on the properties of the wood components with which cooking solutions react, as well as on the composition of cooking solutions and cooking conditions (Kulyashova, 2016).

The problem for the further use of lignosulfonate reagents today is a decrease in the production of sulfite lignosulfonates due to a change in the raw material base and the consistent transition of pulp and paper mills to neutral sulfite methods of technical lignosulfonate production. The resulting products are characterized by a reduced content of the main component, that is lignosulfonate (not more than 49% of the mass, unlike sulfite - 60% of the mass), consisting mainly of low molecular fractions, and also containing insoluble components in the composition (Pat. RF 2038362, 1995). Neutral sulfite liquor is of undoubted interest, since a large proportion of organic substances in it are carbohydrates and salts of low molecular organic acids. However, the possibility of individual use of neutral sulfite liquor requires its modification to obtain a reagent that is stable during electrolyte and temperature aggression and does not adversely affect other properties of the working solution (Badikova et al., 2014). A distinctive feature of drilling reagents obtained by the modification of lignosulfonates is the dependence of their physical and chemical and technological parameters on the quality of the raw material base (Komkova, 2011; Badikova et al., 2016).

In industry, obtaining the ferrochrome lignosulfonate (FCLS) is carried out by modifying the technical lignosulfonate with iron and chromium compounds, followed by neutralization with caustic soda, and then dried to a powder state (Levik, 1982).

However, the industrial obtaining of chrome lignosulfonates is associated with a number of issues, such as the formation of a chromic production waste, incomplete reduction of anionic chromium compounds in the composition of the resulting drilling reagent (Kulyashova, 2016; Badikova et al., 2016)

In this regard, the aim of this paper was to obtain and study the properties of a modified lignosulfonate drilling reagent for effective drilling fluids.

2 MATERIALS AND METHODS

In this paper, lignosulfonates of various cooking methods were used as raw materials for obtaining drilling reagents: sulfite STO (Corporate Standard) 43508418-022-2010 and neutral sulfite TU (Technical Standards) 2455-101-72197712-2013; modifiers, that is iron sulfate as per GOST (State Standard) 6981, sodium dichromate, as per GOST (State Standard) 2651; NTF (nitrilotrimethylphosphonic acid) modifiers TU (Technical Standards) 2439-347-05763441-2001 and TPF (sodium tripolyphosphate) GOST (State Standard) 13493-86 containing phosphonic groups (Badikova et al., 2016).

A drilling reagent based on lignosulfonate modified with salts of polyvalent metals (iron and chromium), manufactured under the trade name of FCLS (ferrochrome lignosulfonate), corresponding to quality indicators, was chosen as an industrial analogue.

Quality indicators of a FCLS reagent are as follows: mass fraction of water is no more than 10%; solubility in water is at least 90%; pH of a 1% aqueous solution is in the range of 4.0-5.0; a dilution rate is at least 50%.

The process of obtaining sulfite liquors, until today, has been predominant and met all the necessary requirements: cheap starting chemicals, high yield of cellulose, the ability to easily obtain from by-products while complying with environmental requirements. However, at present, the standards for the content of pollution in wastewater and gas emissions are tightened, there is a decrease in the quality of the raw materials used for the sulfite cooking method. As a result, pulp and paper mills switch to the processing of low-grade raw materials in a neutral sulfite method that meets environmental safety requirements and contributes to the production of technical lignosulfonates with a reduced content of the main component, that is lignosulfonate (not more than 49% of the mass, unlike sulfite - 60% of the mass), and consists mainly of low molecular fractions (up to 7500 amu, in contrast to sulphite, up to 20,000 amu), and also contains insoluble substances, which makes it impossible to obtain reagents of appropriate quality.

In this regard, additional modification of the lignosulfonate was carried out with compounds containing phosphonic groups (Kulyashova, 2016; Pat. RF 2574659).

Modification of the lignosulfonate feed was carried out as follows: iron (II) sulfate was introduced into the mass of technical lignosulfonate. The mass was maintained with constant stirring for 1.0-1.5 hours at a temperature of 30-40°C. Sodium dichromate was introduced into the resulting mass in the form of an aqueous 15-20% solution. The mass was maintained with constant stirring for 1 hour at a temperature of 30-40°C. Then, a modifying agent was introduced, in the form of an aqueous solution, and again kept for 1 hour under the same conditions. The finished liquid product was neutralized with caustic soda to pH=3.5-5.0. The finished mass was dried to a powder state, first at atmospheric pressure at a temperature of 65÷85°C, then in a vacuum oven to a constant weight (Kulyashova, 2016). The obtained experimental drilling reagents were analyzed according to the requirements of analytical control adopted in the production of reagents that regulate the quality of a drilling fluid (Badikova et al., 2014).

3 RESULTS AND DISCUSSION

As raw materials for obtaining experimental modified lignosulfonate drilling reagents, technical aqueous solutions of lignosulfonates of various cooking methods were used: sulfite and neutral sulfite.

As shown in the references (Badikova et al., 2016; Teptereva et al., 2015), the qualitative characteristics of the obtained drilling reagents are directly conditioned by the chemical composition of the sources of raw materials (sulfite and neutral sulfite lignosulfonate) and modifiers containing phosphophonic groups.

A comparative analysis of the content of functional groups in lignosulfonate feedstock and modified drilling reagents based on it has been carried out. The determination has been carried out by IR spectrometry. The spectra were recorded on a FTIR-8400S (Shimadzu) FT-IR spectrometer in the range 700-4000 cm^{-1} with a device resolution of 4 cm^{-1}.

The obtained IR spectra (Figure 1) of lignosulfonates are characterized by the following absorption bands: 1039-1089 cm^{-1} (SO3 groups); 3200-3600 cm^{-1} (OH groups); 1521 and 1558 cm^{-1} (substituted aromatic lignin ring); 1379 cm^{-1} relate to symmetric vibrations of the terminal methyl group; 1456, 1458 cm^{-1} is the total content of methylene and methyl groups (Kazitsyna et al., 1971).

Figure 1 shows the IR spectrum of the experimental lignosulfonate sample modified with a compound containing phosphonic groups.

The presence of sulfogroups in the lignosulfonate macromolecule gives hydrophilic properties to a water-insoluble polymer.

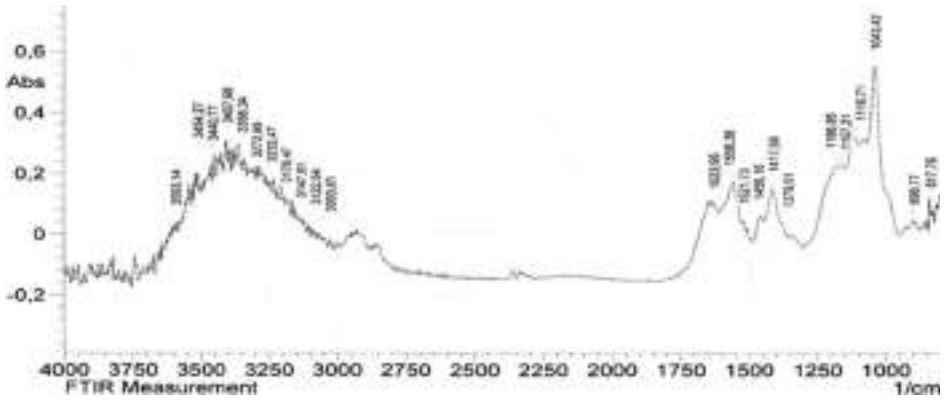

Figure 1. IR spectra of the ferrochrome lignosulfonate sample + TPF (sodium tripolyphosphate).

According to the obtained analysis data by IR spectrometry, it was shown that the samples of modified lignosulfonate reagents were almost identical in the content of functional groups. In the infrared spectrum of the lignosulfonate modified with compounds containing phosphonic groups, absorption bands of the associated P=O bond are observed in the region of 1157-1166 cm^{-1}, which is presumably illustrative of the formation of an additional complex between the phosphonic group introduced into the carboxyl group of the phenylpropane unit of the lignosulfonate, and mainly iron cation (Kazitsyna et al., 1971).

To determine the thermal stability of the reagents tested, a clay mud prepared from Serpukhov mud powder of ПБМВ (PBMV) brand with the following parameters was taken as the basis: NV (nominal viscosity)=64 s, FI (filtration index)=18 cm^3/30 min, η_{pl} ($\eta_{plastic\ viscosity}$) =16 mPas, τ_0=68 dPa (dynamic shear stress), SSS (static shear stress)$_{1/10}$ = 50/64 dPa. The obtained modified drilling reagents were introduced into the clay drilling mud and analyzed according to the GOST analysis methods (Kister, 1972; Darley et al., 1988). The results are presented in Table 1.

The influence of temperature in the range from 20ºC up to 190ºC on the change in technological parameters of the clay mud was determined when the sample was kept for 3 hours in the aging cell 'BOMBA A-B-05' (BOMB A-B-05).

Based on the results obtained in Table 1, it was found that an industrial sample of a drilling reagent, ferrochrome lignosulfonate, is able to effectively reduce the nominal viscosity from 64 up to 30 s, filtering from 18 up to 6 cm^3/30 min, plastic (from 16 up to 12 mPas) and dynamic viscosity from 68 up to 52 dPa, static shear stress from 50/64 up to 15/45 dPa of No. 2 drilling mud with respect to No. 1 initial clay drilling mud. However, drilling fluids are used in a wide variety of mining and geological conditions, for example, when drilling wells at elevated bottomhole temperatures. The influence of temperature on No. 3 drilling fluid in the range up to 190º leads to a decrease in qualitative indicators.

When a drilling reagent based on neutral sulfite liquor modified with TPF (sodium tripolyphosphate) is introduced into No. 5 drilling mud, the nominal viscosity decreases from 64 s up to 36 s and at the same time the heat resistance increases up to 190°C.

When nitriletrimethylenephosphonic acid is modified with a ferrochrome lignosulfonate reagent based on neutral sulfite liquor in No. 4 drilling fluid, the nominal viscosity decreases from 64 s up to 34 s, and it was found that at a concentration of 1% of the mass of introduced modifiers with complex containing properties, the best qualitative indicators were determined, filtration index: 6.5 cm^3/30 min. The addition of FCLS based on sulfite liquor, modified NTF and TPF to drilling fluids No. 6 and 7, reduces the nominal viscosity of No. 1 initial clay

Table 1. The effect of reagents on the parameters of clay drilling mud.

			Solution Properties							
							SSS, dPa		FI,	
№	Solution composition	T,°C 3 h	ρ, g/cm^3	NV, s	η_{pl}, mPas	τ_0, dPa	1 min	10 min	cm^3/30 min	pH
1	Initial clay mud (ICM)	20	1.08	64	16	68	50	64	18.0	9.0
2	ICM+1% FCLS*	20	1.09	30	12	52	15	45	6.0	9.0
3	ICM+1% FCLS*	190	1.08	64	14	98	87	105	9.0	9.1
4	ICM+1 % FCLS*+NTF	190	1.07	34	14	57	15	44	6.5	9.0
5	ICM+1% FCLS*+TPF	190	1.08	36	14	55	17	45	6.5	9.0
6	ICM+1%FCLS**+NTF	195	1.06	25	14	57	15	44	18.0	9.0
7	ICM+1% FCLS**+TPF	195	1.04	30	15	56	15	42	16.0	9.0

* based on NSC (neutral sulfite liquor),
** based on SC (sulfite liquor),
Note: ρ, g/cm3 - density; NV, s - nominal viscosity; η_{pl}, mPas - plastic viscosity; τ_0, mPas - relative viscosity; SSS, dPa - static shear stress; FI, cm^3/30min – filtration index; pH – pH (hydrogen) index.

drilling mud from 64 up to 25-30 s, and the filtration indexes remain almost unchanged compared to ICM No. 1.

According to the research results the influence of drilling reagents on the parameters of clay drilling mud, it was shown that the introduction of modifying agents made it possible to preserve, and in some cases improve the main qualitative characteristics, i.e. nominal viscosity and filtration index, and, among the modifiers used, the best results were achieved with the introduction of NTF or TPF containing phosphonic groups in a drilling reagent based on neutral sulfite liquor, preserving the parameters of drilling fluids No. 4 and 5, even at a temperature up to 190°C.

Modification of lignosulfonates by cations of polyvalent metals that are part of iron sulfate and sodium dichromate in order to obtain ferrochrome lignosulfonates results reagent obtaining, that is a viscosity reducing agent, which is used in a wide range of temperatures and under various conditions (Hornof et al., 1981).

The main qualitative characteristics proved that modified drilling reagents based on neutral sulfite liquor can preserve the property of drilling fluids even at elevated temperatures up to 190ºC.

In this regard, a thermogravimetric analysis of a modified drilling reagent sample for thermal stability was carried out on a TGA-DSC instrument ('Mettler Toledo' company). For this, a weighed portion of the test sample (5-15 mg) was placed in an alumina crucible with a volume of 70 μl. The measurements were carried out in the temperature range from 25°C up to 220°C at a heating rate of 5 deg/min, the atmosphere - air, nitrogen. According to the results of a thermogravimetric analysis of lignosulfonate raw materials and reagents obtained on its basis, it was shown that the temperature of the beginning of decomposition in the raw materials in a neutral sulfite cooking method was 150°C; and in modified drilling reagents was 190ºC and 200ºC, respectively.

The content of iron and chromium compounds was determined by an energy dispersive X-ray fluorescence analysis.

The elemental composition of the drilling reagent samples was determined on an EDX-800 Shimadzu energy dispersive X-ray fluorescence spectrometer with an X-ray tube with a rhodium anode under the following conditions: voltage 15-50 kV, current 20-1000 μA, in vacuum atmosphere, collimator 5 mm, measurement time 15 min. The analysis was carried out by the method of fundamental parameters, provided by software support of the device, using the measurement channels [Ti-U], [C-Sc], [S-K].

Samples for determining the elemental composition undergo minimal preliminary preparation. The sample powder is pressed into tablets on a boric acid substrate by the press at the pressure of 10-15 t (Badikova et al., 2016).

As an example, the results of the analysis of FCLS (industrial analogue) and FCLS + NTF (modified experimental reagent based on neutral sulfite liquor) are shown (Table 2).

The analysis shows that the composition is represented by 10 components. It should be noted that the calculation of the content of elements in the samples is carried out by the

Table 2. Results of comparative laboratory tests of the elemental composition.

Analit	FCLS industrial	FCLS + NTF
S	21.482±0.04	13.324±0.65
Na	9.094±0.84	3.877±0.44
Fe	0.998±0.01	0.849±0.01
P	0.986±0.02	2.754±0.11
Cr	2.089±0.01	0.450±0.02
K	0.579±0.03	0.091±0.12
Ca	0.241±0.17	0.138±0.01
Si	0.256±0.03	0.191±0.02
Cl	0.107±0.09	0.072±0.05
C	64.167±0.26	78.159±1.35

method of fundamental parameters; the determination of elements in the form of oxides without the possibility of indicating valence is carried out formally according to the spectrometer software. C content should be considered as an organic component of the sample. The iron content in FCLS is 0.998% wt., and in the experimental sample is 0.849% wt.; chromium in FCLS is 2.089% wt., experimental reagent is 0.450% wt. The results are confirmed by the spectra.

According to the spectra, the elemental composition of the drilling reagents presented is consistent with tabular photon energies of the main lines of K-series (α, β) and L-series (α, β).

According to the data obtained, it was found that the samples are comparable in terms of the basic elemental composition, but a decrease is observed in the chromium content in the developed modified reagent up to 0.450% wt. as compared with the industrial analogue of FCLS (2.089% wt.), which contributes to a significant reduction in environmental risks when using an experimental reagent.

4 CONCLUSIONS

It was found that when modifying a ferrochromolignosulfonate reagent based on neutral sulfite liquor and/or sulfite liquor with phosphonic compounds, a drilling reagent with improved quality characteristics was obtained: the nominal viscosity is 34 s and 25-30 s, the filtration index is 6.5 cm^3/30 min and 16-18 cm^3/30 min, respectively.

The presented methodology for the modification of the lignosulfonate reagent makes it possible to obtain a drilling reagent, which is stable at high bottomhole temperatures (190-195ºC) and meet the environmental safety requirements by reducing the content of iron to 0.85% by weight. and chromium up to 0.45% by weight.

REFERENCES

Badikova A.D., Kulyashova I.N., Teptereva G.A., Kudasheva F.Kh., Konstantinov K.N. 2009. The effect of lignosulfonate tannidity on the rate of drilling fluid reagent dilution Series: Chemistry and Chemical Technology, V. 52, No. 4, pp. 69–70.

Badikova A.D., Yalalova R.A., Kulyashova I.N., Alekhina I.E., Tashbulatova V.F. 2016. Determination of chromium and iron in the composition of modified lignosulfonate drilling reagents by X-ray fluorescence analysis, Bulletin of the University of Bashkir, T. 21, No. 4, S. 931–934.

Badikova A.D., Yalalova R.A., Kulyashova I.N., Kudasheva F.Kh., Tsadkin M.A., Mortikov E.S. 2016 Modification of neutral sulfite liquors to obtain lignosulfonate drilling reagents, Chemistry and Technology of Fuels and Oils, 2016, No. 6 (598), P. 21–24.

Badikova A.D., Kulyashova I. N., Kudasheva F. Kh. 2014 Lignosulfonates of the neutral sulfite cooking method as a promising raw material for producing drilling reagents, Bashkir Chemical Journal, 2014, V. 21, No. 1, P. 64–66.

Bulatov, A.I., Makarenko P.P., Proselkov Yi. N. 1999. Drilling flushing and grouting solutions: a textbook for universities, M. Nedra, 1999, 424 pp.

Darley H.C.H., Gray G.R., 5th edition. Houston, TX: Gulf Professional Publishing, 1988, 643 p.

Hornof V., Neal G., Bourgeois P., Canad. J., Chem. Engng, 1981, Vol. 59, No. 8, p. 554

Kazitsyna L.A., Kupletskaya N.B. 1971. The use of UV, IR, NMR and mass spectroscopy in organic chemistry: a textbook for universities, M. Higher School, 240 pp.

Kister E.G. 1972. Chemical treatment of drilling fluids, M. Nedra, 392 P.

Komkova, L.P. 2011. Improving the quality of drilling drilling fluids using modified lignosulfonates: Abstract. dis. ... cand. tech. Sciences: 25.00.15.: 1–24.

Kulyashova, I.N. 2016. Improving the quality of drilling drilling fluids with modified neutral sulfite lignosulfonates: Abstract. dis. ... cand. tech. Sciences: 25.00.15.: 1–23.

Levik N.P. 1982. A.S. 956537 USSR. 1982, No. 33, 1 p.

Lurie Yu. Yu. 1984. Chemical analysis of industrial wastewater, M. Chemistry, 142 pp.

Lurie Yu. Yu. 1971. Unified methods of water analysis, M. Chemistry, 375 pp.

Pat. 2098447 Russian Federation, IPC C09K 7/00 (1995.01) A method for producing a lignosulfonate reagent for drilling fluids. 95109485/03 Decl. 06/06/1995, publ. 12/ 10/1997.

Pat. 2038362 Russian Federation, IPC C09K 7/02 (1995.01) Drilling fluid. 93014619/03 Declared 03/ 22/ 1993,publ. 06/ 27/1995.
Pat. 2574659 Russian Federation, IPC C09K 8/03 (2006.01) A method for producing reagents for processing drilling fluids. 2015100383/03 Declared 01/ 12/2015,publ. 02/ 10/2016.
Pat. 2152419 Russian Federation, IPC C09K 7/02 (2000.01) A method for producing a lignosulfonate reagent for drilling fluids. 98116713/03 Decl. 09/ 07/1998,publ. 07/10/2000.
Teptereva G.A., Kulyashova I.N., Asfandiyarov L.Kh., Konesev G.V., Badikova A.D., Chetvertneva I. A. 2015. Reactivity of sulfite liquors as the basis of drilling reagents, Oil and Gas Business, No. 3, P. 91

Advances in Raw Material Industries for Sustainable Development Goals – Litvinenko (Ed)
© 2021 Taylor & Francis Group, London, ISBN 978-0-367-75881-3

Improving the technical and economic efficiency of the Reservoir Pressure Maintenance system (RPM)

Sh.Sh. Zaurbekov
Doctor of Economics, Professor, Vice-Rector, Grozny State Oil Technical University named after Acad. M. D. Millionschikov, Grozny, Russia

M.M. Labazanov
Ph.D., Head of Scientific and Technical Center "Nedra", Grozny State Oil Technical University named after Acad. M.D. Millionschikov, Grozny, Russia

P.U. Musaeva
Laboratory Assistant, ILGGP Scientific and Technical Center Nedra, Grozny State Oil Technical University named after Acad. M.D Millionshchikov, Grozny, Russia

Z.I. Gadaeva
Head of the laboratory "ILGGP" NTC "Nedra", Grozny State Oil Technical University named after Acad. M.D. Millionschikov, Grozny, Russia

T.Kh. Ozdieva
Head of the laboratory "ILGEM" NTC "Nedra", Grozny State Oil Technical University named after Acad. M.D. Millionschikov, Grozny, Russia

I.R. Masarov
Assistant driller, production and exploration wells for oil and gas of the 5th category, Tomsk, Russia

Damzaev
Junior Researcher, Scientific and Technical Center "Nedra", Grozny State Oil Technical University named after Acad. M.D. Millionschikov, Grozny, Russia

ABSTRACT: Waterflooding of oil fields is undoubtedly the most effective way to develop them, providing high rates of oil recovery, significant periods of well flowing and an increase in oil recovery coefficient. Suffice it to say that 95% of all oil produced in the country is accounted for by fields developed using various modifications of waterflooding systems. At the same time, the amount of water pumped into the reservoirs on average doubles the volume of the selected oil.

Naturally, such volumes of injection are associated with huge investments and operating costs, determined by the need to drill injection and water wells, the construction of water intakes, pumping stations, long-term pressure pipelines, commissioning of sewage treatment plants, etc.

So, for example, 381 injection wells were drilled at one of the largest oil fields in the country - Mamontovskoye, 20 water wells from which Apt-Cenomanian water was extracted mechanically, 17 cluster pumping stations were built, each of which owed 7-10 bushes.

The total length of high-pressure pipelines in the field is 656 km. The vast majority of the country's oil fields are equipped with similar RPM systems. The functioning and maintenance of such a complex economy is associated with the large operational costs of small oil production resources should be an increase in the technical and economic efficiency of the reservoir pressure maintenance system. The aforementioned will be caused by an increase in the injectivity of injection wells associated with a decrease in viscosity, both when using directly thermal water for flooding, and when heating injected surface water due to deep heat.

Such an increase in the acceptability of injection wells allows decreasing wellhead injection pressures while maintaining injection volumes, or increasing injection volumes while maintaining these pressures, or reducing the number of injection wells while maintaining wellhead pressures and injection volumes.

1 INTRODUCTION

The most important task in the development and operation of oil fields is the maximum extraction of oil from productive formations. As was shown, the completeness of oil recovery from the reservoirs is characterized by the reservoir recovery coefficient, which varies widely over different fields. Various methods are used to maintain reservoir pressure and increase the coefficient of reservoir recovery, but methods such as injection of water or gas under pressure into productive formations have found the greatest application in practice. (Ozdoeva, Labazanov, Shaipov, Damzaev, 2017).

A system for maintaining reservoir pressure is the process of naturally or artificially maintaining pressure in productive formations of oil deposits at the initial or projected value in order to achieve high rates of oil production and increase the degree of oil recovery. The RPM system during the development of an oil reservoir can be implemented due to the natural active water pressure or water pressure elastic mode, artificial water pressure created as a result of injection of water into reservoir reservoirs during outflow or outflow, as well as during outflow flooding. Depending on the geological conditions and economic development indicators, one or another method of PPD or a combination of them is chosen.

For many decades of development of the oil industry, field development was carried out by drilling only production wells and extracting oil from them through the use of resources of all natural types of reservoir energy. After depletion of reservoir energy and a decrease in bottomhole pressure in production wells, sometimes fields were abandoned to zero when extracting no more than 25-30% of the initial oil reserves in the reservoir.

Artificial water flooding is widespread. At the fields developed with flooding, about 90% of the total oil production is currently produced, more than 2 billion m3 per year is pumped into the reservoirs. The popularity of artificial waterflooding of oil deposits is due to its following advantages:

- availability and free water;
- the relative simplicity of water injection;
- relatively high efficiency of oil displacement by water.

Initially, the use of water flooding was mainly associated with the injection of water into injection wells located in the marginal part of the field (marginal flooding). The principles of near-water flooding - multi-stage development, transfer of injection, shut-off of low-water wells and others - are not widespread. (Shupik 2013).

At present, block systems of in-circuit flooding are justified. With these systems, it is necessary to cut the oil field into blocks of optimal sizes, which exclude the conservation of oil reserves in the inner zones.

The oil industry at the present stage is the most powerful and highly efficient consumer of thermal waters, although for unknown reasons the volumes of thermal waters used in oil production are not taken into account when assessing the consumption of geothermal energy in the country as a whole.

With the use of water flooding, more than 350 fields are developed, providing 96% of the country's total oil production. Water flooding is the main method of developing oil fields. This allows the country to ensure the highest level and rate of oil production in the world.

In recent years, certain difficulties have been outlined in the development of the oil industry, a tendency to reduce the technical and economic indicators of field development, and the pace of development of the industry.

These difficulties and trends are due to modern features of the industry, the main of which can be summarized as follows:

- The deterioration of the structure of reserves, which occurs both in the developed fields, due to their natural depletion and the accelerated development of highly productive parts, and in new fields due to the fact that the latter are characterized by low permeability of reservoirs, high viscosity of oil, high paraffin content in it, small oil-saturated thicknesses, occurrence of oil in the sub-gas parts and oil-water zones, etc. The above complicates the development process, leads to a decrease in oil recovery rates and oil production rates, requires an increase in the efficiency of existing development systems, the use of more active systems with tight well networks in new fields, necessitates the maintenance of not only reservoir pressure, but also temperature, and the use of new, more complex and expensive technologies, etc.
- Depletion and flooding of the country's main developed fields. Almost all of the large fields that provide the main oil production have entered the late stage of development. The commissioning of new capacities in the industry in recent years has been mainly spent on compensating for the increasing losses of production in fields entering the late stage of development, which are characterized by a significant drop in oil production, a rapid increase in water cut in well production, and the transfer of almost the entire stock to mechanized methods of raising the liquid, retirement of some of them from operation, increase in flow rates of wells by fluid, and withdrawal of fluid from the entire facility.

Due to the depletion and watering of the main developed fields from 1980 to 2010. there was an increase in the average water cut of well production from 57.5 to 74.6, a water-oil factor from 1.35 to 2.91, a decrease in fountain production from 45% to 25-30%, an increase in the mechanized well stock from 64.4 to 149.9 thousand., an increase in the volume of injected water from 1.400 to 2 billion m^3.

Field development under these conditions often requires a number of such capital-intensive technological and technical measures to further intensify the development and involve previously uncovered, worse in productivity and operating conditions parts of the deposits, such as additional cutting, creating foci of waterflooding, the transition to areal systems, the formation of fluid withdrawals from individual wells and fields, changing the direction of formation flows, conducting insulating work, etc.

The implementation of these measures requires the drilling of a significant number of additional wells, reconstruction of field facilities, waterflooding capacities, oil treatment and utilization of associated water, and energy re-equipment of the fields.

- Increasing the depth of well drilling in both the "old" and relatively new areas of oil production. Prospects for oil production, especially in the "old" oil producing areas, are associated with access to great depths (about 6000-7000 m). Deposits at these depths are characterized by high initial formation pressure and temperature, a high content of corrosive components (sulfur, hydrogen sulfide, carbon dioxide) in the formation fluids, and the possible manifestation of the plastic properties of oil-bearing rocks. The aforementioned features pose great challenges for science and industry in creating special methods for developing such deposits, and for the necessary drilling and technological equipment.
- A sharp increase in the stock of injection and production wells, especially requiring the use of more labor-intensive and expensive mechanized methods of operation.
- Relocation of the main volumes of oil production to areas with severe climatic conditions. If in 1990 these areas accounted for only about half of the country's oil production in 2010, more than 2/3 of all production falls on these areas. With the aforementioned half-time increase in the stock of producing wells in the country as a whole, a three-fold increase is expected in these areas. The development of oil fields and the operation of wells under these conditions are associated with significant expenditures of fuel and energy resources for own needs. It is clear that the above main features of the current state of oil field development lead to a decrease in the efficiency of their development processes, technical and economic indicators of the development of the industry as a whole. The indicated tendency for their regular decrease is likely to continue in the future. Under these conditions, any positive step towards increasing the marked indicators will be a significant contribution to

solving the most important tasks of the energy program. (Shaipov, Labazanov, Batukaev, Gadaeva, Damzaev, 2017).

In addition to injecting water or gas into the reservoirs, other methods of maintaining reservoir pressure are also used in practice: treating the injected water with surface-active substances (surfactants), injecting carbon dioxide into the reservoirs, and thermal methods. The use of surfactants for additives in injected water in small quantities (0.05-0.1%) significantly reduces the surface tension at the border with oil and with a solid rock surface, reduces the necessary pressure drop for moving oil through the capillaries and contributes to better leaching of oil from the capillaries. According to laboratory studies, oil recovery when using surfactants can increase by 15-16%.

One of the possible ways to maintain reservoir pressure, increase the efficiency and technical and economic indicators of oil field development is to more actively engage and use for this purpose thermal water resources, huge reserves of which are concentrated in the areas where oil production is located, especially in the Tersko-Sunzhenskoye oil and gas region. Some of the promising features of this method of reservoir pressure maintenance are described in this article.

The initial value of the reservoir temperature and its distribution are determined by the geothermal conditions in which the field is located. Typically, the reservoir temperature of oil fields corresponds to the geometric mean gradient in a given geological region. However, significant deviations of formation temperature from this value are also observed. Then it is believed that the reservoir temperature is increased or decreased. High temperature crust zones are called geothermal zones. (Grattoni Carlos, 2003).

In the process of developing an oil field, its reservoir temperature can change significantly. This occurs when substances, mainly water, are injected into the formation with a different temperature than the initial formation, as well as during exothermic reactions in the formation. To a much lesser extent, the reservoir temperature changes due to the throttling of the extracted liquids and gases and hydraulic friction against the formation rocks of the substances filtered in it.

The distribution of reservoir temperature underground and its change in time is called the temperature regime of the field. Temperature changes in oil reservoirs occur mainly due to thermal conductivity and convection.

Oil reservoirs are not thermally insulated from surrounding rocks and from other reservoirs. Therefore, any change in temperature in any section compared to other sections entails its redistribution and heat transfer due to thermal conductivity. The injection into the reservoir of water with a different temperature than the reservoir, and the extraction of oil from the reservoir with reservoir temperature lead to a change in the heat content in the reservoir and, consequently, the reservoir temperature.

Consider the process of oil displacement by water from a homogeneous rectilinear reservoir under conditions when the injected water has a different temperature than the reservoir. For simplicity, we assume that the displacement of oil by water is reciprocating, and the residual oil saturation decreases with increasing temperature according to a certain law.

An increase in the injectivity of the injection well with a decrease in the viscosity of the injected water follows from Darcy's law.

A significant decrease in the viscosity of water with increasing temperature, especially in the range of relatively low reservoir temperatures, causes a significant effect of this factor on the filtration resistance of the bottom-hole zone of the well. The dependence of the viscosity of mineralized water μv on temperature is quite accurately described by the following empirical formula:

$$\mu_v = \left(35 + 0.7M + 0.22M^2\right) / (+ 15.7) \quad (1)$$

where T and M are the temperature and salinity of the water for which the viscosity value is determined.

Bottom water temperature is a function of flow rate, deep wells, geothermal gradient, wellhead temperature, etc. Theoretical assumptions and experience in thermal and per well shows

that at fairly high costs in excess of 300-400 m^3/day. The change in water temperature along the wellbore at steady state is about 3°C/1000m depthTherefore, without resorting to complex solutions of the heat transfer equations in the wellbore, to assess the increase in injectivity of the well, we take the dependence of the bottomhole temperature in the injection well (with an average depth of 3000 m) on its value at the wellhead, in the following simple form:

$$t_c = t_y + 10 \tag{2}$$

where t_c and t_y are the temperature of the injected water at the bottom and at the mouth.

Then, for the axisymmetric flow in the near-well zone of the injection well, for the flow rates of the wellhead temperatures t_{y1} and t_{y2}, one can obtain:

$$\frac{q_2}{q_1} = \frac{\frac{1}{t_y+25.7}\ln\frac{10}{r_c} + \frac{1}{t_{pl}+15.7}\ln\frac{R_k}{10}}{\frac{1}{t_y+25.7}\ln\frac{10}{r_c} + \frac{1}{t_{pl}+15.7}\ln\frac{R_k}{10}} \tag{3}$$

where q_2 and q_1 are flow rates at temperatures ty_1 and ty_2; Rk and r_c are the radii of the drainage zone and the well; t_{pl} - reservoir temperature.

When deriving formula (3), it was assumed that the radius of the zone around the bottom of the injection well cooled to a temperature t_c is 10 m.

The results of estimates for R_k = 500 and r_c = 0.1 m at reservoir temperatures of 80 and 120°C (Figure 1).

The calculations were performed for the ranges of temperature changes of cold and hot (thermal) water characteristic of the conditions of deposits in Western Siberia. From the graph it follows that the increase in flow rate due to the injection of water at a higher temperature depends on the absolute values of wellhead temperatures.

So, for example, if, as a result of injection, thermal waters instead of normal, the temperature on the spine rises from four to 20°C at a reservoir temperature of 80°C, the injectivity increases by 35%. In the case of lifting and pumping thermal Cenomanian water through the same well, due to a decrease in heat loss during the transport of water, we can assume that a temperature of about 45°C is provided at the mouth.

With an increase in the water temperature at the wellhead from 4 to 45°C at a reservoir temperature of 80°C, the injectivity of the well increases by 85%. Thus, an increase in the injectivity of injection wells as a result of an increase in the temperature of the injected water (due to the transition to the injection of thermal water instead of the usual one), contributes to

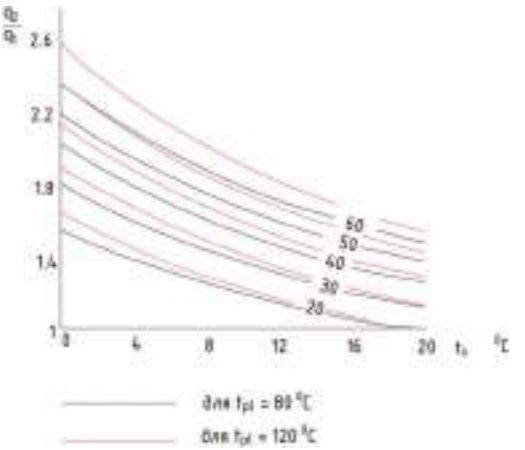

Figure 1. The dependence of the relative increase in the flow rate of the injection well from changes in the temperature of the injected water.

a significant improvement in the technical and economic indicators of the pressure maintenance systems.

The increase in the technical and economic efficiency of RPM systems during the transition to thermal waterflooding, instead of the usual one, is largely associated with the acceleration of the development of RPM systems, with the exception or postponement of large investments in the construction of water intakes, structures and low pressure water pipelines at a later date.

In addition to the noted effects, the transition to flooding with warmer thermal water or surface water heated by deep heat will significantly reduce the pressure loss when pumping water from the pumping station to the bushes. In Western Siberia, pressure losses in high pressure waterways (3–10 km long), especially in winter, reach 15–30 kg/cm^2. Increasing the temperature of the water used for waterflooding is also important for the reliable operation of RPM systems at low temperatures. The noted significant reduces the likelihood of accidents associated with freezing of the mouths in the injection wells of their shafts in the intervals of permafrost distribution.

One of the promising directions of increasing the efficiency of waterflooding is the injection of formation water without lifting them to the surface. A well-known type of such injection is the transfer of water from water reservoirs into a drained oil reservoir. The simplicity of the technology and the exclusion of the aforementioned high costs associated with all ground structures of the RPM systems make this method especially valuable. However, the low filtration characteristics of real reservoir systems, the relatively small pressure differences created by the bypass and the hydrodynamic imperfection of the wells usually determine insufficient volumes of bypassed water. (Gabitov, Safonov, Strizhnev 2005).

The efficiency of the bypass in these cases can be significantly increased by taking measures to increase the pick-up coefficient.

In addition to the noted cost savings associated with the surface structures of the RPM system, it is obvious that in this case all the advantages that are characteristic of flooding the formations with thermal water are retained.

An even more promising and perfect method of flooding without raising the thermal formation water to the surface is the forced downhole pumping of water from the thermal formation into the oil one.

This method is based on the use of submersible pumps of the required capacity, installed directly in the wellbore in such a way as to take the required amount of water from the thermal reservoir and pump it into the water-filled oil reservoir.

Despite the lack of reliable experimental research in downhole injection, it can be assumed that this method, due to its great advantages, will find wide application in the near future.

2 CONCLUSION

The use of formation water instead of surface water, in addition to the listed advantages, allows saving large volumes of fresh water used for PPD systems. There is a shortage of fresh water in many, especially in the newly developed oil producing regions of Western Kazakhstan, the Caspian lowland, and Central Asia. Providing these areas with fresh water is associated with the laying of water pipelines of considerable length.

The volumes of water used to maintain reservoir pressure, as noted above, are huge. So, for example, at one of the largest oil fields of the Soyuz-Mamontovskoye, the annual injection in 1981 reached 49 million m^3 (or 160,000 m^3/day). At the same time, 10 million m^3 of Apt-Cenomanian reservoir water, about 5 million m^3 of wastewater and about 35 million m^3 of fresh water are ending. In total, since 1975, about 252 million m^3 were pumped, of which 150 million m^3 are fresh water. Even larger injection volumes are characterized by the largest oil field - Samotlor.

Currently, water injection at this field has reached 1.5 million m^3/day.

Obviously, the maximum use of thermal water instead of fresh water from surface sources, at such a scale of water flooding, saves huge amounts of fresh water.

It is known that both water from surface sources and associated water must be treated at special facilities before injection into oil reservoirs in order to reduce the content of solids and prevent infection of the reservoirs with sulfate-reducing bacteria

This is associated with significant costs due to the need to use expensive equipment, scarce antiseptics and other reagents.

The use of formation water in the PPD system is usually possible without chemical treatment and purification. For example, for flooding productive formations of oil fields in Western Siberia, thermal waters of powerful water complexes of Apt-Cenomanian and Alb-Cenomanian deposits are used, which lie above productive horizons.

In terms of their physicochemical properties, these waters are close to the waters of productive formations; their displacement does not lead to the formation of precipitation and a decrease in the injectivity of injection wells; they do not require treatment and construction of treatment facilities. One of the drawbacks of surface water sources used for water supply to oil production is the development of microorganisms and algae in the bottom-hole zone of injection wells. In this case, sulfate-reducing bacteria pose the greatest danger. Propagation of these bacteria in the formation leads to the formation of sulfate ions (SO_4^-), clogging the formation as a result of the activity of these bacteria in the formation, sulfides (FeS) are also formed, which in turn react with free iron. In this case, iron sulfide FeS itself is a blocking agent, and the hydrogen sulfide H_2S, which is formed in this case, is a corrosive agent. The noted negative factors are completely eliminated when deep thermal formations are injected into the injection wells of thermal waters.

REFERENCES

Farkhutdinov A.M., Khamitov I.Sh., Cherkasov S.V., Mintsaev M.Sh., Zaurbekov Sh.Sh., Shaipov A. A., Labazanov M.M. 2017. Thermal groundwater of the East Ciscaucasia artesian basin: economic aspects of use on the example of the Khankalsky deposit. Tomsk. News of Tomsk Polytechnic University. Geo-Resource Engineering.

Gabitov G.Kh., Safonov E.H., Strizhnev V.A. and others. 2005. *Improving the reservoir pressure maintenance system is the basis of the effective development of an oil field*. Moscow. Oil industry.

Grattoni Carlos (Great Britain). 2003. *Alternate water and gas injection, gas injection: Proceedings of the 12th European Symposium Enhancing Oil Recovery*. Moscow.

Gumerov A.G., Bazhaikin S.G., Bagmanov A.A. and other. 2006. *The technique of choosing pumping equipment for pumping water into the reservoir in the reservoir pressure maintenance system*. Moscow. Enterprise Standard.

Edited by Kozlovsky E.A. 2001. *Mountain encyclopedia*. Moscow. Soviet Encyclopedia.

Lysenko V.D., Graifer V.I. 2001. *Development of unproductive oil fields*. Moscow. Nedra-Business Center LLC.

Ozdoeva L.I., Labazanov M.M., Shaipov A.A., Damzaev Z.M.E. 2017. *The oil and gas potential of some areas in the Chechen Republic is promising*. Grozny. In the collection: GEOTECHNOLOGIES OF THE XXI CENTURY Materials of the All-Russian Scientific and Practical Conference dedicated to the 100th anniversary of FSBEI HE "GSTU named after Acad. M.D. Millionschikova". Grozny State Oil Technical University named after academician M.D. Millionschikova.

Shaipov A.A., Labazanov M.M., Batukaev A.A., Gadaeva Z.I., Damzaev Z.M.E. 2017. *Prospects for the development of thermal deposits in the Chechen Republic*. Grozny. In the collection: FUNDAMENTAL AND APPLIED RESEARCH: PROBLEMS AND RESULTS Materials of the I International scientific-practical conference dedicated to the 100th anniversary of the FSBEI HE "GSTU named after academician MD Millionschikov": in 2 volumes. Grozny State Oil Technical University named after academician M.D. Millionschikova.

Shupik N.V. 2013. *Improving reservoir pressure maintenance based on leading water flooding*. Moscow. Oil and gas technology.

Zakharova EF, Pashanina O.D., Tronov V.P. 2003. *Improving the reservoir pressure maintenance system at the Berezovsky field*. Moscow. Electronic scientific journal "Oil and Gas Economy".

Zaurbekov Sh. Sh., Mintsaev M.Sh., Labazanov M.M., Shaipov A.A., Batukaev A.A. 2015. *Improving the efficiency of well development in the oil fields of the Tersko-Sunzhenskoye oil and gas region*. Grozny. Territory Neftegaz.

Zaurbekov Sh. Sh., Mintsaev M.Sh., Cherkasov S.V., Labazanov M.M., Shaipov A.A., Damzaev Z.M. E. 2015. *Prospects for oil and gas potential and further areas of geological exploration within the Tersko-Sunzhenskoye oil and gas region*. Grozny. Territory Neftegaz.

Zeigman, Yu.V. 2007. *The operation of reservoir pressure maintenance systems in the development of oil fields: a training manual*. USTU. – Ufa. Oil and gas business.

Advances in Raw Material Industries for Sustainable Development Goals – Litvinenko (Ed)
© 2021 Taylor & Francis Group, London, ISBN 978-0-367-75881-3

Effective axial load as a function of the ultimate stress state of rocks to be drilled

L.K. Gorshkov
Saint-Petersburg military space Academy A. F. Mozhaysky, Saint-Petersburg, Russia

A.N. Dmitriev
St. Petersburg mining University, St. Petersburg, Russia

ABSTRACT: This paper presents the study of the mechanism of well deepening in diamond drilling. Destruction of rocks under diamond drilling is represented by a set of deformation processes arising in rocks when destroying efforts are applied. Modern requirements to the technology and economic feasibility of drilling operations suggest continuous improvement in the field of the mechanism of bottom rock breaking. The article proposes a procedure to analyze situations at well bottom drilling deeper per a revolution of the diamond rock cutting tool. On the basis of the proposed procedure the authors analyze and operating influences to preserve the set and optimum deepening per a revolution are revealed under effective destruction of firm rocks. The estimation method of stress-strain state of rocks to be drilled and the choice of the maximum axial load in diamond drilling of rocks with different physical and mechanical properties.

1 INTRODUCTION

Optimization of drilling modes, improvement and creation of new high-performance rock destruction tools should play a big role in solving the problem of increasing drilling speed. Successful development of drilling technique and technology requires in-depth knowledge of patterns of the rock behavior at the well opening, patterns of rock destruction by the rock-destroying tool, structures, operation and wear of this tool. Thus, the study of the mechanics of bottomhole processes, methods of describing and calculating these processes will allow to develop an effective technology of the rock destruction.

The actual task in the current drilling conditions is to predict the drilling strength of rocks, to determine the concepts of choosing the drilling method and the rock-destroying tool in each individual case. The search for new ways to improve the efficiency and quality of drilling operations without increasing the energy consumption and resource of the rock-destroying tool by modernizing the drilling technology on the example of the method of optimizing the axial load is important for scientific and practical significance.

The problem of evaluating the limit state of rocks to be drilled can be categorized to the group of problems, where the main criteria for the solid body state are excessive crack opening or its complete destruction.

The main resistance parameter of rocks to be drilled is its normative resistance (tensile strength, yield strength, critical resistance, etc.), which determine the level of the maximum axial load on the rock-cutting tool.

2 MATERIALS AND METHODS

To assess the stress-strain state of rocks to be drilled and select the maximum permissible axial load for effective rock destruction in the drilling process, the flat problem solution (one of the

main stresses is zero) of elasticity theory is most often used, at the same time the rocks at the bottom of the well experience normal vertical stress σ_x (Figure 1), normal lateral compression stress σ_y in the horizontal direction and shear stresses τ_{xy} that determine the adhesion of rocks during their destruction.

The above-mentioned normal stresses relate to each other according to the dependence:

$$\sigma_y = \frac{1-\mu}{\mu} \cdot \sigma_x = \lambda \cdot \sigma_x \tag{1}$$

where μ is the Poisson's ratio for the rock to be drilled; λ is the lateral compression ratio.

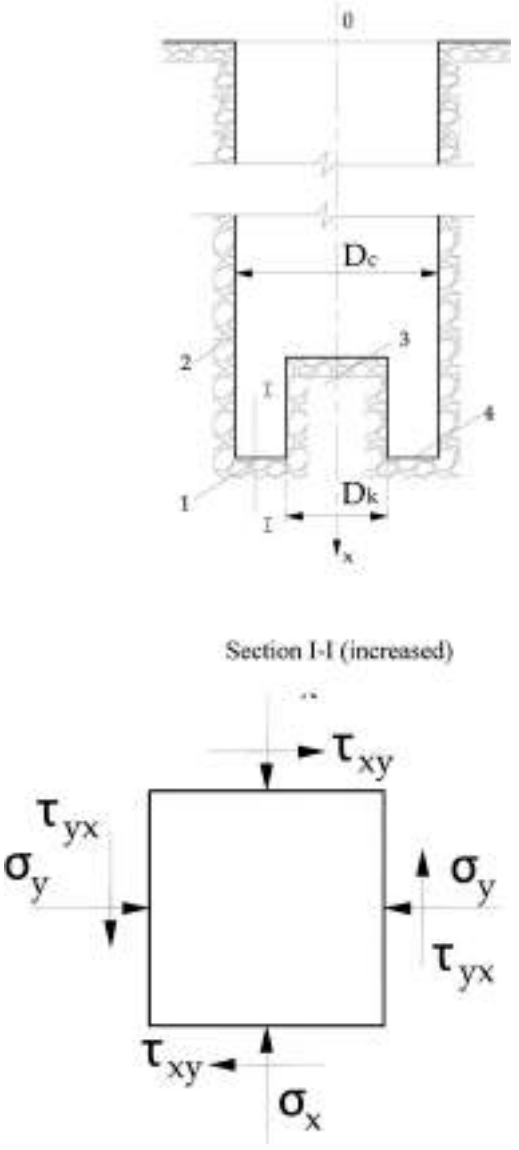

Figure 1. Calculation scheme for determining bottom-hole rock stresses, where: 1-the element of the array to be drilled allocated to the bottom; 2-the walls of the well; 3-the core column; 4-the bottom of the well; σ_x and σ_y normal stresses; τ_{xy} and τ_{yx} tangential stresses on the surfaces of the array element to be drilled.

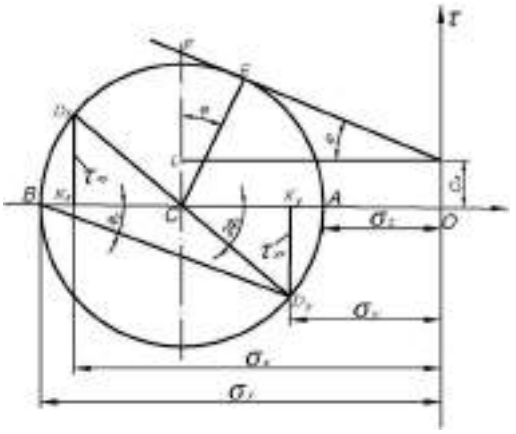

Figure 2. Graphical representation of stress distribution (Mohr circle) on the surfaces of an array element from the well bottom, where: σ_2 and σ_3-the main tension.

The relationship between the stresses σ_x, σ_x and τ_{xy} can be obtained by constructing-for the case in question (see Figure 1) the corresponding Mohr circle (Figure 2), from which its understood that the envelope of the circle at the maximum level of the shear stress is spaced from the center of the circle at a distance

$$\overline{FC} = C_n + \overline{FL}$$

where C_n the grip or the shifting strength of rocks.
If we take into account that
$\overline{FL} = \overline{OC} \cdot tg\varphi$ and $OC = \frac{\sigma_x+\sigma_y}{2}$
we will have

$$\overline{FC} = C_n + \frac{\sigma_x - \sigma_y}{2} \cdot tg\varphi$$

The radius of the Mora circle

$$\overline{CD_x} = \overline{EX},$$

then

$$\overline{CD}_x = \overline{FC} \cdot \cos\varphi = C_n \cdot Cos\ \varphi + \frac{\sigma_x + \sigma_y}{2} \cdot \sin\varphi \tag{2}$$

where φ is the angle of internal friction of the target rock.
From a triangle CD_xK_x (see Figure 2) it follows that, in turn,

$$\overline{CD_x} = \frac{\overline{D_xK_x}}{\sin 2\varphi_0} = \frac{(\sigma_x - \sigma_y) \cdot \mathrm{tg}2\varphi_0}{2 \cdot \sin 2\varphi_0} = \frac{\sigma_x - \sigma_y}{2} \cdot \cos 2\varphi_0, \tag{3}$$

where φ_0-the angle of inclination of the area on which the stress acts σ_x, to the greatest main stress;$0 < \varphi_0 < 0,8$ on average, *0.3 rad* for most cases of drilling in hard rocks are used $\varphi_0 =$.

Equating the right parts of expressions (2) and (3), we obtain

$$\sigma_x = \frac{2C_n \cos\varphi + \sigma_y(\sin\varphi + \cos 2\varphi_0)}{\cos 2\varphi_0 - \sin\varphi}$$

Or

$$\sigma_x = \frac{2C_n + \sigma_y(K + 2\mathrm{tg}\varphi)}{K}, \tag{4}$$

where K is the reducing factor:

$$K = \frac{\cos 2\varphi_0 - \sin\varphi}{\cos\varphi}. \tag{5}$$

Substituting the value σ_y of the dependence (1) in the expression (4) and after some transformations we finally get

$$\sigma_x = \frac{2C_n}{K - \lambda(K + 2\mathrm{tg}\varphi)} \tag{6}$$

The area of the contact surface on which the stress actsσ_x is equal to

$$f_k = \alpha\frac{\pi}{4}\left(D_c^2 - D_k^2\right) \tag{7}$$

Where α-the coefficient characterizing the size of the cutters contact total area ratio with the cross-sectional area of the annular face of the well; for crowns with a diameter of 59 and $76\alpha = 0,06 \div 0,10$ mm, i.e. on average it is possible to use $\alpha = 0,08$; D_c П D_k–diameters of the well and core respectively.

Taking into account the expressions (6) and (7), we can write the expression for the maximum axial load on the well bottom during core drilling

$$P_{np} = \sigma_x \cdot f_k$$

Or

$$P_{np} = \frac{\alpha \cdot \pi \cdot C_n(D_c^2 - D_k^2)}{2[K + 2tg\ \varphi]} \tag{8}$$

The adhesion of rocks C_n in the formula (8) can be expressed through the strength of rocks on uni-axial compression $\sigma_{сж}$ and the coefficient of internal friction φ (Bock, 1983):

$$C_n = \frac{\sigma_{сж}}{2\,\mathrm{tg}\left(\frac{\pi}{4} + \frac{\varphi}{2}\right)}.$$

3 RESULTS AND DISCUSSION

Using the given calculation method, it is possible to determine the maximum axial loads during drilling of rocks with different physical and mechanical properties and different drilling capacity.

Table 1. Physical and mechanical properties of rocks.

№	Formation rock	modulus of elasticity E, 10^5 *MPa*	Poisson's ratio, μ	coefficient of lateral compression, λ	One-axial compressive strength $\sigma_{сж}$, *MPA*	Internal friction angle φ, *grad.*	Rock adhesion C_n, *MPa*
1.	Basalt	1,0	0,28	0,39	290	50	52,7
2.	Granit	0,55 – 0,9	0,25	0,33	210	48	40,3
3.	Gabbro	1,05	0,34	0,51	200	46	40,4
4.	Limestone	0,2 – 0,9	0,22	0,28	110	50	20,0
5.	Sandstone	0,1 – 0,7	0,30	0,43	105	47	20,7
6.	Hard shale	0,4	0,25	0,33	75	45	15,6
7.	Siltstone	0,3	0,26	0,35	60	43	13,0
8.	Argillite	0,2	0,24	0,32	45	42	10,0

Table 2. Ultimate axial loads of some rocks during drilling by diamond crowns with diameters of 59 and 76 mm.

№	Formation rock	Category of rocks by drillability	Shorthand multiplier K	σ_x, MPa	Maximum axial loading, kN	
					Calculation results $P_{пр}$	Recommendations [4]
1.	Basalt	X	0,71	127,9	7–15/11–19	8–15/12–17
2.	Granit	IX - X	0,199	134,3	8–16/12–21	8–15/12–17
3.	Gabbro	IX	0,233	85,8	6–11/8–14	6–12/8–13
4.	Limestone	VII - VIII	0,171	73,5	5–9/7–12	6–8/8–12
5.	Sandstone	VII	0,213	51,8	4–7/5–9	4–8/5–10
6.	Hard shale	VII	0,239	62,4	4–8/6–10	4–8/5–10
7.	Siltstone	VI	0,265	54,0	4–7/5–9	4–8/5–10
8.	Argillite	V - VI	0,279	51,8	4–7/5–8	4–7/5–8

As an example, Table 1 shows the data of physical and mechanical properties (Bulychev, 1989; Gorshkov, 1992) calculations of some rocks, drilled by diamond crowns, and in Table 2-values of limit axial loads for the same rocks drilled with crowns of 59 mm (in the numerator) and 76 mm (in the denominator) diameters in comparison with other data (Gorshkov, 2000).

From Table 2 conclusions can be made that the limiting axial loads calculated by the proposed method are satisfactorily correlated with their values obtained experimentally from the device "ВИТР". Some deviations of the compared data are explained by inaccuracies in determining the coefficient of internal friction of rocks and the value of the lateral compression coefficient, depending both on the depth of the well in the drilling interval and on geological and tectonic conditions, as well as a fairly rough averaging of the coefficient α in formula (7), which is determined by the level of bulky diamond saturated crowns (Gorshkov, 1992).

4 CONCLUSIONS

Using of the described technique, it is possible to determine the most optimal operating conditions of the rock-destroying tool.

The validity of the technique is confirmed by the close convergence of the results of the theoretical and experimental studies. The statistical evaluation of the results of the experimental

studies showed that the error is not more than 5%. Nevertheless, the calculation showed sufficient simplicity and practical applicability of the proposed method for determining the maximum permissible axial loads in diamond drilling, at least at the preliminary stage, which is confirmed by the results of the study (Blinov et al., 1983).

REFERENCES

Bock H. Introduction to the mechanics of rocks. - M .: Mir, 1983.

Bulychev N.S. Mechanics of underground structures in the examples and tasks. - M .: Nedra, 1989.

Gorelikov V.G. The classification and analysis of the methods of determining the diamond's number involved in the destruction of rock/Yu.V. Lykov, Baatarkhuu Gantulga. The collection of the master and postgraduate student's research, 2014. № 9/156, - pp. 115–117.

Gorshkov L.K. Temperature modes of diamond drilling/L.K. Gorshkov, V.G. Gorelikov.– M.: Nedra, 1992. - p. 73.

Gorshkov L.K. Assessment of the stress-strain state of the diamond crown matrix during dynamic interaction with a mountain massif/L.K. Gorshkov, V.I. Spirin// Collection of "Geological study and use of the subsoil", Vol. 3. - M .: Geoinformmak, 2000. - p. 3–14.

Neskoromnykh V.V. Rock destruction in geological survey. [Razrushenie gornyh porod pri provedenii geologo-razvedochnyh rabot]. Uchebnik-Textbook. Krasnoyarsk: Publ.H. SFU, 2012, 297 p.

Reference guide of the master exploration drilling/ G.A. Blinov, V.I. Vasiliev, Yu.V. Baklanov and others. - L .: Nedra, 1983.

Advances in Raw Material Industries for Sustainable Development Goals – Litvinenko (Ed)

Polymer compositions for well killing operation in fractured reservoirs

S.R. Islamov
Postgraduate student, Saint Petersburg Mining University, St. Petersburg, Russia

A.V. Bondarenko
Student, Saint Petersburg Mining University, St. Petersburg, Russia

A.F. Gabibov
Student, Saint Petersburg Mining University, St. Petersburg, Russia

D.V. Mardashov
PhD, Associate professor, Saint Petersburg Mining University, St. Petersburg, Russia

ABSTRACT: This article describes the results of physical, chemical and rheological properties of the frame and gel forming compositions, which are crosslinked systems prepared based on soluble silicates. The aim of this work is to increase the well killing efficiency during well service operations in the conditions of fractured carbonate reservoirs, high gas-oil ratio and abnormally low reservoir pressure. The technology of well killing during well service operation involves sequential injection into the well. The considered compositions showed that they could be used in conditions of reservoir temperatures from 20°C to 90°C, which consists in the possibility of injection these compositions into a typical well and selling them into the bottom-hole formation zone due to their low viscosity after preparation and slow cross-linking speed. Laboratory tests showed the high efficiency of the use of blocking polymer compositions, and opened new directions for further research, namely, the need for a cycle of laboratory and field tests of the considered compositions, which will allow us to choose and justify the optimal technological and economic parameters of the operation. The results can be applied to increase the well killing efficiency of oil and gas wells in complicated conditions during well service operations.

1 INTRODUCTION

Currently, based on the assessment of reserves, the share of carbonate reservoirs accounts for about 60% of hydrocarbon fields and about the same amount of oil production in the world. The development of such reservoirs is complicated by the presence of an extensive network of natural and artificial (as a result of hydraulic fracturing) fractures, high heterogeneity, complex structure of the pore space, hydrophobic properties of reservoir rocks and abnormally low reservoir pressure.

The considered characteristic features of carbonate reservoirs can lead to low coverage of the formation impact, low displacement efficiency, quick well flooding, gas breakthrough, and, as a result, a rapid decline in oil production (Bouts et al. 1997; Dorman & Udvary 1996; Rogachev & Strizhnev 2006).

The presence of reservoirs with similar characteristics in the field requires a special, differentiated approach to planning well killing operations related to the development and selection of blocking composition. The correct selection of blocking compositions for well killing requires careful laboratory tests for specific objects of the planned application.

Failure to comply with the above conditions when planning activities at the well may lead to the loss of significant volumes of process fluids, increase the repair and response time, which, ultimately, will lead to an increase in the cost of well service operations (Dandekar 2013; Jouenne et al. 2006).

An advanced solution in the development of blocking fluids is the use of cross-linked polymer compositions with time-controlled gelation. The rate of change of viscosity can be adjusted to more efficiently carry out technological operations.

Technologies using the described polymer compositions have proven to be a reliable method for isolating highly permeable reservoir intervals in order to prevent water and gas breakthrough into production wells (Gumerova & Yarkeyeva 2017).

As part of this work, the physical, chemical and rheological properties of the frame and gel forming compositions were selected and studied as blocking polymer fluids for well killing.

These compositions are crosslinked systems based on soluble silicates. In this case, a silicate gel is formed when an aqueous solution with a relatively high pH, containing a sufficient amount of orthosilicic acid ester monomer or orthosilicic acid oligomers, experiences a decrease in its pH, or is exposed to hardness cations (Volkov et al. 2019; Musabirov et al. 2019; Tokunov & Saushin 2004).

The technology for well killing during well service operation involves sequential injection of frame and gel forming compositions into the well.

The procedure for conducting laboratory physical, chemical and rheological tests of compositions consisted of several consecutive stages:

1) determination of density;
2) assessment of thermal stability;
3) assessment of destruction;
4) determination of effective viscosity and static shear stress;
5) determination of the gelation time of cross-linked compositions.

2 MATERIALS AND METHODS

2.1 *Investigation of physical and chemical properties of compositions*

The frame-forming composition is an opaque non-uniform white liquid. When injected into the reservoir, the liquid phase is separated, and the dry residue is "baked" at elevated temperatures, forming a strong frame-forming screen for isolating intervals with increased fracturing. This feature of the composition allows to reduce the fluid loss into the well during well killing operation.

In turn, the gel-forming compositions are a transparent homogeneous liquid, which due to its high viscosity has a low filtration index in the reservoir, and is also able to prevent gas breakthrough in high gas-oil ratio conditions. At the same time, the gel-forming composition was prepared in two versions with a gel-forming agent for low (20°C) and high (90°C) temperatures.

The density of the frame and gel forming compositions was determined by the pycnometric method according to (GOST 3900-85 2006) and amounted to 1045 kg/m^3 and 1015 kg/m^3 for low temperatures, and for high temperatures - 1022 kg/m^3), respectively. This value of the density of the studied compositions allows them to be used at normal and reduced values of reservoir pressure (Galimkhanov et al. 2019; Rogachev & Kondrashev 2016).

To assess the thermal stability, the prepared composition fulfilled in a thermostat at a temperature of 20°C or 90°C for 3 days (average duration of well service operation). Then the state of the composition under study and the change in its appearance were visually evaluated. The composition was considered unstable when the water phase was isolated, stratified, and precipitated.

The destructibility of the frame and gel forming compositions was evaluated visually at temperatures of 20°C and 90°C for 24 hours by mixing the destructor with the studied blocking compositions in 1:1 ratios. A 10% aqueous solution of sodium hydroxide was used as the

destructor of the gel-forming composition, and a mixture of 12% hydrochloric and 5% hydrofluoric acids was used for the destruction of the frame-forming composition.

2.2 *Determination of the rheological properties of the compositions*

The study of rheological properties of the frame and gel forming compositions consisted in determining the following parameters:

- effective viscosity at 300 rpm;
- "viscosity curves" (dependence of the effective viscosity on the shear rate or rotor speed);
- Static shear stress after gelation of cross-linked compositions in the controlled shear rate mode by plotting the dependence of the shear stress τ on the shear rate D, determining the shear stress at which the structure of the composition begins to collapse and move;
- time of gelation of cross-linked compositions in the "dynamic" mode by measuring the effective viscosity μ_{eff} of the composition in time at a given shear rate equal to the rate of injection of the composition into the well, and in the "static" mode of oscillating stresses by measuring the complex viscosity in time.

The construction of the "viscosity curve" and the determination of the static shear stress was carried out for the frame and gel forming compositions. Static shear stress characterizes the initial pressure gradient at which the structure of the composition collapses and moves (Strizhnev 2010).

Experiments to determine the gelation time were performed only for cross-linked compositions that are nonlinear gels.

Determination of rheological characteristics is carried out according to (GOST 1929-87 2002) with the use of automated rotary viscometer Rheotest RN 4.1 (Figure 1). Measurements were made using a cylindrical measuring system.

I. Sequence of studies of linear (non-crosslinked) compositions:

1. Modeling the process of starting the movement of the composition (destruction of the structure of the composition). The static shear stress is determined by plotting the dependence of the shear stress on the shear rate in the controlled shear stress mode. The static shear stress is equal to the value of the shear stress τ, preceding the destruction of the structure of the composition, and characterizes the beginning of the movement of the composition. The conditions of the experiment:
   – pre-exposure of the composition in the measuring cell for 15 minutes;
   – experiment time t = 0-500 s;

Figure 1. Rotational automated viscometer Rheotest RN 4.1.

– shear stress τ = 0-2000 Pa;
– temperature T = 20-90°C, respectively.

2. Determination of the effective viscosity was carried out in the controlled shear rate "viscosity curve" (CR test - Controlled Rate). The essence of the research method was to obtain the dependence of the effective viscosity (shear stress) on the shear rate (rotational speed) with a gradual increase in the last parameter from 0 to 300 s^{-1}. The conditions of the experiment:
– experiment time t = 0-300 s;
– shear rate γ = 0-300 s^{-1};
– temperature T = 20-90°C, respectively.

II. Due to the fact that the gel-forming composition changes the viscosity over time, it was decided to conduct a step-by-step study of rheological characteristics according to the following scheme (Raupov & Oprikova 2018; Ryabokon 2009):

1. Modeling the state of the composition immediately after preparation at the wellhead to assess filterability in the inter-tube space or in a column of tubing. The effective viscosity of the composition at different shear rates is determined by removing the "viscosity curve". The conditions of the experiment:
– experiment time t = 0-300 s;
– shear rate γ = 0-300 s^{-1};
– temperature T = 20°C.
2. Modeling the process of pumping the composition through the tube space into the well, taking into account the uniform temperature change along the well bore. The gelation time is determined at a constant shear rate. The conditions of the experiment:
– experiment time t = 85 min;
– shear rate γ = 21.8 s^{-1};
– temperature T = 20-90°C (for the composition applicable at 20°C, the experiment temperature T = 20°C).
3. Modeling the process of pumping the composition into the space of the production string. The determination of the gelation time at a constant shear rate continues. The conditions of the experiment:
– experiment time t = 15 min;
– shear rate γ = 7.1 s^{-1};
– temperature T = 90°C (for a composition applicable at 20°C, the experiment temperature T = 20°C).
4. Modeling the process of holding the composition for the reaction time (the end of the crosslinking process) at the reservoir temperature. The time of gelation in the static mode of oscillating stresses is determined (Elchin et al. 2019; Quintero et al. 2017). The conditions of the experiment:
– experiment time t = 3 h;
– the oscillation frequency of the rotor f = 1 Hz;
– voltage modulus G = 10 Pa;
– temperature T = 90°C (for a composition applicable at 20°C, the experiment temperature T = 20°C).
5. Modeling the process of starting the movement of the composition (destruction of the structure of the composition). The static shear stress is determined by plotting the dependence of the shear stress on the shear rate in the controlled shear stress mode. The conditions of the experiment:
– experiment time t = 0-500 s;
– shear stress τ = 0-2000 Pa;
– temperature T = 90°C (for the composition used at 20°C, the experiment temperature T = 20°C).
6. Modeling the state of the composition after injection into the well to assess changes in its effective viscosity. The effective viscosity of the composition at different shear rates is determined by removing the "viscosity curve". The conditions of the experiment:

– experiment time t = 0-300 s;
– shear rate γ = 0-300 s^{-1};
– temperature T = 90°C (for the composition used at 20°C, the experiment temperature T = 20°C).

3 RESULTS AND DISCUSSION

The evaluation of thermal stability of frame-forming composition (Table 1) revealed that 15 min after preparation of the composition at 20°C and 90°C of the composition is given up to 20 and 25% of water, respectively. When further thermostating, the amount of water released remains virtually unchanged. At the same time, the producer of the frame-forming composition allows the release of water in a small amount from the volume of the composition. Therefore, it was decided that the frame-forming composition is thermal stable at 20°C and 90°C and is able to maintain its physical and chemical properties during well service and workover operations.

At the same time, when the gel-forming composition was thermostated, no visible changes in appearance were observed during the entire period time.

It is worth noting that the requirement for such a type of composition in well killing operation is their complete or partial destructibility when exposed to a destructor. Compositions that do not meet these conditions cannot be recommended for use. Since this entails a deterioration of the reservoir's filtration and reservoir properties, as well as difficulties in developing and bringing the well back to normal after well service and workover operations.

The destructibility of the frame and gel forming compositions was evaluated visually at temperatures 20-90°C for 24 hours by mixing the destructor with the studied blocking compositions in 1:1 ratios. A 10% aqueous solution of sodium hydroxide was used as the destructor of the gel-forming composition, and a mixture of 12% hydrochloric and 5% hydrofluoric acids was used for the destruction of the frame-forming composition.

As a result of evaluating the destruction of the frame and gel forming compositions (Table 2) it was found that these compositions can be recommended for use in the well-killing process. The results of evaluating the destruction of the frame and gel compositions showed the following:

– the gel-forming composition is completely destroyed within 1 and 3 hours with a 10% aqueous NaOH solution at 90 and 20°C, respectively;
– the frame-forming composition is destroyed by 75% within 24 hours with a mixture of 12% hydrochloric and 5% hydrofluoric acids (mud acid) at 90 and 20°C, respectively. The future observation showed insignificant changes because when reacting with a frame-forming composition, mud acid loses reactivity.

Summarized results of rheological tests of the compositions are presented in Table 3.

The results of determining the gelation time under the conditions of injection of cross-linked compounds are shown in Figures 2-3.

Based on the results presented in (William et al. 1996), the higher the static shear stress, the greater the pressure gradient blocking composition is able to withstand without collapsing. The same conclusions are valid when the effective viscosity increases, since it increases its structural strength.

Table 1. Results of determining the thermal stability of the frame and gel forming compositions.

No.	Composition name	Thermal stability at 20°C for 3 days	Thermal stability at 90°C for 3 days	Remark
1	Frame-forming	+	+	Allocation of up to 20 and 25% of water, respectively
2	Gel-forming	+	+	–

Table 2. Results of evaluation of the destruction processes of the frame and gel forming compositions.

No.	Composition name	Temperature, °C	Destruction results	Destruction time, h	Destructor	Recommendation for use
1	Frame-forming	20	Partially	1 (50%) 24 (75%)	12% HCl + 5% HF	Recommended
2	Frame-forming	90	Partially	1 (50%) 24 (75%)	12% HCl + 5% HF	Recommended
3	Gel-forming	20	Completely	3 (100%)	10% aqueous NaOH solution	Recommended
4	Gel-forming	90	Completely	1 (100%)	10% aqueous NaOH solution	Recommended

Table 3. Results of rheological studies of the frame and gel forming compositions.

No.	Composition name	Effective viscosity (mPa·s) after preparation at N = 300 rpm	Effective viscosity (mPa·s) after crosslinking at N=300 rpm	Static shear stress, Pa
1	Frame-forming at 20°C	27	–	2.66
2	Frame-forming at 90°C	64	–	3.38
3	Gel-forming at 20°C	10.7	17.4	126
4	Gel-forming at 90°C	8	600	648

Notes:
"–"means that the effective viscosity for these compositions was not measured, since these compositins are not "cross-linked" and their viscosity does not depend on time

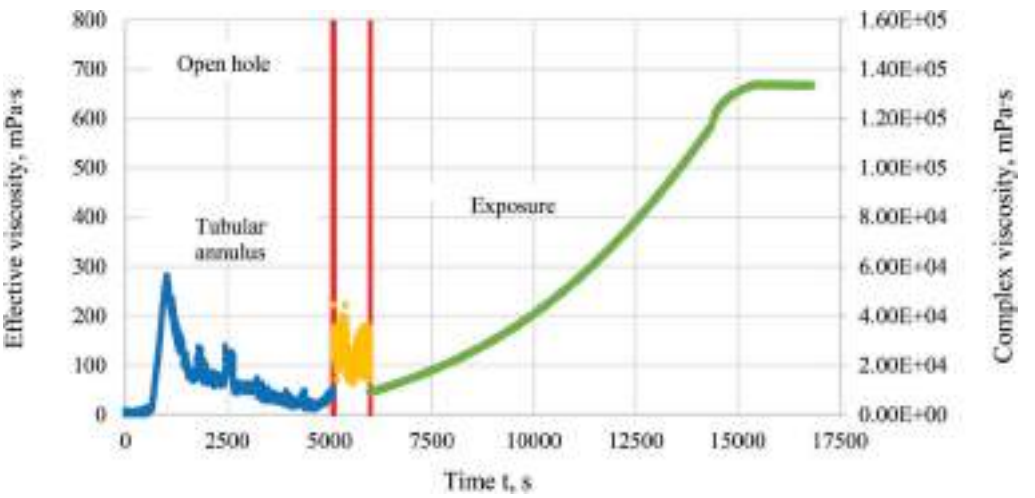

Figure 2. Dynamics of effective and complex viscosity of the gel-forming composition (90°C).

Based on the results of determining the crosslinking time in the process of modeling the injection of a gel-forming composition (used for 20°C) into a conditional well, it was found that:

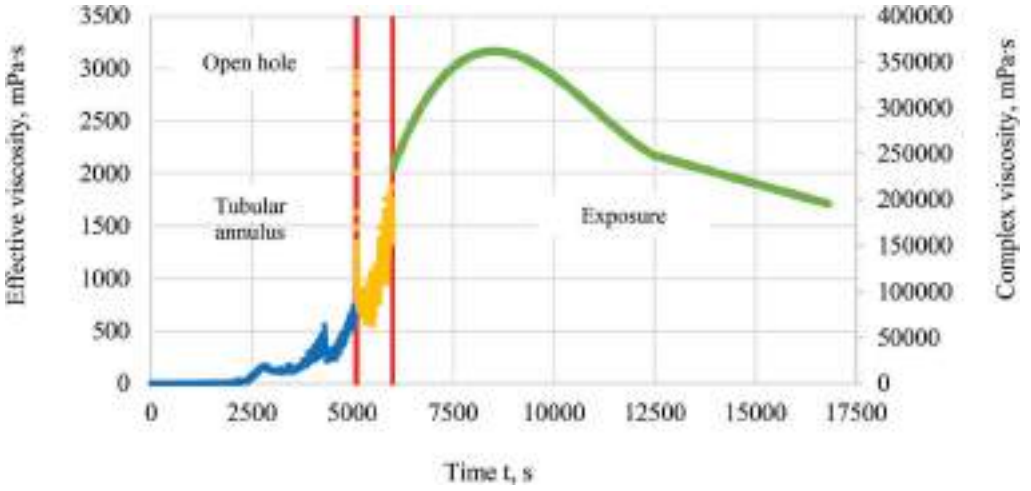

Figure 3. Dynamics of effective and complex viscosity of the gel-forming composition (20°C).

– the crosslinking process begins during the injection of the compound into the inter-tube space. The induction period of the beginning of gelation is about 40 minutes after the preparation of the composition.
– the process of crosslinking the composition ends after its injection into the well, during the technical settling of the well. The induction period of the end of gelation is about 2 h 20 min after preparation of the composition.

Based on the results of determining the crosslinking time in the process of modeling the injection of a gel-forming composition (used for 90°C) into a conditional well, it was found that:

– the crosslinking process begins during the injection of the compound into the inter-tube space. The induction period of the beginning of gelation is about 12 minutes after the preparation of the composition.
– the process of crosslinking the composition ends during its injection into the inter-tube space.

The induction period of the end of gelation is about 18 minutes after the preparation of the composition. After injection of the composition into the well, during the technical settling of the well, structure formation is observed, characterized by an increase in the complex viscosity, which ends after 4 hours from the moment of preparation of the composition. In order to increase the technological efficiency (for example, to prevent mechanical destruction of the gel during its injection into the well) of the silencing process using the gel-forming composition used for 90°C, it is recommended to adjust the content of the components so that the gel-forming process ends after the composition is fully injected into the well.

4 CONCLUSION

Based on the laboratory tests of physical, chemical and rheological properties of the frame and gel forming compositions, the following findings have been established:

1. Compositions in the conditions of low (20°C) and high (90°C) temperatures are thermostable during the entire researched period (3 days).
2. The results of evaluating the destruction of the frame and gel compositions showed the following:

– the gel-forming composition is completely destroyed within 1 and 3 hours with a 10% aqueous NaOH solution at 90 and 20°C, respectively;
– the frame-forming composition is destroyed by 75% within 24 hours with a mixture of 12% hydrochloric and 5% hydrofluoric acids (mud acid) at 90 and 20°C, respectively. The future observation showed insignificant changes because when reacting with a frame-forming composition, mud acid loses reactivity.

3. The gel (8 and 10.7 mPa·s) and frame (64 and 27 mPa·s) forming compositions at 20 and 90°C, respectively, have a low effective viscosity after preparation, which allows us to conclude that they are technologically efficient when injected into the well;
4. Gel-forming composition can have a high blocking capacity, since their static shear stress is 648 Pa at low temperatures (20°C) and 126 Pa at high temperatures (90°C).

The results of physical, chemical and rheological studies of frame and gel forming compositions have shown that they can be used in conditions of reservoir temperatures from 20°C to 90°C, which consists in the possibility of injection these compositions into a typical well and selling them into the bottom-hole formation zone due to their low viscosity after preparation and slow cross-linking speed. However, based on the results of the conducted studies, it is recommended to adjust the content of the components of the gel-forming composition (used for 90°C) so that the gel-forming process ends after the composition is injected into the well in full.

In addition, the use of destruction allows to reduce the negative impact of this technology on filtration characteristics of the bottomhole formation zone after well killing due to the reduction of the coefficient of relative changes in permeability and pressure gradient the start of oil flow when "development" wells.

To address the problem of well killing in complicated conditions, it is necessary to conduct a cycle of laboratory and field tests of the considered compositions, which will allow to select and justify the optimal technological and economic parameters of the operation.

REFERENCES

Bouts, M.N., Ruud, A.T. & Samuel, A.J. 1997. Time Delayed and Low-Impairment Fluid-loss Control Using a Succinoglycan Biopolymer with an Internal Acid Breaker. *SPE Journal*, *doi: 10.2118/31085-PA*, *21-23 December*. Texas: Houston.

Dandekar, A.Y. 2013. *Petroleum Reservoir Rock and Fluid Properties*. Boca Raton: CRC press.

Dorman, J. & Udvary, F. 1996. Comparative Evaluation of Temporary Blocking Fluid Systems for Controlling Fluid Loss Through Perforations. *SPE Formation Damage Control Symposium*, *doi: 10.2118/31081-MS*, 14-15 February. Louisiana: Lafayette.

Elchin, F.V., Azizagha, A.A., Vugar, V.G. & Nurana, V.N. 2019. Water Shutoff Using Crosslinked Polymer Gels. *SPE Annual Caspian Technical Conference*, *doi: 10.2118/198351-MS*, *16-18 October*. Azerbaijan: Baku.

Galimkhanov, A., Okhotnikov, D., Ginzburg, L., Bakhtin, A., Sidorov, Y., Kuzmin, P., Kulikov, S., Veliyev, G. & Badrawi, M. 2019. Successful Implementation of Managed Pressure Drilling Technology Under the Conditions of Catastrophic Mud Losses in the Kuyumbinskoe Field. *SPE Russian Petroleum Technology Conference*, *doi: 10.2118/196791-MS*, *22-24 October*. Russia: Moscow.

GOST 3900-85. 2006. *Oil and Oil products. Density Determination Methods*. Moscow: Publishing Standards.

GOST 1929-87. 2002. *Oil Products. Methods for Determination of Dynamic Viscosity on a Rotational Viscometer*. Moscow: Publishing Standards.

Gumerova, G.R. & Yarkeyeva, N.R. 2017. Technology of using cross-linked polymer compositions. *Journal of Oil & Gas Business*, 2, 63–79.

Jouenne, S., Klimenko, A. & Levitt, D. 2016. Tradeoffs Between Emulsion and Powder Polymers for EOR. *SPE Improved Oil Recovery Conference*, *doi: 10.2118/179631-MS*, *11-13 April*. Oklahoma: Tulsa.

Musabirov, M.Kh., Kuryashov, D.A., Garifov, K.M., Dmitriyeva, A.Y. & Abusalimov E.M. 2019. Developing structure-forming colloidal systems for matrix acidizing of porous-fractured carbonate reservoirs. *Oil Industry Journal*, 6, 71–73.

Quintero, L., Ponnapati, R. & Felipe, M. 2017. Cleanup of Organic and Inorganic Wellbore Deposits Using Microemulsion Formulations: Laboratory Development and Field Applications. *Offshore Technology Conference*, *doi: 10.4043/27653-MS*, *1-4 May*. Texas: Houston.
Raupov, I.R. & Oprikova, V.Y. 2018. The results of laboratory studies of the rheological characteristics of the crosslinked polymer composition. *Bulatovskie chteniya*, 2, 63–66.
Rogachev, M.K. & Strizhnev, K.V. 2006. *Complication Control During Oil Production*. Moscow: Nedra Business Center.
Rogachev, M.K. & Kondrashev, A.O. 2016. Substantiation of the technology of in-situ waterproofing in low-permeability res*er*voirs. *Journal of Mining Institute*, 217, 55–60.
Ryabokon, S.A. 2009. *Technological Fluids for Completion and Well Service Operations*. Krasnodar: Prosveshcheniye-Yug.
Strizhnev, K.V. 2010. *Repair and Insulation Works in Wells: Theory and Practice*. St. Petersburg: Nedra.
Tokunov, V.I. & Saushin, A.Z. 2004. *Process Fluids and Compositions for Increasing the Productivity of Oil and Gas Wells*. Moscow: Nedra.
Volkov, V., Turapin, A., Ermilov, A., Vasyutkin, S., Fomin, D. & Sorokina, A. 2019. Experience of Gas Wells Development in Complex Carbonate Reservoirs in Different Stages of Development. *SPE Russian Petroleum Technology Conference*, *doi:10.2118/196915-MS*, *22-24 October*. Russia: Moscow.
William, E., Syed, A. & Mingjie, K. 1996. Effects of Completion Fluid Loss on Well Productivity. *SPE Formation Damage Control Symposium*, *doi: 10.2118/31137-MS*, *14-15 February*. Louisiana: Lafayette.

Advances in Raw Material Industries for Sustainable Development Goals – Litvinenko (Ed)
© 2021 Taylor & Francis Group, London, ISBN 978-0-367-75881-3

Paper methodology for pipe steels in hydrogen containing environments. Review

A.B. Arabey
Gazprom, St. Petersburg, Russia

V.A. Egorov, K.B. Konischev & Semenov
Gazprom VNIIGAZ LLC, Moscow reg., Russia

ABSTRACT: The review article provides test methods for pipe steels in environments containing hydrogen. The authors analyze test procedures designed for determination of pipe steel properties to provide further estimation of their serviceability for transmission of hydrogen-containing natural gas. The fatigue properties of the pipe metal decrease with increasing hydrogen content in the gas mixture. The method of determining the of the fatigue crack growth rate is promising for pipe metal in gas mixture containing hydrogen.It has been established that hydrogen impacts gas mixture compression. This fact should be taken into account when selecting operation modes for compressor stations.

Keywords: hydrogen embrittlement, hydrogen-methane gas mixture, fatigue damage, crack growth rate, strength properties

1 INTRODUCTION

Hydrogen can be considered as a clean energy carrier, similar to electricity (Nitsh & Voigt, 1988), (Aksyutin et al., 2017). Using the existing natural gas (NG) grid for the hydrogen service has been being considered over the past decades.It has been found, that transporting hydrogen using an existing natural gas network is technically feasible (Bedel & Junker, 2006). Existing gas transmission system (GTS) can be used for hydrogen-containing natural gas as well. Hydrogen embrittlement of carbon steels that the major pipelines are made of can impose restrictions on transmission of hydrogen-methane gas mixtures through GTS. Hydrogen embrittlement of steels has been investigated by a number of scientists (Nanninga et al., 2010), (Marhi & Somerday, 2008), (Kolachev, 1985), (Nagumo, 2016). These studies analyze hydrogen impact only on metal that stays tensile enough after exposure to hydrogen. At the same time, most of metallic materials have reduced resistance to fatigue damage and high fatigue crack growth rate in hydrogen environments (Marhi & Somerday, 2012). Changing the hydrogen concentration in the gas mixture leads to unsteady operation of the GTS (Guandalini et al., 2015). Recently, the American Society of Mechanical Engineers (ASME) has adopted a code specifically for hydrogen piping and pipelines: ASME Pressure Piping Code B31.12. Additionally, ASME has adopted new language in the Boiler and Pressure Vessel Code (Section VIII, Division 3, Article KD-10) for qualifying pressure vessels for hydrogen service. These rules can be adopted for pipelines as well, as part of a fitness-for-service management program (Baek et al., 2017). This work is motivated by a desire to describe the approach of fracture mechanics to serviceability for pipelines distributing mixed hydrogen and natural gas.

2 MATERIAL AND TEST METHODS

A hydraulic servo controlled testing machine Instron with an autoclave was used to measure the mechanical properties of specimens in mixtures natural gas and hydrogen (ASTM G142-2016). Chamber material is insensitive to hydrogen embrittlement and is able to resist up to 20 MPa gaseous hydrogen pressure. Tests were conducted with API-5L X80 pipe samples (Figure 1) (ASTM G142 2016), (ASTM E647 2000).

Mechanical properties of the pipe metal have been determined by standard specimens. Fatigue crack growth tests have been carried out within this study on the compact tension specimens in accordance with (ISO 7539-6 2018).

Test environment: hydrogen-methane gas mixture with hydrogen content varying from 0 % to 50 %. Tests have been performed under 12 MPa. For safety reasons methane was replaced by nitrogen.

3 TEST RESULTS

Authors (Meng et al., 2017) were determined that the change in hydrogen content in gas mixture didn't influence tensile properties (Figure 2).

The influence of added hydrogen on tensile behavior of thesmooth specimens is shown in Figure 3.

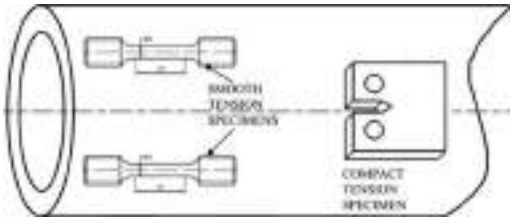

Figure 1. Specimens for tests from API-5L X80 pipe.

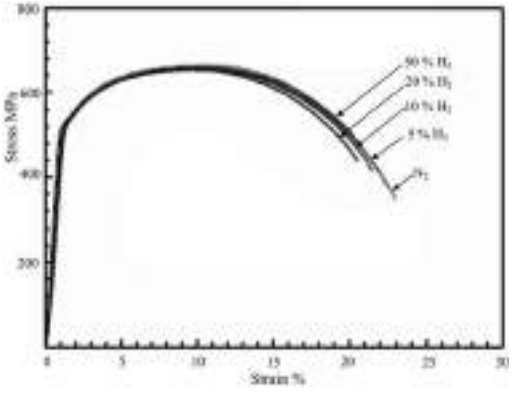

Figure 2. Influence of added hydrogen on the tensile of the smooth tension specimens.

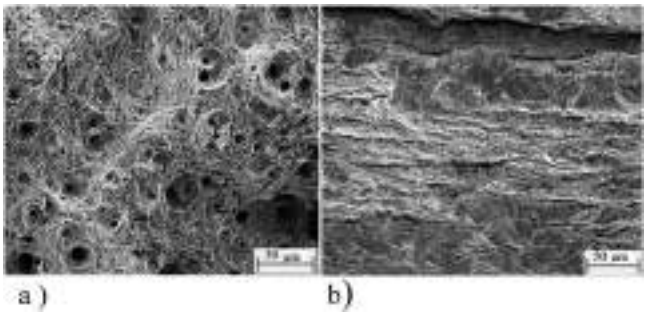

Figure 3. Fractured surfaces of the smooth specimens in: a) nitrogen and; b) hydrogen blend 20 %.

The reduction of area specimens and hydrogen embrittlement index is calculated as follows:

$$R_A = 1 - (S_k/S_0) \tag{1}$$

$$E_I(\%) = \frac{R_A^{N_2} - R_A^{H_2}}{R_A^{N_2}} \times 100 \tag{2}$$

where R_A = the reduction of area specimen in N_2 and H_2 blends; S_k = cross-section area of the specimen after failure; S_0 = cross-section area of the specimen before failure; E_I = specimen hydrogen embrittlement index (E_I = 0 means no hydrogen embrittlement E_I = 100 % is value for maximum embrittlement).

The indexes for various hydrogen blends are shown in Table 1.

Authors (Meng et al., 2017) have suggested that gaseous hydrogen content increasing in gas mixture from 0 % to 50 % results in metal embrittlement of high-strength API-5L X80 pipes. Fatigue crack growth rate escalates by an order of magnitude when moving from neutral nitrogen to gaseous mixtures of nitrogen and hydrogen. Fatigue crack growth rate also builds up with hydrogen content increase in gas mixture from 5 % to 50 %. Simultaneous hydrogen exposure and mechanical loads on pipe steel can lead to hydrogen embrittlement. For this reason there is a need to understand the problem of reversed pipeline loads in hydrogen-containing environments. The influence of cyclic loads on crack growth rate of API-5L X80 pipe steel in pure nitrogen and hydrogen blends is shown in Figure 4.

The effect of hydrogen on the properties of API-5L X80 was investigated by similar methods (Briottet et al., 2011). It has been established that «fatigue crack growth rate» parameter is more sensitive to alternation of hydrogen content, than to any changes in mechanical properties of pipe steel. For air and hydrogen environments fatigue crack growth rates in shown in Figure 5.

The fatigue crack growth rate increases by at least an order of magnitude in hydrogen compared to air. This difference explained by interaction between hydrogen and dislocations in API-5L X80 steel.

Specialists of the Institute of Standards and Technologies (the USA) were engaged in the study of hydrogen embrittlement and simulated fatigue crack growth processes on API-5L

Table 1. Hydrogen embrittlement of API-5L X80 steel.

H_2 content, %	0	5	10	20	50
E_I index, %	0	3,39	4,32	15,88	16,77

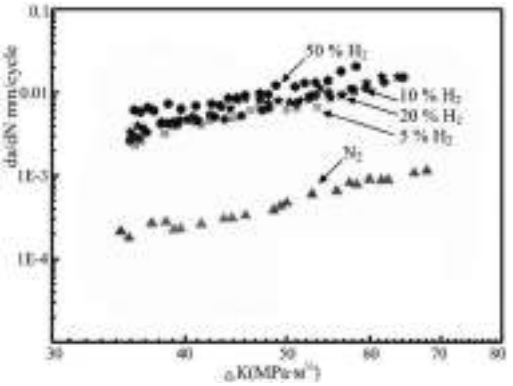

Figure 4. Da/dN versus ΔK curves in nitrogen gas and hydrogen blends.

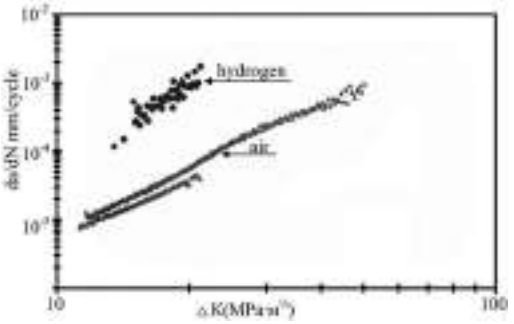

Figure 5. Fatigue crack growth rate behavior in air and hydrogen gas.

X100 steel (Amaro et al., 2014). Studies have shown that the fatigue crack growth rate in air and in environments with different hydrogen pressure varied (Figure 6).

Authors determined that fatigue crack growth rate depended on hydrogen content. Upgrading of hydrogen pressure from 1.72 MPa to 20.68 MPa can double the growth rate.

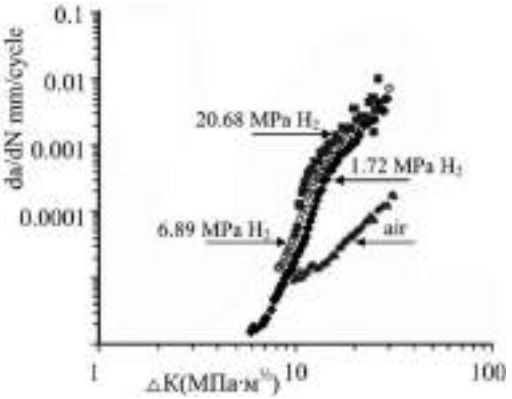

Figure 6. Fatigue crack growth rate behavior in air and hydrogen gas.

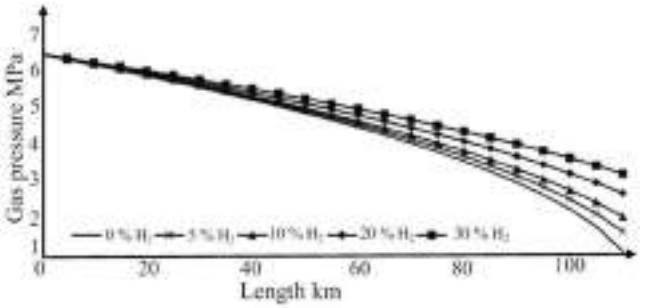

Figure 7. Gas pressure drop in pipeline for different hydrogen fractions in mixture with natural gas.

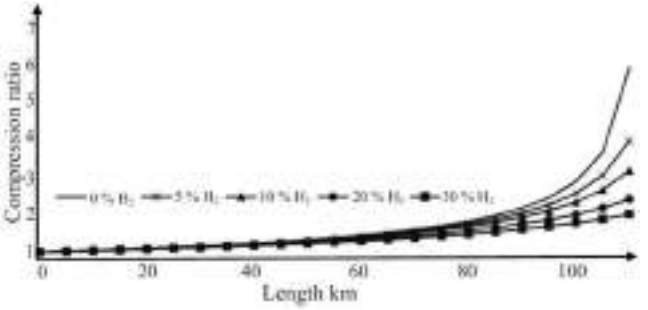

Figure 8. Compression ratio for mixture gas depending from the pipeline length.

In addition to pipes, compressor station, belong to GTS. Therefore, should be paid attention to physic parameters hydrogen transportation by pipeline GTS (Zabrzeski et al., 2017). For example hydrogen is much less viscous, and thus it can decrease Joule-Thompson effect in terms of pressure drop (Shimko, 2005). A mixture of natural gas and hydrogen in the pipeline 600 mm was investigated. The hydrogen content in natural gas modified from 0 % to 30 %. The gas temperature was to be 7 ºC and initial gas pressure 6.4 MPa (Zabrzeski et al., 2019). Correlation between gas pressure, hydrogen content and pipeline length is shown in Figure 7.

Simulated conditions for hydrogen-containing natural gas transmission through existing GTS must take into account operation of compressor stations. Figure 8 shows relationship of compression and the length of a pipeline that transmits hydrogen-containing natural gas.

Thus, hydrogen strongly influences variation of the process of natural gas compression.

4 CONCLUSIONS

Increase in hydrogen content in gas mixtures from 5 % to 50 % does not have significant impact on traditional mechanical properties of high-strength API-5L X80 pipe steels. Variation of fatigue crack growth rate depends on hydrogen content in pipe steel and is sensitive to the level of hydrogen content in metal. Fatigue crack growth rate determination method can be prospective in terms of selection of the best chemical composition of the pipe steel that is not exposed to negative hydrocarbon impact during transmission of methane-hydrogen mixtures.It is necessary to give consideration to physical properties of hydrogen when selecting compression and transmission modes for methane-hydrogen mixtures via existing GTS.

REFERENCES

Aksyutin O.E., Ishkov A.G., Romanov K.V., Teterevlev R.V., Khloptsov V.G., Kazaryan V.A., Stolyarevsky A. Ya. Power content of methane-hydrogen fuel under the conditions of transition to low-carbon economy. Gazovaya promyshlennost = Gas industry. Special edition №1/750/2017, 82–85.

Amaro R.L., Rustagi N., Findley K.O., Drexler E.S., Slifka A.J. Modeling the fatigue crack growth of X100 pipeline steel in gaseous hydrogen. International Journal of Fatigue 59 (2014) 262–271.

ASTM E647-00 Standard test method for measurement of fatigue crack growth rates.

ASTM G142-2016 Standard test method for determination of metals to embrittlement in hydrogen containing environments at high pressure, high temperature, or both.

Baek U.B., Nahm S.H. Kim W.S. Ronevich, J.A. and San M. Compatibility and suitability of existing steel pipelines for transport of hydrogen-natural gasblendshttps://hysafe.info/wp-content/uploads/2017_papers/228.pdf

Bedel L., Junker M. Naturel gas pipelines for hydrogen transportation WHEC 16/ 13-16June 2006-Lyon France.

Briottet L., Moro I., Lemoine, P. Quantifying the hydrogen embrittlement of pipe steel for safety considerations. Available from: http://conference.ing.unipi.it/ichs2011/papers/186.pdf

Guandalini G., Colbertaldo P., Campanari S. Dynamic Quality Tracking of Natural Gas and Hydrogen Mixture in a Portion of Natural Gas Grid Energy Procedia 75 (2015) 1037–1043.

ISO 7539-6:2018 Corrosion of metals and alloys-Stress corrosion testing-Part 6: Preparation and use of pre-cracking specimens for tests under constant load or constant load or constant.

Kolachev B.A. Hydrogen embrittlement of metals. Moscow. Metallurgy. 1985.

Marhi C.S. and Somerday B.P. Technical reference on hydrogen compatibility of materials: plain carbon ferritic steels: C-Mn alloys. Sandia National Laboratories Report No. SAND2008-1163.

Marhi C.S. and Somerday B.P. Technical reference on hydrogen compatibility of materials. Sandia National Laboratories Report No. SAND2012-7321, Livermore CA, 2012.

Meng B., Gu C., Zhang L., Zhou C., Li X., Zhao Y., Zheng J., Chen X., Han Y. Hydrogen effects on X80 pipeline steel in high-pressure natural gas/hydrogen mixtures. International Journal of Hydrogen Energy 42(2017) 7404–7412.

Nagumo M., Fundamentals of hydrogen embrittlement ISBN 978-981-10-0160-4, 2016.

Nanninga N.E., Slifka A.J., Levy Y.S. and White C. A review of fatigue crack growth for pipeline steels exposed to hydrogen. Journal of Research of the National Institute of Standards and Technology, 115 No.6, 2010, 437–452.

Nitsh J. and Voigt C. Launch concepts for non-fossil hydrogen, 1988, Springer, Berlin.

Shimko M.A. V.E.1 Combined Reverse-Brayton Joule Thompson hydrogen liquefaction cycle. Available from: http://www.hydrogen.energy.gov/pdfs/progress05/v_e_1_shimko.pdf

Zabrzeski Ł., Janusz P., Liszka K., Łaciak M. and Szurlej A. The effect of hydrogen transported through gas pipeline on the functioning of gas compression station work AGH Drilling, Oil, Gas 2017/34.

Zabrzeski L., Janusz1 P., Liszka K., Łaciak M., Szurlej A. Hydrogen-natural gas mixture compression in case of transporting through high-pressure gas pipelines. Available from: https://iopsciennce.iop.org/article/10.1088/1755-1315/214/1/012137/pdf

Advances in Raw Material Industries for Sustainable Development Goals – Litvinenko (Ed)

Investigation of pump-ejector systems characteristics for water alternating gas injection

A.N. Drozdov
Doctor of Engineering Sciences, Professor, Peoples Friendship University of Russia, Moscow, Russia

S.D. Karabaev
Post-graduate student of Peoples Friendship University of Russia, Moscow, Russia

N.P. Olmaskhanov
Post-graduate student of Peoples Friendship University of Russia, Moscow, Russia

Y.A. Gorbyleva
Post-graduate student of Peoples Friendship University of Russia, Moscow, Russia

I.M. Narozhnyy
Senior lecturer of Peoples Friendship University of Russia, Moscow, Russia

E.I. Gorelkina
Post-graduate student of Peoples Friendship University of Russia, Moscow, Russia

ABSTRACT: In this article, the experiments conducted to increase the efficiency of the use of pumping-ejector systems used for the enhanced oil recovery metod. This method is the water alternating gas injection. Water alternating gas injection implies the injection of alternately water and gas, or a water-gas mixture - simultaneous water alternating gas. The purpose of these experiments is to study the jet apparatus characteristics at high pressures at the ejector's intake (0-0.3 MPa), as well as to develop a new calculation methodology for the rheometer. Studies were conducted on a laboratory bench, allowing research at various gas flow rates. The article presents new dependencies for the three possible stand designs that allow recalculation of gas flow. The new rheometer calculation methodology can reduce the inaccuracy from 20% to 1.8%. The results of experiments that, the maximum value of the ejector efficiency is equal to 32.5%, and the injection rate varies from 1 - 1.14, under these experiments conditions.

Keywords: pump-ejector systems, characteristic of liquid-gas ejector, water alternating gas injection

1 INTRODUCTION

Simultaneous water alternating gas (SWAG) injection is a combination of conventional water-flooding and gas injection techniques. Unlike water, which takes up small hydrophilic pores and bottleneckings in the flooded zone of the reservoir, pumped gas as a non-wetting phase takes large hydrophobic pores, and the top of the reservoir under the action of gravitational forces (Drozdov et al. 2006). These aspects of oil displacement have led to reasonability of maintaining reservoir pressure by water and gas injection. At the same time, the displacement profile is also aligned, and the formation coverage is increased. Various authors carried out laboratory filtration experiments on the displacement of oil and hydrocarbon liquids from the reservoir by water, gas and various combinations of these agents. The results of experiments (Piyakov et al. 1992) on the use of water alternating gas (WAG) injection showed that the

injection of gas and water, regardless of the type of gas used and the stage of flooding, contributes to an increase in the displacement efficiency. The value of the increase of displacement efficiency is a function of the gas agent composition. The minimum increase of 7-8% was obtained in experiments using nitrogen; upon injection of dry hydrocarbon gas, the increase was 15–16%; with an increase in the content of intermediate components C_2-C_4 in a hydrocarbon gas, the displacement efficiency increased. The series of experiments on core samples (Fatemi et al. 2013), taking into account the wettability of the reservoirs, proves the effectiveness of the use of WAG compared to injecting water or gas separately.

Experiments (Stepanova 2003) suggested that the most significant effect of WAG was observed for media with mixed wettability, when hydrophobic surfaces form through paths along large pores, while smaller ones remain hydrophilic. The direct observation of physical processes occurring in a porous medium during WAG was carried out on the water-wet glass micromodel (Sohrabi et al. 2000). Various water alternating gas technologies over the past decades have been applied at almost a hundred fields in the world, both abroad and in our country. The successful ratio of using WAG according to data in foreign practice exceeds 90% (Berge 2002).

With the simultaneous injection of water and gas, the greatest effect according to the data (Egorov 2006, Liskevich 1973, Drozdov 2006) is achieved when the gas content of the water-gas mixture is in the range of 25-75%. Now abroad, dry or enriched hydrocarbon gases, as well as carbon dioxide, are usually injected into WAG technologies. The most commonly reported increase in oil recovery during WAG is approximately 5%, but, as noted in some fields, oil recovery may increase by 20%. Studies (Lei et al. 2016) have shown the efficiency of WAG CO_2 for multilayer formation.

In the article (Christensen et al. 2001) extensive review of the WAG injection process has been presented. The increase in oil production of the considered fields is about 5-10%. To obtain the effect of WAG and to avoid early breakthrough of the injection gas, it is necessary to have a good idea of the phase of the behavior of the reservoir oil and injection gas mixtures, as well as the heterogeneity of the reservoir.

The experimental study of WAG and SWAG injection schemes with CO_2 (Kamali 2017) is aimed at determining the function of co-optimization function for CO_2 storage and incremental oil production. Experiments are run to represent immiscible, near-miscible, and miscible displacements. Numerical simulations show a remarkable reduction in gas relative permeability for the WAG and SWAG displacements compared with continuous-gas-injection displacements, as a result of which the vertical-sweep efficiency of CO_2 is improved.

A comprehensive review of WAG field displacements and their effect on oil recovery and produced-gas/water ratio has been presented in the literature (Stalkup 1983; Christensen et al. 2001).

The vast simulation study (Nygård & Andersen 2020) has been performed investigating immiscible WAG injection focusing on mechanisms such as mobility, gravity, injected volume fractions, reservoir heterogeneity, gas entrapment, and relative permeability hysteresis.

Scientists (Hoare & Coll 2018, Kumar et al. 2017, Khorsandi et al. 2017; Alzayer & Sohrabi 2018) note the influence of hysteresis relative permeability on the effectiveness of WAG. It is often expected that the gas phase will show large hysteresis effects (Hoseini et al. 2011). Hysteresis lowers gas mobility and hence improves the gas/oil mobility ratio and reduces gravity segregation. The first effect is always positive, but the second is mainly positive in more uniform reservoirs where gravity segregation has a negative effect on recovery. In heterogeneous reservoirs, reducing gravity segregation can lead to the oil in low-permeability layers remaining unswept. (Nygård & Andersen 2020)

Most foreign fields with WAG technologies are located in Canada, the USA and Norway (Skauge & Stensen 2003, Christensen et al. 2001, Cone 1970, Quale et al. 2000, Righi & Pascual 2007, Shi et al. 2008, Stoisits et al. 1995, Choudhary et al. 2011, Gbadamosi et al. 2018, Olalotiti-Lawal et al.2018).

In Russia, experimental work on the WAG was carried out at the Sovetskoye and Vakhskoye (Kryuchkov 2002), Ilishevskoye (Shuvalov et al. 2008), Alekseevskoye (Vafin 2008, Zaripov 2006), Novogodnee (Zakirov et al. 2006), Vostochno-Perevalnoye (Zatsepin & Chernikov 2007, Chubanov et al. 2008) and at the Sredne-Hulymskoye fields (Chubanov et al. 2008).

In foreign practice, complex and expensive equipment that requires large capital investments, high-quality maintenance and competent operation – gas treatment units, pumps and high pressure compressors – is used to implement gas and water exposure. Attempts to apply the WAG compressor technology at the Samotlorskoye and Novogodnoye fields under Russian conditions, despite the enormous costs, were ultimately discontinued.

So the traditional technology of SWAG injection is not widely used in domestic oil fields. The main problem is the absence of effective processes and technologies for water and gas pumping into injection wells. In this situation, the use of jet technology, in particular pump-ejector systems, may turn out to be a very attractive solution.

In previously published papers (Krasilnikov 2010, Drozdov et al. 2008), laboratory studies of pump-ejector systems were carried out at constant pressure at the jet apparatus intake P_{in} (0; 0.5 MPa) with different values of relative power pressure drop created in the ejectors working nozzle ΔP_p. In this article, the characteristics of an ejector with a constant ΔP_p with a relative outlet pressure drop ΔP_o created by a jet apparatus were considered.

2 PURPOSE

The purpose of this work is to characterize the pump-ejector system at high pressures at the jet apparatus intake within 0 – 0.3 MPa. Additionally, the differential pressure gauge should be calibrated with the creation of a new calculation methodology.

3 MATERIALS AND METHODS

Investigations of the pump-ejector system was carried out on the laboratory bench (Figure 1) which worked in the following way. The power liquid (water) from the tank 1 enters the intake of a multistage centrifugal pump 2. Next, the power fluid is forced to the nozzle of the jet apparatus 3 and injects, depending on the experimental conditions, either gas from tank 1 or gas from the atmosphere, which is regulated by valves 12 and 13.

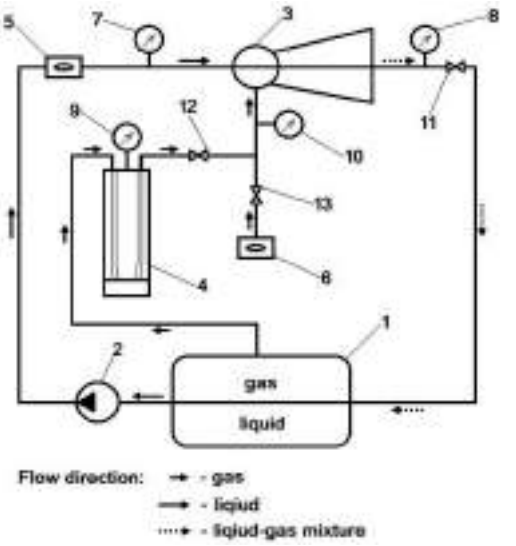

Figure 1. Diagram of the stand for the pump-ejector system investigation: 1 - liquid-gas tank; 2 - multistage centrifugal pump; 3 - ejector; 4 - differential pressure gauge; 5 - fluid meter; 6 - gas meter; 7, 8, 9 - manometers; 10 - pressure-vacuum meter; 11, 12, 13 - control valves and gate valves.

The flow rate of the power fluid injected into the nozzle is measured by a fluid meter 5. Depending on the conditions, the flow rate of the injected gas is measured by a differential pressure gauge 4 when high pressure gas is injected, or by a gas meter 6 when atmospheric air is injected. The pressures in front of the working nozzle of the jet apparatus and at the output from its diffuser were measured using manometers 7 and 8. The pressure at the ejector's intake was measured with a pressure – vacuum meter 10. Different operating modes and pressures were generated by a control valve 11.

Measured parameters during the experiment: fluid rate, gas rate from the tank, gas rate from the atmosphere, power pressure in front of the nozzle, pressure at the ejector's intake and output pressure. The efficiency of the ejector η_g during gas injection is determined by the ratio of the effective power N_e to total power N_t (Drozdov 2014):

$$\eta_g = \frac{N_e}{N_t} = \frac{\mathrm{Q}_{g.in} P_{in} \ln \frac{\mathrm{P_o}}{\mathrm{P_{in}}}}{\mathrm{Q}_p(P_o)} = \frac{\mathrm{u_g} p_{in} \ln \frac{\mathrm{P_o}}{\mathrm{P_{in}}}}{(P_p - P_0)}, \tag{1}$$

where $\mathrm{Q_{g.in}}$ – volumetric gas rate in the suction chamber;
p_{in} – pressure in the suction chamber (intake chamber);
$\mathrm{P_o}$ – outlet pressure of the ejector;
P_p – power pressure in front of the nozzle;
Q_p – volumetric power fluid rate;
$\mathrm{u_g} = \mathrm{Q_{g.in}}/\mathrm{Q}_p$ is the volumetric injection coefficient in the suction chamber.
Technical water is used as a power liquid and air as a gas. Relative pressure drop:

$$\frac{\Delta \mathrm{P_c}}{\Delta \mathrm{P_p}} = \frac{P_c - P_{\pi \mathrm{p}}}{P_p - P_{\pi \mathrm{p}}} \tag{2}$$

where $\Delta \mathrm{P_c}$,$\Delta \mathrm{P_p}$ – pressure drops created by the jet apparatus and the working nozzle of the ejector respectively.

Differential pressure gauge DT-50 was used to determine the gas rate from the tank. Generally, it is used to measure the flow rate of non-aggressive gases, vapors and liquids by determining the pressure drop across the orifice plate or other throttle body.

Additional tubes were used for the accuracy and to increase the measurement range for gas rate (Figure 2). Were used 3 schemes of gas flow which dependences on the degree of gas rate.

The "right" scheme is used at pressures P <0.18 MPa, which is activated by opening the valve 7 and closing the valve 6. The "left" scheme is used at pressures of 0.18<P<0.26 MPa, where the valves open vice versa to the "right" scheme. The "general" scheme is used when P>0.26 MPa, where both valves open. Theoretically, after getting the calibration curve at any pressure level, other pressure values can be obtained using the following equation:

$$Q_2 = Q_1 \sqrt{\frac{\lambda_1}{\lambda_2} \frac{P_1}{P_2}}, \tag{3}$$

where Q_1, Q_2 – the gas rates in the rheometer at pressures P_1 and P_2 respectively; λ_1, λ_2 – resistance values at P_1 and P_2 respectively.

For a quadratic zone of gas flow in a tube, as is well known $\lambda_1 = \lambda_2$, where at the same water level difference in the differential pressure gauge, we obtain:

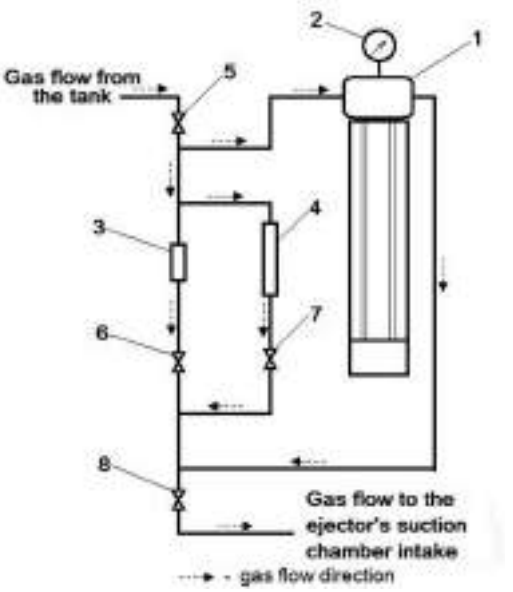

Figure 2. Diagram of a differential pressure gauge with variable parameters of the measurement range: 1 - differential pressure gauge; 2 - manometer; 3 - copper tube (shortened); 4 - copper tube (elongated); 5, 6, 7, 8 - valves and gate valves.

$$Q_2 = Q_1 \sqrt{\frac{P_1}{P_2}}, \tag{4}$$

In article (Drozdov 1982) it is pointed out that in the calibration process where brass tubes with an internal diameter of 4-6 mm was used at pressure under 0.6 MPa, the resistance values are not equal $\lambda_1 \neq \lambda_2$. Analytical determination of λ with the required accuracy depending on pressure and flow rate by formula (3) is difficult to perform. Due to it, the calibration dependencies were built at the same pressures as in the experiments pressures values. Since our studies are carried out with 6 mm tubes at pressures below 0.6 MPa, it is necessary to introduce correction factors for formula (2).

Calibration of the differential pressure gauge was carried out in this way. Calibration curves were registered at pressures of 0.1; 0.14; 0.18; 0.22; 0.26; 0.3 MPa. Gas rates at appropriate pressures were calculated based on 0.1 MPa by the formula (4). After that, the deviations between the calculated and actual values were estimated. According to the deviations, correction factors were found, and flow rates based on new formula were calculated. Next will be presented the results.

4 RESULTS AND DISCUSSION

This section presents the results of experimental studies of the pump-ejector system and calibration of the differential pressure gauge.

4.1 *Differential pressure gauge*

Because of the calibration carried out, it was possible to achieve sufficient accuracy of the new calculation methodology (Table 1, Table 2, Table 3). The following formula was obtained for the "right" scheme:

Table 1. The results of the calibration of the differential pressure gauge for the "right" scheme.

P, MPa	Old method (Δ, %)	New method (Δ, %)
0,14	9,9	1,14
0,18	16,8	1,78
0,22	22,7	1,71
0,26	26,3	1,62
0,3	28,7	1,35

Table 2. The results of the calibration of the differential pressure gauge on the "left" scheme.

P, MPa	Old method (Δ, %)	New method (Δ, %)
0,14	9,1	1,37
0,18	15,4	1,11
0,22	18,9	0,99
0,26	23,1	1,01
0,3	25,4	1,15

Table 3. The results of the calibration of the differential pressure gauge on the "common" scheme.

P, MPa	Old method (Δ, %)	New method (Δ, %)
0,14	9,7	1,86
0,18	14,7	1,5
0,22	20,0	1,66
0,26	23,0	1,83
0,3	25,2	1,44

$$Q_2 = Q_1 * \sqrt{\frac{P_1}{P_2}} * \left(-5,04 * (\Delta P)^2 + 2,38 * (\Delta P) + 1,01\right), \tag{5}$$

where Q_1,Q_2 – volumetric gas rates in differential pressure gauge at pressure P_1, P_2 respectively;

$$\Delta P = P_2 - P_1$$

.

During the calibration of the differential pressure gauge on the "right" scheme, the following results are obtained:

- according to the old method, the averaged inaccuracy is 20.88 %;
- according to the new method, the averaged inaccuracy does not exceed 1.8 %.

The next formula was obtained for "left" scheme:

$$Q_2 = Q_1 \times \sqrt{\frac{P_1}{P_2}} \times \left(-3,08 * (\Delta P)^2 + 1,75 * (\Delta P) + 1,03\right), \quad (6)$$

During the calibration of the differential pressure gauge on the "right" scheme, received the following indicators:

- according to the old method, the averaged inaccuracy is 18.52 %;
- according to the new method, the averaged inaccuracy does not exceed 1.9 %.

The next formula was obtained for "common" scheme:

$$Q_2 = Q_1 \times \sqrt{\frac{P_1}{P_2}} \times \left(-3,53 * (\Delta P)^2 + 1,83 * (\Delta P) + 1,03\right), \quad (7)$$

During the calibrating for the "common" system, we obtained the following indicators:

- according to the old method, the averaged inaccuracy is 18.52%
- according to the new method inaccuracy does not exceed 1.9%.

4.2 *Characteristics of the pump-ejector system*

After the calibration of the differential pressure gauge, the pressure-energy characteristics of the ejector were obtained (Figure 3, Figure 5). The maximum efficiency of ejector η_g during gas injection is obtained 0.325, where the relative pressure drop is $\Delta P_o/\Delta P_p = 0.315$, injection coefficient u_g in the suction chamber is 1.13 at intake pressure $P_{in} = 0.26$ MPa and outlet pressure $P_o = 0.636$ MPa. The minimum efficiency of ejector η_g during gas injection is obtained 0.245, where the relative pressure drop is $\Delta P_o/\Delta P_p = 0.294$, injection coefficient in the suction chamber is $u_g = 1.14$ under intake pressure $P_{in} = 0.05$ MPa and outlet pressure $P_o = 0.397$ MPa. It can also be noted that in the pressure range $P_{in} = 0.05$ - 0.3 MPa the injection coefficient in the suction chamber is varies from 1 to 1.14.

After that, a graph of maximum efficiencies η_g was plotted to the function of intake pressures P_{in} (Figure 4.). This graph shows that the difference between the maximum and

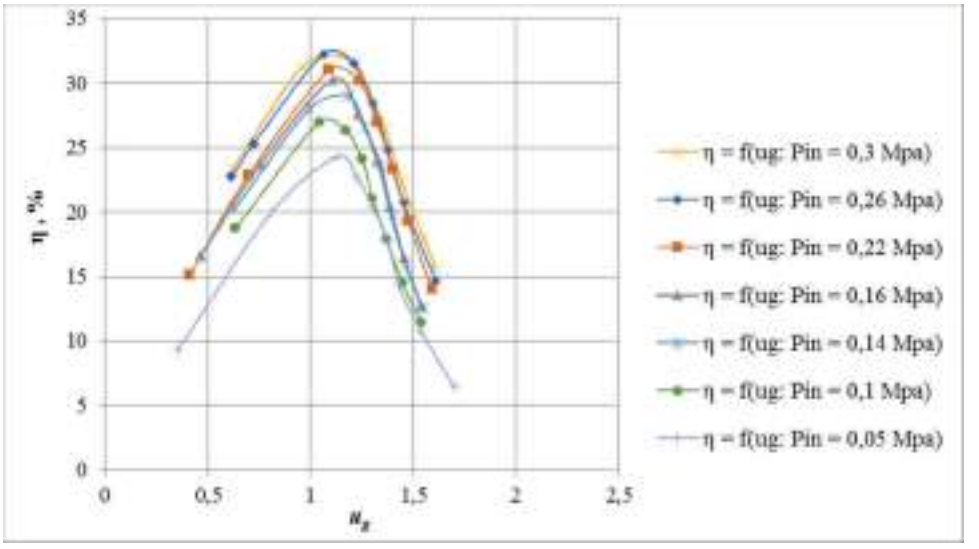

Figure 3. The ejector efficiencies η_g to the function of injection coefficient u_g.

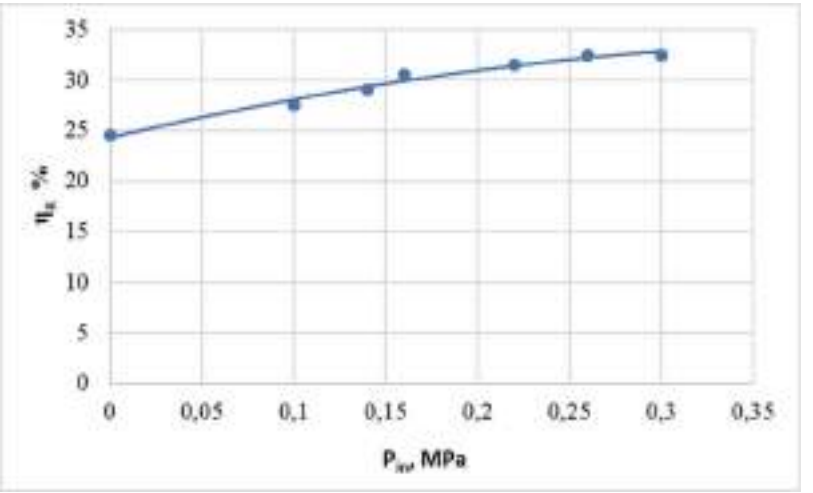

Figure 4. The maximum efficiencies η_g to the function of intake pressure P_{in}.

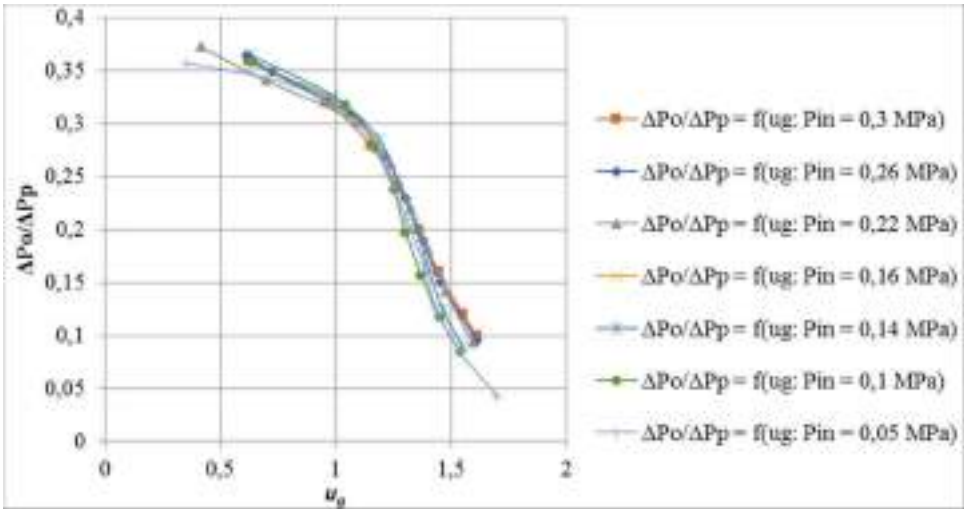

Figure 5. The relative pressure drop $\Delta P_o/\Delta P_p$ to the function of injection coefficient u_g.

minimum values is 0.078. The value of η_g gradually increases to P_{in} = 0.26 MPa and after this point some decline is observed.

5 CONCLUSION

Research and calculations have shown that, the new calculation methodology of the differential pressure gauge makes it possible to calculate gas rates with an inaccuracy of no more than 1.8%.

The obtained pressure-energy characteristics for high pressures at the ejector's intake in the range from 0.05 to 0.3 MPa allow us to conclude that the maximum efficiency at this condition, do not exceed 32.5%. The volumetric injection coefficient rates range from 1 to 1.14. It is

worth noting that after the intake pressure of 0.26 MPa, there is some decrease in the efficiency, which can be assessed in further studies at higher intake pressure P_{in}.

ACKNOWLEDGMENT

The publication has been prepared with the support of the «RUDN University Program 5-100».

REFERENCES

Alzayer, H. & Sohrabi, M. 2018. Water-Alternating-Gas Injection Simulation—Best Practices *SPE EOR Conference at Oil and Gas West Asia*, 26–28 *March*: SPE-190346-MS Oman: Muscat

Berge, L.I., Stensen, J.A., Crapez, B. & Quale, E.A. 2002. SWAG Injectivity Behavior Based on Siri Field Data*Improved Oil Recovery Symposium*, 13-17 *April*: SPE 75126 Oklahoma: Tulsa.

Choudhary, M.K., Dezabala, E., Solis, H.A. & Narvaez, J. Z. Z. 2011. Design, Implementation and Performance of a Down-Dip WAG Pilot *International Petroleum Technology Conference*, 15-17 *November*: IPTC-14571-MS Thailand: Bangkok

Christensen, J. R., Stenby, E. H. and Skauge, A. 2001. Review of WAG Field Experience. *SPE Res Eval & Eng* 4 (2): 97–106.

Chubanov, O.V., Harlanov, S.A. & Nurgaliev, R.G. 2008. Development and implementation of water alternating gas injection methods for enhanced oil recovery at RITEK *Territory of NEFTEGAZ* vol. 9: 42–48

Cone, C. 1970. Case history of the University Block-9 (Wolfcamp) field – a gas-water injection secondary recovery project *Journal of Petroleum Technology* XII, vol. 22:1485–1491.

Drozdov, A.N. 1982. *Development of methods for calculating the characteristics of a submersible centrifugal pump for the operation of wells with low pressures at the entrance to the pump* Cand. Sci. Dissertation Moscow p 212

Drozdov, A.N., Egorov, Yu.A., Verbitsky, V.S., Dengaev, A.V. & Lambin, D.N. 2006. Methods and technology of water alternating gas injection influence to oil reservoirs *Territory NEFTEGAZ* vol 2: 54–58

Drozdov, A.N., Krasilnikov, I.A. & Verbitsky V.S. 2008. Investigation of the characteristics of pumping-ejector systems for water-gas impact on the formation *Territory NEFTEGAZ* vol 2: 60–63

Drozdov, A.N. 2014. Problems of simultaneous water alternating gas injection and its solutions *Oil industry* vol 2: 2–6

Egorov, Yu.A. 2006 *Development of water-alternated-gas technology using pump-ejector systems to increase oil recovery* Cand. Sci. Dissertation Moscow p 169

Fatemi, S.M. & Sohrabi, M. 2013. Experimental investigation of near-miscible water-alternating-gas injection performance in water-wet and mixed-wet systems *SPE Journal* vol. 18(1): 114–123.

Gbadamosi, A. O., Kiwalabye, J., Junin, R. & Augustine, A. 2018. A review of gas enhanced oil recovery schemes used in the North Sea *Journal of Petroleum Exploration and Production Technology* vol. 8:1373–1387

Hoare, G. & Coll, C. 2018. Effect of Small/Medium Scale Reservoir Heterogeneity on the Effectiveness of Water, Gas and Water Alternating Gas WAG Injection. *SPE Europec featured at the 80th EAGE Conference and Exhibition*, 11–14 *June*: SPE-190855-MS Denmark: Copenhagen

Hoseini, J., Masoudi, R., Mousavi Mirkalaei, S. M. et al. 2011. Investigating the Effect of Hysteresis Modelling on Numerical Simulation of Immiscible WAG Injection. *International Petroleum Technology Conference,* 15–17 *November: IPTC-15055-MS*. Thailand: Bangkok

Kamali, F., Hussain, F. & Cinar, Y. 2017. An Experimental and Numerical Analysis of Water-Alternating-Gas and Simultaneous-Water-and-Gas Displacements for Carbon Dioxide Enhanced Oil Recovery and Storage *SPE Journal* vol. 22 (2): 18

Khorsandi, S., Li, L., & Johns, R. T. 2017. Equation of State for Relative Permeability, Including Hysteresis and Wettability Alteration *SPE Journal* vol. 22 (6):1915–1928.

Krasilnikov, I.A. 2010. *Development of methods for calculating the characteristics of liquid-gas ejectors for well operation and water alternating gas influence on the reservoir using pump-ejector systems* Cand. Sci. Dissertation Moscow p 144

Kryuchkov, V.I. 2002. *The use of water-gas systems based on petroleum gas to increase oil recovery*. Cand. Sci. Dissertation Bugulma p 193

Kumar, J., Agrawal, P. & Draoui, E. 2017. A Case Study on Miscible and Immiscible Gas-Injection Pilots in a Middle East Carbonate Reservoir in an Offshore Environment. *SPE Res Eval & Eng* 20 (1): 19–29. SPE-181758-PA.

Lei, H., Yang, S., Zu, L., Wang, Z. & Li, Y. 2016. Oil recovery performance and CO_2 storage potential of CO_2 water-alternating-gas injection after continuous CO_2 injection in a multilayer formation *Energy & fuels* vol. 30 (11): 8922–8931.

Liskevich, E.I. & Ostrovsky, Yu.M. 1973. Oil displacement by gas-water mixtures *Oil field development, proceedings of UkrNIIIPND* vol. 11-12: 233–240.

Nygård, J. I. & Andersen, P. Ø. 2020. Simulation of Immiscible Water-Alternating-Gas Injection in a Stratified Reservoir: Performance Characterization Using a New Dimensionless Number *SPE Journal* SPE-200479-PA

Olalotiti-Lawal, F., Onishi, T., Datta-Gupta, A., Fujita, Y., Watanabe, D. & Hagiwara, K. 2018. Post-Combustion CO_2 WAG Pilot in a Mature Field: Model Calibration and Optimization *SPE Annual Technical Conference and Exhibition*, 24-26 *September:* SPE-191472 Texas: Dallas

Piyakov, G.N., Yakovlev, A.P., Kudashev, R.I. & Romanova, E.I. 1992. The study of the efficiency of water alternating gas injection (on the example of the Yu_1 layer of the Kogalymskoye field) *Oil industry* vol. 1: 38–39.

Quale, E.A., Crapez, B., Stensen, J.A. & Berge, L.I.B. 2000. SWAG Injection on the Siri Field - An Optimized Injection System for Less Cost, SPE 65165, *SPE European Petroleum Conference held in Paris*, France, *October*, 24–25 France: Paris

Righi, E.F. & Pascual, M. 2007. Water-Alternating-Gas Pilot in the Largest Oil Field in Argentina: Chihuido de la Sierra Negra, Neuquen Basin. *SPE Latin American and Caribbean Petroleum Engineering Conference*, 15-18 *April 2007:* SPE 108031. Argentina: Buenos Aires.

Shi, W., Corwith, J., Bouchard, A., Bone, R. & Reinbold E. 2008. Kuparuk MWAG Project after 20 Years *SPE/DOE Improved Oil Recovery Symposium*, 19-23 *April 2008:* SPE 113933. Oklahoma: Tulsa.

Shuvalov, A.V., Samigullin, I.F. & Suleymanov, A.A. 2008. Pilot-industrial work at JSOC Bashneft related to the introduction of gas and water alternating gas injection *Materials of the VII Interregional Conference "Geology, Minerals, and Geoecology Problems of Bashkortostan, the Urals and Neighboring Territories"*, 2008, *November*: 239–241

Skauge, A. & Stensen, J.O. 2003. A review of field experience in water alternating gas injection. *Reports of the 1st International Conference "Oil Recovery - 2003", May* 19-23: 119–120. Russia: Moscow

Sohrabi, M., Henderson, G.D., Tehrani, D.H & Danesh A. 2000. Visualisation of oil recovery by water alternating gas (WAG) injection using high pressure micromodels-water-wet system *SPE Annual Technical Conference and Exhibition*.

Stalkup, F. I. 1983. *Miscible Displacement*. Richardson, Texas: Monograph Series, Society of Petroleum Engineers.

Stepanova, G.S. 2003 New methods of gas and water-alternated-gas injection of oil reservoirs *Drilling and Oil*, vol. 9: 18–20.

Stoisits, R.F., Krist, G.J., Ma, T.D., Rugen, J.A., Kolpak, M.M. & Payne, R.L. 1995. Simultaneous Water and Gas Injection Pilot at the Kuparuk River Field, Surface Line Impact *SPE Annual Technical Conference*, *Oct.* 1995*:* SPE 30645

Vafin, R.V. 2008. Improving the efficiency of water-alternated-gas technology on the reservoir at the Alekseevskoye field *Neftepromyslovoe delo* vol. 2: 33–35

Zakirov, S.N., Indrupsky, I.M., Levochkin, V.V., Fakhretdinov, R.N. & Ostapchuk, S.S. 2006. Water-alternated-gas injection on the Novogodnee field *Oil industry*, vol.12: 40–43.

Zaripov, M.S. 2006. *Improving the technology of water alternating gas injection, preparation and injection of working agents into the reservoir* Abstract of Cand. Sci. Dissertation Ufa p 24

Zatsepin, V.V. & Chernikov, E.V. 2007. Some issues of the implementation of water alternating gas injection at the Vostochno-Perevalnoye field *Oil Industry* vol. 2: 44–47.

Advances in Raw Material Industries for Sustainable Development Goals – Litvinenko (Ed)
© 2021 Taylor & Francis Group, London, ISBN 978-0-367-75881-3

The choice of fluid and thermal grid of the organic Rankine cycle in the conditions of its application at the oil refineries

M.A. Peretyatko
Ph.D. student, Saint-Petersburg Mining University, Saint-Petersburg, Russia

P.V. Yakovlev
Professor, Saint-Petersburg Mining University, Saint-Petersburg, Russia

V.A. Lebedev
Professor, Saint-Petersburg Mining University, Saint-Petersburg, Russia

A.S. Deev
Postgraduate student, Saint-Petersburg Mining University, Saint-Petersburg, Russia

ABSTRACT: The article discusses the problem of choosing the working fluid for the Rankine organic cycle. This is done by analyzing the parameters of the ORC unit on these Freon's. It is proposed to use low-grade heat of technological units for oil refining as a heat source for the organic Rankine cycle unit. Currently, a significant part of the available low-grade heat from oil refineries is lost into the atmosphere. The installation of the organic Rankine cycle allows the use of this heat to generate an expensive energy resource - electricity. This is the advantage of this installation over other methods of utilizing low-grade heat. At the moment, there is no clear methodology for choosing a working fluid for the organic Rankine cycle, that used at an oil refinery. For comparison, the following freons were selected: r245fa, r152a and r404a. To solve this problem, a model that calculates such indicators as thermal efficiency, coolant flow rate and electric power of the installation, for the simplest scheme of the organic Rankine cycle was built. The article also provides an analysis of the results obtained by modeling the comparison of the considered working bodies. To assess the feasibility of using the unit with selected coolant, the economic effect of its implementation was evaluated.

1 INTRODUCTION

In the modern world, more and more attention is paid to the problem of improving energy efficiency. One of the tasks of increasing energy efficiency is the development of methods for recycling of low-grade heat. Low-potential heat sources include flows of various substances and gases with a temperature of not more than 300°C. Such sources are very common in the oil, metallurgical chemical and other industries.

Consider the refining industry in more detail. The technological process of oil refining is not perfect in terms of the full use of thermal energy. Thermal energy supplied to oil at refineries is used only by 30%. About 35% of it discharged into the atmosphere using circulation water system or air-cooling units, about 10-15% released into the atmosphere from surfaces of equipment and about 15% released into the atmosphere with flue gases (Burdygina, 2003). According to estimates, at refineries with a capacity of 5-6 million tons per year of crude oil, at least 15 MW of low potential heat with a temperature of at least 150°C are discharged into the atmosphere.

One of the modern ways of recycling this low-grade heat is organic Rankine cycle (ORC). ORC is used to generate electricity. The schematic diagram of the OCR unit is shown in Figure 1.

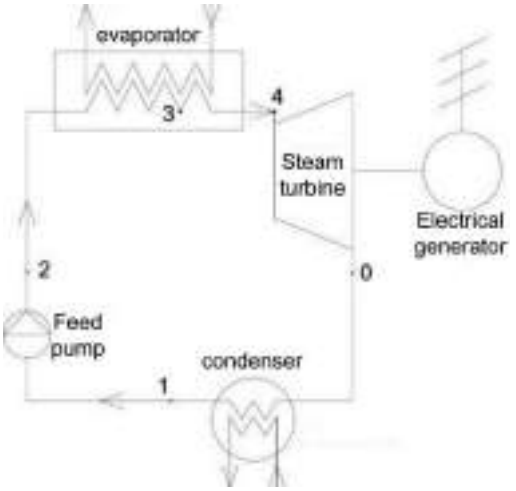

Figure 1. Schematic diagram of the OCR unit.

OCR works on the same principle as the classical Rankine cycle with water as a fluid. The main difference between organic fluid and water is a low boiling point, which allows steam to be generated at low temperatures of heat sources.

For the normal operation of a steam turbine, it is necessary, to have a large pressure difference, which is different for various fluids. In this regard, depending on the temperature conditions of the thermal scheme of the organic Rankine cycle, it is necessary to determine the compound that will be used as a working fluid. When choosing different compounds, you must follow rules:

— Work, done by steam in the turbine, should be as much as possible;
— Thermal conductivity of the fluid should be as large as possible for more efficient heat transfer in the evaporator and condenser;
— Fluid must be stable at high temperatures;
— Fluid should be environmentally friendly and safe.

Based on these criteria, for further consideration, the following freons were selected: r245fa, r152a, r404a. The parameters of the considered working fluid are presented in Table 1.

These freons have already been used as a coolant for ORC, but under other conditions. It is advisable to consider them for specific conditions of use at a refinery.

One of the main indicators of the effectiveness of the Rankine cycle is the thermal efficiency of the cycle. In this case, the thermal efficiency of the cycle will depend on the selected compound. Based on this fact, the choice of the working fluid will be made according to the highest thermal efficiency of the cycle. Further in the work, an unit working on the selected fluid will be considered.

Consider freon r245fa as a working fluid for the proposed heat recovery unit at oil refineries. The p-h diagram of the ORC with r245fa is shown in Figure 2.

Table 1. Parameters of the considered working fluid.

Parameter	Value		
	r245fa	r152a	r404a
Molar mass, g/mol	134,1	66,1	97,6
Boiling point, °C	15,3	-24	-46,3
Specific thermal capacity in a liquid state at normal pressure, kJ/kg K	1,36	1,8	1,62
Ozone depletion potential	0	0	0
Global warming potential	1030	140	3750

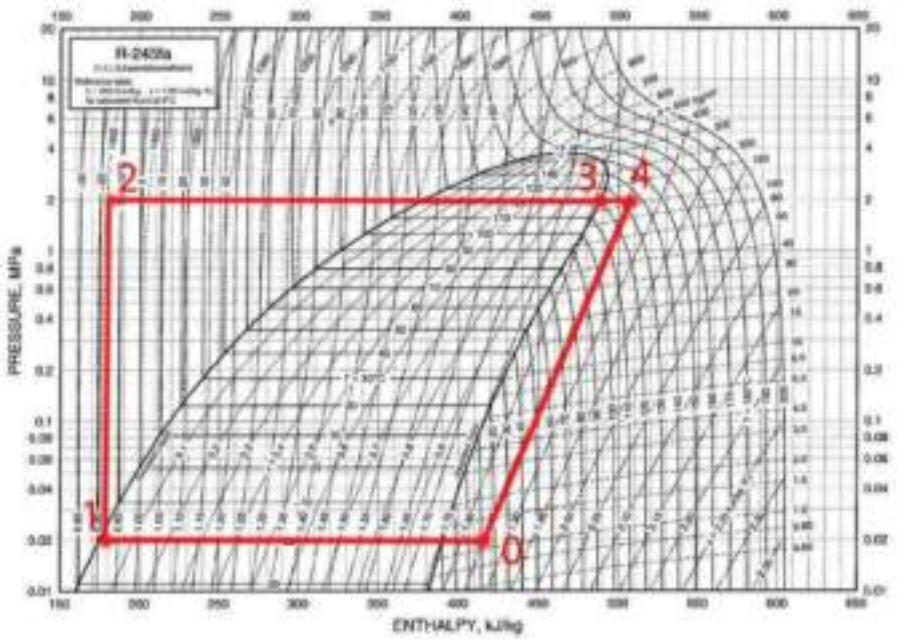

Figure 2. P-h diagram of the ORC with r245fa.

The following algorithm was used to determine the installation efficiency:

— The value of the temperature of the quenching compound in the condenser and power of the low-potential heat source and its temperature are set. The temperature of the low-grade heat source determines the maximum attainable temperature of the organic fluid;
— The enthalpies of the fluid at the characteristic points of the cycle are determined. The characteristic points of the cycle on r245fa are presented in Table 2;
— Further, the thermal efficiency of the unit, the work done by steam in the turbine and its adiabatic power are determined from the values of enthalpies in the evaporator and condenser;
— Then, the power of the feed pump is determined. Power of the ORC unit, taking into account the operation of the feed pump, the energy loss in the generator and the internal efficiency of the turbine is determined.

Then, in a similar way, calculation was performed for the remaining freons. To facilitate the calculations, a model of the OCR unit was built in Microsoft Excel. This model automatically calculates all parameters of the cycle after entering the initial data. °C

For comparison, several freons as a working fluid in the ORC, the temperature range of the quenching compound is assumed to be the same (from -20°C to 20°C), as well as the values of the internal efficiency of the turbine (86%) and the efficiency of the generator (95%). Then we

Table 2. Characteristic points of the cycle on r245fa.

Point	Enthalpy, кJ/kg	Note
0	410	End of expansion in a turbine
1	175	At the exit of the condenser
2	185	At the entrance to the evaporator
3	480	At the exit of evaporator
4	505	At the exit of the superheater

compare technical performance of the unit with different fluids. The most suitable compound is the one at which the power of the unit is greatest.

One of the problems of ORC is low efficiency. Thermal efficiency of these installations usually does not exceed 28% (Casati, 2014). One of the methods for increasing efficiency is the improvement of the cycle arrangement. However, this method leads to a complication of the design of the unit and an increase in its cost. For this reason, we built computer model that allows you select the most optimal cycle diagram of the ORC unit. The selection is made according to the following principle:

— The technical parameters of three cycle diagrams are calculated (simple circuit, circuit with economizer, circuit with intermediate steam overheating and economizer);
— Economical indicators of each circuit are determined;
— The optimal cycle diagram is selected based on the economic performance.

The calculation of the technical indicators of the unit without intermediate overheating of the steam and with economizer was carried out similarly to the algorithm for choosing the working fluid. The difference is that in this calculation the power of the feed pump is not taken into account.

Consider the OCR unit with an economizer. The thermal circuit of this unit is shown on Figure 3.

This scheme is used to increase the efficiency of the cycle. Economizer is installed between the turbine and the condenser and it heat the condensate after the feed pump in front of the evaporator by cooling the steam leaving the turbine to a condensation temperature 20°C.

The calculation of the technical indicators of the unit with an economizer was carried out similarly to the above algorithm; however, the calculation is complicated due to the need to make the heat balance of the economizer. From the heat balance equation, the enthalpy of the heated refrigerant at the outlet of the economizer is determined.

Next, a thermal circuit is calculated with an intermediate superheat of the steam and an economizer (Figure 4).

The calculation of the technical indicators of the unit operating according to this thermal scheme was carried out similarly to the calculation of the scheme with the economizer; however, the calculation is complicated by adding two characteristic points of the cycle: after high-pressure section and before low pressure section. It is necessary to set the value of the pressure of steam after the high-pressure section (0.6 MPa in this case), as well as to compile the heat balance of the intermediate superheater of the steam. The initial enthalpy of steam in the low pressure section is calculated from the heat balance equation.

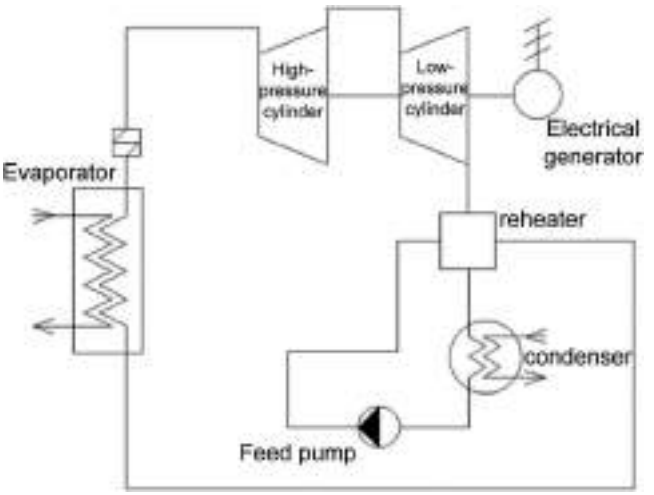

Figure 3. Thermal circuit of OCR unit with an economizer.